Advances
in Clinical and Experimental Medicine

WROCLAW
MEDICAL UNIVERSITY

Advances
in Clinical and Experimental Medicine

Editorial Policy

Contents

Feasibility and safety of high-power ablation of atrial fibrillation with contact force-sensing catheter: The lesion size index-guided ablation

Abdul Shokor Parwani[A–F], Felix Hohendanner[B–D,F], Amelie Kluck[B,C,E,F], Florian Blaschke[C,E,F], Burkert Pieske[A,E,F], Leif-Hendrik Boldt[A,C,E,F]

Charité-Universistätsmedizin Berlin, Campus Virchow Klinikum, Germany

A – research concept and design; B – collection and/or assembly of data; C – data analysis and interpretation;
D – writing the article; E – critical revision of the article; F – final approval of the article

Abstract

Background. Radiofrequency (RF) ablation is a commonly used method of atrial fibrillation (AF) treatment. High-power short-duration (HPSD) ablation has been suggested as a method to reduce procedure times whilst creating safe and lasting lesions. High-power ablation with contact force (CF)-sensing technology catheters might aid in a further improvement of safety whilst generating lasting transmural lesions.

Objectives. We report our experience using lesion size index (LSI)-guided 50 W ablation with a CF-sensing catheter of AF.

Materials and methods. We performed LSI-guided 50 W point-by-point ablation using a CF-sensing catheter (TactiCath). Target LSI at the anterior left atrium (LA) was 5.0 and at the posterior LA it was 4.5.

Results. Altogether, 4641 RF lesions were created in 86 consecutive patients. To reach a mean LSI of 4.9 ±0.01, a mean RF ablation time of 14.3 ±0.1 s was applied with a mean CF of 13.4 ±0.1 g. The RF time per lesion at the anterior wall of LA was 15.9 ±0.2 s, while it was 13 ±0.2 s at the posterior wall of LA. We observed force time integral (FTI) values between 36 g and 310 g. Procedure duration was 107 ±4 min with a RF ablation time of 15.4 ±0.6 min. No audible steam pops occurred. No pericardial effusion was observed. After a 1-year follow-up, no adverse events were reported and 83% of patients had no symptomatic arrhythmia recurrence.

Conclusions. We provide evidence for the safety and efficacy of LSI-guided 50 W ablation using the TactiCath CF-sensing ablation catheter. These data support the use of high-power ablation with CF sensing technology to improve both safety and efficacy.

Key words: atrial fibrillation, high-power ablation, lesion size index, contact force sensing

716

A.S. Parwani et al. Lesion size index-guided high-power ablation

Background

Generation of transmural lesions for targeted ablation of atrial tachycardia circuits or substrate and pulmonary vein isolation has been proven to be of high clinical value for the treatment of atrial rhythm disorders. Different energy forms are used to create these lesions. Radio-frequency (RF) energy is still the most commonly used energy form. To achieve transmural and lasting lesions, different settings of RF energy have been suggested with different relative contributions of the resistive or conductive heating phase.[1]

Recently, high-power (≥50 W) short-duration (HPSD) RF ablation with irrigated non-contact force has been shown to be safe while reducing procedure and ablation time, as compared to the traditional lower-power (e.g., 35 W) longer-duration ablation.[2,3] Moreover, lesion width has been suggested to be increased in HPSD as compared to traditional ablation techniques, owing to the fact that a substantial fraction of the ablation time is the resistive heating phase.[4]

Ablation with contact force (CF)-sensing technology catheters has been linked to enhanced procedural safety and efficacy in traditional ablation settings.[5–10] Lesion size index (LSI) is a multiparametric index introduced to improve lesion formation. It incorporates time, power, CF, and impedance data recorded during RF ablation with CF-sensing technology catheters.[11,12] The LSI-guided high-power ablation with CF-sensing technology catheters might aid in a further improvement of safety while generating lasting transmural lesions.

Objectives

We aim to examine the clinical safety and efficacy of LSI-guided 50 W ablation with CF-sensing catheter in patients with atrial fibrillation (AF).

Materials and methods

Study population

We included all consecutive patients that underwent RF ablation for AF with a LSI-guided 50 W ablation protocol in our clinic. All clinical, imaging and procedural data were recorded. The AF type was categorized as paroxysmal when lasting <1 week, or persistent when lasting >1 week and when electrical cardioversion was performed. The study protocol was approved by the human ethics committee of the Charité-Universistätsmedizin Berlin, Germany (application No. EA2/099/20). The study is in accordance with the Declaration of Helsinki.

Procedure and ablation settings

Prior to ablation procedures, a transesophageal echocardiogram was performed to exclude atrial thrombus formation, and transthoracic echocardiography was used to obtain measures of left atria and left ventricle, as previously described.[13] Oral anticoagulation therapy with vitamin K antagonists were continued, targeting an international normalized ratio between 2 and 3. Direct oral anticoagulation was paused on the morning of the procedure and resumed after the procedure.

During ablation, patients were sedated by using boluses of midazolam (3–5 mg) and a continuous infusion of propofol (1.5–4 mg/kg/h). Fluoroscopic guided transseptal puncture was performed and intravenous (i.v.) unfractioned heparin (initial bolus 100 U/kg) was administered with an intraprocedural activated clotting time between 300 s and 400 s. A biplane angiography of the left atrium (LA) was performed in angulations of RAO 30° and LAO 60° prior to ablation.

In all cases, the Abbott Ensite Precision™ system (Abbott, St. Paul, USA) was used for 3-D electroanatomic mapping with a single dispersive electrode. A decapolar Abott circular mapping catheter (Inquiry Optima™) or the multipolar HD grid catheter (both from Abbott) were used for creating a 3-D map of the atrium and for documenting pulmonary vein (PV) potentials. In all cases, a point-by-point circumferential ablation of PVs was performed.

Lesions were generated using a 3.5-mm open-tip irrigated TactiCath Quartz ablation catheter (Abbott) with the Abbott Agilis™ steerable sheath (Abbott). The TactiCath Quartz ablation catheter utilizes 3 fibers for optical force sensing via infrared laser light.[12,14] It was continuously flushed with 2 mL/min of normal saline solution during mapping. Flush rate was increased to 30 mL/min during ablation with a 1-second pre-flushing period before and 2-second post-flushing period after the ablation. The RF energy was generated using an Ampere RF generator (Abbott) with a maximal temperature of 43°C at 50 W both at the anterior and posterior left atrial wall.

The RF energy delivery was initiated at a stable CF between 10 g and 30 g. In our LSI-guided approach, we terminated RF energy delivery when a target LSI of 5.0 for the anterior LA wall and a target LSI of 4.5 for the posterior LA wall were reached. This conservative ablation approach was chosen to minimize the complication rate. The RF energy delivery for linear lesions was also performed with a LSI-guided 50 W ablation protocol, with a targeted LSI of 5.0 at the anterior LA wall and 4.5 at the posterior LA wall. The target inter-lesion distance was 4 mm.

The LSI is generated from CF, impedance, power, RF duration and, most importantly, in vivo experimental data of lesion generation. The underlying formula is based

on an empirical model derived from >3000 lesions in animal models and human tissue.[11] It accounts for a time-independent resistive and a time-dependent diffusive heating component (see also Calzolari et al. and Mattia et al.[11,15]), and considers the nonlinear lesion formation observed in vivo.

After encircling the veins, entry and exit block were confirmed using an Abbott circular mapping catheter (Inquiry Optima™; Abbott) or the multipolar HD grid mapping catheter, by documenting lack of vein potentials and failure of pacing inside the vein.

Study outcomes

For each patient, we recorded the pre-ablation clinical characteristics. For each ablation pulse, we obtained duration of RF application, impedance, power, CF, force time integral (FTI), and LSI. All ablation parameters were analyzed and grouped according to the different atrial regions: left/right upper and lower PV and anterior/posterior LA wall. Furthermore, the rate of acute pulmonary vein isolation (PVI), total RF ablation time, fluoroscopy time, and procedure time (skin-to-skin) were documented. The occurrence of steam pops was noted by the operators. Transthoracic echocardiography was performed after the procedure on the same day to exclude pericardial effusion.

For determination of early recurrence, all measures were taken to obtain electrocardiography (ECG) documentation in case of reported symptoms suggestive of arrhythmia recurrence at the 3- and 12-month follow-up visits. This includes either a 24-hour Holter ECG or a 12-lead ECG at the time of the follow-up visit. Symptomatic patients were classified as recurrences.

Statistical analyses

Continuous variables are shown as mean ± standard deviation (SD). Categorical variables are described as numbers or percentages. A correlation between type of AF (paroxysmal or persistent) and binary variables was analyzed with Pearson's χ^2 test. Comparisons of metric variables between paroxysmal and persistent AF were evaluated with Mann–Whitney U test, thereby accounting for not nominally distributed variables. A value of $p < 0.05$ was used to indicate statistical significance.

Results

Patient characteristics

A total of 86 patients with symptomatic AF were consecutively included in this study. Patients' baseline clinical characteristics are given by AF type in Table 1. The mean age in the study group was 66 ±1 years. Mean CHA_2DS_2-Vasc score was 2.8 ±0.2. Mean LA diameter was 40.4 ±0.8 mm and mean left ventricular ejection fraction (LVEF) was 52 ±1%.

The majority of patients were concomitantly treated with a ß-blocker and inhibitors of the renin-angiotensin-aldosterone system (Table 2). There was no statistically significant difference in baseline characteristics between patients with paroxysmal AF and persistent AF other than statin and ACEi/AT1R use, which was more frequent in patients with persistent AF.

Most patients underwent de novo PVI (59% of all procedures) for persistent or paroxysmal AF. De novo PVI was

Table 1. Clinical characteristics by AF type

Clinical characteristics	All patients n = 86	Persistent AF n = 41 (48%)	Paroxysmal AF n = 45 (52%)	p-value
Age [years]	66 ±1	66 ±1	66 ±2	0.92
Male sex	55 (64%)	26 (63%)	29 (64%)	0.92
CAD	29 (34%)	18 (44%)	11 (24%)	0.06
Sleep apnea	3 (3%)	1 (2%)	2 (4%)	0.61
Prior stroke/TIA	9 (10%)	5 (12%)	4 (9%)	0.62
Hypertension	81 (94%)	39 (95%)	42 (93%)	0.72
IDDM/NIDDM	15 (17%)	11 (27%)	4 (9%)	**0.03**
Pacemaker	8 (9%)	3 (7%)	5 (11%)	0.55
LVEF [%]	52 ±1	49.5 ±11.2	54.1 ±9.9	0.06
LA size [mm]	40.4 ±0.8	42.1 ±1.2	38.9 ±1.0	0.06
CHA2DS-VASc	2.8 ±0.2	3.2 ±0.2	2.4 ±0.3	**0.01**
EHRA score	2.4 ±0.1	2.4 ±0.2	2.4 ±0.1	0.75
NYHA score	2.2 ±0.2	2.1 ±0.3	2.2 ±0.5	0.94
AADs failed	11 (13%)	6 (15%)	5 (11%)	0.63

AF – atrial fibrillation; LA – left atrium; CAD – coronary artery disease; TIA – transitory ischemic attack; LVEF – left ventricular ejection fraction; AAD – antiarrhythmic drugs; (N)IDDM – (non-)insulin dependent diabetes mellitus; EHRA – European Heart Rhythm Association; NYHA – New York Heart Association. Values in bold are statistically significant.

Table 2. Overview of the medications at baseline

Medication	All patients n = 86	Persistent AF n = 41 (48%)	Paroxysmal AF n = 45 (52%)	p-value
ß-blocker	74 (86%)	37 (90%)	37 (82%)	0.28
Statine	29 (34%)	22 (54%)	7 (16%)	**<0.01**
ACEi/AT1R	54 (63%)	31 (76%)	23 (51%)	**0.02**
Antiarrhythmic	11 (13%)	6 (15%)	5 (11%)	0.63
OAK	77 (90%)	39 (95%)	38 (84%)	0.11

ACEi/AT1R – inhibitors of the renin-angiotensin-aldosterone system; OAK – oral anticoagulation; AF – atrial fibrillation. Values in bold are statistically significant.

Table 3. Overview of different ablation approaches according to the underlying rhythm disorder

Ablation type	All patients n = 86	Persistent AF n = 41 (48%)	Paroxysmal AF n = 45 (52%)	p-value
De novo PVI	51 (59%)	22 (54%)	29 (64%)	0.31
Re-PVI	35 (41%)	19 (46%)	16 (36%)	0.31
Anterior mitral line	6 (7%)	3 (7%)	3 (7%)	0.47
Isthmus mitral line	2 (2%)	0 (0%)	2 (4%)	0.17
Roof line	5 (6%)	2 (5%)	3 (7%)	0.72
RA isthmus line	8 (9%)	3 (7%)	5 (11%)	0.55

AF – atrial fibrillation; PVI – pulmonary vein isolation; RA – right atrium.

Table 4. Ablation parameters LSI, power [W], impedance drop, FTI, and CF [g] in comparison of the anterior wall with the posterior wall

Ablation location	LSI	Power [W]	Impedance drop	FTI	CF [g]
Anterior (PV only)	4.9 ±0.6	47 ±2	18 ±7	173 ±79	13 ±7
Posterior (PV only)	4.6 ±0.5	47 ±2	17 ±5	142 ±60	12 ±6

LSI – lesion size index; FTI – force time integral; CF – contact force; PV – pulmonary vein.

especially prevalent in paroxysmal AF patients (Table 3). However, there were no statistically significant differences in the ablation strategy.

In the remaining patients, re-isolation of the PVs was performed. Additionally, patients with re-isolation of PVs underwent linear ablation in case of inducible left atrial tachycardias.

Procedural data

A total of 4641 RF lesions were obtained with an average of 51 ±3 lesions per patient. The LSI-guided 50 W ablation was used for all lesions. Mean procedure duration was 107.7 ±4.8 min (range: 58–187 min), with a mean total RF time of 15.4 ±0.8 min (range: 10.5–39.9 min). Mean RF time per lesion was 14.3 ±0.1 s (range: 6–50 s) and the mean LSI was 4.9 ±0.01 (range: 3.9–6.9; Fig. 1).

The PVI or freedom from atrial tachycardia inducibility (in cases of atrial tachycardia) were achieved in all patients without major adverse events.

Mean LSI at the anterior part of the LA was 5 ±0.01. Mean LSI at the posterior part of the LA was 4.6 ±0.01. Mean energy delivery time to reach a LSI of 5.0 was 15.9 ±0.2 s. Mean application time to reach a LSI of 4.5 was 13 ±0.2 s (Fig. 2).

The RF duration, FTI and impedance drop showed a continuous increase along with higher LSI ranges. However,

most importantly, even high LSI values above 5.5, characterized by RF duration of 17.2 ±1.3 s and a CF of 22.7 ±0.8 g, led to no audible or tactile steam pops or adverse events in any of the 4641 RF applications (Fig. 2).

Safety and outcome

Overall, with regard to efficacy and safety, a complete isolation of the pulmonary veins with entry and exit block or freedom from AT inducibility was achieved in all patients without major adverse events. No audible steam pops occurred and no pericardial effusion was observed. Furthermore, in none of the studied patients, a transient ischemic attack or stroke occurred. At 1-year follow-up, no additional adverse events occurred (especially atrio-esophageal fistula, symptomatic pulmonary vein stenosis or phrenic nerve palsy). Freedom from AF or atrial tachycardia was achieved in 83% of all patients.

Discussion

In the present study, we investigated LSI-guided 50 W ablation using TactiCath CF ablation catheter for the treatment of left atrial tachycardia (AF and/or left macro-reentrant atrial tachycardia). We determined ablation
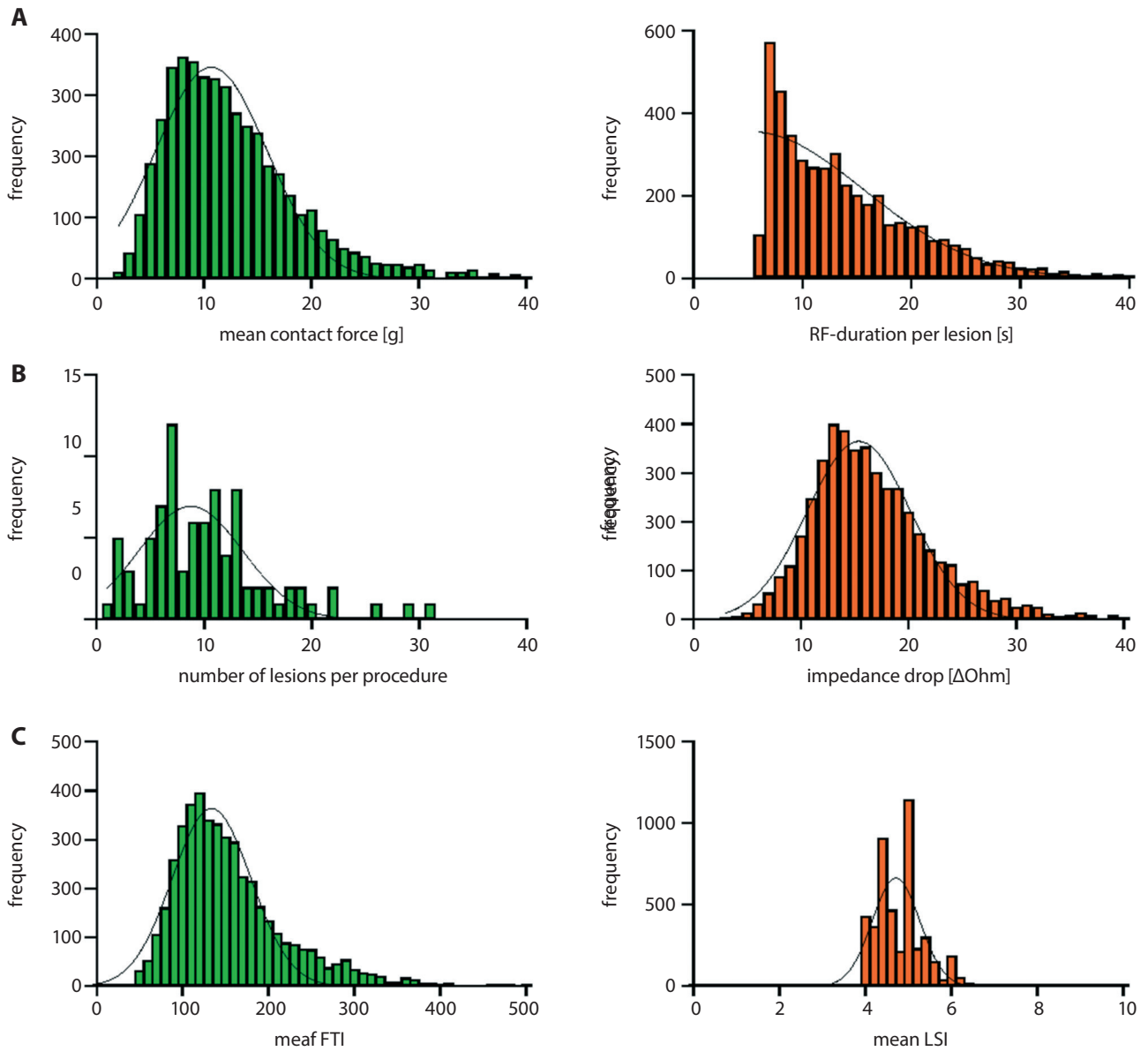
Fig. 1. Ablation parameters. A. Contact force (CF) and radiofrequency (RF) duration per lesion; B. Lesion per procedure and impedance drop; C. Force time integral (FTI) and mean lesion size index (LSI)
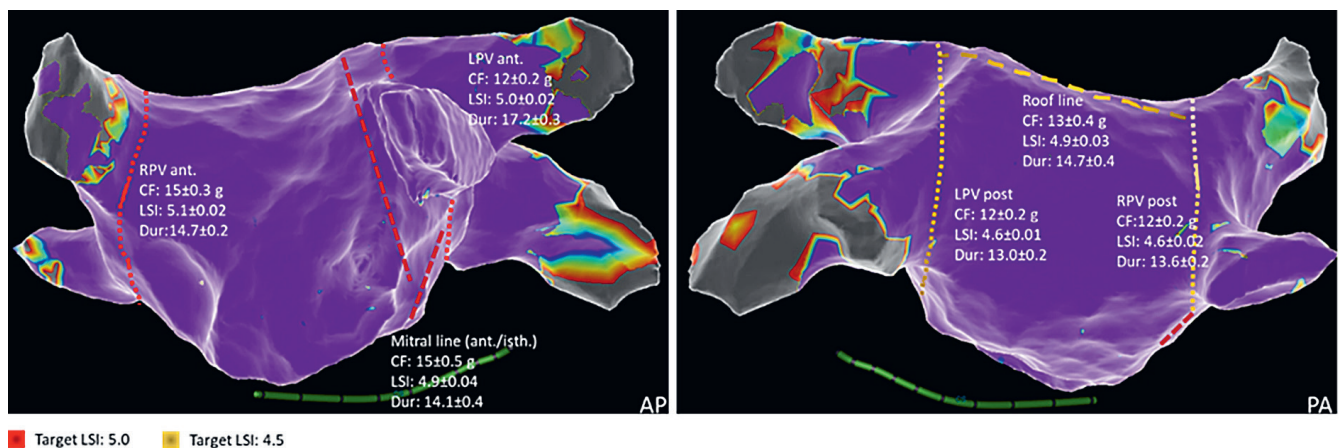
Fig. 2. Three-dimensional electroanatomic map of the LA indicating ablation sites and the respective CF as well as LSI and RF duration

CF – mean contact force in gram; LSI – lesion size index; Dur – RF duration in seconds per lesion; RF – radiofrequency; LA – left atrium. RPV – right pulmonary vein; LPV – left pulmonary vein.

parameters for different atrial regions and provided catheter- and ablation-related data for different LSI ranges for qualitative and quantitative lesion characterization.

The main finding of this study is that a target LSI of 5.0 at the anterior left atrial wall and 4.5 at the posterior left atrial wall (including left atrial lines) can be safely reached using the TactiCath CF-sensing catheter with an energy delivery of 50 W. With a mean CF of 22.7 ±0.8 g, energy delivery time up to 17 s showed no complications. It was also associated with short procedure times and RF energy delivery, and low risk for arrhythmia recurrences.

The impact of CF catheters and high-power (e.g., >35 W) ablation techniques on long-term outcomes has been studied in several trials.[6,16–18] In a previous study, the sole use of CF catheters or high-power ablation was associated with a particularly high success rate in patients with paroxysmal AF.[19]

High-power ablation creates lesions with equal volumes as compared to standard settings; however, they are wider and less deep, most likely due to the increased resistive heating component.[20] Previous studies evaluating 50 W ablations using non-CF catheters[16,21,22] showed a better long-term freedom from AF and shorter fluoroscopy and procedural times without an increase in complication rates, when compared with 35 W ablations using non-CF catheters.[2,3] In our previous experience using 35 W ablation, mean RF application time was 30 min for atrial ablation procedures.[23] In the present study, the total RF and procedure times were further decreased as compared to our traditional lower-power (i.e., 30–35 W) ablation approach.

Ablation with a CF-sensing catheter with an appropriate CF has been shown to achieve a higher 1-year freedom from AF when compared with non-CF-sensing ablation catheters.[18,20] Prediction of lesion size is an important aspect of safe and effective RF ablation, especially considering the known variability of myocardial wall thickness. The FTI values above 400 g have been recommended and a wide range of FTI values has been reported for LSI-targeted ablation in a low-power (25–30 W) approach.[15] In the present study, we observed FTI values between 36 ±2 and 310 ±15. As reported by Winkle et al.,[16] the high variability of FTI makes it an inferior target parameter as compared to LSI guidance. Physicians should be aware that FTI values during high-power ablation may be low despite creating an effective lesion. Traditional FTI cutoffs should be abandoned in high-power ablation.

The LSI has been shown to be a good predictor of lesion size in low-power ablation settings.[11,16] A LSI of 4.5 at the posterior left atrial wall and a LSI of 5.0 at the anterior left atrial wall have been suggested by some studies to predict effective lesion formation.[11,24] Moreover, several animal studies support the use of 50 W ablation using CF catheters for 5–10 s.[24–26]

Yet, the appropriate target LSI in high-power ablation using a CF-sensing still needs to be determined. For example, Winkle et al., using a CF-sensing catheter and 50 W ablation strategy as in our study, used a target LSI of 6.0 in patients in AF and a mix of LSI and "loss of pace capture" strategy in patients in sinusrhythm. Their average RF duration per lesion was 11.2 ±3.7 s. As in our study, they could also safely isolate all PVs with short procedure and RF ablation time.[16]

In our study, to reach an average LSI of 4.9 ±0.01, we needed an average energy delivery time of 14.3 ±0.1 s with a mean CF of 13.6 ±9.1 g. It is important to emphasize that an appropriate CF between 10 g and 30 g appears to be paramount to avoid unnecessary RF energy delivery, which may lead to edema formation, which in turn makes an effective lesion creation at this particular site more difficult or even impossible, thereby increasing the risk for reconnection and arrhythmia recurrence.

Limitations

The main limitation of this study is the consecutive enrolment design and the single-center experience. We did not compare LSI-guided high-power ablation to LSI-guided traditional lower-power (e.g., 35 W) longer-duration ablation protocol. Nevertheless, the study could demonstrate that LSI-guided 50 W ablation proved to be safe, with high acute success rates and short procedure time, whilst also being effective in reducing documented arrhythmia recurrences. As we included both patients with de novo pulmonary vein isolations and patients with redo procedures in our study, we observed an excellent arrhythmia-free survival of 83% during the 1-year follow-up.

Conclusions

We provide evidence for the safety and efficacy of LSI-guided 50 W ablation using the TactiCath CF ablation catheter. We show that a target LSI of up to 5.0 in 50 W ablation strategy is safe and associated with short procedure times and a low symptomatic arrhythmia recurrence rate.

ORCID iDs

Abdul Shokor Parwani https://orcid.org/0000-0003-2043-7050
Felix Hohendanner https://orcid.org/0000-0002-0194-4615
Amelie Kluck https://orcid.org/0000-0002-8414-5121
Florian Blaschke https://orcid.org/0000-0001-7193-0318
Burkert Pieske https://orcid.org/0000-0002-64665306
Leif-Hendrik Boldt https://orcid.org/0000-0002-3320-0880

References

1. Kottmaier M, Popa M, Bourier F, et al. Safety and outcome of very high-power short-duration ablation using 70 W for pulmonary vein isolation in patients with paroxysmal atrial fibrillation. *Europace*. 2020;22(3):388–393. doi:10.1093/europace/euz342
2. Vassallo F, Cunha C, Serpa E, et al. Comparison of high-power short-duration (HPSD) ablation of atrial fibrillation using a contact force-sensing catheter and conventional technique: Initial results. *J Cardiovasc Electrophysiol*. 2019;30(10):1877–1883. doi:10.1111/jce.14110

3. Castrejon-Castrejon S, Martinez Cossiani M, Ortega Molina M, et al. Feasibility and safety of pulmonary vein isolation by high-power short-duration radiofrequency application: Short-term results of the POWER-FAST PILOT study. *J Interv Card Electrophysiol*. 2020; 57(1):57–65. doi:10.1007/s10840-019-00645-5

4. Bourier F, Duchateau J, Vlachos K, et al. High-power short-duration versus standard radiofrequency ablation: Insights on lesion metrics. *J Cardiovasc Electrophysiol*. 2018;29(11):1570–1575. doi:10.1111/jce.13724

5. Kimura M, Sasaki S, Owada S, et al. Comparison of lesion formation between contact force-guided and non-guided circumferential pulmonary vein isolation: A prospective, randomized study. *Heart Rhythm*. 2014;11(6):984–991. doi:10.1016/j.hrthm.2014.03.019

6. Reddy VY, Shah D, Kautzner J, et al. The relationship between contact force and clinical outcome during radiofrequency catheter ablation of atrial fibrillation in the TOCCATA study. *Heart Rhythm*. 2012; 9(11):1789–1795. doi:10.1016/j.hrthm.2012.07.016

7. Squara F, Latcu DG, Massaad Y, Mahjoub M, Bun SS, Saoudi N. Contact force and force-time integral in atrial radiofrequency ablation predict transmurality of lesions. *Europace*. 2014;16(5):660–667. doi:10.1093/europace/euu068

8. le Polain de Waroux JB, Weerasooriya R, et al. Low contact force and force-time integral predict early recovery and dormant conduction revealed by adenosine after pulmonary vein isolation. *Europace*. 2015;17(6):877–883. doi:10.1093/europace/euu329

9. Yokoyama K, Nakagawa H, Shah DC, et al. Novel contact force sensor incorporated in irrigated radiofrequency ablation catheter predicts lesion size and incidence of steam pop and thrombus. *Circ Arrhythm Electrophysiol*. 2008;1(5):354–362. doi:10.1161/CIRCEP.108.803650

10. Matsuda H, Parwani AS, Attanasio P, et al. Atrial rhythm influences catheter tissue contact during radiofrequency catheter ablation of atrial fibrillation: Comparison of contact force between sinus rhythm and atrial fibrillation. *Heart Vessels*. 2016;31(9):1544–1552. doi:10.1007/s00380-015-0763-0

11. Calzolari V, De Mattia L, Indiani S, et al. In vitro validation of the lesion size index to predict lesion width and depth after irrigated radiofrequency ablation in a porcine model. *JACC Clin Electrophysiol*. 2017; 3(10):1126–1135. doi:10.1016/j.jacep.2017.08.016

12. Shah DC, Lambert H, Nakagawa H, Langenkamp A, Aeby N, Leo G. Area under the real-time contact force curve (force-time integral) predicts radiofrequency lesion size in an in vitro contractile model. *J Cardiovasc Electrophysiol*. 2010;21(9):1038–1043. doi:10.1111/j.1540-8167.2010.01750.x

13. Hohendanner F, Romero I, Blaschke F, et al. Extent and magnitude of low-voltage areas assessed by ultra-high-density electroanatomical mapping correlate with left atrial function. *Int J Cardiol*. 2018; 272:108–112. doi:10.1016/j.ijcard.2018.07.048

14. Bourier F, Gianni C, Dare M, et al. Fiberoptic contact-force sensing electrophysiological catheters: How precise is the technology? *J Cardiovasc Electrophysiol*. 2017;28(1):109–114. doi:10.1111/jce.13100

15. Mattia L, Crosato M, Indiani S, et al. Prospective evaluation of lesion index-guided pulmonary vein isolation technique in patients with paroxysmal atrial fibrillation: 1-year follow-up. *J Atr Fibrillation*. 2018; 10(6):1858. doi:10.4022/jafib.1858

16. Winkle RA, Moskovitz R, Hardwin Mead R, et al. Atrial fibrillation ablation using very short duration 50 W ablations and contact force sensing catheters. *J Interv Card Electrophysiol*. 2018;52(1):1–8. doi:10.1007/s10840-018-0322-6

17. Winkle RA, Mead RH, Engel G, Patrawala RA. Atrial fibrillation ablation: "Perpetual motion" of open irrigated tip catheters at 50 W is safe and improves outcomes. *Pacing Clin Electrophysiol*. 2011;34(5):531–539. doi:10.1111/j.1540-8159.2010.02990.x

18. Reddy VY, Dukkipati SR, Neuzil P, et al. Randomized controlled trial of the safety and effectiveness of a contact force-sensing irrigated catheter for ablation of paroxysmal atrial fibrillation: Results of the TactiCath Contact Force Ablation Catheter Study for Atrial Fibrillation (TOCCASTAR) study. *Circulation*. 2015;132(10):907–915. doi:10.1161/CIRCULATIONAHA.114.014092

19. Winkle RA, Mead RH, Engel G, et al. High-power, short-duration atrial fibrillation ablations using contact force sensing catheters: Outcomes and predictors of success including posterior wall isolation. *Heart Rhythm*. 2020;17(8):1223–1231. doi:10.1016/j.hrthm.2020.03.022

20. Leshem E, Zilberman I, Tschabrunn CM, et al. High-power and short-duration ablation for pulmonary vein isolation: Biophysical characterization. *JACC Clin Electrophysiol*. 2018;4(4):467–479. doi:10.1016/j.jacep.2017.11.018

21. Kanj MH, Wazni O, Fahmy T, et al. Pulmonary vein antral isolation using an open irrigation ablation catheter for the treatment of atrial fibrillation: A randomized pilot study. *J Am Coll Cardiol*. 2007;49(15):1634–1641. doi:10.1016/j.jacc.2006.12.041

22. Bunch TJ and Day JD. Novel ablative approach for atrial fibrillation to decrease risk of esophageal injury. *Heart Rhythm*. 2008;5(4):624–627. doi:10.1016/j.hrthm.2007.11.007

23. Huemer M, Wutzler A, Parwani AS, et al. Comparison of the anterior and posterior mitral isthmus ablation lines in patients with perimitral annulus flutter or persistent atrial fibrillation. *J Interv Card Electrophysiol*. 2015;44(2):119–129. doi:10.1007/s10840-015-0033-1

24. Parwani AS, Hohendanner F, Bode D, et al. The force stability of tissue contact and lesion size index during radiofrequency ablation: An ex-vivo study. *Pacing Clin Electrophysiol*. 2020;43(3):327–331. doi:10.1111/pace.13891

25. Bhaskaran A, Chik W, Pouliopoulos J, et al. Five seconds of 50–60 W radio frequency atrial ablations were transmural and safe: An in vitro mechanistic assessment and force-controlled in vivo validation. *Europace*. 2017;19(5):874–880. doi:10.1093/europace/euw077

26. Ali-Ahmed F, Goyal V, Patel M, Orelaru F, Haines DE, Wong WS. High-power, low-flow, short-ablation duration-the key to avoid collateral injury? *J Interv Card Electrophysiol*. 2019;55(1):9–16. doi:10.1007/s10840-018-0473-5

Increased local miR-21 expressions are linked with clinical severity in lumbar disc herniation patients with sciatic pain

Zhen-Fei Zou[A,C,D], Jing-Pei He[B–D], Yan-Lian Chen[A,B,E], Hai-Lin Chen[A,D–F]

Department of Anesthesiology, Maoming People's Hospital, China

A – research concept and design; B – collection and/or assembly of data; C – data analysis and interpretation;
D – writing the article; E – critical revision of the article; F – final approval of the article

Address for correspondence
Hai-Lin Chen
E-mail: chl20130630@163.com

Abstract

Background. The miR-21 has been implicated in the process of neuroinflammation as well as neuropathic pain.

Objectives. To explore the relationship between the plasma and local expression of miR-21 with disease severity of lumbar disc herniation (LDH) patients with sciatic pain.

Materials and methods. Ninety-two LDH patients with sciatic pain and 25 scoliosis patients as painless controls were enrolled in the current study. Samples from nucleus pulposus (NP), annulus fibrosus (AF) and soft tissues around nerve root (STANR) were obtained. The plasma and local expressions of miR-21 were detected with quantitative reverse transcription polymerase chain reaction (qRT-PCR). The visual analogue scale (VAS) for lumbar pain and leg pain, and Japanese Orthopedic Association (JOA) score were selected to evaluate the clinical severity. The degree of disc compression on nerve was evaluated using the Pfirrmann grade based on the magnetic resonance imaging (MRI) findings. For the convenience of analysis, LDH patients with sciatic pain were classified into a severe pain (SP) group (VAS ≥ 6) and a mild-moderate pain (MP) group (VAS < 6). Receiver operating characteristic (ROC) curve analysis was performed to detect the potential diagnostic power of miR-21 with regard to the Pfirrmann grade.

Results. There were no significant differences in serum miR-21 expressions among SP LDH patients, MP LDH patients and scoliosis painless controls. Local expressions of miR-21 in STANR, AF and NP were all drastically upregulated in the SP group in comparison with the MP group and scoliosis painless group. Local NP and STANR miR-21 expressions were positively associated with the Pfirrmann grade. Local miR-21 expressions in STANR and AF were positively associated with VAS score and negatively related to JOA score. The ROC curve analysis indicated that both STANR and AF miR-21 expressions may serve as significant diagnostic factors for the Pfirrmann grade.

Conclusions. Increased local miR-21 expressions are linked with clinical severity of LDH in patients with sciatic pain.

Key words: miR-21, lumbar disc herniation, sciatic pain, clinical severity

Background

Among the degenerative abnormalities of the lumbar spine, lumbar disc herniation (LDH) has been the most common diagnosis and reason for spinal surgeries in adults.[1] Around 2–3% of the world population was affected by LDH, bringing great social and economic burden as well as experiencing impaired life quality. The prevalence of LDH was 4.8% in men and 2.5% in women over 35 years of age.[2] Sciatica is the most important symptom of LDH. It causes radiating leg pain that follows a dermatomal pattern, along with the distribution of sciatic nerve into the foot and toes.[3] Coughing can make the pain worse, and patients may experience a variety of symptoms such as sensory symptoms, gait deformity, unilateral spasm of the paraspinal muscles, as well as limited forward flexion of the lumbar spine.[4]

So far, it has been acknowledged that sciatica in the LDH was a direct result of nerve root compression. Nevertheless, LDH has different mechanisms which were hard to be simply explained by mechanical compromise.[5] In recent years, studies have demonstrated the biological activity of the herniated tissue in the expression of inflammatory mediators.[6] Besides, it has been shown that the protruded nucleus pulposus (NP)-induced neuroinflammatory response was pivotal for radicular pain.[7] Neuroinflammation, due to periphery-to-central nervous system (CNS) cross-talk through proinflammatory mediators, could result in chronic pain in LDH patients.[8] The herniated NP also resulted in the autoimmune-mediated inflammatory response, involving multiple cytokines, such as tumor necrosis factor alpha (TNF-α) and interleukin (IL)-6.[9]

As a class of small non-coding RNAs, microRNAs (miR-NAs) play critical roles in regulating gene expression and essential physiological and pathological processes. Even though they represent just 1–3% of the human genome, it has been found that miRNAs have the ability to regulate around 30% of the protein-encoding genes in humans.[10–12] Recent works have shown that miRNAs could promote or suppress the inflammatory process, and either exacerbate or attenuate the pathological results of uncontrolled neuroinflammation.[13] For example, miR-210 could induce microglial activation and regulate microglia-mediated neuroinflammation in neonatal hypoxic-ischemic encephalopathy.[14] The miR-146a negatively regulates neuroinflammation in neurons, microglia and astrocytes.[15] The miR-124 acts as a key negative regulator of neuroinflammation by reducing inflammatory mediators and restricting microglia to an inactive state.[16] Studies found that the maladjustment of miRNAs expressions is related to the occurrence and development of LDH and sciatica. For example, miR-223 in exosome-like vesicles is related to a decreased risk of persistent pain in LDH patients.[17] Increased circulating miR-17 expressions are correlated with the intensity of lumbar radicular pain (LRP) in LDH patients.[18] The miR-124-3p could alleviate neuropathic pain in a chronic sciatic nerve injury model.[19]

The miR-21 is one of the most widely studied miRNAs and is highly present in many cell types. The miR-21 expression is also upregulated in many disease status including cancer, cardiovascular disease, inflamed tissue, etc.[20] In active immune cells, including macrophages, neutrophils, mast cells, as well as T cells, miR-21 is highly expressed.[20] In the injured dorsal root ganglion (DRG) neurons, miR-21 is specifically upregulated and causally involved in the late phase of neuropathic pain.[21] It has been also demonstrated that the delivery of miR-21 derived from neurons to macrophages polarizes these cells into a proinflammatory or pronociceptive phenotype.[22] In addition, silencing miR-21 expression in sensory neurons could prevent both the development of neuropathic allodynia as well as the macrophage recruitment in the DRG.[22] As a fibrosis-associated miRNA, miR-21 promotes the inflammation in ligamentum flavum tissues by the activation of IL-6 expression, leading to ligamentum flavum fibrosis, hypertrophy and final spinal canal stenosis.[23] These findings implicate that miR-21 may play an important role in lumbar-related disease. On the other hand, the rupture of the annulus fibrosus (AF) can lead to a foreign body reaction resulting from NP that guides neovascularization,[24] which is accompanied by macrophage infiltration. The subsequent macrophage infiltration is believed to aggravate pain symptoms and sciatica through the production of various cytokines.[25] In contrast, macrophage infiltration may also have a positive effect on relieving symptoms through inducing a phagocytic resorption process, mediated by anti-inflammatory cytokines.[26] Previous studies found that miR-21 could promote macrophage infiltration under various conditions.[27,28]

Objectives

All the abovementioned studies indicated that miR-21 may serve as an important promoter for facilitating the sciatica in LDH patients. However, there were no studies illustrating the relationship between miR-21 expression and LDH severity. Therefore, this study was designed to detect whether circulating or local miR-21 expressions are related to the clinical severity of LDH patients with sciatica.

Materials and methods

Study patients

From May 2020 to May 2021, 92 LDH patients who received discectomy were enrolled in the study. All LDHs were confirmed with magnetic resonance imaging (MRI) with unilateral sciatica, regardless of lumbar pain existence. Inclusion criteria were determined as follows: 1) definite lower level and single segment (L4~L5 or L5~S1) disc herniation on MRI, consistent with related clinical signs, as well as symptoms of LRP (straight leg raising (SLR) < 60°)

with either a short-term (2–4 weeks) severe or long-term (4–12 weeks) moderate leg pain; 2) patients did not receive nonsteroidal anti-inflammatory drugs (NSAIDs) or nerve nutrition drugs for at least 1 week before the surgery. Exclusion criteria were as follows: 1) patients with serious functional diseases in multiple organs, including the heart, lung, liver, kidney, etc.; 2) patients with blood system diseases, cancer or other systemic diseases; 3) patients with incarcerated, central, free, or giant LDH; 4) patients with foot drop or cauda equina syndrome; 5) patients with spondylolisthesis or spinal stenosis. At the same time, 25 scoliosis patients, without any signs of lumbar and radicular pain or degenerative disc disease were recruited as controls. All the controls did not have any signs of LDH identified using MRI. This study protocol was approved by the ethics committee of Maoming People's Hospital and conducted according to the Declaration of Helsinki. Patients provided an informed consent before any study-specific procedures were performed.

Laboratory examination

Venous blood was extracted from all participants before 9 AM after an overnight fast, and placed at room temperature for 2 h, followed by centrifugation for 20 min at 1900 × g. The miRNeasy Serum/Plasma Kit (Qiagen, Hilden, Germany) was used to isolate the total RNA from 200 µL of serum, according to the manufacturer's instructions. Up to the present, there was no housekeeping miRNA available that is normalized for the miRNA expression in serum/plasma. Hence, the samples were treated with U6 RNA (5 nmol/L) as the spiked-in RNA, after the addition of miRNeasy.

For tissue examination, total RNA was extracted from NP, AF and soft tissues around nerve root (STANR) using a Trizol kit (Thermo Fisher Scientific, Waltham, USA). The extracted RNA was then reversely transcribed into complementary DNA (cDNA), using PrimeScript™ II 1st Strand cDNA Synthesis Kit (TaKaRa Bio Inc., Kusatsu, Japan). The relative expression of miR-21 was determined using a TaqMan™ MicroRNA Assay (GeneCopoeia, Guangzhou, China) and SYBR® Premix Ex Taq™ kit (Ta-KaRa Bio Inc.). The fold change relative to internal reference was computed based on the relative quantitative $2^{-\Delta\Delta Ct}$ method: $\Delta\Delta Ct = \Delta Ct$ (target gene) – ΔCt (internal reference). The U6 was adopted as an internal reference of miR-21. The primers were listed as below: miR-21 forward primer: 5'-GTGCAGGGTCCGAGGT-3', reverse primer: 5'-GCCGCTAGCTTATCAGACTGATGT-3'; U6 forward primer: 5'-CTCGCTTCGGCAGCACA-3', reverse primer: 5'-AACGCTTCACGAATTTGCGT-3'.

Definition of compression degree

According to the Pfirrmann grade,[29] the compression degree was evaluated through an axial cut MR image at the level of maximal disc herniation, to grade the unilateral traversing nerve root compromise due to the herniating disc: grade 0 (normal) – no compromise of the root is seen; grade 1 (contact) – there is a visible contact of disc material with the nerve root, and the normal epidural fat layer between the two is not evident, while the nerve root has a normal position and there is no dorsal deviation; grade 2 (deviation) – the nerve root is displaced dorsally by disc material; grade 3 (compression) – the nerve root is compressed between disc material and the wall of the spinal canal (it may appear flattened or be indistinguishable from the disc material). Only patients with Pfirrmann grade ≥1 were enrolled in the study. The image findings were assessed by 2 experienced radiologists, and the kappa value was computed to examine the consistency of the results. As recommended by Landis and Koch,[30] the kappa value was graded as following: 0–0.20: slight agreement; 0.21–0.40: fair agreement; 0.41–0.60: moderate agreement; 0.61–0.80: substantial agreement; 0.81 or higher: excellent agreement; 1.00: absolute agreement.

Assessment of clinical severity

The degree of pain was determined using the visual analogue scale (VAS) score, whereas the functional ability was determined with Japanese Orthopedic Association (JOA) score. The VAS scale was presented as a line segment with a length of 10 cm, representing 10 points in total (1 cm for 1 point): 0 points indicates no pain and 10 points indicates an extremely severe pain. The higher the score, the more severe the pain.[31] Since the number of cases in our study was comparatively small, the median number of 0–10, 5.5 (rounding up to 6) was used to categorize the severity of pain. Besides, lumbar pain, numbness or pain of lower limbs, SLR test, walking ability, esthesia, activities of daily living (ADL), muscle strength, as well as bladder function were all assessed using JOA score. The score of JOA ranges from 0 to 29 points, where higher scores indicate less pain and better function.[32] Both VAS and JOA scores are widely used in the evaluation of pain and function states in many diseases.

Statistical analyses

Statistical analyses were carried out using IBM SPSS v. 21.0 software (IBM Corp., Armonk, USA). The statistical graph was created using Prism 8.0 (GraphPad, San Diego, USA). Data were described as mean ± standard deviation (SD) or median (interquartile range (IQR)). The distribution data of miR-21 expressions was tested using Kolmogorov–Smirnov test. The statistical analysis showed that the data of miR-21 expressions were normally distributed. The Student's t-test was carried out to compare the differences between the groups. One-way analysis of variance (ANOVA) was applied to statistically test the differences among ≥3 groups, followed by Dunn's post hoc tests. The Spearman's correlation analysis was used

to examine the association of miR-21 expression with VAS and JOA scores. Area under the curve (AUC) was tested for statistical analysis, with regard to receiver operating characteristic (ROC) curve analysis. The values of $p < 0.05$ were considered statistically significant.

Results

Demographic data

There were significant differences in age ($p < 0.001$). Besides, there were no significant differences in disease duration between severe pain (SP) and mild-moderate pain (MP) groups (median 6.3 compared to 6.0, $p > 0.05$). Demographic characteristics are listed in Table 1.

Table 1. Demographic characteristics

Variable	Severe pain (n = 44)	Mild-moderate pain (n = 48)	Control (n = 25)	p-value
Sex (F/M)	19/25	24/24	11/14	0.783
Age [years]	37.2 ±5.8	38.5 ±6.0[NS]	20.1 ±4.1	<0.001
Disease duration [months]	6.3 (2–42)	6.0 (1–44)[NS]	80 (56–136)	<0.001
BMI [kg/cm²]	23.6 ±2.4	23.2 ±2.5	23.1 ±2.6	0.469

One-way analysis of variance (ANOVA) was applied, followed by Dunn's post hoc tests. BMI – body mass index; NS – not statistically significant compared with the severe pain group after the post hoc analysis.

Serum and local miR-21 expressions in LDH patients and controls

Based on the degree of pain, LDH patients with sciatica were divided into the SP group (VAS ≥ 6; n = 44) and the MP group (VAS < 6; n = 48). Additionally, 25 scoliosis patients without pain were enrolled as painless controls. No significant differences of serum miR-21 expressions were found between control and LDH patients (1.00 ±0.04 compared to 1.00 ±0.06, t = 0.936, p = 0.404; Table 2). Also, no significant differences of serum miR-21 expressions were found between the MP group and SP group when Student's t-test was used (1.00 ±0.05 compared to 1.00 ±0.06, t = 0.942; p = 0.399; Table 3). Compared to the controls, miR-21 expressions in NP, STANR and AF were all significantly higher in the LDH group (t = 9.58, 2.58 ±0.87 compared to 0.99 ±0.06, p < 0.001, t = 9.136, t = 13.16, all p < 0.001; Table 2). Subsequently, the local miR-21 expression in the SP as well as the MP groups was further compared. We found that NP (3.25 ±0.40 compared to 1.96 ±0.70, t = 10.700, p < 0.001) as well as STANR (2.75 ±0.61 compared to 2.42 ±0.55, t = 2.776, p = 0.007), but not AF (2.68 ±0.62 compared to 2.49 ±0.58, t = 1.472, p = 0.144) miR-21 expressions were significantly increased in the SP group in comparison with MP group (Table 3).

Table 2. Comparison of miR-21 expression between control and lumbar disc herniation (LDH) patients

miR-21 expression	Control	LDH	p-value
NP miR-21 expression	1.00 ±0.06	2.58 ±0.87	<0.001
AF miR-21 expression	1.00 ±0.06	2.58 ±0.60	<0.001
STANR miR-21 expression	1.00 ±0.05	2.60 ±0.58	<0.001
Serum miR-21 expression	1.00 ±0.04	1.00 ±0.06	0.404

Student's t-test was used to compare miR-21 expression between control and LDH patients. NP – nucleus pulposus; AF – annulus fibrosus; STANR – soft tissues around nerve root.

Table 3. Comparison of miR-21 expression between control and lumbar disc herniation (LDH) patients

miR-21 expression	Mild-moderate pain	Severe pain	p-value
NP miR-21 expression	1.96 ±0.70	3.25 ±0.40	<0.001
AF miR-21 expression	2.49 ±0.58	2.68 ±0.62	0.144
STANR miR-21 expression	2.42 ±0.55	2.75 ±0.61	0.007
Serum miR-21 expression	1.00 ±0.05	1.00 ±0.06	0.399

Student's t-test was used to compare miR-21 expression between control and LDH patients. NP – nucleus pulposus; AF – annulus fibrosus; STANR – soft tissues around nerve root.

Correlation between serum/local miR-21 expressions and Pfirrmann grade in LDH patients

The possible relationship between serum/local miR-21 expressions and compression degree to sciatic nerve was further explored through Pfirrmann grading system. In the LDH patients, there were 26, 36 and 30 patients with Pfirrmann grade 1, 2 and 3, respectively. Through Student's t analysis, we found that LDH patients with Pfirrmann grade 3 had drastically higher NP and STANR miR-21 expressions than LDH patients with Pfirrmann grade 2 (NP: 2.39 ±0.21 compared to 2.17 ±0.26, t = 2.209, p = 0.031; STANR: 2.90 ±0.54 compared to 2.57 ±0.60, t = 2.316, p = 0.024; Table 4). Furthermore, LDH patients with Pfirrmann grade 2 demonstrated markedly increased NP and STANR miR-21 expressions compared to LDH patients with Pfirrmann grade 1 (NP: 2.17 ±0.26 compared to 2.06 ±0.16, t = 2.844, p = 0.006; STANR: 2.57 ±0.60 compared to 2.22 ±0.48, t = 2.467, p = 0.017; Table 4). The Spearman's correlation analysis showed that both NP and STANR expressions were positively related to Pfirrmann grade (NP: r = 0.423, p < 0.001; STANR: r = 0.440, p < 0.001; Fig. 1A,B). We performed ROC curve analysis to explore the diagnostic value of local miR-21 with regard to Pfirrmann grade. The ROC curve analysis indicated that both NP (Pfirrmann grade 1 compared to 2: AUC = 0.728, p = 0.002; Pfirrmann grade 2 compared to 3: AUC = 0.680, p = 0.013; Fig. 2A,B) and STANR (Pfirrmann grade 1 compared to 2: AUC = 0.682, p = 0.015; Pfirrmann grade 2 compared to 3: AUC = 0.665, p = 0.022) miR-21

Table 4. Comparison of miR-21 expression among different Pfirrmann grades

miR-21 expression	Grade 1	Grade 2	Grade 3
NP miR-21 expression	2.06 ±0.16	2.17 ±0.26*	2.39 ±0.21#
STANR miR-21 expression	2.22 ±0.48	2.57 ±0.60*	2.90 ±0.54#
Serum miR-21 expression	0.98 ±0.06	1.01 ±0.06ns	1.00 ±0.06ns

Student's t-test was used to compare miR-21 expression of grade 1 compared to grade 2, as well as grade 2 compared to grade 3; *p < 0.05 compared to grade 1; #p < 0.05 compared to grade 2; ns – not significant; NP – nucleus pulposus; STANR – soft tissues around nerve root.

expressions may serve as significant diagnostic factors for the Pfirrmann grade (Fig. 2C,D). However, there were no significant differences in serum miR-21 expressions among different Pfirrmann grades (1–3) detactable with one-way ANOVA (0.98 ±0.06 compared to 1.01 ±0.06 compared to 1.00 ±0.06, respectively, F = 0.387, p = 0.681; Table 4). Besides, serum miR-21 expressions were not significantly associated with Pfirrmann grades (r = 0.107, p = 0.310).

Association of local miR-21 expression levels with VAS and JOA scores

The associations of miR-21 expressions in STANR and NP with VAS and JOA scores were then investigated. The Spearman's correlation analysis showed that miR-21 expressions in both NP and STANR were positively linked to VAS (NP: r = 0.592, p < 0.001; STANR: r = 0.432, p < 0.001; Fig. 3A,B) and negatively associated with JOA scores (NP: r = −0.493, p < 0.001; STANR: r = −0.436, p < 0.001; Fig. 3C,D).

Discussion

Lumbar radicular pain was first described by Hippocrates in the 14th century BC.[33] Most of the pathophysiologic mechanisms in animal models as well as experimental studies underpinning sciatica have been explored. However, the relevant neoplastic, infectious or degenerative conditions have remained unexplored. In addition to mechanical deformation, the pathophysiologic mechanisms of sciatica may also be related to inflammation, immunology and neurophysiology.

Neuropathic and inflammatory pain promote a large number of persisting adaptations at the cellular and molecular level, allowing even transient tissue or nerve damage to elicit changes in cells that contribute to the development of chronic pain and associated symptoms.[34] In recent years, authors who were striving to achieve a consensus of opinion related to the pathogenesis of neuropathic or inflammatory pain, in their works have been devoting increasingly more attention to the importance of an epigenetic component.[35] The advances in the basic and clinical sciences over these years have substantiated the belief that neuropathic or inflammatory pain could be partially regulated by epigenetic factors.[36] The miRNAs do not only function as one of the most important epigenetic machineries, but also are epigenetically modified by DNA methylation and histone modification like any other protein-coding gene.[37]

The current study investigated the effect of serum/local miR-21 expression on disease severity in LDH patients with sciatica. We found that local miR-21 expression was significantly higher than in controls, indicating that local miR-21 may take part in the process of sciatica in LDH patients. In this study, we did not observe any significant differences in serum miR-21 expressions between LDH patients and controls, indicating that LDH causing radicular pain is a local event instead of a systematic process. On the other hand, sometimes, microRNA expressions in the serum are not stable and may be affected by many other conditions.

Additionally, we found that local miR-21 levels of NP and STANR were positively linked to VAS score and negatively related to JOA score. As mentioned before, the herniated tissue is not inert but very active in expressing inflammatory mediators. Both the chemical irritation caused by the NP-released bioactive substances and an autoimmune response against itself can also induce the inflammation. We extended these findings and demonstrated that higher local NP and STANR miR-21 expressions in LDH patients are linked to the increased radicular pain.
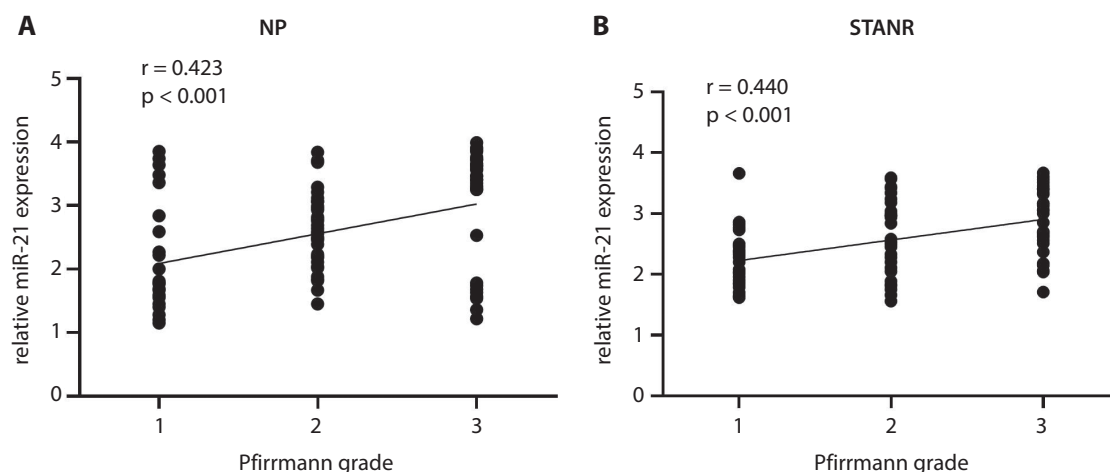
Fig. 1. A. Spearman's correlation analysis between local nucleus pulposus (NP) miR-21 expressions and Pfirrmann grade (n = 92); B. Spearman's correlation analysis between local soft tissues around nerve root (STANR) miR-21 expressions and Pfirrmann grade (n = 92)
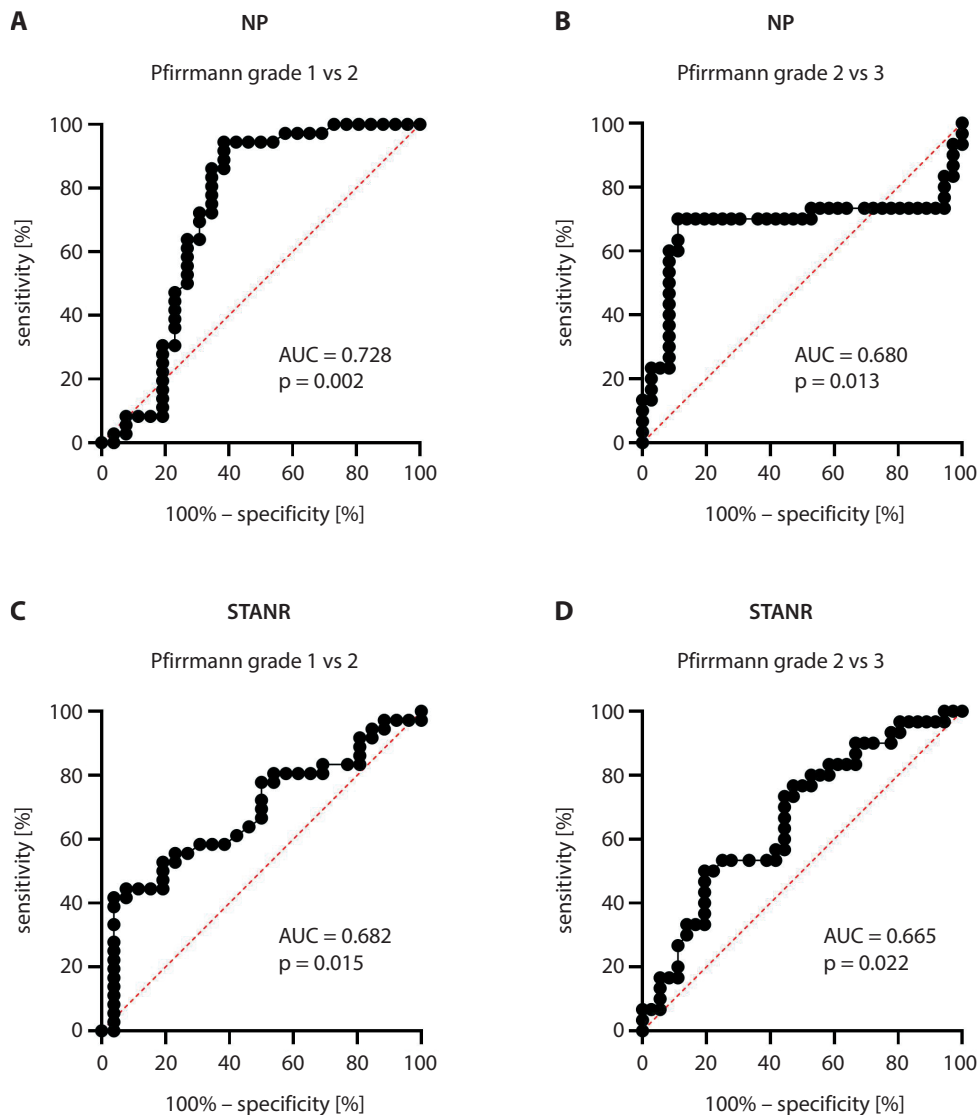
Fig. 2. Area under curve (AUC) was tested for statistical analysis. A. Receiver operating characteristic (ROC) curves of nucleus pulposus (NP) miR-21 expression with regard to Pfirrmann grade 1 (n = 26) compared to Pfirrmann grade 2 (n = 30); B. ROC curves of NP miR-21 expression with regard to Pfirrmann grade 2 (n = 30) compared to Pfirrmann grade 3 (n = 36); C. ROC curves of annulus fibrosus (AF) miR-21 expression with regard to Pfirrmann grade 1 (n = 26) compared to Pfirrmann grade 2 (n = 30); D. ROC curves of AF miR-21 expression with regard to Pfirrmann grade 2 (n = 30) compared to Pfirrmann grade 3 (n = 36)

STANR – soft tissues around nerve root.

The following ROC curve analysis showed that both NP and STANR miR-21 expressions may serve as a significant diagnostic factor for the Pfirrmann grade, indicating that the more the disk is herniated, the higher the miR-21 is expressed. The herniated disk tissues also affect the STANR, but not in AF. This may be attributed to the fact that increased miR-21 expressions originate from the degenerated disk. Many researchers focused on the proinflammatory role of NP around the nerve root. As reported in studies, NP had both inflammatogenic and leucotactic effects.[38,39] An animal study also reported that autologous NP applied to the lumbar nerve roots of rats led to a reduced blood flow to the DRG as well as an elevated endoneurial fluid pressure.[40] The miR-21 has been implicated to play a role in causing the inflammatory and neuropathic pain in previous studies. Simeoli et al. found that pain neurons in DRG release exosomes containing miR-21 after nerve injuries. These exosomes are then absorbed by the immune cells in the surrounding, further contributing to the local inflammation as well as neuropathic pain.[41] Chemokines produced by Schwann cells and satellite cells promote monocyte/macrophage infiltration at the site of injury and DRG. When they blocked the release of miR-21 from the exosomes of DRG pain neurons, they played an anti-inflammatory role and prevented the neuropathic pain in mice.[41]

Limitations

There were some limitations that should be taken into account. First, the sample size was relatively small. More samples would be needed to identify the findings of our study. Second, we only examined serum and local miR-21 expressions. The investigation of other miRNAs or related inflammatory cytokines may reveal much more valuable information.

Conclusions

We found that local NP and AF miR-21 expressions were significantly upregulated in LDH patients with sciatica
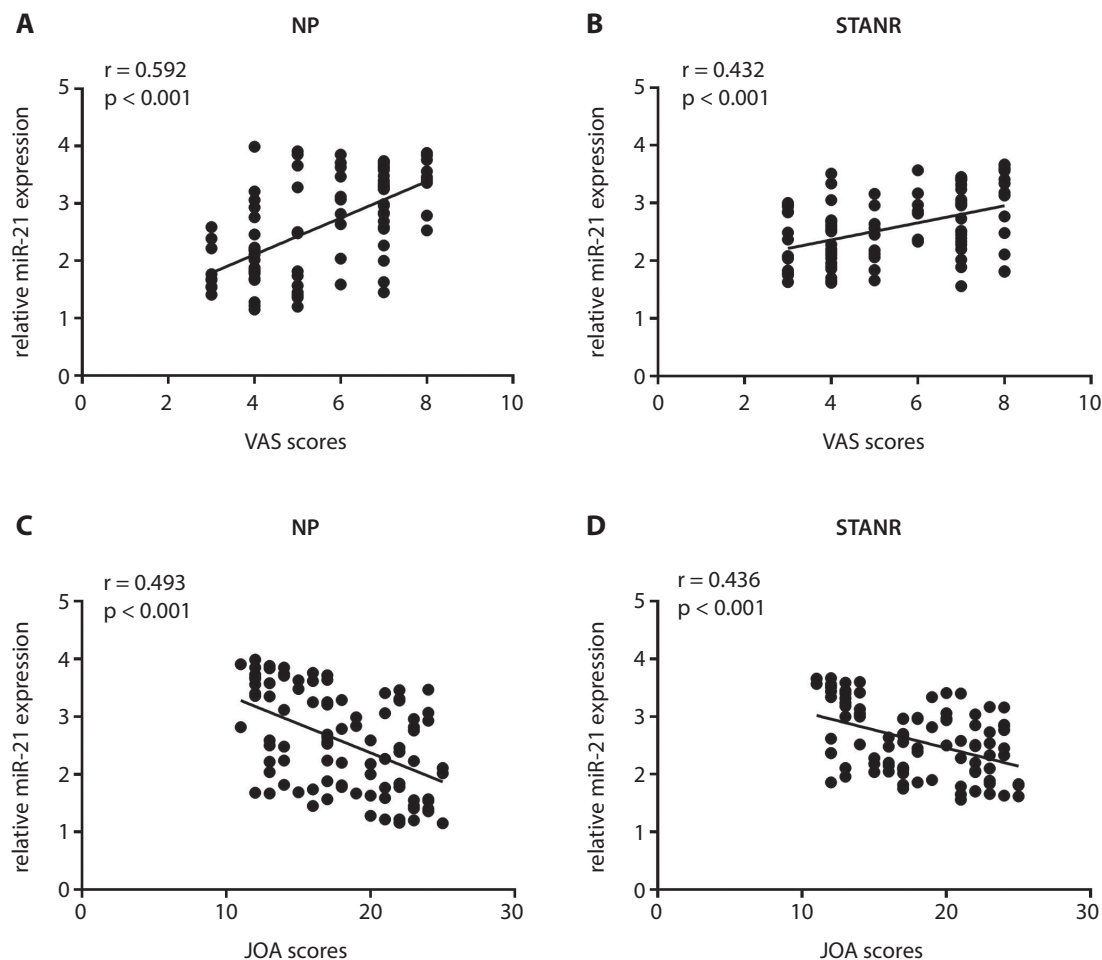
Fig. 3. A. Spearman's correlation analysis between nucleus pulposus (NP) miR-21 expressions and visual analogue scale (VAS) scores (n = 92); B. Spearman's correlation analysis between soft tissues around nerve root (STANR) miR-21 expression and VAS scores (n = 92); C. Spearman's correlation analysis between NP miR-21 expressions and Japanese Orthopedic Association (JOA) scores (n = 92); D. Spearman's correlation analysis of STANR miR-21 expression with JOA scores (n = 92)

compared to controls, and local miR-21 expressions were positively correlated with disease severity of LDH. Local interventions that target miR-21 and its related signaling in LDH patients require further study.

ORCID iDs

Zhen-Fei Zou https://orcid.org/0000-0002-5079-9389
Jing-Pei He https://orcid.org/0000-0003-2165-5308
Yan-Lian Chen https://orcid.org/0000-0001-7159-6807
Hai-Lin Chen https://orcid.org/0000-0001-5326-8842

References

1. Benzakour T, Igoumenou V, Mavrogenis AF, Benzakour A. Current concepts for lumbar disc herniation. *Int Orthop*. 2019;43(4):841–851. doi:10.1007/s00264-018-4247-6
2. Vialle LR, Vialle EN, Suárez Henao JE, Giraldo G. Lumbar disc herniation. *Rev Bras Ortop*. 2015;45(1):17–22. doi:10.1016/S2255-4971(15)30211-1
3. Douglas S. Sciatic pain and piriformis syndrome. *Nurse Pract*. 1997;22(5):166–168. PMID:9172241.
4. Kääriä S, Leino-Arjas P, Rahkonen O, Lahti J, Lahelma E, Laaksonen M. Risk factors of sciatic pain: A prospective study among middle-aged employees. *Eur J Pain*. 2011;15(6):584–590. doi:10.1016/j.ejpain.2010.11.008
5. Blamoutier A. Nerve root compression by lumbar disc herniation: A French discovery? *Orthop Traumatol Surg Res*. 2019;105(2):335–338. doi:10.1016/j.otsr.2018.10.025
6. Cosamalón-Gan I, Cosamalón-Gan T, Mattos-Piaggio G, Villar-Suárez V, García-Cosamalón J, Vega-Álvarez JA. Inflammation in the intervertebral disc herniation. *Neurocirugia (Astur : Engl Ed)*. 2021;32(1):21–35. doi:10.1016/j.neucir.2020.01.001

7. Park HW, Ahn SH, Kim SJ, et al. Changes in spinal cord expression of fractalkine and its receptor in a rat model of disc herniation by autologous nucleus pulposus. *Spine (Phila Pa 1976)*. 2011;36(12):E753–E760. doi:10.1097/BRS.0b013e3181ef610b
8. Palada V, Ahmed AS, Finn A, Berg S, Svensson CI, Kosek E. Characterization of neuroinflammation and periphery-to-CNS inflammatory crosstalk in patients with disc herniation and degenerative disc disease. *Brain Behav Immun*. 2019;75:60–71. doi:10.1016/j.bbi.2018.09.010
9. Cuéllar JM, Borges PM, Cuéllar VG, Yoo A, Scuderi GJ, Yeomans DC. Cytokine expression in the epidural space: A model of noncompressive disc herniation-induced inflammation. *Spine (Phila Pa 1976)*. 2013;38(1):17–23. doi:10.1097/BRS.0b013e3182604baa
10. Araldi E, Chamorro-Jorganes A, van Solingen C, Fernandez-Hernando C, Suarez Y. Therapeutic potential of modulating microRNAs in atherosclerotic vascular disease. *Curr Vasc Pharmacol*. 2013;13(3):291–304. PMID:26156264.
11. Ivey KN, Srivastava D. MicroRNAs as developmental regulators. *Cold Spring Harb Perspect Biol*. 2015;7(7):a008144. doi:10.1101/cshperspect.a008144
12. Economou EK, Oikonomou E, Siasos G, et al. The role of microRNAs in coronary artery disease: From pathophysiology to diagnosis and treatment. *Atherosclerosis*. 2015;241(2):624–633. doi:10.1016/j.atherosclerosis.2015.06.037
13. Slota JA, Booth SA. MicroRNAs in neuroinflammation: Implications in disease pathogenesis, biomarker discovery and therapeutic applications. *Noncoding RNA*. 2019;5(2):35. doi:10.3390/ncrna5020035
14. Li B, Dasgupta C, Huang L, Meng X, Zhang L. MiRNA-210 induces microglial activation and regulates microglia-mediated neuroinflammation in neonatal hypoxic-ischemic encephalopathy. *Cell Mol Immunol*. 2020;17(9):976–991. doi:10.1038/s41423-019-0257-6
15. Li YY, Cui JG, Dua P, Pogue AI, Bhattacharjee S, Lukiw WJ. Differential expression of miRNA-146a-regulated inflammatory genes in human primary neural, astroglial and microglial cells. *Neurosci Lett*. 2011;499(2):109–113. doi:10.1016/j.neulet.2011.05.044

16. Makeyev EV, Zhang J, Carrasco MA, Maniatis T. The microRNA miR-124 promotes neuronal differentiation by triggering brain-specific alternative pre-mRNA splicing. *Mol Cell*. 2007;27(3):435–448. doi:10.1016/j.molcel.2007.07.015

17. Moen A, Jacobsen D, Phuyal S, et al. MicroRNA-223 demonstrated experimentally in exosome-like vesicles is associated with decreased risk of persistent pain after lumbar disc herniation. *J Transl Med*. 2017;15(1):89. doi:10.1186/s12967-017-1194-8

18. Hasvik E, Schjølberg T, Jacobsen DP, et al. Up-regulation of circulating microRNA-17 is associated with lumbar radicular pain following disc herniation. *Arthritis Res Ther*. 2019;21(1):186. doi:10.1186/s13075-019-1967-y

19. Zhang Y, Liu HL, An LJ, et al. miR-124-3p attenuates neuropathic pain induced by chronic sciatic nerve injury in rats via targeting EZH2. *J Cell Biochem*. 2019;120(4):5747–5755. doi:10.1002/jcb.27861

20. Sheedy FJ. Turning 21: Induction of miR-21 as a key switch in the inflammatory response. *Front Immunol*. 2015;6:19. doi:10.3389/fimmu.2015.00019

21. Sakai A, Suzuki H. Nerve injury-induced upregulation of miR-21 in the primary sensory neurons contributes to neuropathic pain in rats. *Biochem Biophys Res Commun*. 2013;435(2):176–181. doi:10.1016/j.bbrc.2013.04.089

22. Malcangio M. Role of the immune system in neuropathic pain. *Scand J Pain*. 2019;20(1):33–37. doi:10.1515/sjpain-2019-0138

23. Sun C, Tian J, Liu X, Guan G. MiR-21 promotes fibrosis and hypertrophy of ligamentum flavum in lumbar spinal canal stenosis by activating IL-6 expression. *Biochem Biophys Res Commun*. 2017;490(3):1106–1111. doi:10.1016/j.bbrc.2017.06.182

24. Kobayashi S, Meir A, Kokubo Y, et al. Ultrastructural analysis on lumbar disc herniation using surgical specimens: Role of neovascularization and macrophages in hernias. *Spine (Phila Pa 1976)*. 2009;34(7):655–662. doi:10.1097/BRS.0b013e31819c9d5b

25. Djuric N, Yang X, El Barzouhi A, et al. Lumbar disc extrusions reduce faster than bulging discs due to an active role of macrophages in sciatica. *Acta Neurochir*. 2020;162:79–85. doi:10.1007/s00701-019-04117-7

26. Woertgen C, Rothoerl RD, Brawanski A. Influence of macrophage infiltration of herniated lumbar disc tissue on outcome after lumbar disc surgery. *Spine (Phila Pa 1976)*. 2000;25(7):871–875. doi:10.1097/00007632-200004010-00017

27. Sahraei M, Chaube B, Liu Y, et al. Suppressing miR-21 activity in tumor-associated macrophages promotes an antitumor immune response. *J Clin Invest*. 2019;129(12):5518–5536. doi:10.1172/JCI127125

28. Qu S, Shen Y, Wang M, Wang X, Yang Y. Suppression of miR-21 and miR-155 of macrophage by cinnamaldehyde ameliorates ulcerative colitis. *Int Immunopharmacol*. 2019;67:22–34. doi:10.1016/j.intimp.2018.11.045

29. Pfirrmann CW, Dora C, Schmid MR, Zanetti M, Hodler J, Boos N. MR image-based grading of lumbar nerve root compromise due to disk herniation: Reliability study with surgical correlation. *Radiology*. 2004;230(2):583–588. doi:10.1148/radiol.2302021289

30. Landis JR, Koch GG. The measurement of observer agreement for categorical data. *Biometrics*. 1977;33(1):159–174. PMID:843571.

31. Heller GZ, Manuguerra M, Chow R. How to analyze the Visual Analogue Scale: Myths, truths and clinical relevance. *Scand J Pain*. 2016;13:67–75. doi:10.1016/j.sjpain.2016.06.012

32. Fujiwara A, Kobayashi N, Saiki K, Kitagawa T, Tamai K, Saotome K. Association of the Japanese Orthopaedic Association score with the Oswestry Disability Index, Roland–Morris Disability Questionnaire, and short-form 36. *Spine (Phila Pa 1976)*. 2003;28(14):1601–1607. PMID:12865852.

33. Marketos SG, Skiadas P. Hippocrates: The father of spine surgery. *Spine (Phila Pa 1976)*. 1999;24(13):1381–1387. doi:10.1097/00007632-199907010-00018

34. Finnerup NB, Kuner R, Jensen TS. Neuropathic pain: From mechanisms to treatment. *Physiol Rev*. 2021;101(1):259–301. doi:10.1152/physrev.00045.2019

35. Descalzi G, Ikegami D, Ushijima T, Nestler EJ, Zachariou V, Narita M. Epigenetic mechanisms of chronic pain. *Trends Neurosci*. 2015;38(4):237–246. doi:10.1016/j.tins.2015.02.001

36. Ueda H, Uchida H. Epigenetic modification in neuropathic pain. *Curr Pharm Des*. 2015;21(7):849–867. doi:10.2174/1381612820666141027113923

37. Piletič K, Kunej T. MicroRNA epigenetic signatures in human disease. *Arch Toxicol*. 2016;90(10):2405–2419. doi:10.1007/s00204-016-1815-7

38. McCarron RF, Wimpee MW, Hudkins PG, Laros GS. The inflammatory effect of nucleus pulposus: A possible element in the pathogenesis of low-back pain. *Spine (Phila Pa 1976)*. 1987;12(8):760–764. doi:10.1097/00007632-198710000-00009

39. Olmarker K, Blomquist J, Strömberg J, Nannmark U, Thomsen P, Rydevik B. Inflammatogenic properties of nucleus pulposus. *Spine (Phila Pa 1976)*. 1995;20(6):665–669. doi:10.1097/00007632-199503150-00006

40. Yabuki S, Kikuchi S, Olmarker K, Myers RR. Acute effects of nucleus pulposus on blood flow and endoneurial fluid pressure in rat dorsal root ganglia. *Spine (Phila Pa 1976)*. 1998;23(23):2517–2523. doi:10.1097/00007632-199812010-00006

41. Simeoli R, Montague K, Jones HR, et al. Exosomal cargo including microRNA regulates sensory neuron to macrophage communication after nerve trauma. *Nat Commun*. 2017;8(1):1778. doi:10.1038/s41467-017-01841-5

Clinical characteristics and survival analysis of patients with hepatocellular carcinoma after hepatitis B virus turning negative

Hong Li[1,A–F], Wen-Min Guo[2,A,C–F], Qian Xie[3,A–F], Xiu Sun[4,B], Qiong Wang[5,B]

[1] Department of Infectious Diseases, Shunde Hospital of Southern Medical University, Foshan, China

[2] Department of Infectious Diseases, The First Hospital of Shanxi Medical University, Taiyuan, China

[3] ECG Room, Shanxi Cardiovascular Research Institute, Taiyuan, China

[4] Hepatology Department, Ditan Hospital of Capital Medical University, Beijing, China

[5] Department of Infectious Diseases, Weinan Central Hospital, China

A – research concept and design; B – collection and/or assembly of data; C – data analysis and interpretation;
D – writing the article; E – critical revision of the article; F – final approval of the article

Address for correspondence
Hong Li
E-mail: HongL2021@126.com

Abstract

Background. Hepatitis B virus (HBV) infection is one of the most common infections, affecting 248 million people worldwide. Hepatitis B virus can progress to cirrhosis, liver failure and hepatocellular carcinoma (HCC).

Objectives. To analyze the clinical characteristics and survival time of HCC occurrence in patients with HBV infection after virus turning negative.

Materials and methods. The Kaplan–Meier and log rank survival analysis were performed to compare the overall survival (OS) of the patients with HCC in different groups.

Results. The 1-, 3- and 5-year OS rates of the 104 investigated patients were 76.4%, 54.4% and 20.5%, respectively. The median survival time was 37 months. The median survival time of HBV-DNA-negative group was longer than that of the HBV-DNA-positive group (negative compared to positive: 42 compared to 36, p = 0.003). The 5-year OS rate of patients receiving antiviral therapy before HCC diagnosis in the HBV-DNA-negative group was higher than that in the HBV-DNA-positive group (negative compared to positive: 53.0% compared to 0%, p = 0.022). There was no significant difference in the 5-year OS rate in patients who did not receive antiviral therapy before HCC diagnosis between HBV-DNA-negative and HBV-DNA-positive groups (p = 0.195).

Conclusions. Among HBV-infected patients, a significant proportion of virus-negative patients develop liver cancer and require long-term continuous monitoring. A long-term effective antiviral therapy can improve the survival rate of patients with liver cancer. This study revealed important clinical characteristics of HCC patients and provided useful information for their clinical management and monitoring.

Key words: HBV-DNA, hepatocellular carcinoma (HCC), hepatitis B virus (HBV), survival rate

732

H. Li et al. HCC and hepatitis B virus negative

Background

Hepatitis B virus (HBV) infection is one of the most common infections, affecting 248 million people worldwide.[1] Hepatitis B virus causes chronic infection in patients and can lead to cirrhosis, hepatocellular carcinoma (HCC) and other serious liver diseases.[2] Primary liver cancer is the 5th most frequent cancer and the 2nd main reason of cancer death worldwide.[3,4] The main pathological types of primary liver cancer include HCC, intrahepatic cholangiocarcinoma (ICC) and hepatocellular carcinoma combined with cholangiocarcinoma (CHCC-CC).[5] Hepatocellular carcinoma accounts for more than 90% of primary liver cancer cases, and in China, more than 90% of patients suffering from primary liver cancer die from HCC each year, which is associated with a rising rate of annual HBV infection.[6,7] In addition, genetic conditions leading to chronic liver disease, such as hemochromatosis and alpha-1 antitrypsin deficiency, also increase the risk of HCC.[8] Hepatocellular carcinoma occurs mainly in the context of cirrhosis, hepatitis B or C virus infection or nonalcoholic steatohepatitis.[9] Hepatocellular carcinoma is the most rapidly rising cause of cancer-related deaths in developed countries and is anticipated to increase further.[9,10] Chronic HBV or hepatitis C virus (HCV) infection are the most common causes of HCC,[9–11] accounting for 78.5% of HCC-related deaths worldwide in 2013.[3] It is a global public health threat that causes considerable liver-related morbidity and mortality.[12]

So far, serum HBV-DNA level has become a major marker for monitoring virus replication and evaluating the efficacy of antiviral therapy in patients with chronic HBV infection.[13] In clinical practice, HBV replication can be assessed by viral DNA load.[14] A study has proven that the excessive degree of HBV-DNA is an independent threat component for the occurrence of HCC.[15] Another study showed that when HBV-DNA stages were less than 2000 IU/mL, the chance of HCC remained, with an annual incidence of 0.06%.[16] However, it is still unknown how the clinical features and survival rates of HCC in HBV-infected individuals differ from those in HBV-negative patients. The prognosis of patients with liver cancer has been very poor, with a 5-year survival rate of less than 20%.[17] However, there is little data on the survival trends in HCC patients for whom the HBV was tested negative.

Objectives

The aim of this study was to analyze the traits and survival time of HCC occurrence in patients with HBV infection after HBV turning negative.

Materials and methods

Ethical approval

All patients signed informed consent. The study protocol was in line with the ethics guidelines of the Declaration of Helsinki and approved by the local ethics committee of the First Hospital of Shanxi Medical University (approval No. K028).

Patients

All patients with HCC caused by HBV infection diagnosed at the Department of Infectious Diseases of the First Hospital of Shanxi Medical University from June 2014 to June 2017 were included. During diagnosis of HCC, according to the titer of HBV-DNA, the patients were divided into 2 groups: HBV-DNA-negative group and HBV-DNA-positive group.

Inclusion and exclusion criteria

All patients met the following inclusion criteria: HBV infection and diagnosis in accordance to the Chronic Hepatitis B Prevention and Control Guidelines (2015 Edition).[18] Hepatocellular carcinoma was diagnosed in accordance to the Guidelines for Diagnosis and Treatment of Primary Liver Cancer in China (2017).[19] Exclusion criteria were as follows: patients coinfected with different viruses, including HCV, hepatitis D virus (HDV) or human immunodeficiency virus (HIV), and patients with different liver diseases, including alcohol-related or non-alcohol-related liver disease, autoimmune liver disease, drug-induced liver diseases, and other factors.

Follow-up

Until June 30, 2017, all hospitals followed up the patients using both passive and active approaches, with active follow-up by telephone every 3 months. In addition, hospital staff linked patient records to local population-based cancer registry data, which provided the information on their survival. The survival time of the patients was calculated starting from the date of HCC diagnosis to the last follow-up date, and the survival time of the patients who had already died was calculated from the date of HCC diagnosis to the patient's death.

Data collection

Patients were directly questioned and the past medical records were collected and thoroughly analyzed for the diagnosis of HCC, including the following: 1) general information: gender, age, history of diseases, personal history, family history, etc.; 2) laboratory examination: HBV-DNA, hepatitis B serologic test, platelet (PLT) count test,

serum alanine aminotransferase (ALT), serum albumin (ALB), total bilirubin (TBIL), alpha-fetoprotein (AFP), etc.; 3) other data: use of antiviral drugs, survival rate after HCC diagnosis, etc.

Statistical analyses

Statistical evaluation was carried out with the use of SPSS (v. 26.0; IBM Corp., Armonk, USA) and Stata (v. 12.0; Stata-Corp LLC, College Station, USA) software. The 1-, 3- and 5-year overall survival (OS) rates and median survival time were analyzed using the Kaplan–Meier method. The differences between the survival curves were analyzed using the log rank test. Two-sided values of $p < 0.05$ were considered statistically significant.

Results

Baseline data of liver cancer patients investigated

A total of 104 individuals were recruited in this study, including 61 patients in HBV-DNA-negative group and 43 patients in HBV-DNA-positive group. The age of patients in the HBV-DNA-negative group, which consisted of 48 (78.69%) males and 13 (21.31%) females, was between 50 and 63 years, with a median of 62 years. According to the data, 18 (29.51%) patients were smokers, 8 (13.11%) patients had diabetes and there were 15 (24.59%) patients with HBV family history. Also, 47 (77.05%) patients were diagnosed with HCC complicated with cirrhosis; 43 (70.49%) patients had received antiviral therapy before HCC diagnosis; 35 (57.38%) patients had normal body mass index (BMI) (18.5–23.0 kg/m²). As for the HBV-DNA-positive group, including 31 (72.09%) males and 12 (27.91%) females, the patients ranged in age from 43 to 62 years, with a median of 52 years. In this group, 13 (30.23%) patients were smokers, 4 (9.30%) patients had diabetes and there were 14 (32.56%) individuals with HBV family history. Also, 40 (93.02%) patients were complicated with cirrhosis, 11 (25.58%) patients had received antiviral therapy before HCC diagnosis and 25 (58.14%) individuals had normal BMI (18.5–23.0 kg/m²). Compared with HBV-DNA-positive group, patients in the HBV-DNA-negative group had lower proportion of liver cirrhosis (77.05% compared to 93.02%, $p = 0.034$) and higher proportion of receiving antiviral therapy (70.49% compared to 25.58%, $p < 0.001$) (Table 1).

With regard to results obtained from hepatitis B serologic test, the difference in hepatitis B e-antigen (HBeAg)/ hepatitis B e-antibody (HBeAb) between the HBV-DNA-negative group and the HBV-DNA-positive group was statistically significant ($p = 0.021$). Moreover, the proportion of HBeAg (+)/HBeAb (–) was lower (16.39% compared to 34.88%), and the proportion of HBeAg (+)/HBeAb (–) was higher (31.15% compared to 11.63%) in the HBV-DNA-negative group than

that in the HBV-DNA-positive group, while the proportion of HBeAg (+)/HBeAb (–) was almost the same (52.46% compared to 53.49%) in these 2 groups. The other measurements also showed that the proportion of patients with normal ALT level (<40 U/L) in the HBV-DNA-negative group was higher than that in the HBV-DNA-positive group (55.74% compared to 27.91%, $p = 0.017$). There was no statistically significant distinction between 2 groups regarding TBIL ($p = 0.181$) and ALB ($p = 0.065$) levels. In PLT comparison, the proportion of people with normal PLT level (100–300 × 10⁹/L) in the HBV-DNA-negative group was lower than that in the HBV-DNA-positive group (49.18% compared to 60.47%). However, the difference between the 2 groups regarding AFP was not statistically significant ($p = 0.128$). The details of the analysis are presented in Table 1.

Survival and univariate analysis

At the end of the follow-up period, there were 35 deaths due to liver cancer, 1 patient survived for more than 5 years and the median survival time was 37 months (95% confidence interval (95% CI): [32.13; 41.87]). The 1-, 3- and 5-year survival rates after the HCC diagnosis were 76.4%, 54.4% and 20.5%, respectively (Fig. 1A). In the HBV-DNA-negative group, there were 15 liver cancer deaths, median survival time was 42 months (95% CI: [31.19; 52.81]), and 1-, 3-, and 5-year survival rates after the HCC diagnosis were 84.9%, 64.6% and 15.9%, respectively. However, in the HBV-DNA-positive group, the median survival time was 36 months (95% CI: [11.68; 60.32]) and the 1-, 3- and 5-year survival rates after the HCC diagnosis were 64.2%, 40.3% and 0%, respectively. The survival rate of HBV-DNA-negative group was higher than that of HBV-DNA-positive group, and the difference was statistically significant ($\chi^2 = 8.864$; $p = 0.003$; Fig. 1B). A further analysis of the patients who acquired antiviral remedy before the HCC diagnosis confirmed that 1-, 3- and 5-year survival rates were 87.0%, 66.3% and 53.0% in the HBV-DNA-negative group and 58.9%, 29.5% and 0% in the HBV-DNA-positive group, respectively. There was a substantial distinction in the survival rate between the 2 groups ($\chi^2 = 5.285$; $p = 0.022$; Fig. 1C). For patients with no antiviral therapy before the HCC diagnosis in the HBV-DNA-negative and the HBV-DNA-positive groups, 1-, 3- and 5-year survival rates were 75.0%, 56.3% and 0%, and 66.9%, 31.8% and 0%, respectively. There was no large difference in survival rates ($\chi^2 = 1.679$; $p = 0.195$), but the survival rate of the HBV-DNA-negative group was relatively high (Fig. 1D).

Relationship between antiviral therapy and survival time

The median survival time of patients receiving antiviral therapy before the HCC diagnosis was 42 (95% CI: [33.93; 50.07]) months, and that of patients without antiviral

Table 1. Baseline data of 104 patients with liver cancer

Characteristics	HBV-DNA-negative patients n (%)	HBV-DNA-positive patients n (%)	p-value*
Total number of cases	61 (100)	43 (100)	–
Gender Male Female	 48 (78.69) 13 (21.31)	 31 (72.09) 12 (27.91)	0.438
Age [years] ≤44 45–54 55–64 65–74 ≥75	 3 (4.92) 22 (36.07) 23 (37.70) 11 (18.03) 2 (3.28)	 14 (32.56) 11 (25.58) 11 (25.58) 5 (11.63) 2 (4.65)	0.045
Smoking status Never-smoker Smoker	 43 (70.49) 18 (29.51)	 30 (69.77) 13 (30.23)	0.937
Diabetes Absent Present	 53 (86.89) 8 (13.11)	 39 (90.70) 4 (9.30)	0.757
Family history of HBV Absent Present	 46 (73.41) 15 (24.59)	 29 (67.44) 14 (32.56)	0.372
Liver cirrhosis Absent Present	 14 (22.95) 47 (77.05)	 3 (6.98) 40 (93.02)	0.034
Antiviral treatment Absent Present	 18 (29.51) 43 (70.49)	 32 (74.42) 11 (25.58)	<0.001
BMI [kg/m²] <18.5 18.5–23.0 ≥23.0	 3 (4.92) 35 (57.38) 23 (37.70)	 3 (6.98) 25 (58.14) 15 (34.88)	0.905
HBsAg <225 ≥225	 33 (54.10) 28 (45.90)	 19 (44.19) 24 (55.81)	0.319

Characteristics	HBV-DNA-negative patients n (%)	HBV-DNA-positive patients n (%)	p-value*
HBeAg/HBeAb (+)/(−) (−)/(−) (−)/(+)	 10 (16.39) 19 (31.15) 32 (52.46)	 15 (34.88) 5 (11.63) 23 (53.49)	0.021
HBcAb <45 ≥45	 37 (60.66) 24 (39.34)	 23 (53.49) 20 (46.51)	0.466
PLT [10⁹/L] <100 100–300 >300	 31 (50.82) 30 (49.18) 0 (0.00)	 15 (34.88) 26 (60.47) 2 (4.65)	0.021
ALT [U/L] <40 40–80 81–120 >120	 34 (55.74) 17 (27.86) 5 (8.20) 5 (8.20)	 12 (27.91) 19 (44.19) 5 (11.62) 7 (16.28)	0.017
TBIL [µmol/L] <17.1 17.1–34.2 >34.2 35–55	 18 (29.51) 24 (39.34) 19 (31.15) 41 (67.21)	 5 (11.63) 23 (53.49) 15 (34.88) 23 (53.49)	0.181
ALB [g/L] <35 35–55	 20 (32.79) 41 (67.21)	 20 (46.51) 23 (53.49)	0.065
AFP [ng/mL] ≤20 20–400 ≥400	 27 (44.26) 13 (21.31) 21 (34.43)	 14 (32.56) 17 (39.53) 12 (27.91)	0.128

HBV – hepatitis B virus; HBsAg – hepatitis B surface antigen; HBeAg – hepatitis B e-antigen; HBeAb – hepatitis B e-antibody; HBcAb – hepatitis B core antibody; BMI – body mass index; PLT – platelets; ALT – alanine aminotransferase; TBIL – total bilirubin; ALB – albumin; AFP – alpha-fetoprotein; *Student's t-test was used for continuous variables and χ^2 test was used for categorical variables.

therapy was 31 (95% CI: [24.74; 37.26]) months. The 1-, 3- and 5-year survival rates for both groups were 81.4%, 58.5% and 19.5%, and 70.6%, 29.6% and 0%, respectively. There was no significant difference between the survival rates of the 2 groups (χ^2 = 2.885; p = 0.089) (Fig. 2A). In addition, there was no large difference between the survival rate of patients treated with sustained antiviral for more than 2 years and those treated with antiviral therapy for less than 2 years (χ^2 = 0.454; p = 0.500) (Fig. 2B). However, patients who underwent antiviral treatment for more than 2 years before the diagnosis of HCC experienced a higher 3- and 5-year survival rates than patients without the treatment (66.3% and 39.8% compared to 31.5% and 0%, respectively).

Discussion

In recent years, with the emergence of nucleotides and their analogues, the clinical prognosis of HBV-associated end-stage liver disease has significantly improved. However, some patients still develop HCC after viral negative transformation, suggesting that the inhibition of viral replication and liver inflammation alone cannot eliminate HCC. This study collected and compared the characteristics of HBV-related HCC patients at diagnosis and after turning positive or negative, in order to provide the scientific evidence for the occurrence and clinical regularity of HCC after HBV infection. Up to now, the therapy of HCC has involved mainly surgical treatments, antiviral therapy and a few other methods. Patients with HBV-associated HCC have significantly improved survival rates when the combination therapy model is employed.

In this study, 83.65% of individuals were diagnosed with cirrhosis complicated with HCC, which was consistent with the data from the previous research stating that cirrhosis is a high risk factor for HEB complicated with HCC.[20,21] This study discovered that the percentage of patients with cirrhosis was considerably different between HBV-DNA-positive group and HBV-DNA-negative group, and the percentage of patients with cirrhosis was lower in the HBV-DNA-negative group. Therefore, some HBV-DNA-negative patients with chronic HEB will develop
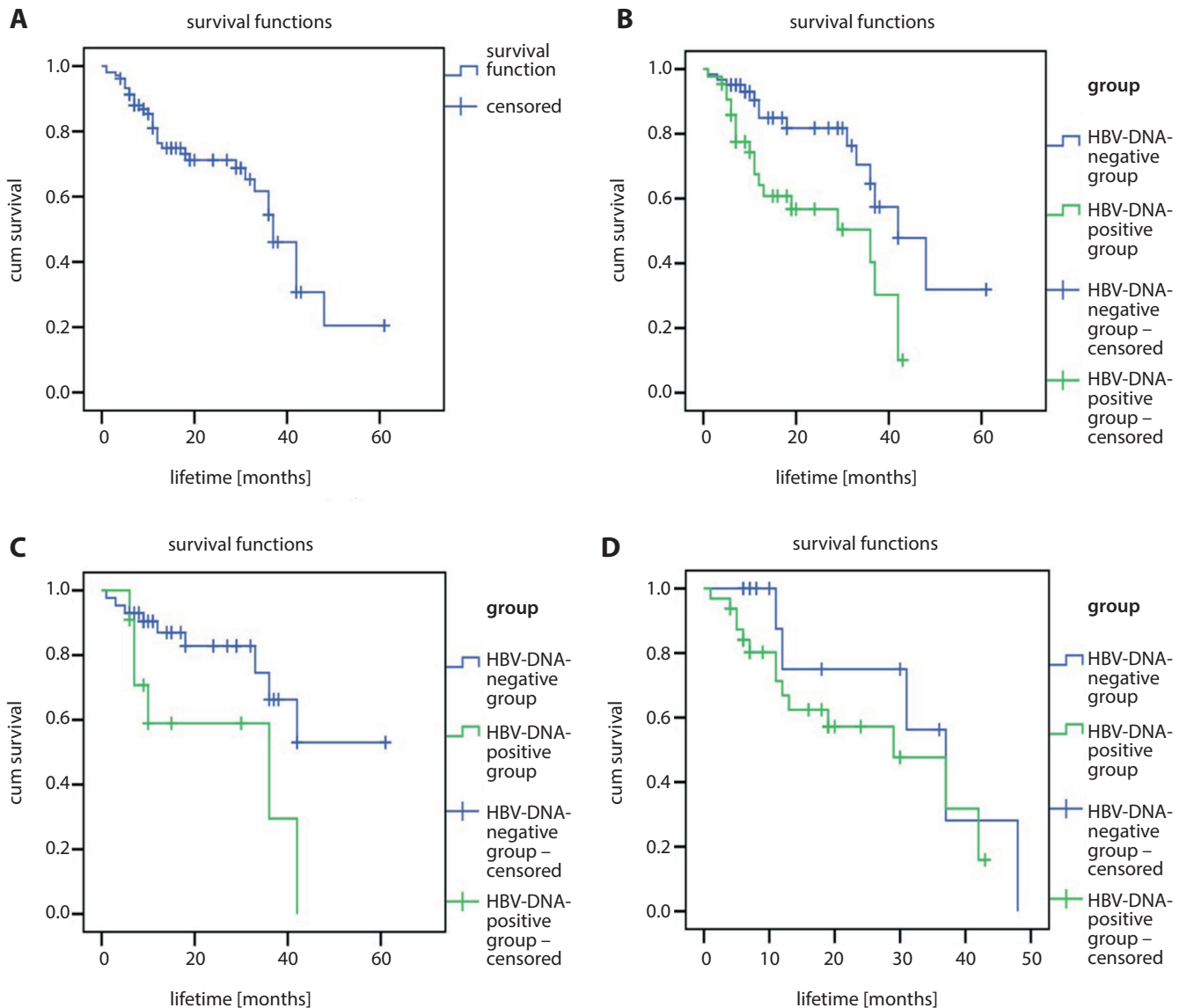
Fig. 1. Survival analysis curve. A. Overall survival curve; B. Survival curves of the hepatitis B virus (HBV)-DNA negative group and HBV-DNA-positive group; C. Survival curves of HBV-DNA-negative group and HBV-DNA-positive group with antiviral treatment; D. Survival curves of HBV-DNA-negative group and HBV-DNA-positive group without antiviral treatment

HCC even if it does not progress to liver cirrhosis. In this regard, we hypothesized that some HBV-DNA-negative patients had received a long-term antiviral therapy before progressing to cirrhosis, and that antiviral treatment can improve or reverse liver fibrosis and cirrhosis. A study has shown that entecavir (ETV) could significantly improve or reverse hepatic fibrosis or cirrhosis in HBeAg-negative or HBeAg-positive individuals, and the Ishak fibrosis scores improved by 88%.[22] Lok have collected and analyzed the results of nucleotide analogues (NAs) that were observed for more than 10 years.[23] They found that 1 year of NAs treatment reduced liver inflammation in 50~70% of chronic hepatitis B (CHB) patients. After 3–5 years of long-term treatment, fibrosis and cirrhosis could be resolved in most patients.

Antiviral remedy is the key to deal with chronic HBV infection. Effective antiviral remedy can lengthen the survival time of patients with liver cancer. Long-term research on lamivudine (LAM) and adefovir (ADV) has proven that antiviral remedy reduces the occurrence of HCC in patients with chronic HBV infection.[24] A multicenter study in Taiwan additionally confirmed that 4-year ETV treatment appreciably reduced the danger of liver cancer, cirrhosis events and mortality in patients with hepatic B-associated cirrhosis, with a 60% reduction of the threat of liver cancer as compared to the non-antiviral group.[25] A retrospective study in 632 patients with hepatitis-associated liver cancer found that the 2-year survival rate of patients with hepatitis-associated liver cancer before and after antiviral remedy was significantly greater than that of patients without antiviral therapy ($\chi^2 = 33.792$; $p = 0.000$, $\chi^2 = 33.179$; $p = 0.000$).[26] Therefore, antiviral remedy before and after HCC diagnosis is beneficial. In our study, 43 HBV-DNA-negative and 11 HBV-DNA-positive
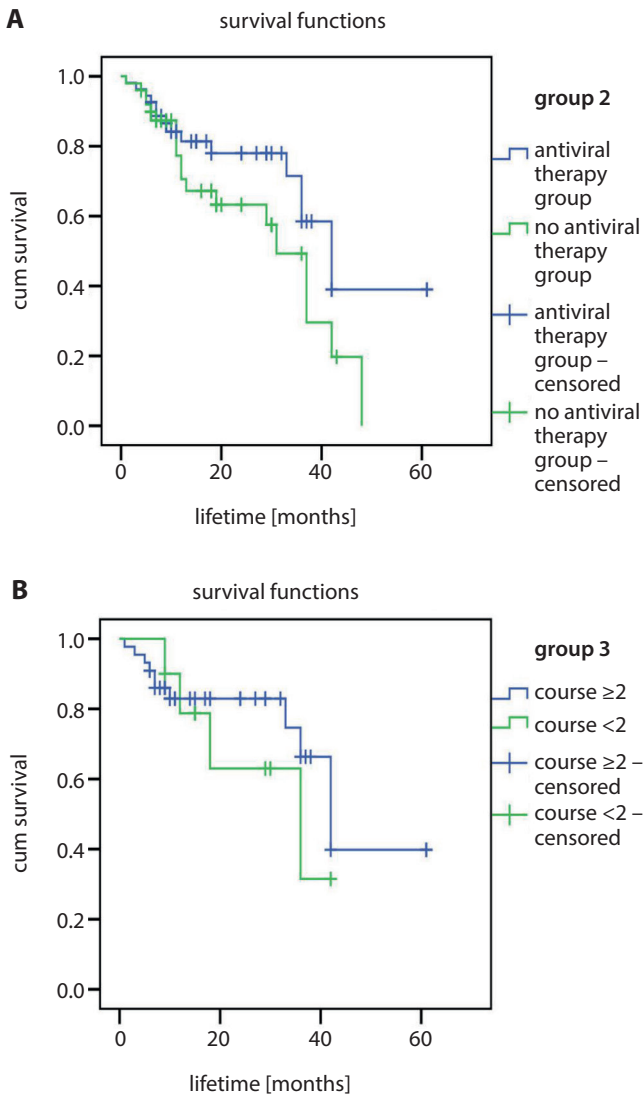
Fig. 2. Relationship between antiviral therapy and survival time.
A. Survival curves of patients with antiviral and no antiviral therapy;
B. Survival curves of patients with antiviral course ≥2 years and <2 years

patients received effective antiviral therapy. The remaining 32 individuals who did not obtain antiviral cure developed liver cancer. This was constant with the study by Choi et al. stating that not receiving effective antiviral treatment is an independent cause of HCC in patients with hepatic B cirrhosis.[27] In addition, there was no significant difference in 1-, 3- and 5-year survival rates between patients who were administered antiviral remedy before diagnosis and those who did not (χ^2 = 2.885; p = 0.089). This may be associated with the older age of patients in the antiviral remedy group at the time of HCC diagnosis, different treatment measures taken after HCC diagnosis and the application of antiviral drugs.

Different researchers have different views on the relationship between HBeAg and HCC. In an 8-year prospective follow-up study of 18,154 HBeAg-positive patients in Taiwan, these patients were found to have a relatively high risk of liver cancer, which was 6 to 7 times higher than

in the HBeAg-negative patients.[28] Zhou et al. determined that there was no significant difference between the incidence of HCC and serum E-antigen positivity in patients with chronic HBV infection.[29] Another study reported an even higher risk of HCC in HBeAg-negative patients.[30] In our study, HBeAg-negative patients accounted for a large proportion of the whole study population. Compared with the HBV-DNA-positive group, HBeAg+/HBeAb− ratio was lower and HBeAg−/HBeAb− ratio was higher in the HBV-DNA-negative group. We speculated that this was related to a long-term antiviral remedy in the HBV-DNA-negative group. Some patients were negative for HBeAg after treatment, but no serological changes of HBeAg were observed. This does not rule out the possibility that some HBeAg-negative patients with chronic HBV are tested negative right now, but were HBV-DNA-positive before undergoing antiviral treatment, mainly due to mutations in anterior C and BCP regions of the virus strain during the immune clearance period.[31] After a long-term antiviral therapy, the expression of the mutated HBeAg was highly reduced and HBV-DNA became negative. Whether it is necessary to further define the HBeAg and HBeAb of patients before antiviral treatment needs to be further examined.

Watanabe et al. found that the PLT level was related to the improvement in patients with HBV-associated HCC, and low PLT level was an independent indicator of the possible occurrence of HCC.[32] A study has shown that the peripheral blood PLT count of HBV-associated HCC patients is different and dynamic.[33] The peripheral blood PLT count of patients with early HCC was considerably lower than that of patients with advanced HCC. Some scholars believe that HCC can synthesize PLT biotin, which can cause paraneoplastic PLT hyperplasia. The larger the tumor size, the more often the synthesis of bopoietin and the higher the peripheral blood PLT count.[34] In this study, HBV-DNA-negative patients had lower PLT levels than HBV-DNA-positive ones. This may be associated with the greater number of HBV-DNA-negative patients receiving antiviral therapy and regular follow-up. Most patients in the HBV-DNA-positive group were diagnosed with advanced HCC, resulting in PLT accompanied by paracancerous hyperplasia.

In our study, the serum ALT level was decreased in the HBV-DNA-negative group, which may be associated with the higher percentage of antiviral treatment in the HBV-DNA-negative group. Antiviral remedy can enhance liver inflammation. Consistent with the results obtained by Furman et al., serum ALT levels were lower in HCC patients with negative HBV-DNA during medium and long-term NAs treatment than in HCC patients with positive HBV-DNA.[35]

With the global implementation of infant HBV vaccination programs, the incidence of HBV virus infection in birth cohorts has gradually declined. However, due to the long incubation period of HBV infection, an immense percentage of patients with chronic HBV infection develop HCC or even die. In 2009, Nguyen et al. found that the prognosis

of HBV-related HCC was very poor, the median survival time was less than 16 months, and the 1-, 3- and 5-year survival rates were 36–67%, 10–56% and 15–26%, respectively.[36] In this study, the median survival time of HCC patients was 37 months, and the 1-, 3- and 5-year survival rates were 76.4%, 54.4% and 20.5%, respectively.

The HBV-DNA stages (negative or positive) are also associated with the prognosis of HBV-associated HCC patients. One study has proven that the 2-year survival rate of HBV-DNA-negative group is higher than that of HBV-DNA-positive group (p = 0.007).[37] Stratified evaluation confirmed that HBV-DNA was associated with survival rate, and the difference between the 500 IU/mL HBV-DNA group and the 105 IU/mL HBV-DNA group was statistically significant (p = 0.009), suggesting that the higher the baseline HBV-DNA level, the lower the survival rate and the worse the prognosis after the HCC diagnosis. In this study, there was a significant distinction in the survival rate between HBV-DNA-negative and HBV-DNA-positive group (χ^2 = 8.846; p = 0.003). Similarly to previous studies, patients in the HBV-DNA-negative group survived longer. The difference between the 2 groups may be related to HBV reactivation (PHR) after liver cancer treatment. One of the risk factors for the recurrence of liver cancer is HBV activation.[26] The occurrence of PHR may be related to surgical resection and interventional therapy of HCC. Lao et al. found a PHR risk after hepatectomy or transarterial chemoembolization (TACE).[38] Preoperative HBV-DNA level, hepatic blood flow, degree of cirrhosis, and other factors are related to PHR, even if the preoperative HBV-DNA titer is less than 500 copies/mL, there is still a risk of postoperative virus infection. Lai and Yuen also conducted a similar study.[24] The HBV-associated HCC patients with negative HBV-DNA were at risk of hepatitis B reactivation after TACE, and PHR could further damage liver function and affect the prognosis of a patient. A further analysis of the individuals treated with antiviral therapy before HCC showed that the HBV-DNA-negative group had longer survival time and higher survival rate than the HBV-DNA-positive group, which was related to the dual effect of antiviral remedy and the negative HBV-DNA.

Limitations

The sample size of our study was relatively small, and further multicenter studies with large sample size are needed to confirm the outcomes of the study.

Conclusions

In summary, HBV-infected patients are at hazard of developing HCC even after turning virus-negative. When diagnosed with HCC, most patients have received long-term and effective antiviral therapy, thus decreasing the degree of cirrhosis, which indicates that antiviral therapy is one of the effective means for the remedy of liver cancer. At the same time, continuous monitoring of the disease is necessary to achieve early detection, diagnosis and therapy of HCC.

ORCID iDs

Hong Li https://orcid.org/0000-0002-7425-8309

References

1. Schweitzer A, Horn J, Mikolajczyk RT, Krause G, Ott JJ. Estimations of worldwide prevalence of chronic hepatitis B virus infection: A systematic review of data published between 1965 and 2013. *Lancet.* 2015;386(10003):1546–1555. doi:10.1016/S0140-6736(15)61412-X
2. Wu CC, Chen YS, Cao L, Chen XW, Lu MJ. Hepatitis B virus infection: Defective surface antigen expression and pathogenesis. *World J Gastroenterol.* 2018;24(31):3488–3499. doi:10.3748/wjg.v24.i31.3488
3. GBD 2013 Mortality and Causes of Death Collaborators. Global, regional, and national age-sex specific all-cause and cause-specific mortality for 240 causes of death, 1990–2013: A systematic analysis for the Global Burden of Disease Study 2013. *Lancet.* 2015;385(9963):117–171. doi:10.1016/S0140-6736(14)61682-2
4. Fitzmaurice C, Dicker D, Pain A, et al.; Global Burden of Disease Cancer Collaboration. The Global Burden of Cancer 2013. *JAMA Oncol.* 2015;1(4):505–527. doi:10.1001/jamaoncol.2015.0735
5. Gao YX, Yang TW, Yin JM, et al. Progress and prospects of biomarkers in primary liver cancer (Review). *Int J Oncol.* 2020;57(1):54–66. doi:10.3892/ijo.2020.5035
6. Yu SJ, Kim YJ. Hepatitis B viral load affects prognosis of hepatocellular carcinoma. *World J Gastroenterol.* 2014;20(34):12039–12044. doi:10.3748/wjg.v20.i34.12039
7. European Association For The Study Of The Liver; European Organisation For Research And Treatment Of Cancer. EASL-EORTC clinical practice guidelines: Management of hepatocellular carcinoma. *J Hepatol.* 2012;56(4):908–943. doi:10.1016/j.jhep.2011.12.001
8. Orcutt ST, Anaya DA. Liver resection and surgical strategies for management of primary liver cancer. *Cancer Control.* 2018;25(1):1073274817744621. doi:10.1177/1073274817744621
9. Villanueva A. Hepatocellular carcinoma. *N Engl J Med.* 2019;380(15):1450–1462. doi:10.1056/NEJMra1713263
10. Forner A, Reig M, Bruix J. Hepatocellular carcinoma. *Lancet.* 2018;391(10127):1301–1314. doi:10.1016/S0140-6736(18)30010-2
11. de Martel C, Maucort-Boulch D, Plummer M, Franceschi S. Worldwide relative contribution of hepatitis B and C viruses in hepatocellular carcinoma. *Hepatology.* 2015;62(4):1190–1200. doi:10.1002/hep.27969
12. Seto WK, Lo YR, Pawlotsky JM, Yuen MF. Chronic hepatitis B virus infection. *Lancet.* 2018;392(10161):2313–2324. doi:10.1016/S0140-6736(18)31865-8
13. Yuen MF, Gane EJ, Kim DJ, et al. Antiviral activity, safety, and pharmacokinetics of capsid assembly modulator NVR 3-778 in patients with chronic HBV infection. *Gastroenterology.* 2019;156(5):1392–1403.e7. doi:10.1053/j.gastro.2018.12.023
14. Tan L, Wu ZQ, Zhao C, et al. A perspective of the relationship of serum HBV DNA and HBsAg apportioned by the same hepatic parenchyma cell volume with inflammation in the natural history of chronic hepatitis B. *Ann Palliat Med.* 2021;10(2):1388–1395. doi:10.21037/apm-20-635
15. Chen CJ, Yang HI, Su J, et al. Risk of hepatocellular carcinoma across a biological gradient of serum hepatitis B virus DNA level. *JAMA.* 2006;295(1):65–73. doi:10.1001/jama.295.1.65
16. Chen JD, Yang HI, Iloeje UH, et al. Carriers of inactive hepatitis B virus are still at risk for hepatocellular carcinoma and liver-related death. *Gastroenterology.* 2010;138(5):1747–1754. doi:10.1053/j.gastro.2010.01.042
17. Allemani C, Weir HK, Carreira H, et al. Global surveillance of cancer survival 1995–2009: Analysis of individual data for 25,676,887 patients from 279 population-based registries in 67 countries (CONCORD-2). *Lancet.* 2015;385(9972):977–1010. doi:10.1016/S0140-6736(14)62038-9
18. Hou J, Wang G, Wang F, et al. Guideline of prevention and treatment for chronic hepatitis B (2015 update). *J Clin Transl Hepatol.* 2017;5(4):297–318. doi:10.14218/JCTH.2016.00019

19. Zhou J, Sun HC, Wang Z, et al. Guidelines for Diagnosis and Treatment of Primary Liver Cancer in China (2017 Edition). *Liver Cancer.* 2018;7(3):235–260. doi:10.1159/000488035

20. Moon JC, Kim SH, Kim IH, et al. Disease progression in chronic hepatitis B patients under long-term antiviral therapy. *Gut Liver.* 2015;9(3):395–404. doi:10.5009/gnl14170

21. Orito E, Hasebe C, Kurosaki M, et al. Risk of hepatocellular carcinoma in cirrhotic hepatitis B virus patients during nucleoside/nucleotide analog therapy. *Hepatol Res.* 2015;45(8):872–879. doi:10.1111/hepr.12427

22. Chang TT, Liaw YF, Wu SS, et al. Long-term entecavir therapy results in the reversal of fibrosis/cirrhosis and continued histological improvement in patients with chronic hepatitis B. *Hepatology.* 2010;52(3):886–893. doi:10.1002/hep.23785

23. Lok ASF. Hepatitis: Long-term therapy of chronic hepatitis B reverses cirrhosis. *Nat Rev Gastroenterol Hepatol.* 2013;10(4):199–200. doi:10.1038/nrgastro.2013.13

24. Lai CL, Yuen MF. Prevention of hepatitis B virus-related hepatocellular carcinoma with antiviral therapy. *Hepatology.* 2013;57(1):399–408. doi:10.1002/hep.25937

25. Su TH, Hu TH, Chen CY, et al. Four-year entecavir therapy reduces hepatocellular carcinoma, cirrhotic events and mortality in chronic hepatitis B patients. *Liver Int.* 2016;36(12):1755–1764. doi:10.1111/liv.13253

26. Xie ZB, Wang XB, Fu DL, Zhong JH, Yang XW, Li LQ. Postoperative hepatitis B virus reactivation in hepatitis B virus-related hepatocellular carcinoma patients with hepatitis B virus DNA levels <500 copies/mL. *Onco Targets Ther.* 2016;9:4593–4603. doi:10.2147/OTT.S104300

27. Choi J, Kim HJ, Lee J, Cho S, Ko MJ, Lim YS. Risk of hepatocellular carcinoma in patients treated with entecavir vs tenofovir for chronic hepatitis B: A Korean nationwide cohort study. *JAMA Oncol.* 2019;5(1):30–36. doi:10.1001/jamaoncol.2018.4070

28. Yang HI, Lu SN, Liaw YF, et al. Hepatitis B e antigen and the risk of hepatocellular carcinoma. *N Engl J Med.* 2002;347(3):168–174. doi:10.1056/NEJMoa013215

29. Zhou XP, Hu XL, Zhu YM, Qu F, Sun SJ, Qian YL. Comparison of semen quality and outcome of assisted reproductive techniques in Chinese men with and without hepatitis B. *Asian J Androl.* 2011;13(3):465–469. doi:10.1038/aja.2010.164

30. Papatheodoridis GV, Lampertico P, Manolakopoulos S, Lok A. Incidence of hepatocellular carcinoma in chronic hepatitis B patients receiving nucleos(t)ide therapy: A systematic review. *J Hepatol.* 2010;53(2):348–356. doi:10.1016/j.jhep.2010.02.035

31. Elefsiniotis IS, Glynou I, Magaziotou I, et al. HBeAg negative serological status and low viral replication levels characterize chronic hepatitis B virus-infected women at reproductive age in Greece: A one-year prospective single center study. *World J Gastroenterol.* 2005;11(31):4879–4882. doi:10.3748/wjg.v11.i31.4879

32. Watanabe T, Tokumoto Y, Joko K, et al. Effects of long-term entecavir treatment on the incidence of hepatocellular carcinoma in chronic hepatitis B patients. *Hepatol Int.* 2016;10(2):320–327. doi:10.1007/s12072-015-9647-8

33. Ma KL, Liu J, Gao M, et al. The effects of failure of low density lipoprotein receptor expression induced by inflammation on radial artery foam cell formation in patients with end-stage renal disease [in Chinese]. *Zhonghua Nei Ke Za Zhi.* 2013;52(6):464–468. PMID:24059991.

34. Carr BI, Guerra V. Thrombocytosis and hepatocellular carcinoma. *Dig Dis Sci.* 2013;58(6):1790–1796. doi:10.1007/s10620-012-2527-3

35. Furman D, Chang J, Lartigue L, et al. Expression of specific inflammasome gene modules stratifies older individuals into two extreme clinical and immunological states. *Nat Med.* 2017;23(2):174–184. doi:10.1038/nm.4267

36. Nguyen VTT, Law MG, Dore GJ. Hepatitis B-related hepatocellular carcinoma: Epidemiological characteristics and disease burden. *J Viral Hepat.* 2009;16(7):453–463. doi:10.1111/j.1365-2893.2009.01117.x

37. Fitzgerald S, Chao J, Feferman Y, Perumalswami P, Sarpel U. Hepatitis B and hepatocellular carcinoma screening practices in Chinese and African immigrant-rich neighborhoods in New York City [published online as ahead of print on October 28, 2016]. *J Racial Ethn Health Disparities.* 2016. doi:10.1007/s40615-016-0296-y

38. Lao XM, Luo G, Ye LT, et al. Effects of antiviral therapy on hepatitis B virus reactivation and liver function after resection or chemoembolization for hepatocellular carcinoma. *Liver Int.* 2013;33(4):595–604. doi:10.1111/liv.12112

39. Zhou J, Sun HC, Wang Z, et al. Guidelines for Diagnosis and Treatment of Primary Liver Cancer in China (2017 Edition). *Liver Cancer.* 2018;7(3):235–260. doi:10.1159/000488035

Influence of formalized Predialysis Education Program (fPEP) on the chosen and definitive renal replacement therapy option

Ewa Wojtaszek[A–F], Joanna Matuszkiewicz-Rowińska[A–C,E,F], Paweł Żebrowski[B,F], Tomasz Głogowski[B,F], Jolanta Małyszko[D–F]

Department of Nephrology, Dialysis and Internal Medicine, Warsaw Medical University, Poland

A – research concept and design; B – collection and/or assembly of data; C – data analysis and interpretation;
D – writing the article; E – critical revision of the article; F – final approval of the article

Address for correspondence
Jolanta Małyszko
E-mail: jolmal@poczta.onet.pl

Abstract

Background. It is widely accepted that patients with chronic kidney disease (CKD) should play an active role in the selection of renal replacement therapy (RRT) option. However, patients' knowledge about CKD and treatment options is limited. The implementation of structured education program and shared decision-making may result in a better preparation to RRT, more balanced choice of dialysis modalities and better access to kidney transplantation (TX).

Objectives. The aim of this long-term study was to assess the impact of formalized Predialysis Education Program (fPEP) on knowlege on RRT options, as well as on selected and definitive therapy.

Materials and methods. The study included 435 patients (53% men, mean age 60 years) with CKD stage 4 and 5, participating in fPEP at our center. The program included at least 3 visits, during which balanced information about all RRT options was presented and self-care and informed decision-making were encouraged. The knowledge about RRT options before and after fPEP attendance, and selected and definitive RRT options were assessed.

Results. Ninety-two percent of patients received prior nephrology care. After fPEP completion, in most patients, the knowledge about CKD and RRT options and selected preferred modality improved – 40% of participants chose hemodialysis (HD), 32% peritoneal dialysis (PD) and 18% TX. During the observation period, 4% of patients died before commencement of dialysis, 2.7% received preemptive kidney transplant, 8.6% were placed on transplant waiting list, and 94% started dialysis (30% PD and 70% HD). Among those who chose PD, 69% started PD and 24% started HD; the leading causes of the discrepancy between choosing and receiving PD was the deterioration in clinical condition (50%) and change of decision (32%).

Conclusions. The fPEP increases CKD patients' knowledge on RRT methods. The implementation of a decision-making process based on fPEP leads to a satisfying distribution between modalities, with a good concordance between chosen and definitive modality.

Key words: end-stage renal disease, chronic kidney disease, renal replacement therapy, predialysis education, modality selection

Background

International guidelines for treatment of kidney disease recommend informing the patient about all renal replacement therapy (RRT) options, as well as involving them in the process of selection of treatment modality and promoting the informed patient decision-making.[1,2] When implemented properly, predialysis education programs may produce many benefits: deferred initiation of dialysis, less emergency dialysis starts, more balanced distribution of RRT options, less anxiety and fear, and probably better survival.[3–7]

It has been recognized that predialysis care and preparation for end-stage renal disease (ESRD) in Poland is suboptimal, contributing to the unbalanced distribution of RRT modalities and high morbidity and mortality after the initiation of dialysis. Despite dissemination of practice guidelines, predialysis education in Poland is provided infrequently, and if provided, its comprehensibility seems to be suboptimal.

In 2004, based on the general principles of multidisciplinary predialysis care clinics, the formalized Predialysis Education Program (fPEP) adapted to Polish organizational, social and cultural circumstances has been developed and implemented in the Department of Nephrology, Dialysis and Internal Diseases of Warsaw Medical University, Poland. Since 2005, it has become a part of clinical practice of predialysis care and remains ongoing.

Objectives

The aim of the present study was to assess the impact of fPEP on knowledge of RRT options, and chosen and definitive modality at the start of RRT treatment.

Materials and methods

This is an observational, prospective, long-term, single-center study aimed at determining the impact of formalized PEP on 435 chronic kidney disease (CKD) patients transitioning from CKD care to RRT. The fPEP was developed for the purpose of clinical practice in Department of Nephrology, Dialysis and Internal Medicine, Warsaw Medical University, Poland. Anonymized patient data were extracted from patient files prepared for the needs of fPEP and provided to the research team. According to Polish law, for educational interventions, ethics committee approval is not applicable.

Study population

The study included patients participating in fPEP at our center between January 2005 and December 2019. Patients were referred to fPEP regardless of potential contraindications to specified RRT modalities. The inclusion criteria were as follows: 1) CKD stage 4 or 5; 2) completion of education process (at least 2 visits) with a certificate issued; 3) initiation of dialysis or kidney transplantation (TX) or death at the end of the study. The exclusion criteria were: 1) incomplete education (only 1 visit and/or lack of certificate); 2) education after urgent-start dialysis; 3) education before return to dialysis due to transplanted kidney failure. The following demographic and clinical data were registered: age, sex, family status, duration of nephrology care, knowledge of kidney disease and different treatment options, cause of kidney failure and comorbidities (diabetes, coronary artery disease, heart failure, cerebrovascular disease, peripheral atherosclerosis, chronic pulmonary disease, chronic liver disease, cancer), potential medical, psychological and social contraindications to particular RRT options, and kidney function (measured with estimated glomerular filtration rate (eGFR)) at fPEP commencement.

Study protocol

Patients with advanced renal failure (eGFR ≤ 20 mL/min) with their families or caregivers are referred to the participation in fPEP. Nephrologists and highly trained nurses experienced in all RRT modalities are involved in the education process. The basic schedule includes 3 individual (face-to-face) meetings lasting 60–90 min (further visits are possible at the initiative of the patient or the educational team). Subsequent visits are arranged every 2–4 weeks. Educational materials to help discuss specific issues are available, as well as a presentation of dialysis equipment and meetings with patients treated with various RRT methods.

To improve the communication between educational team members, each visit is documented using short forms containing most important information about the patient, confirming acquisition of information provided to the patient during previous visit, and outlining the educational content planned for the next meeting.

Visit 1

During the first visit, a "patient profile" is created to establish an education plan tailored to the needs and cognitive abilities of the patient, and to identify contraindications and/or prejudice to any therapy option. This includes a history of kidney disease, comorbidities, symptoms of renal failure, patient's current life situation, degree of independence, as well as lifestyle and employment. The knowledge about the disease and motivation to participate in the treatment process are assessed using self-prepared questionnaire with a grading scale based on the Polish school grading scale (1–6). Regardless of the CKD stage, the explanation of the progressive and irreversible nature of CKD and its adverse effects on the functioning of other organs is essential. The analysis of test results allows for showing the relationship between deteriorating kidney

function and the changes in the patient's wellbeing. This is a background to discuss ways to slow down the progression of kidney disease and prevent its complications, and to emphasize patient's participation in the process. Discussing the symptoms of renal failure, the importance of patient self-control and timely preparation and initiation of RRT is the final part of the 1st visit.

Visit 2

The next visit (or visits) is devoted to the presentation and discussion of RRT options – TX, peritoneal dialysis (PD) and hemodialysis (HD). Regardless of the patient's preferences or potential indications and contraindications to any treatment method, all options are presented to establish the complementarity of RRT.

Visit 3

The 3rd visit (and sometimes more visits) is devoted to assessing the patient's understanding and acquisition of the information provided during previous meetings. It serves to clarify doubts and to rediscuss misunderstood problems, and offers an opportunity to learn more about the RRT method chosen by the patient.

At the end of the education process, post-fPEP assessment of CKD and RRT options knowledge evaluation are performed, and training certificate is issued, indicating the patient's preferred method of RRT. Most patients continue nephrology care, but, if indicated, further steps for preparation to the selected option are implemented.

Statistical analyses

Data are presented as median (interquartile range (IQR)) or frequencies and percentages for categorical variables. Differences between study groups were tested using the Mann–Whitney U test and Kruskal–Wallis test, and differences in the relative frequencies were tested using the Pearson's χ^2 test. A value of $p < 0.05$ was considered statistically significant. Univariate and multivariable logistic regression was used to determine the association between demographics, clinical factors, as well as factors associated with fPEP attendance (post-fPEP knowledge of RRT methods and personal selection), and selected and definitive RRT modality. Four models for HD, PD and TX selection (M1 – post-fPEP HD, PD and TX knowledge, M2 – M1+age and Charlson Comorbidity Index (CCI), M3 – M2+eGFR, M4 – M3+nephrology care), and definitive HD or PD treatment (M1 – post-fPEP HD, PD and TX knowledge and personal HD or PD selection, M2 – M1+age and CCI, M3 – M2 + eGFR, M4 – M3+nephrology care) were assessed. The models were ranked using Akaike Information Criterion (AIC). The models with lowest AIC value were considered to have the highest support explaining selection and definitive RRT modality. In Table 1 and Table 2, we added the details of statistical analyses regarding factors associated with the selection of RRT method (Table 1) and details of statistical analysis concerning factors associated with definitive dialysis modality (Table 2).

All statistical calculations were performed using STATISTICA software package v. 13 (StatSoft Polska, Kraków, Poland).

Table 1. Details of statistical analysis regarding factors associated with the selection of renal replacement therapy (RRT) method

HD choice										
Log likelihood	R^2 Cox–Snell	R^2 Nagelkerke	likelihood ratio test			Wald test			Hosmer–Lemeshow test	
			χ^2	df	p-value	χ^2	df	p-value	χ^2	p-value
−242.939	0.207	0.280	101.224	3	<0.0001	56.242	3	<0.0001	0.209	0.976
−240.896	0.215	0.290	105.310	5	<0.0001	58.142	5	<0.0001	6.449	0.597
−238.307	0.220	0.298	108.487	6	<0.0001	60.310	6	<0.0001	6.525	0.585
−238.711	0.222	0.300	109.680	7	<0.0001	60.677	7	<0.0001	1.592	0.991
PD choice										
−231.921	0.173	0.242	82.732	3	<0.0001	26.695	3	<0.0001	5.447	0.141
−226.544	0.193	0.270	93.486	5	<0.0001	35.899	5	<0.0001	13.263	0.103
−217.280	0.227	0.317	112.014	6	<0.0001	48.571	6	<0.0001	12.352	0.136
−215.283	0.234	0.327	116.008	7	<0.0001	51.171	7	<0.0001	7.362	0.498
TX choice										
−145.093	0.125	0.228	58.550	3	<0.0001	20.212	3	<0.001	0.474	0.788
−120.868	0.218	0.395	107.001	5	<0.0001	45.165	5	<0.0001	5.100	0.746
−119.427	0.223	0.405	109.882	6	<0.0001	45.070	6	<0.0001	4.477	0.811
−116.577	0.233	0.423	115.582	7	<0.0001	48.667	7	<0.0001	4.264	0.832

df – degrees of freedom; HD – hemodialysis; PD – peritoneal dialysis; TX – kidney transplantation; M1 – Model 1 – post formalized Predialysis Education Program (fPEP) HD, PD and TX knowledge; M2 – Model 2 – M1+age and Charlson Comorbidity Index (CCI); M3 – Model 3 – M2+estimated glomerular filtration rate (eGFR); M4 – Model 4 – M3+nephrology care.

Table 2. Details of statistical analysis regarding factors associated with definitive dialysis modality

Model	AIC	log likelihood	R^2 Cox–Snell	R^2 Nagelkerke	likelihood ratio test			Wald test			Hosmer–Lemeshow test	
					χ^2	df	p-value	χ^2	df	p-value	χ^2	p-value
Definitive HD												
M1	388.220	−189.110	0.347	0.478	185.981	4	<0.0001	70.333	4	<0.0001	5.703	0.126
M2	379.633	−182.816	0.366	0.504	198.567	6	<0.0001	76.870	6	<0.0001	15.480	0.054
M3	329.543	−156.771	0.437	0.602	250.657	7	<0.0001	104.535	7	<0.0001	4.936	0.764
M4	320.164	−151.082	0.452	0.622	262.036	8	<0.0001	101.208	8	<0.0001	11.732	0.163
Definitive PD												
M1	319.799	−120.202	0.380	0.545	208.170	3	<0.0001	76.699	3	<0.0001	2.768	0.597
M2	252.405	−226.544	0.474	0.679	279.564	5	<0.0001	85.889	5	<0.0001	1.629	0.990
M3	228.116	−107.058	0.504	0.724	305.853	6	<0.0001	108.371	6	<0.0001	5.018	0.756
M4	228.433	−106.216	0.506	0.726	307.566	7	<0.0001	111.112	7	<0.0001	4.191	0.833

AIC – Akaike Information Criterion; df – degrees of freedom; HD – hemodialysis; PD – peritoneal dialysis; M1 – Model 1 – post formalized Predialysis Education Program (fPEP) HD, PD and TX knowledge; M2 – Model 2 – M1+age and Charlson Comorbidity Index (CCI); M3 – Model 3 – M2+estimated glomerular filtration rate (eGFR); M4 – Model 4 – M3+nephrology care.

Results

Among 652 patients registered in our fPEP between January 2005 and December 2019, 435 met predefined inclusion criteria to the present study. Demographic and clinical characteristics of the studied group are presented in Table 3.

Based on the data collected in the "patient profile" and discussions among the educational team members, 97 (22%) patients were deemed not suitable for free choice of dialysis modality. Medical contraindications to PD were revealed in 29 (7%), social contraindications in 10 (2%) and psychological contraindications in 58 (13%) patients. However, psychological contraindications were considered absolute only in 25 (6%) patients, when PD assisted by family was not possible.

Table 3. Demographic and clinical characteristics of the studied group (n = 435)

Parameter	Value
Age [years] ≥65 years of age, n (%)	Me = 61; IQR = 23 n = 200 (46)
Male sex, n (%)	n = 231 (53)
CCI	Me = 6; IQR = 5
eGFR at fPEP commencement [mL/min]	Me = 16; IQR = 7

The cause of kidney disease, n (%)
  diabetic nephropathy
  glomerulonephritis
  hypertensive/vascular
  interstitial nephropathy
  ADPKD
  other
  unknown
	
	n = 87 (20)
	n = 115 (26)
	n = 118 (27)
	n = 49 (11)
	n = 36 (8)
	n = 14 (3)
	n = 16 (4)

Nephrology care, n (%) Nephrology care >1 year, n (%)	n = 399 (92) n = 291 (67)
Living alone, n (%)	n = 105 (24)
Employed, n (%)	n = 222 (51)

Me – median; IQR – interquartile range; CCI – Charlson Comorbidity Index; eGFR – estimated glomerular filtration rate; fPEP – formalized Predialysis Education Program; ADPKD – autosomal dominant polycystic kidney disease.

Absolute contraindications to TX were found in 115 (26%) patients. They resulted from high comorbidity burden (CCI ≥ 9). In patients with CCI < 9, contraindications or limitations to eligibility for TX were evaluated individually.

The knowledge about kidney disease and RRT methods

At baseline, 252 (58%) patients had had at least sufficient (43% sufficient, 15% good) knowledge about kidney disease. Only 30 (7%) fPEP participants had had at least perceived knowledge about all RRT modalities, 248 (57%) about HD and 104 (24%) about TX. Surprisingly, 400 (92%) of patients had had no knowledge or even never heard about PD.

After fPEP completion, 383 (88%) participants improved their knowledge about kidney disease and 239 (55%) patients proved to have knowledge about all RRT options; 387 (89%) about HD, 326 (75%) about PD and 248 (57%) about TX.

Finally selected RRT option

After fPEP completion, 59 (14%) of participants did not make a final decision, while 376 (86%) patients indicated their preferred RRT option – 176 (40%) patients HD and 140 (32%) PD, and among those who were deemed eligible to transplantation (324), 60 patients (18%) selected TX.

Patients unable to indicate a preferred modality were significantly older (69 ±13 years compared to 60 ±16 years, Mann–Whitney U test: U = 6725.5; p < 0.0001) and had higher comorbidity burden (CCI 8 ±3 compared to 6 ±3, Mann–Whitney U test: U = 6905.5; p < 0.0001) and better preserved kidney function (eGFR 22 ±5 mL/min compared to 17 ±5 mL/min, Mann–Whitney U test: U = 4268.0; p < 0.0001). They had lesser knowledge on HD (53% compared

Table 4. Characteristics of patients who chose their preferable renal replacement therapy (RRT) option (n = 376)

Variable	Chose HD n = 176	Chose PD n = 140	Chose TX n = 60	HD vs PD vs TX	p-value
Age [years]	Me = 67; IQR = 18	Me = 59; IQR = 21.5	Me = 44; IQR = 19	74.21*	<0.0001
Male sex (%)	59	53	42	4.37#	0.09
CCI	Me = 7; IQR = 4	Me = 6; IQR = 5	Me = 2; IQR = 2	76.76*	<0.0001
eGFR [mL/min]	Me = 16; IQR = 5	Me = 14.5; IQR = 7	Me = 15.6; IQR = 4.5	6.37*	<0.05
Nephrology care (%)	93	88	98	6.9#	<0.05
Post-fPEP knowledge about HD (%)	91	98	98	11.25#	<0.01
Post-fPEP knowledge about PD (%)	59	99	95	86.83#	<0.0001
Post-fPEP knowledge about TX (%)	39	75	97	79.21#	<0.0001

Me – median; IQR – interquartile range; * – Kruskal–Wallis test; # – χ^2 test; HD – hemodialysis; PD – peritoneal dialysis; TX – kidney transplantation; CCI – Charlson Comorbidity Index; eGFR – estimated glomerular filtration rate; fPEP – formalized Predialysis Education Program.

Table 5. AIC ranks for models tested for likelihood of selecting specific RRT modality

Model	HD choice	PD choice	TX choice
	AIC	AIC	AIC
Model 1 – post-fPEP HD, PD and TX knowledge	493.879	471.843	298.187
Model 2 – M1+age, CCI	493.793	465.089	253.736
Model 3 – M2+eGFR	492.615	448.560	252.855
Model 4 – M3+nephrology care	493.423	446.567	249.155

AIC – Akaike Information Criterion; HD – hemodialysis; PD – peritoneal dialysis; TX – kidney transplantation; CCI – Charlson Comorbidity Index; eGFR – estimated glomerular filtration rate; fPEP – formalized Predialysis Education Program; RRT – renal replacement therapy; M1 – Model 1 – post formalized Predialysis Education Program (fPEP) HD, PD and TX knowledge; M2 – Model 2 – M1+age and Charlson Comorbidity Index (CCI); M3 – Model 3 – M2+estimated glomerular filtration rate (eGFR); M4 – Model 4 – M3+nephrology care.

to 89%, χ^2 = 33.66, degrees of freedom (df) = 1; p < 0.0001), PD (51% compared to 75%, χ^2 = 24.76, df = 1; p < 0.0001) and TX (26% compared to 57 %, χ^2 = 27.35, df = 1; p < 0.0001).

In Table 4, characteristics of the patients who indicated preferred RRT options are presented.

Selection of preferred RRT modality was associated with knowledge about this method. For HD selection, all assessed models were comparable (ΔAIC < 2); however, for PD and TX selection, the full model (M4) reached the lowest AIC value (Table 5). In Table 6, the full model (M4) for HD, PD and TX selection is presented in details.

Definitive RRT option

During study period, 407 (94%) patients started dialysis – 283 (70%) HD and 124 (30%) PD. Death in predialysis period occurred in 19 (4%) cases, and 9 (2.7%) patients received preemptive kidney transplant. Figure 1 shows patient flow and the distribution of selected and definitive RRT options.

The best concordance between selected and definitive modality was noticed for HD (98%). Despite their personal choice, 43 patients did not start PD – 9 patients died before dialysis and 34 (24%) started HD. The most prevalent reason of the discrepancy between indicated and definitive modality was the deterioration of clinical condition and losing independence – 17 (50%). Eleven (32%) patients changed their decision, and in 6 (18%) cases Tenckhoff

Table 6. Factors associated with the selection of RRT option in multivariate logistic regression (Model 4)

Variable	Choice of HD				Choice of PD				Choice of TX			
	OR	95% CI	Wald stat	p-value	OR	95% CI	Wald stat	p-value	OR	95% CI	Wald stat	p-value
Age	1.02	0.9; 1.05	3.72	0.05	0.99	0.96; 1.02	0.19	0.7	0.99	0.95; 1.02	0.29	0.6
CCI	0.95	0.83; 1.1	0.35	0.5	1.28	1.1; 1.5	10.47	0.001	0.56	0.42; 0.76	14.33	0.0002
eGFR	0.96	0.92; 1.0	3.0	0.08	0.9	0.86; 0.95	17.36	<0.0001	1.05	0.98; 1.13	1.68	0.19
Nephrology care (yes)	1.57	0.68; 3.6	1.14	0.3	0.44	0.19; 0.99	3.91	0.05	7.17	0.89; 57.49	3.44	0.06
Post-fPEP knowledge about HD (yes)	28.13	9.07; 87.23	33.39	<0.0001	0.63	0.08; 4.9	0.19	0.7	0.21	0.009; 4.7	0.97	0.3
Post-fPEP knowledge about PD (yes)	0.062	0.023; 0.17	30.63	<0.0001	55.17	8.93; 341.02	18.62	<0.0001	1.83	0.37; 9.13	0.55	0.5
Post-fPEP knowledge about TX (yes)	0.47	0.26; 0.86	6.041	0.01	2.47	1.3; 4.69	7.73	0.005	7.9	0.96; 65.13	3.67	0.05

RRT – renal replacement therapy; OR – odds ratio; 95% CI – 95% confidence interval; HD – hemodialysis; PD – peritoneal dialysis; TX – kidney transplantation; CCI – Charlson Comorbidity Index; eGFR – estimated glomerular filtration rate; fPEP – formalized Predialysis Education Program.

Fig. 1. Patient flow and the distribution of selected and definitive renal replacement therapy (RRT) options

*pts eligible to TX
PEP Predialysis Education Program
HD hemodialysis
PD peritoneal dialysis
TX kidney transplantation
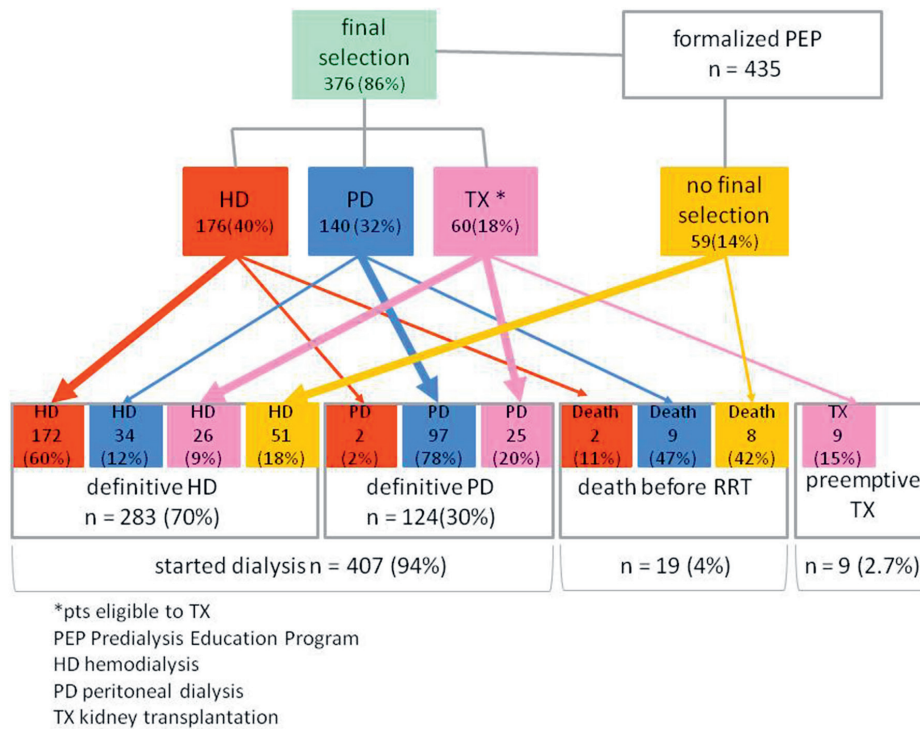
Table 7. Patient characteristics according to definitive dialysis method (n = 407)

Variable	Definitive HD n = 283	Definitive PD n = 124	HD vs PD	p-value
Age [years]	Me = 63; IQR = 18	Me = 52; IQR = 25	9081*	<0.0001
Male sex (%)	54	50	0.75#	0.5
CCI	Me = 7; IQR = 5	Me = 4; IQR = 4	10389.5*	<0.0001
eGFR	Me = 17; IQR = 7	Me = 13; IQR = 5	8698*	<0.0001
Nephrology care (%)	94	89	15.5#	0.06
Post-fPEP knowledge about HD (%)	87	98	310.84#	<0.001
Post-fPEP knowledge about PD (%)	66	100	260.22#	<0.0001
Post-fPEP knowledge about TX (%)	46	82	193.06#	<0.0001
Selected RRT modality (%) HD PD TX	 61 12 9	 2 78 20	319.67#	<0.0001

Me – median; IQR – interquartile range; * – Mann–Whitney U test; # – χ² test; HD – hemodialysis; PD – peritoneal dialysis; TX – kidney transplantation; CCI – Charlson Comorbidity Index; eGFR – estimated glomerular filtration rate; fPEP – formalized Predialysis Education Program; RRT – renal replacement therapy.

catheter implantation was abandoned due to extensive intraperitoneal adhesions.

During the study period, 51 (85%) patients who indicated TX as their preferred modality had to start dialysis therapy; however, 28 (47%) of them were placed on transplant list before dialysis. More often, the patients started PD (60%). The characteristics of the patients who finally started therapy on PD and HD are presented in Table 7.

The initiation of PD and HD therapy was strongly associated with the choice and knowledge about the modality; however, PD knowledge decreased the probability of HD initiation. The model including all assessed parameters reached the lowest AIC value for prediction of definitive dialysis modality (Table 8). The details are presented in Table 9.

Table 8. AIC ranks for models tested for likelihood of definitive RRT modality

Model	Definitive HD AIC	Definitive PD AIC
Model 1 – post-fPEP HD, PD and TX knowledge and personal HD or PD selection	388.220	319.799
Model 2 – M1+age, CCI	379.633	252.405
Model 3 – M2+eGFR	329.543	228.116
Model 4 – M3+nephrology care	320.164	228.433

AIC – Akaike Information Criterion; RRT – renal replacement therapy; HD – hemodialysis; PD – peritoneal dialysis; TX – kidney transplantation; CCI – Charlson Comorbidity Index; eGFR – estimated glomerular filtration rate; fPEP – formalized Predialysis Education Program.

Table 9. Factors associated with definitive dialysis modality in multivariate logistic regression (Model 4)

Variable	Definitive HD				Definitive PD			
	OR	95% CI	Wald stat	p-value	OR	95% CI	Wald stat	p-value
Age	1.03	1.0; 1.07	4.22	0.04	0.93	0.89; 0.96	10.63	<0.0001
CCI	0.86	0.71; 1.03	2.68	0.1	0.94	0.77; 1.14	2.33	0.5
eGFR	1.24	1.16; 1.33	42.17	<0.0001	0.82	0.75; 0.89	35.28	<0.0001
Nephrology care	6.19	2.07; 18.58	10.61	0.001	0.49	0.20; 1.23	2.27	0.1
Selected HD (yes)	54.03	19.37; 150.65	58.15	<0.0001	–	–	–	–
Selected PD (yes)	–	–	–	–	74.82	30.73; 182.13	90.37	<0.0001
Post-fPEP knowledge about HD (yes)	10.72	1.11; 103.73	4.19	0.04	3.18	0.69; 14.71	2.19	0.1
Post-fPEP knowledge about PD (yes)	0.07	0.008; 0.58	6.04	0.01	55.65	6.63; 226.12	67.20	<0.0001
Post-fPEP knowledge about TX (yes)	0.77	0.34; 1.76	0.37	0.5	2.52	1.28; 4.96	7.15	0.007

OR – odds ratio; 95% CI – 95% confidence interval; HD – hemodialysis; PD – peritoneal dialysis; TX – kidney transplantation; CCI – Charlson Comorbidity Index; eGFR – estimated glomerular filtration rate; fPEP – formalized Predialysis Education Program.

Discussion

In this single-center study, we present the results of the implementation of fPEP in the population of Polish patients with CKD and its influence on selected and definitive RRT method.

Potential contraindications to specified RRT options or perceived mental limitations were not restrictive for the referral to education. In fact, it is quite common not to offer PD to obese patients and to patients with a history of surgical abdomen procedures or with polycystic kidney disease, not to offer HD if the problem with vascular access is anticipated, and to not discuss RRT options when some mental limitations are perceived. These contraindications or limitations are often unjustified, and regardless of them patients have the right to obtain comprehensive information and make an informed decision.

In our study, despite long-term nephrology care, 42% patients had no knowledge about kidney disease. Only 8% knew about PD and only 7% had at least perceived knowledge about all methods. Our results stand out significantly from the literature data.[3,8,9] In our study, nephrology care was associated with the knowledge about kidney disease and HD, but not PD and TX.

Most of the patients proved to be receptive to the psycho-educational intervention we used. Post-fPEP assessment revealed that 89% patients had knowledge about HD, 75% about PD, 57% about TX, and 55% about all RRT options. It seems comparable to previous data; however, more often, the impact of educational intervention on the choice or receipt of RRT method was assessed.[5–7,10–13] Knowledge on a given method not necessarily must mean its choice. It is an essential factor in making a personal, informed decision and adjusting a treatment option to the patient's needs and expectations, making patients willing to learn more about the preferred method. However, one should be aware that in treatment decision-making, CKD patients very often do not use objective knowledge, but rather are guided by their feelings, beliefs, the possibility of family support, or the impact of the treatment on their quality of life.[14,15]

In our study, elderly patients with higher comorbidity burden proved to be less susceptible to educational intervention. One possible explanation for this association may be cognitive impairment due to vascular or Alzheimer's disease; however, it is worth remembering that after the age of 65, even without additional pathologies, the cognitive functions in terms of information processing, memory and understanding abstraction deteriorate. Therefore, the method, rapidity and perhaps the scope of education should be tailored to these limited perception capabilities. In the authors' opinion, for all patients in question, one-to-one sessions may be the optimal method of education. Sensitive and tactful communication, motivational interviewing to engage the patient to change behaviors, and providing well-balanced, unbiased information are considered key factors for successful education. Repeating the most important information and making sure that the discussed issues have been understood by the patient, as well as positive feedback from the patients about what they have learned can ensure that they received the most as possible comprehensive information necessary for shared decision-making.[2,16,17]

The distribution between selected dialysis methods in our study was almost equal – 40% patients chose HD and 32% chose PD, which is in line with previous studies.[5–7,10–13] Nevertheless, such distribution can be associated with additional factors that extend beyond patient choice, including patient characteristics, healthcare system, reimbursement policy, provider factors such as "home dialysis first" policy, or clinician behavior.

In our cohort, 22% of patients have been considered not suitable for free personal choice of dialysis modality, which is similar to previous data.[13,18,19] Medical and psychological (or both) contraindications for the choice of PD were the most common. In general, old age and high comorbidity burden are perceived as contraindications to PD and those patients are less likely to receive PD, even

though they have decreased mortality risk on PD.[20] However, quite a large group of elderly patients consciously chose HD because of concerns about the lack of support, being a burden on the family and social isolation. It appears to be, in a certain sense, an expression of a wider problem of shortcomings in healthcare systems and social care in many countries in the face of an aging population. In some countries, the use of assisted PD has been suggested to increase the probability of the choice and the prevalence of PD.[21,22]

The knowledge about PD was strongly associated with PD selection, while reducing the likelihood of HD choice. It was also reported in previous studies and a meta-analysis by Devoe et al.[5,6,10,19,23]

Our study encompassed patients who, at the end of the follow-up, had established outcome (initiation of dialysis, TX or death). During the study period, 94% of fPEP participants began dialysis – 70% of patients started HD and 30% started PD. It is in sharp contrast to the Polish and international ESRD statistics, where PD incidence and prevalence is well below these values.[24–26]

Patient flow analysis revealed that 98% patients who selected HD started HD, and 69% who indicated PD as preferred option finally started PD. Generally, this is in concordance with the data from previous educational studies.[6,10,11,13,19,27–29] In fact, in our study, 1/3 of patients who had selected PD have not started the treatment – 6% died before dialysis commencement and 24% eventually began HD treatment, predominantly due to deterioration in clinical condition and loss of independence (50%). One-third of fPEP participants with final PD selection had changed their mind before the dialysis began. At least in part, the deterioration in their clinical condition or a change in family or social circumstances may be associated with the re-evaluation of the decision. Nevertheless, timing of modality education, regular follow-up, repeating education when needed, and support may be essential to support the decision.[10,17,19] In our study, patients who initiated PD have had lower eGFR at the time of education, thus the period between selecting and starting dialysis was certainly shorter. Seventy eight percent of patients who ultimately started PD chose PD as preferred option, while 20% had to start dialysis despite final TX selection. Patients who chose PD were significantly younger and had lower comorbidity burden; however, the most important factors associated with initiation of PD were PD knowledge and final PD selection, but not CCI.

Final HD selection was strongly associated with initiation of HD, and 60% of patients started HD in accordance with their choice. The 2nd most populous group commencing HD were those who have been unable to indicate preferred RRT option during the education process. They were significantly older, had higher commodity burden and presented the weakest response to the educational intervention compared to other groups of patients. It is possible that older patients have fear or no interest in being

an active part of the decision-making process, and prefer to transfer responsibility for medical decision to the doctor or family.[14,15,30] To overcome these barriers, the following solutions may be effective: allowing more time for the patient to reach a decision, involve family members in the education process or arrange contact with other patients. Nevertheless, in these patients, optimal preparation and elective dialysis start is perceived as the benefit of predialysis education.[6,28]

We assumed that, according to recommendations, all patients with advanced kidney disease should be informed about the possibility of TX.[1,31] For the purpose of fPEP, we assumed that patients with CCI ≥ 9 (26%) had absolute contraindications to TX, and we decided not to discuss this option during the education process. In some patients, when relative contraindications or limited eligibility to TX had been established, individual consultations regarding suitability for transplantation have been provided.

At baseline, ¼ of fPEP participants had had the knowledge about TX, which is comparable to the reports from other patient populations.[3,8,9] Participation in fPEP resulted in doubling the number of patients with TX knowledge, and 60 (18%) patients indicated TX as preferred RRT option.

During the follow-up, 2.7% of patients received preemptive TX, while 8.6% of patients were placed on transplant waiting list before dialysis initiation. Our results appear to be worse than Poltransplant data; however, it should be emphasized that the single-center nature of our study may limit the value of the comparison with nationwide data.[32] Regardless of this, our data seem to confirm the evidence that predialysis education attendance increases the probability of placement on transplant waiting list before dialysis initiation[7] and preemptive TX.[6,33]

The RRT modality decision-making is a complex process requiring an appropriate and individualized educational process. Identification and acknowledgement of emotions should be a first step in building effective communication and education to ensure that patients received knowledge appropriate for shared decision-making. Therefore, the emotional support and creation of an atmosphere of mutual trust between the patient and the educational team was one of the essential elements of our program; however, the evaluation of this factor on fPEP results is impossible. Our study also supports the opinion that there is no single education curriculum that can be applied to all CKD patients, and thus education must be flexible and tailored to each patient.

Limitations

We are aware of the limitations of our study, being a single-center and observational study. However, this single-center character allowed for the implementation of consistent approach to education and shared decision-making, and exclusion of bias connected with center and educational team characteristics. The 2nd limitation was

the lack of control group; however, we assessed the influence of formalized Predialysis Education Program on the chosen RRT modality in relation to the pre-education period. In a real-life scenario, the standard group of patients such as described in this study is under nephrology care, and sometimes even not under nephrology care, and the patients have no opportunity for any education regarding RRT modality. Due to lack of choice, these patients cannot serve as controls to the group who was offered predialysis education. Therefore, as in the educational studies, we chose to compare the knowledge of RRT options and chosen and definitive modality at the start of RRT treatment.

Nevertheless, it would be desirable to evaluate the effectiveness of fPEP in the entire population of Polish CKD patients transitioning from conservative care to RRT. The implementation of this educational intervention may be beneficial not only to patients but also to the whole healthcare system. However, we are fully aware that the legacy of the pandemic includes all the shortcomings of telemedicine, lack of access to specialists and lots of "crash-landers" (patients with late referral for dialysis) coming to dialysis units. Thus, all the educational programs were either suspended or limited and this situation has been affecting the choice or rather lack of choice of RRT modality for patients with advanced stages of CKD.

Conclusions

The implementation of fPEP improves patients' knowledge and willingness to shared decision-making. This results in a balanced choice between PD and HD, and increases the incidence of PD and likely access to TX. It would be valuable to evaluate in randomized trials or large observational studies the influence of specific educational process elements, and the contribution of patient-specific factors to its effectiveness.

ORCID iDs

Ewa Wojtaszek ⓘ https://orcid.org/0000-0001-5970-8466
Joanna Matuszkiewicz-Rowińska
ⓘ https://orcid.org/0000-0001-7644-823X
Paweł Żebrowski ⓘ https://orcid.org/0000-0003-2826-0253
Tomasz Głogowski ⓘ https://orcid.org/0000-0001-8198-5646
Jolanta Małyszko ⓘ https://orcid.org/0000-0001-8701-8171

References

1. Stevens PE, Levin A; KDIGO Work Group. Evaluation and management of chronic kidney disease, Synopsis of the kidney disease: Improving global outcomes. *Kidney Int Suppl*. 2013;3(1):135–150. doi:10.1038/kisup.2012.72
2. Moss AH. Shared decision making in dialysis: The new RPA/ASN guideline on appropriate initiation and withdrawal of treatment. *Am J Kidney Dis*. 2001;37(5):1081–1091. doi:10.1016/s0272-6386(05)80027-7
3. Mehrotra R, Marsh D, Vonesh E, et al. Patient education and access of ESRD patients to renal replacement therapies beyond in-center hemodialysis. *Kidney Int*. 2005;68(1):378–390. doi:10.1111/j.1523-1755.2005.00453.x
4. Devins GM, Mendelssohn DC, Barre PE, Binik YM. Predialysis psycho-educational intervention and coping styles influence time to dialysis in chronic kidney disease. *Am J Kidney Dis*. 2003;42(4):693–703. doi:10.1016/s0272-6386(03)00835-7
5. Shukla AM, Easom A, Singh M, et al. Effects of comprehensive predialysis education program on the home dialysis therapies: A retrospective cohort study. *Perit Dial Int*. 2017;37(5):542–547. doi:10.3747/pdi.2016.00270
6. Prieto-Velasco M, Quiros P, Remon C. Spanish Group for the Implementation of a Shared Decision Making Process for RRT Choice with Patient Decision Aid Tools. *PLoS One*. 2015;10(10):e0138811. doi:10.1371/journal.pone.0138811
7. Kurella Tamura M, Li S, Chen SC, et al. Educational programs improve the preparation for dialysis and survival of patients with chronic kidney disease. *Kidney Int*. 2014;85(3):686–692. doi:10.1038/ki.2013.369
8. Finkelstein FO, Story K, Firanek C, et al. Perceived knowledge among patients cared for by nephrologists about chronic kidney disease and end-stage renal disease therapies. *Kidney Int*. 2008;74(9):1178–1184. doi:10.1038/ki.2008.376
9. Gray NA, Kapojos JJ, Burke MT, et al. Patient kidney disease knowledge remains inadequate with standard nephrology outpatient care. *Clin Kidney J*. 2016;9(1):113–118. doi:10.1093/ckj/sfv108
10. Manns BJ, Taub K, Vanderstraeten C, et al. The impact of education on chronic kidney disease patients' plans to initiate dialysis with self-care dialysis: A randomized trial. *Kidney Int*. 2005;68(4):1777–1783. doi:10.1111/j.1523-1755.2005.00594.x
11. Lacson E Jr, Wang W, DeVries C, et al. Effects of nationwide predialysis educational program on modality choice, vascular access, and patient outcomes. *Am J Kidney Dis*. 2011;58(2):235–242. doi:10.1053/j.ajkd.2011.04.015
12. Shukla AM, Hinkamp C, Segal E, et al. What do the US advanced kidney disease patients want? Comprehensive pre-ESRD Patient Education (CPE) and choice of dialysis modality. *PLoS One*. 2019;14(4):e0215091. doi:10.1371/journal.pone.0215091
13. Heaf J, Heiro M, Peterson A, et al. Choice of dialysis modality among patients initiating dialysis: Results of the Peridialysis study. *Clin Kidney J*. 2020;14(9):2064–2074. doi:10.1093/ckj/sfaa260
14. Song MK, Lin FC, Gilet GA, et al. Patient perspectives on informed decision-making surrounding dialysis initiation. *Nephrol Dial Transplant*. 2013;28(11):2815–2823. doi:10.1093/ndt/gft238
15. Morton RL, Tong A, Howard K, et al. The views of patients and caregivers in treatment decision making for chronic kidney disease: Systematic review and thematic synthesis of qualitative studies. *BMJ*. 2010;340:c112. doi:10.1136/bmj.c112
16. Isnard Bagnis C, Crepaldi C, Dean J, et al. Quality standards for predialysis education: Results from a consensus conference. *Nephrol Dial Transplant*. 2015;30(7):1058–1066. doi:10.1093/ndt/gfu225
17. Goovaerts T, Isnard Bagnis C, Crepaldi C, et al. Continuing education: Preparing patients to choose a renal replacement therapy. *J Ren Care*. 2015;40(1):62–75. doi:10.1111/jorc.12106
18. Mendelssohn DC, Mujais SK, Soroka SD, et al. A prospective evaluation of renal replacement therapy eligibility. *Nephrol Dial Transplant*. 2008;24(2):555–561. doi:10.1093/ndt/gfn484
19. Goovaerts T, Jadoul M, Goffin E. Influence of a pre-dialysis education programme (PDEP) on the mode of renal replacement therapy. *Nephrol Dial Transplant*. 2005;20(9):1842–1847. doi:10.1093/ndt/gfh905
20. van de Luijtgaarden MWM, Noordzij M, Steli VS, et al. Effects of comorbid and demographic factors on dialysis modality choice and related patient survival in Europe. *Nephrol Dial Transplant*. 2011;26(9):2940–2947. doi:10.1093/ndt/gfq845
21. Bèchade C, Lobbedez T, Ivarsen P, Povlsen JV. Assisted peritoneal dialysis for older people with end-stage renal disease: The French and Danish Experience. *Perit Dial Int*. 2015;35(6):663–666. doi:10.3747/pdi.2014.00344
22. Iyasere OU, Brown EA, Johansson L, et al. Quality of life and physical function in older patients on dialysis: A comparison of assisted peritoneal dialysis with hemodialysis. *Clin J Am Soc Nephrol*. 2016;11(3):423–430. doi:10.2215/CJN.01050115
23. Devoe DJ, Wong B, James MT, et al. Patient education and peritoneal dialysis modality selection: A systematic review and meta-analysis. *Am J Kidney Dis*. 2016;68(3):422–433. doi:10.1053/j.ajkd.2016.02.053

24. The United States Renal Data System (USRDS). USRDS 2020 Annual Data Report. https://adr.usrds.org/2020/end-stage-renal-disease/11-international-comparisons. Accessed June 5, 2021.

25. The Registry of the European Renal Association – European Dialysis and Transplant Association (ERA-EDTA). Annual Report 2011. https://www.era-edta-reg.org/files/annualreports. Accessed June 5, 2021.

26. Dębska-Ślizień A, Rutkowski B, Rutkowski P, et al. Actual condition of renal replacement therapy in Poland in year 2017 [in Polish]. *Nefrol Dial Pol*. 2018;22:133–140. https://nefroldialpol.pl/wp-content/uploads/2021/02/NDP-3-4-2020_RAPORT-A-Debska.pdf

27. Ribitsch W, Haditsch B, Otto R, et al. Effects of a pre-dialysis patient education program on the relative frequencies of dialysis modalities. *Perit Dial Int*. 2013;33(4):367–371. doi:10.3747/pdi.2011.00255

28. Marron B, Martinez Ocana JC, Salgueira M, et al. Analysis of patient flow into dialysis: Role of education in choice of dialysis modality. *Perit Dial Int*. 2005;25(Suppl 3):S56–S59. PMID:16048258.

29. Liebman SE, Bushinsky DA, Dolan JG, Veazie P. Differences between dialysis modality selection and initiation. *Am J Kidney Dis*. 2012;59(4):550–557. doi:10.1053/j.ajkd.2011.11.040

30. Dahlan RA, Alsuwaida AO, Farrash MS, et al. Let us listen to patients: Underutilization of peritoneal dialysis from patients' perspectives. *Perit Dial Int*. 2017;37(5):574–576. doi:10.3747/pdi.2016.00321

31. Chadban SJ, Ahn C, Axelrod DA, et al. KDIGO Clinical Practice Guideline on the evaluation and management of candidates for kidney transplantation. *Transplantation*. 2020;104(4S1 Suppl 1):S1–S103. doi:10.1097/TP.0000000000003136

32. Poltransplant. Biuletyn Informacyjny Poltransplantu. www.poltransplant.pl/Download/Biuletyn2020. Accessed July 25, 2021.

33. Cankaya E, Cetinkaya R, Keles M, et al. Does predialysis education program increase the number of pre-emptive renal transplantation? *Transpl Proc*. 2013;45(3):887–889. doi:10.1016/j.transproceed.2013.02.075

Interprofessional collaboration in the renal care settings: Experiences in the COVID-19 era

*Ewa Pawłowicz-Szlarska[1,A–D,F], *Maria Sawościan[2,A–D,F], Klaudia Lipińska[2,B–D,F], Kaja Kendyś[2,B–D,F], Michał Nowicki[1,A,C–F]

[1] Department of Nephrology, Hypertension and Kidney Transplantation, Medical University of Lodz, Poland

[2] Student Scientific Society affiliated with the Department of Nephrology, Hypertension and Kidney Transplantation, Medical University of Lodz, Poland

A – research concept and design; B – collection and/or assembly of data; C – data analysis and interpretation;
D – writing the article; E – critical revision of the article; F – final approval of the article

Address for correspondence
Michał Nowicki
E-mail: michal.nowicki@umed.lodz.pl

Abstract

Background. The role of interprofessional collaboration (IPC) in healthcare is increasingly emphasized. Due to significant comorbidity in renal patients who require highly specialized procedures, proper IPC is an essential component in renal care. During the coronavirus disease 2019 (COVID-19) pandemic, the existing and proven collaboration mechanisms were put to the test.

Objectives. To assess IPC in the renal care settings in the era of COVID-19 pandemic.

Materials and methods. The survey consisted of the Assessment of Interprofessional Team Collaboration Scale II (AITCS-II) (3 subscales – partnership, cooperation and coordination, maximum of 5 points), questions about work conditions and factors influencing work during the pandemic, as well as demographic data. The survey was distributed in 8 renal care settings (4 hospital wards with dialysis units and 4 individual dialysis units); 127 participants filled out the survey; 26.8% of participants were physicians, 68.5% nurses and 4.7% other staff members, i.e., administrative assistants. Mean work experience in their current team was 16.8 ±11.7 years among nurses and 11.6 ±9.7 years among physicians.

Results. Interprofessional collaboration was assessed by physicians and nurses, respectively, as follows: partnership 4.03 ±0.79 compared to 3.58 ±0.73 (p = 0.003), cooperation 4.28 ±0.59 compared to 3.71 ±0.72 (p = 0.0002), and coordination 3.83 ±0.87 compared to 3.48 ±0.82 (p = 0.04). The specific workplace did not influence the IPC rates; 49.9% of physicians and 40.1% of nurses agreed or strongly agreed that the collaboration worsened during the pandemic; 47% of physicians and 42.4% of nurses admitted that the communication has significantly deteriorated. An increased level of stress, new procedures and fear of getting infected with severe acute respiratory syndrome coronavirus 2 (SARS-CoV-2) were, according to the participants, the most significant factors for the worsening of IPC.

Conclusions. The exceptional circumstances faced during the pandemic have a significant impact on IPC, which may influence patients' satisfaction and safety. An active support for healthcare teams in the field of IPC is especially important in this challenging reality.

Key words: COVID-19, interprofessional collaboration, nephrology, renal care

Background

In recent years, many studies have shown the key role of interprofessional collaboration (IPC) in healthcare and its impact on work processes and patients' safety.[1] The IPC has become an important factor in well-functioning medical teams.[2] The collaboration among healthcare professionals, regardless of medical domain, is essential in creating a synergy to provide efficient, safe and high-quality patient care.[3] Multifunctional teams tend to be more productive and innovative in coping with risk assessment and management. It has been proven that IPC may lead to improved healthcare systems and outcomes.[4] Good practice of IPC has been associated with improved health outcomes, including decreased mortality rate.[5] Consequently, more and more emphasis is placed on interprofessional education (IPE), which leads to medical students valuing the need of proper IPC.[6]

In the study by Tonelli et al., the complexity of patients seen by different medical specialists was assessed and compared using 9 factors of complexity including the number of comorbidities, presence of mental illness, number of types of physicians involved in each patient's care, number of physicians involved in each patient's care, number of prescribed medications, number of emergency department visits, rate of death, rate of hospitalization, and rate of placement in a long-term care facility.[7] It was concluded that nephrologists deal with the most complex patients, as compared to 12 other specialties. Obviously, the complexity of renal patients affects all healthcare professionals taking care of this group of patients.

The significant complexity of patients with kidney diseases and the need to provide care to patients who need highly specialized medical procedures require an appropriate collaboration between medical and nursing staff as well as other healthcare professionals.

Taking into account the abovementioned factors, the collaboration in nephrology is addressed more and more often in the scientific reports. For instance, a feasible strategy of the use of electronic collaboration tool such as Slack (Slack Technologies, San Francisco, USA), which facilitates real-time conversational communication in a private or semiprivate virtual workspace, was described recently.[8] Fulton et al. developed and evaluated an interprofessional palliative care and geriatrics curriculum for nephrology teams, concluding that IPC may result in improved management of patients with chronic kidney disease (CKD) or end-stage kidney disease.[9] A qualitative analysis of IPC between nephrologists and intensive care unit (ICU) practitioners revealed significant difficulties stemming from discordant preferences about the aggressiveness of renal replacement therapy, based on different understanding of physiology, goals of care and acuity.[10]

While the coronavirus disease 2019 (COVID-19) pandemic has overrun the world with numerous cases and deaths, it has also challenged the healthcare systems, putting the existing guidelines and solutions to test.[11] It is suggested that many of these challenges can be addressed by placing a greater emphasis on the use of IPE to underpin and support effective collaborative working.[12] As it was indicated by Goldman and Xyrichis, studying IPC during the COVID-19 pandemic is an important goal for health services research in the months and years to come, both to reinforce the current response and prepare for future challenges.[13]

Objectives

Bearing in mind the complexity of nephrology patients, the new challenges posed by the pandemic and the need to study work-related challenges in the COVID-19 era, we decided to conduct research in order to assess IPC in nephrology facilities in the era of the severe acute respiratory syndrome coronavirus 2 (SARS-CoV-2) pandemic.

Participants and methods

Study survey and design

A 41-item study survey comprised the Assessment of Interprofessional Team Collaboration Scale II (AITCS-II)[14,15] and a section of self-created questions about working during the COVID-19 pandemic.

The AITCS-II is a validated tool that consists of 3 subscales: (1) partnership – 8 items; (2) cooperation – 8 items; and (3) coordination – 7 items. Each item is rated on a 5-point Likert scale where: 1 – never; 2 – rarely; 3 – occasionally; 4 – most of the time; and 5 – always. Subscale scores were calculated by averaging the mean values of all 3 subscale items, whereas the total score was determined by taking an average of all 3 subscales. The survey was translated into by the researchers with the consent of the authors of the survey.

The questionnaire was preceded by demographic data collection, which included additional specifications associated with our research:

– job specification (for physicians) – a registrar; a resident; a specialist; other;

– unit of employment – clinical nephrology ward; dialysis center; both;

– prevalent unit of employment (for employees working in both type of units);

– weekly work time;

– holiday leave – complete; partial; neither;

– work experience in years;

– team experience in current place of employment.

The 2nd part of the questionnaire consisted of 3 parts. In the 1st one, the participants were asked to assess the change in the collaboration and working conditions

during the SARS-CoV-2 pandemic on a 1–5 Likert-type scale. In the 2nd part, they were provided with 9 possible explanations for the change in the working conditions and were asked to choose the factors they found most crucial in creating the differences. In the last, non-obligatory section, the participants were invited to provide their own opinions and concerns regarding the pandemic and IPC in the COVID-19 era.

Surveys were collected from January 14 to May 6, 2021, across 4 hospital nephrology wards integrated with dialysis units and 4 individual dialysis units located in 1 province (voivodeship) in Central Poland.

The study protocol was approved by the local ethics committee of Medical University of Lodz (approval No. RNN/30/12/KE of January 12, 2021).

Study group

The study group comprised 127 participants, including 87 nurses, 34 physicians and 6 participants who also completed the survey and were the representatives of other professions – e.g., administrative personnel. The characteristics of the study group are provided in Table 1. The participants were approached directly and provided with printed copies of the questionnaire, which were collected upon completion.

Statistical analyses

Due to a greatly limited number of other types of professionals represented in the study group, only the answers of nurses and physicians (n = 121) were analyzed statistically. Statistical analysis was performed using Statistica v. 13.1 PL software (StatSoft Inc., Tulsa, USA). Graphs were plotted with the use of Microsoft Excel Office 365 (Microsoft Corp., Redmond, USA). The normality of the distribution of the continuous variables was assessed with Shapiro–Wilk test. Mann–Whitney U test was used for comparisons between 2 independent groups. Nonparametric comparisons of more than 2 groups were performed with Kruskal–Wallis test. Nonparametric correlations were assessed with Spearman's method. Pearson's χ^2 test was used for comparisons of categorical data. There was 1.2% of missing data in AITCS-II items. More missing data occurred in the demographic part of the survey, where pairwise deletion was performed. To determine internal consistency reliability, Cronbach's alpha was calculated for each subscale of the AITCS-II. It amounted to 0.91, 0.94 and 0.93 for partnership, cooperation and coordination, respectively.

Results

The results of the AITCS-II for nurses and physicians are provided in Table 2. No statistically significant differences ($p > 0.05$) in AITCS-II and its subscale scores were found between nurses working mostly in dialysis and hospital settings; also, no statistically significant differences were found between physicians, as presented in Table 3. No statistically significant correlations between partnership, collaboration and coordination rates and age as well as the length of professional experience (overall and in the current team) in nurses and doctors were found; these correlations are provided in Table 4. Also, no statistically significant differences in AITCS-II overall score were found with regard

Table 1. The study group characteristics

Characteristic	Nurses (n = 87)	Physicians (n = 34)	Other professions (n = 6)
Females, n (%)	87 (100)	22 (64.7)	6 (100)
Males, n (%)	0 (0)	12 (35.3)	0 (0)
Age [years], mean ±SD	49.7 ±9.7	44.5 ±13.2	49.7 ±5.1
Length of experience in the current team [years], mean ±SD	16.8 ±11.7	11.6 ±9.7	11.3 ±8.8
Place of work			
In-patient hospital settings, n (%)	9 (10.5)	6 (17.6)	1 (16.7)
Dialysis units, n (%)	60 (69.8)	11 (32.4)	5 (83.3
Both units, n (%)	17 (19.7)	17 (50)	0 (0)

SD – standard deviation.

Table 2. Mean score of Assessment of Interprofessional Team Collaboration Scale II (AITCS-II) and its subscales in nurses and physicians

AITCS-II and subscales scores	Nurses	Physicians	p-value*
AITCS-II overall (mean ±SD)	3.59 ±0.66	4.06 ±0.7	0.0018[a]
Partnership (mean ±SD)	3.58 ±0.73	4.03 ±0.79	0.0034[b]
Cooperation (mean ±SD)	3.71 ±0.72	4.28 ±0.59	0.0002[c]
Coordination (mean ±SD)	3.48 ±0.82	3.83 ±0.87	0.0406[d]

*Mann–Whitney U test; U values: [a] – 939.5; [b] – 971.0; [c] – 823.5; [d] – 1124.0. SD – standard deviation.

Table 3. Mean score of Assessment of Interprofessional Team Collaboration Scale II (AITCS-II) and its subscales in nurses and physicians working mostly in hospital settings and dialysis units

AITCS-II and subscales scores	Hospital settings	Dialysis units	p-value*
Nurses			
AITCS-II overall (mean ±SD)	3.51 ±0.54	3.61 ±0.69	0.5791
Partnership (mean ±SD)	3.55 ±0.48	3.59 ±0.77	0.6267
Cooperation (mean ±SD)	3.63 ±0.81	3.73 ±0.72	0.7788
Coordination (mean ±SD)	3.32 ±0.55	3.51 ±0.86	0.3302
Physicians			
AITCS-II overall (mean ±SD)	4.05 ±0.73	4.07 ±0.68	0.9293
Partnership (mean ±SD)	4.08 ±0.78	3.97 ±0.83	0.6696
Cooperation (mean ±SD)	4.24 ±0.67	4.35 ±0.47	0.9286
Coordination (mean ±SD)	3.8 ±0.83	3.89 ±0.96	0.7223

*Mann–Whitney U test. SD – standard deviation.

Table 4. Correlation coefficients (r) and p-values of Spearman's correlations between Assessment of Interprofessional Team Collaboration Scale II (AITCS-II) subscale scores and age and length of professional experience in nurses and physicians

Score	Age	Overall length of professional experience	Length of professional experience in the current team
Nurses			
Partnership score	r = −0.004, p = 0.9732	r = −0.031, p = 0.7861	r = −0.204, p = 0.074
Cooperation score	r = 0.161, p = 0.146	r = 0.142, p = 0.2057	r = 0.155, p = 0.1763
Coordination score	r = 0.065, p = 0.56	r = 0.037, p = 0.7437	r = −0.029, p = 07972
Physicians			
Partnership score	r = −0.156, p = 0.3869	r = −0.174, p = 0.3249	r = −0.248, p = 0.1643
Cooperation score	r = 0.132, p = 0.465	r = 0.093, p = 0.5998	r = −0.032, p = 0.8595
Coordination score	r = 0.147, p = 0.4142	r = 0.122, p = 0.4929	r = −0.036, p = 0.8441

to weekly worktime (p = 0.7752, Kruskal–Wallis test) and the use of the holiday leave (p = 0.1917, Kruskal–Wallis test).

Briefly, 49.9% of physicians and 40.1% of nurses agreed or strongly agreed that IPC worsened during the pandemic; 47% of physicians and 42.4% of nurses stated that the communication between these 2 groups has significantly deteriorated in the COVID-19 era; 44.8% of nurses agreed or strongly agreed that since the outbreak of the pandemic, they could have relied only on themselves, while only 17.7% of physicians stated so (χ^2 = 7.25, df = 1, p = 0.0071).

The factors regarded by nurses and physicians as crucial in creating the differences in the IPC during the pandemic are provided in Fig. 1. An increased level of stress, the rapid change of procedures at the time of pandemic and fear of SARS-CoV-2 infection were considered to be most important.

Nine participants (7%) expressed their additional opinions and concerns regarding the interprofessional collaboration in the COVID-19 era. The quotes are provided in Table 5. Participants pointed out the lesser amount of time spent with patients due to the new procedures, physical and psychological exhaustion of the staff members, and insufficient reimbursement at the time of pandemic.

Discussion

Our results indicate that IPC in the COVID-19 era is an important challenge, as the self-assessed perceptions of both collaboration and communication reported by nurses and physicians significantly worsened. The exceptional circumstances faced in the time of pandemic have an impact on IPC in healthcare, which may influence patients' satisfaction and safety, and thus, IPC should be addressed and improved.

What is important, physicians rated IPC in all ATICS-II subscales significantly higher than nurses in our study population. Previous literature regarding IPC also showed the varied approaches of physicians and nurses to doctor–nurse cooperation.[16] Our findings are consistent with the research conducted by Carney et al. proving that physicians rate IPC higher than the nursing staff.[17] Possible reasons of this phenomenon may comprise the differences in education, role expectations, gender distribution, and approach to practice.[18] It was proven that nurses are trained to communicate more holistically, using the "story" of the patient, while physicians tend to communicate using the "headlines".[19] According to Tang et al.,[20] the factors affecting physician–nurse collaboration include
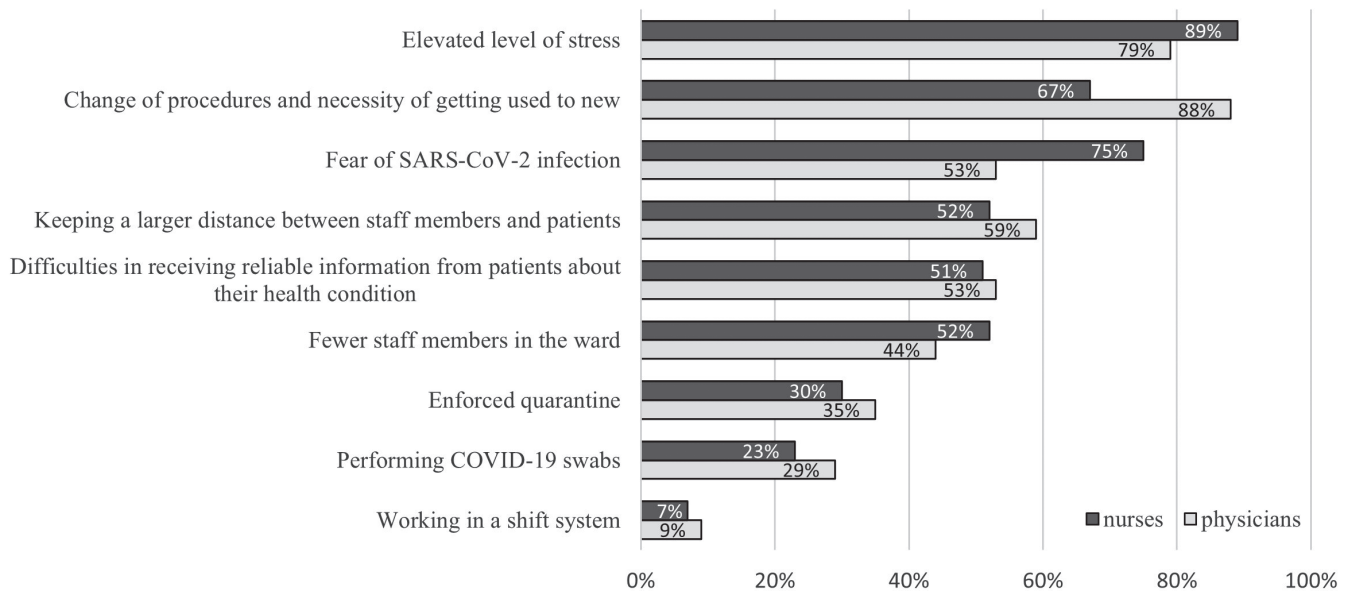
Fig. 1. Factors influencing the quality of interprofessional collaboration during the severe acute respiratory syndrome coronavirus 2 (SARS-CoV-2) pandemic

COVID-19 – coronavirus disease 2019.

Table 5. Participants reflections on factors influencing interprofessional collaboration in renal care settings during the pandemic

Participant	Quotation – factors influencing interprofessional collaboration in renal care settings during the pandemic
Female, physician, 33 years old	Extending the time needed to prepare for the patient visit and the use of PPE, while necessary, extends also the time from the call for help from the patient to the moment when the patient receives it. It has a negative impact on our work; it's both stressful for the doctors/nurses and dangerous for the patients. Extending the duration of the procedures due to the use of PPE comes at the price of time allocated to COVID-negative patients and has a negative influence on the teamwork.
Female, physician, 37 years old	My assessment is that the cooperation in the doctors' teams is better than the cooperation between doctors and nurses. I would say that there are some individuals who damage the general reputation.
Female, physician, 32 years old	The negative influence – patient and personnel isolation, lack of possibility to exchange opinions easily. The PPE greatly limits the nonverbal communication (the face masks require "screaming" instead of a conversation, inability to observe lip movement makes it more difficult for patients with advanced age or sickness to understand). The positive influence – the increase in adherence to sanitary procedures, more frequent hand sanitization, PPE usage.
Female, nurse, 24 years old	Increase of physical and psychological exhaustion due to the sanitary procedures, protective clothing, the number of obligations, limited time. Working with COVID-positive patients is more labor-consuming and requires more time, which is already in shortage, as well as physical strength. It is often that you work with COVID patients alone in order to limit the contact and it is obvious that you cannot do everything single-handedly, and if you do, it comes at the price of health deterioration.
Female, physician, 26 years old	Problematic access to the patient increases the unease in their families and distrust of the doctors and healing process, the diagnosis and quality of care for the patient. The patients themselves feel alienated, detached from their close ones, scared, all of which exacerbate the prognosis. Because of the necessity to wear the protective coverall, the doctor–patient contact is superficial – the physicians limit themselves to necessary procedures, and the patients focus more on the coverall than the person wearing it, which makes them scared.
Female, nurse, 50 years old	No increase in salary to make up for the difficult conditions results in a negative impact on eagerness and work commitment.
Female, nurse, 60 years old	Lack of appropriate payment for working in such difficult pandemic conditions, with COVID-positive patients. Also, lack of any kind word in tough times, no interest or support.
Female, nurse, 50 years old	No cooperation with the ward management staff.
Female, physician, 58 years old	Lack of possibility to transfer COVID-positive patients to dialysis stations; employees on sick leave.

PPE – personal protective equipment; COVID – coronavirus disease.

communication, respect and trust, unequal power, understanding professional roles, and task prioritizing.

On the other hand, some reports showed that nurses have a more positive attitude towards IPC than physicians. Physicians viewed physician–nurse collaboration as less important than nurses, but rated the quality of collaboration higher than nurses.[20] As reported by Mahboube et al., nurses, compared to physicians, showed a more positive attitude toward shared education and teamwork, caring as opposed to curing and physicians'

dominance.[21] The experiences gathered during the CO-VID-19 pandemic and their impact on IPC are a new and, to the knowledge of researchers, unexplored aspect of renal patient care.

The reflections on the work-related experiences and perceptions of renal healthcare team members on the front lines of the COVID-19 pandemic were presented by Zerbi et al.[22] This editorial, in which free statements on work during the pandemic were shared by 3 nurses, 2 nurse's aides and 1 psychologist, gave only a narrative insight into the situation and provided no quantitative data on working environment in these extraordinary circumstances. The importance of cooperation between nurses during the crisis and the significance of shared experiences for strengthening mutual understanding were emphasized by the participants.

When it comes to dealing with the pandemic crisis, an interesting initiative was the creation of the mobilizer team in one of academic medical center in the USA.[23] The mobilizer team consisted of clinical and operational administrative leaders and its task was to provide a 24-hour support to the front line teams. It gave various specialists a chance to work together, sometimes for the first time. Subsequently, it created partnerships between these specialists and provided an opportunity for the development of IPC in the healthcare system. The situations such as pandemic show that mechanisms and procedures aiming to manage a team in a crisis are greatly needed and should be constantly improved and developed. It also indicates a huge need to introduce and evolve IPE programs, taking into account current global challenges.

Limitations

Limitations of our study include the assessment of perceptions rather than staff behavior or patient outcomes; the latter would give another perspective on actual IPC practice. Results were gathered only from voluntary respondents. The data were gathered in 1 province in 1 country, so the generalizability of our results across other countries and regions all around the globe is limited, and the cultural aspects as well as healthcare organization may bias the potential comparisons. Also, no comparison with the pre-pandemic situation was possible due to lack of assessment of IPC using similar study design. However, to the best of our knowledge, our research is the first report on work-related perceptions focused on IPC of renal care practitioners during the COVID-19 pandemic and corresponds with the need for further research in this area.

Conclusions

We found that partnership, cooperation and coordination are perceived as significantly worse by nurses than physicians. The IPC worsened significantly during the pandemic both according to physicians and nurses.

The communication between nurses and physicians also deteriorated. The factors which may influence IPC practice in face of the pandemic challenge included an increased level of stress, rapid changes of the procedures and fear of SARS-CoV-2 infection. Our data suggest that an active support for renal care teams in the field of collaboration, partnership, cooperation, and coordination is especially important in this challenging reality.

ORCID iDs

Ewa Pawłowicz-Szlarska   https://orcid.org/0000-0001-8864-4131
Maria Sawościan   https://orcid.org/0000-0003-4171-1637
Klaudia Lipińska   https://orcid.org/0000-0003-4723-9572
Kaja Kendyś   https://orcid.org/0000-0002-2065-543X
Michał Nowicki   https://orcid.org/0000-0002-0823-5440

References

1. Reeves S, Pelone F, Harrison R, Goldman J, Zwarenstein M. Interprofessional collaboration to improve professional practice and healthcare outcomes. *Cochrane Database Syst Rev*. 2017;6(6):CD000072. doi:10.1002/14651858.CD000072.pub3
2. Karam M, Tricas-Sauras S, Darras E, Macq J. Interprofessional collaboration between general physicians and emergency department teams in Belgium: A qualitative study. *Int J Integr Care*. 2017;17(4):9. doi:10.5334/ijic.2520
3. Wei H, Corbett RW, Ray J, Wei TL. A culture of caring: The essence of healthcare interprofessional collaboration. *J Interprof Care*. 2020; 34(3):324–331. doi:10.1080/13561820.2019.1641476.
4. Morley L, Cashell A. Collaboration in healthcare. *J Med Imaging Radiat Sci*. 2017;48(2):207–216. doi:10.1016/j.jmir.2017.02.071
5. Spaulding EM, Marvel FA, Jacob E, et al. Interprofessional education and collaboration among healthcare students and professionals: A systematic review and call for action. *J Interprof Care*. 2019;35(4): 612–621. doi:10.1080/13561820.2019.1697214
6. Zechariah S, Ansa BE, Johnson SW, Gates AM, Leo G. Interprofessional education and collaboration in healthcare: An exploratory study of the perspectives of medical students in the United States. *Healthcare (Basel)*. 2019;7(4):117. doi:10.3390/healthcare7040117
7. Tonelli M, Wiebe N, Manns BJ, et al. Comparison of the complexity of patients seen by different medical subspecialists in a universal healthcare system. *JAMA Netw Open*. 2018;1(7):e184852. doi:10.1001/jamanetworkopen.2018.4852
8. Lin J. Picking up the slack: Collaboration tools to build community and increase productivity in nephrology. *Semin Nephrol*. 2020;40(3): 298–302. doi:10.1016/j.semnephrol.2020.04.009
9. Fulton AT, Richman K, Azar M, et al. A novel interprofessional palliative care and geriatrics curriculum for nephrology teams. *Am J Hosp Palliat Care*. 2020;37(11):913–917. doi:10.1177/1049909120915462
10. Clapp JT, Diraviam SP, Lane-Fall MB, et al. Nephrology in the academic intensive care unit: A qualitative study of interdisciplinary collaboration. *Am J Kidney Dis*. 2020;75(1):61–71. doi:10.1053/j.ajkd.2019.05.030
11. Butler SM. After COVID-19: Thinking differently about running the healthcare system. *JAMA*. 2020;323(24):2450–2451. doi:10.1001/jama.2020.8484
12. Gray R, Sanders C. A reflection on the impact of COVID-19 on primary care in the United Kingdom. *J Interprof Care*. 2020;34(5):672–678. doi:10.1080/13561820.2020.1823948
13. Goldman J, Xyrichis A. Interprofessional working during the COVID-19 pandemic: Sociological insights. *J Interprof Care*. 2020;34(5):580–582. doi:10.1080/13561820.2020.1806220
14. Orchard CA, King GA, Khalili H, Bezzina MB. Assessment of Interprofessional Team Collaboration Scale (AITCS): Development and testing of the instrument. *J Contin Educ Health Prof*. 2012;32(1):58–67. doi:10.1002/chp.21123
15. Orchard C, Pederson LL, Read E, Mahler C, Laschinger H. Assessment of Interprofessional Team Collaboration Scale (AITCS): Further testing and instrument revision. *J Contin Educ Health Prof*. 2018;38(1):11–18. doi:10.1097/CEH.0000000000000193

16. House S, Havens D. Nurses' and physicians' perceptions of nurse–physician collaboration: A systematic review. *J Nurs Adm*. 2017;47(3):165–171. doi:10.1097/NNA.0000000000000460

17. Carney BT, West P, Neily JB, Mills PD, Bagian JP. Improving perceptions of teamwork climate with the Veterans Health Administration medical team training program. *Am J Med Qual*. 2011;26(6):480–484. doi:10.1177/1062860611401653

18. Mannahan CA. Different worlds: A cultural perspective on nurse–physician communication. *Nurs Clin North Am*. 2010;45(1):71–79. doi:10.1016/j.cnur.2009.10.005

19. Makary MA, Sexton JB, Freischlag JA, et al. Operating room teamwork among physicians and nurses: Teamwork in the eye of the beholder. *J Am Coll Surg*. 2006;202(5):746–752. doi:10.1016/j.jamcollsurg.2006.01.017

20. Tang CJ, Chan SW, Zhou WT, Liaw SY. Collaboration between hospital physicians and nurses: An integrated literature review. *Int Nurs Rev*. 2013;60(3):291–302. doi:10.1111/inr.12034

21. Mahboube L, Talebi E, Porouhan P, Orak RJ, Farahani MA. Comparing the attitude of doctors and nurses toward factor of collaborative relationships. *J Family Med Prim Care*. 2019;8(10):3263–3267. doi:10.4103/jfmpc.jfmpc_596_19

22. Zerbi S, Resmini B, Merlino M, et al. Inferno, disruption, concern, sense of community, teamwork, tears: Reflections by renal healthcare team members on the front lines of the COVID-19 pandemic. *J Nephrol*. 2021;34(1):7–10. doi:10.1007/s40620-020-00921-y

23. Stifter J, Terry A, Phillips J, Heitschmidt M. A short report on an interprofessional mobilizer team: Innovation and impact during the COVID-19 pandemic. *J Interprof Care*. 2020;34(5):716–718. doi:10.1080/13561820.2020.1813696

The arterial stiffness changes in hemodialysis patients with chronic kidney disease: The impact on mortality

Konrad Rekucki[1,A–F], Agnieszka Sławuta[2,A,B,D–F], Dorota Zyśko[3,C,E], Katarzyna Madziarska[4,A–F]

[1] Department of Cardiology, T. Marciniak Lower Silesian Specialist Hospital, Wrocław, Poland

[2] Department of Internal and Occupational Diseases, Hypertension and Clinical Oncology, Wroclaw Medical University, Poland

[3] Department of Emergency Medicine, Wroclaw Medical University, Poland

[4] Department of Nephrology and Transplantation Medicine, Wroclaw Medical University, Poland

A – research concept and design; B – collection and/or assembly of data; C – data analysis and interpretation;
D – writing the article; E – critical revision of the article; F – final approval of the article

Abstract

Background. Patients with kidney disease suffer from high cardiovascular risk due to classic and disease-specific risk factors. Arterial stiffness is a novel cardiovascular risk factor whose role is yet to be established. High-resolution echo-tracking is a developing method for the assessment of local arterial stiffness.

Objectives. To assess carotid stiffness in patients on long-term hemodialysis (HD) using high-resolution echo-tracking and to analyze the impact of arterial stiffness on mortality in the mid-term follow-up.

Materials and methods. Fifty-eight HD patients (28 female (F), 30 male (M)) underwent clinical examination, laboratory tests and carotid stiffness assessment. Local arterial stiffness parameters such as beta stiffness index (β), Young's modulus (Ep), arterial compliance (AC), and one-point pulse wave velocity (PWVβ) were measured both before and after HD, allowing to calculate their change (Δ). The survival of patients was analyzed up to 48 months. The multivariate analysis of survival with the use of Cox proportional hazard stepwise regression was performed to determine the factors significantly correlated with the survival.

Results. After 48 months, 33 patients were alive (16 F, 17 M) and 25 patients (12 F, 13 M) died. The deceased group was significantly older (66.5 ±12.3 years compared to 56.6 ±17.8 years), had more pronounced coronary artery disease (percutaneous coronary intervention (PCI) 36% compared to 9%, $p < 0.05$, respectively). Deceased patients had significantly higher ΔAC than survivors. The results showed that age, history of PCI, left ventricular ejection fraction (LVEF), ΔAC, fasting glucose, serum total protein, sodium level after HD, and potassium level before HD were significantly associated with mortality.

Conclusions. Echo-tracking-based arterial stiffness assessment in patients with chronic kidney disease (CKD) yields the clinical information regarding mid-term mortality risk. A paradoxical increase in AC is among independent risk factors for mid-term mortality in patients undergoing maintenance HD. The proper estimation of the correlations among vascular, hemodynamic and sympathetic-dependent changes in a given patient with kidney failure is complex.

Key words: hemodialysis, chronic kidney disease, arterial stiffness, mortality, echo-tracking

Background

Cardiovascular diseases are the leading cause of death in patients with chronic kidney disease (CKD).[1] These patients suffer from high cardiovascular risk due to traditional and disease-specific risk factors. Arterial stiffness has been proven to be independently associated with a higher global risk of death in patients suffering from CKD.[2] The measurement of local arterial stiffness in CKD patients may be of particular value due to the limitations of classic diagnostic methods in this group of patients,[3,4] such as electrocardiographic exercise test or stress echocardiography.[5] These patients are less likely to have the classic symptoms of myocardial ischemia, hence the need to look for new tools to improve clinical evaluation. Damage to the kidneys also limits the possibility of using tests with contrast media – coronary angiography and computed tomography.[3] In this group of patients, the diagnostic value of laboratory exponents of cardiovascular function, such as N-terminal pro B-type natriuretic peptide (NT-proBNP) or cardiac troponin, is also lower.[6,7] Chronic kidney disease is affecting 10–16% of the world population.[8–10] As glomerular filtration rate (GFR) decreases, the likelihood of hypertension increases.[11] People with CKD are also characterized by an increased tendency to develop advanced atherosclerotic lesions.[12] It should be emphasized that the presence of classic cardiovascular risk factors such as diabetes, hypertension, nicotinism, and dyslipidemia does not sufficiently explain the clear increase in the risk of cardiovascular death in patients with CKD.[4,10]

Stiffness is one of the properties of arteries resulting from the vessel wall structure, in particular from the ratio of collagen to elastic fibers.[13,14] Left ventricular contraction causes an ejection of a certain volume of blood into the systemic circulation. The appearance of additional blood volume in the ascending aorta causes its distension, which is possible due to its high elasticity. This distension is then transferred to the distal parts of the arterial system, forming a pulse wave. The pulse wave, reaching the resistance vessels, is reflected due to the increase in the stiffness of arteries. The reflected wave returns to the ascending aorta in diastole, supporting coronary perfusion. The final shape of the pulse wave is therefore a result of a progressive wave and reflected wave. The increase in the stiffness of arteries, particularly in the aorta, leads to a shorter distance between the heart and the place where the reflected wave is formed, as well as to an increase in pulse wave speed. This causes many adverse effects on the cardiovascular system. The resulting reduction in diastolic blood pressure impairs coronary perfusion. At the same time, high central blood pressure leads to an increase in left ventricular afterload in the pressure overload mechanism. Therefore, an increase in arterial stiffness is a part of the development of hypertension, ischemic heart disease and heart failure.[15,16] Both aging and diseases such as essential hypertension, diabetes and CKD contribute to the increase in arterial stiffness.[17–19]

High-resolution echo-tracking is a direct and noninvasive method of the evaluation of local arterial stiffness. It is obtained by ultrasound examination at one point of the arterial system, usually at the site of the common carotid artery. According to experts from the European Society of Cardiology (ESC), it is recognized that methods for measuring local arterial stiffness, such as high-resolution echo-tracking, are useful in pathophysiology and therapy studies.[13] In recent years, the interest in using high-resolution echo-tracking in patients with CKD has increased.[20–22] There is growing evidence that carotid stiffness assessment may contribute to a better risk stratification of CKD patients. Studies have shown that carotid stiffness parameters obtained with high-resolution echo-tracking may be used in prediction of all-cause mortality in patients with kidney failure treated with hemodialysis (HD).[21]

Objectives

The aim of the study was to assess local arterial stiffness parameters in patients undergoing maintenance HD and relate these parameters to mortality in the mid-term follow-up.

Materials and methods

Study design and participants

This was a prospective cohort study. The analysis was performed in 58 patients (28 women and 30 men) with kidney failure treated with HD at Dialysis Center in Department of Nephrology and Transplantation Medicine (Wroclaw Medical University, Wrocław, Poland). Hemodialysis sessions were conducted 3 times a week for 4 h per session. The study group was formed in 2015 and patients were observed until 2019. The patients included in the study were free of active infection. We excluded patients with persistent or permanent atrial fibrillation, history of malignancy and diseases requiring immunosuppressive treatment.

All patients were treated with erythropoietin and intravenous iron supplementation according to standards. Beta-blockers, angiotensin converting enzyme (ACE) inhibitors, angiotensin receptor blockers (ARBs), calcium channel blockers, and alpha blockers were used in the treatment of hypertension. All patients were dialyzed using a native arteriovenous fistula.

The study was approved by Institutional Ethics Committee of the Wroclaw Medical University, Poland.

Variables and data sources

In all subjects, data on cardiovascular morbidity and causes of kidney failure were collected. Clinical data of patients were extracted from the hospital records.

At the study onset, the following factors were analyzed: baseline characteristics, duration of dialysis, adequacy of dialysis (Kt/V), body mass index (BMI), and laboratory parameters. Blood samples were collected prior to the initiation of HD session. Routine laboratory tests were measured in the Central Hospital Laboratory, University Hospital in Wrocław, Poland, as a part of the standard care.

Heart rate, blood pressure measurements and carotid elasticity with echo-tracking technique were investigated at the study onset, before and after a single mid-week HD session. All patients underwent transthoracic echocardiogram.

Assessment of local arterial stiffness

Images were obtained with an Aloka Alpha 6 ultrasonograph (Aloka Co., Ltd., Tokyo, Japan) equipped with an integrated and automated Doppler and high-resolution echo-tracking system using a linear probe. Patients were examined in supine position 15 min before the start of HD and 15 min after the end of HD. A clear ultrasonographic visualization of both anterior and posterior wall of the common carotid artery opposite to the arteriovenous fistula was taken 1–2 cm below bifurcation in the longitudinal axis. Consequently, after establishing the intima-media complex, the echo-tracking samples were positioned at the end of intima, with an 1 kHz sampling rate for continuous detection of movement of the arterial wall. Thus, a graphical representation of change in the diameter of the artery was recorded as a waveform. Three to five evolutions were recorded to obtain a representative waveform.

To calculate local arterial stiffness parameters, it is necessary to register high-resolution echo-tracking, heart cycle and blood pressure. Heart cycle was recorded using standard electrocardiographic limb leads I, II and III. Blood pressure was measured over the brachial artery opposite the arteriovenous fistula in supine position, directly before the ultrasonographic examination.

As a result, the following parameters were calculated:

– β – beta stiffness index – ratio of the natural algorithm of systolic/diastolic blood pressure to the relative change in diameter:

$$\beta = \ln (Ps/Pd)/[(Ds - Dd)/Dd]$$

where: ln – the natural logarithm, Ps – systolic blood pressure, Pd – diastolic blood pressure, Ds – diameter of the artery in systole, Dd – diameter of the artery in diastole;

– Ep – epsilon, Young's modulus:

$$Ep = (Ps - Pd)/[(Ds - Dd)/Dd]$$

– AC – arterial compliance, calculated from the arterial cross-section and blood pressure:

$$AC = \pi(Ds{\times}Ds - Dd{\times}Dd)/[4{\times}(Ps - Pd)]$$

– PWVβ – one-point pulse wave velocity, derived from the time delay between the 2 consecutive waveforms representing the diastole of the artery, with the use of beta stiffness index:

$$PWV\beta = \sqrt{(\beta{\times}Pd/2{\times}r)}$$

where: β – beta stiffness index, Pd – diastolic blood pressure, r – blood density (1.050 kg/m^3).

The change (Δ) in carotid stiffness parameters was calculated as follows: $\Delta\beta = \beta$ after HD – β before HD; $\Delta Ep = Ep$ after HD – Ep before HD; $\Delta AC = AC$ after HD – AC before HD; $\Delta PWV\beta = PWV\beta$ after HD – PWVβ before HD.

Statistical analyses

Statistical analyses were performed using STATISTICA v. 12 (TIBCO Software, Palo Alto, USA). Continuous variables were checked for the distribution using the Shapiro–Wilk W test and if the value of p was < 0.05, the assumption for normality was discarded. The Shapiro–Wilk W test showed normal distribution for the following variables: age, adequacy of HD, ultrafiltration during HD session, BMI, all echocardiographic parameters, echo tracking parameters except for Ep after HD, all blood pressure and heart rate parameters, and laboratory parameters except for fasting glucose, C-reactive protein (CRP) and high-density lipoprotein (HDL) cholesterol. Continuous variables with normal distribution were presented as means and standard deviations (SDs), and compared according to the survival groups (deceased compared to alive) with Student's t-test. Continuous variables without normal distribution were presented as medians and interquartile ranges (IQRs) and compared using Mann–Whitney U test. Discrete variables were presented as counts and percentages, and compared using χ^2 test. The comparison of the investigated parameters between the deceased patients depending on the causes of death (non-cardiovascular compared to cardiovascular mortality) was performed separately.

The multivariate survival analysis with the use of Cox proportional hazard stepwise regression was performed based on a model in which the dependent variable was the survival time since the inclusion in the study, while independent variables incorporated in the analysis were characteristics which differed in the one-way analysis with a significance of p < 0.15 between the 2 evaluated groups (survivors and non-survivors), or were relevant from the clinical point of view. In case of highly correlated variables such as heart rate before HD and heart rate after HD, serum total protein and serum total albumin, history of coronary artery disease and history of percutaneous coronary intervention (PCI), AC after HD and change in the arterial compliance (ΔAC), the more statistically significant variable was chosen. The following variables were considered for multivariate analysis: age, hypertension, history of PCI, left ventricular ejection fraction (LVEF), ΔAC, heart rate after HD, hemoglobin, serum total protein, fasting glucose, CRP, low-density lipoprotein (LDL) cholesterol, urea after HD, creatinine before HD, sodium level after HD, and potassium level before HD.

The survival analysis using Cox proportional hazard regression analysis was performed with the Cox proportional hazard analysis module. In the assumptions of the model, the reliability of Efron was selected, and models were created taking into account all effects and using the forward method. Then, Cox regression assumptions were assessed by analyzing Martingale-based residuals for survival models and Schoenfeld residuals over time, visually assessing a plot of the residuals compared to time. The correlation of residuals and time was examined using the Spearman's correlation. In case of finding a variable that violates the assumptions of the Cox proportional hazard regression, the variable was excluded from the model.

Receive operating characteristic (ROC) analysis was performed to find the cutoff point of echo-tracking parameters which differ between survivors and non-survivors. The Kaplan–Meier curve was constructed and the log-rank test was performed to present the survival in the groups of patients chosen on the basis of the founded cutoff points, as described above.

The multiple stepwise regression analysis was performed to find the association between echo-tracking parameters and age, gender, diabetes, and the presence of cardiovascular complications assessed as at least one of the following: previous myocardial infarction, stroke, history of coronary artery bypass graft surgery, or PCI. The variance inflation factor was assessed as the diagonal elements of the inverse correlation matrix. The Durbin–Watson test was performed to examine the autocorrelation of the residuals.

The results were considered statistically significant when the p-value was < 0.05.

Results

Clinical characteristics of the investigated patients at study onset are presented in Table 1.

Thirty-three patients from the initial cohort of 58 (56.89%) survived the whole 48-month observation period. Of the non-survivors, 11 patients (44%) died of cardiovascular diseases and 14 patients (56%) died of non-cardiovascular causes. The comparison of the investigated parameters between deceased and surviving patients is depicted in Table 2–4. The comparison of the investigated parameters between deceased patients depending on the causes (non-cardiovascular compared to cardiovascular mortality) is depicted in Table 5–7. The predictors of the overall mortality among the studied patients using Cox proportional hazards model are depicted in Table 8.

Based on the data obtained in the study, we created a multivariate analysis of survival with the use of Cox proportional hazard stepwise regression. The dependent variable was the survival of the whole 48-month observation period. Independent variables were: age, hypertension, history of PCI, LVEF, ΔAC, heart rate after HD, hemoglobin, fasting glucose, serum total protein, CRP, LDL cholesterol,

urea after HD, creatinine before HD, sodium level after HD, and potassium level before HD. The stepwise forward model showed that factors which significantly correlated with survival were: age, history of PCI, LVEF, ΔAC, fasting glucose, serum total protein, sodium level after HD, and potassium level before HD.

In Fig. 1, a plot of Martingale-based residuals compared to survival time was depicted. In Table 9, the Spearman's correlation between Schoenfeld residuals of the model and survival time was shown.

The ROC curve analysis was performed to find the cutoff point between patients who survived the 48-month observation period and the deceased. In the Fig. 2, the ROC curve analysis for the ΔAC in survivors and non-survivors was presented. The cutoff point aimed at differentiating the groups was −0.06 mm^2/kPa. The area under curve was 0.71; 95% confidence interval (95% CI): [0.56; 0.85]; p = 0.005.

In Fig. 3, the crude Kaplan–Meier survival curves for the difference in survival regarding ΔAC for patients with ΔAC ≥ −0.06 and ΔAC < −0.06 are presented. Patients with ΔAC ≥ −0.06 have worse outcome than patients with ΔAC < −0.06. We assessed the significant cutoff point of survival as −0.06 mm^2/kPa.

The stepwise multivariate regression analysis revealed that age was only associated with β after HD, with Ep after HD and with PWVβ after HD. However, gender, diabetes

Table 1. Clinical characteristics of the investigated patients at study onset

Variables	
Age [years], mean (SD)	60.9 (±16.3)
Male gender, n (%)	30 (51.7)
Duration of HD therapy [months], median (IQR)	39 (13.7–85.4)
Adequacy of dialysis [Kt/V], mean (SD)	1.39 (±0.34)
Hypertension, n (%)	43 (74.1)
Diabetes mellitus, n (%)	22 (37.9)
BMI [kg/m^2], mean (SD)	25.9 (±5.4)
The cause of kidney failure	
Chronic glomerular disease, n (%)	18 (31)
Diabetic nephropathy, n (%)	5 (8.6)
Polycystic kidney disease, n (%)	5 (8.6)
Interstitial nephropathy, n (%)	7 (12.1)
Hypertensive nephropathy, n (%)	18 (31)
Other, n (%)	5 (8.6)
Cardiovascular morbidity	
Coronary artery disease, n (%)	25 (43.1)
Myocardial infarction, n (%)	9 (15.5)
PCI, n (%)	12 (20.7)
CABG, n (%)	5 (8.6)
Stroke, n (%)	10 (17.2)

SD – standard deviation; IQR – interquartile range; BMI – body mass index; PCI – percutaneous coronary intervention; CABG – coronary artery bypass graft; HD – hemodialysis.

Table 2. Comparison of the investigated parameters between deceased and surviving patients with kidney failure treated with HD – basic characteristics

Variables	Deceased n = 25	Surviving n = 33	p-value
Age [years], mean (SD)	66.5 (±12.3)	56.6 (±17.8)	0.021[t]
Male gender, n (%)	13 (52)	17 (51.5)	0.971
Duration of HD therapy [months], median (IQR)	46.9 (21–112.4)	33 (12–85)	0.236[u]
Adequacy of HD [Kt/V], mean (SD)	1.5 (±0.3)	1.4 (±0.4)	0.293[t]
Ultrafiltration during HD session [mL], mean (SD)	1792.0 (±922.4)	1692.4 (±786.4)	0.659[t]
Hypertension, n (%)	20 (80)	23 (69.7)	0.375
Diabetes mellitus, n (%)	12 (48)	10 (30.3)	0.169
BMI [kg/m^2], mean (SD)	25.2 (±6.1)	26.4 (±4.8)	0.410[t]
The cause of kidney failure			
Chronic glomerular disease, n (%)	6 (24)	12 (36.4)	0.314
Diabetic nephropathy, n (%)	3 (12)	2 (6.1)	0.745
Polycystic kidney disease, n (%)	0 (0)	5 (15.2)	0.118
Interstitial nephropathy, n (%)	4 (16)	3 (9.1)	0.694
Hypertensive nephropathy, n (%)	10 (40)	8 (24.2)	0.199
Other, n (%)	2 (8)	3 (9.1)	0.745
Cardiovascular morbidity			
Coronary artery disease, n (%)	14 (56)	11 (33.3)	0.084
Myocardial infarction, n (%)	6 (24)	3 (9.1)	0.235
PCI, n (%)	9 (36)	3 (9.1)	0.029
CABG, n (%)	3 (12)	2 (6.1)	0.745
Stroke, n (%)	4 (16)	6 (18.2)	0.894

[t] – variables compared using Student's t-test; [u] – variables compared using Mann–Whitney U test; other variables were compared using χ^2 test; SD – standard deviation; HD – hemodialysis; IQR – interquartile range; BMI – body mass index; PCI – percutaneous coronary intervention; CABG – coronary artery bypass graft.

Table 3. Comparison of the investigated parameters between deceased and surviving patients with kidney failure treated with HD – cardiological and vascular assessment

Variables	Deceased n = 25	Surviving n = 33	p-value
Echocardiographic features			
LVESd [mm], mean (SD)	35.0 (±7.3)	32.9 (±7.7)	0.311
LVEDd [mm], mean (SD)	53.6 (±7.3)	52.1 (±6.9)	0.420
LA diameter [mm], mean (SD)	42.6 (±6.9)	41.5 (±6.2)	0.517
Aortic diameter [mm], mean (SD)	33.6 (±4.8)	32.3 (±4.9)	0.352
IVSd [mm], mean (SD)	13.8 (±2.2)	13.2 (±2.3)	0.339
PWd [mm], mean (SD)	12.1 (±1.9)	11.5 (±1.4)	0.175
LVEF [%], mean (SD)	51.1 (±11.6)	57.5 (±9.1)	0.022
Echo-tracking parameters			
β before HD, mean (SD)	8.2 (±3.5)	8.7 (±4.5)	0.674
β after HD, mean (SD)	7.4 (±3.0)	8.1 (±3.8)	0.494
Δβ, mean (SD)	−1.4 (±3.6)	−1.4 (±3.6)	0.665
Ep [kPa] before HD, mean (SD)	117.4 (±58.5)	117.8 (±63.3)	0.979
Ep [kPa] after HD, mean (IQR)	96.0 (72.0–129.5)	94.5 (72.0–126.5)	0.920[u]
ΔEp [kPa], mean (SD)	−21.0 (±54.5)	−7.5 (±52.8)	0.376
AC [mm^2/kPa] before HD, mean (SD)	0.87 (±0.34)	0.78 (±0.33)	0.333
AC [mm^2/kPa] after HD, mean (SD)	1.04 (±0.42)	0.76 (±0.31)	0.007
ΔAC [mm^2/kPa], mean (SD)	0.22 (±0.29)	0.00 (±0.28)	<0.001
PWVβ [m/s] before HD, mean (SD)	6.1 (±1.5)	6.1 (±1.5)	0.854
PWVβ [m/s] after HD, mean (SD)	5.7 (±1.1)	6.0 (±1.4)	0.502
ΔPWVβ [m/s], mean (SD)	−0.2 (±1.3)	−0.4 (±1.3)	0.545
Blood pressure and heart rate			
SBP before HD [mm Hg], mean (SD)	144.8 (±22.6)	138.3 (±24.1)	0.320
SBP after HD [mm Hg], mean (SD)	133.3 (±21.0)	134.3 (±28.0)	0.887
DBP before HD [mm Hg], mean (SD)	73.6 (±11.4)	74.9 (±16.4)	0.762
DBP after HD [mm Hg], mean (SD)	74.8 (±13.7)	74.6 (±13.9)	0.949
Heart rate before HD, mean (SD)	78.2 (±14.6)	73.1 (±12.8)	0.066
Heart rate after HD, mean (SD)	81.0 (±13.9)	73.6 (±14.6)	0.066

[u] – variables compared using Mann–Whitney U test; other variables were compared using Student's t-test; LVESd – left ventricular end-systolic diameter; LVEDd – left ventricular end-diastolic diameter; LA – left atrium; IVSd – intraventricular septum thickness in diastole; PWd – posterior wall thickness in diastole; LVEF – left ventricular ejection fraction; SD – standard deviation; HD – hemodialysis; IQR – interquartile range; β – beta stiffness index; Ep – epsilon; AC – arterial compliance; PWVβ – one-point pulse wave velocity; SBP – systolic blood pressure; DBP – diastolic blood pressure.

and the presence of cardiovascular complications were not related to any parameters of arterial stiffness. The results of the stepwise multiple regression analyses were presented in Table 10–12.

Discussion

In the present study, we observed that the change in AC correlates with mid-term survival in patients undergoing maintenance HD. The AC is a parameter proportional to change in cross-sectional area of the artery, and inversely proportional to the change in blood pressure. In general population, the higher the AC, the more elastic the artery is. Previous studies have shown that the decrease in pulse pressure – which is a basic surrogate of arterial stiffness – after HD is connected with a longer survival of patients undergoing maintenance HD.[23] In contrary, the results of our study show that subjects with ΔAC equal or higher than −0.06 mm^2/kPa had shorter survival time in the mid-term follow-up than patients with ΔAC below the cutoff

point. The Kaplan–Meier survival curves drifted apart after 600 days. Furthermore, the lone value of AC after HD was also correlated with worse outcome – survivors were characterized by a significantly lower AC after HD than deceased patients. We have not observed such correlation in AC before HD or for any other of the calculated carotid

Table 4. Comparison of the investigated parameters between deceased and surviving patients with kidney failure treated with HD – laboratory parameters

Variables	Deceased n = 25	Surviving n = 33	p-value
Hemoglobin [g/dL], mean (SD)	10.1 (±1.9)	11.1 (±4.1)	0.068
Serum total protein [g/dL], mean (SD)	6.7 (±0.7)	6.3 (±0.8)	0.068
Serum albumin [g/dL], mean (SD)	3.6 (±0.4)	3.8 (±0.5)	0.096
Fasting glucose [mg/dL], mean (IQR)	114.0 (91.0–168.0)	103.0 (90.0–131.0)	0.230^u
CRP [mg/L], mean (IQR)	10.7 (3.9–28.3)	5.5 (3.4–10.6)	0.045^u
Uric acid [mg/dL], mean (SD)	6.0 (±1.3)	6.4 (±1.6)	0.315
Total cholesterol [mg/dL], mean (SD)	177.2 (±42.1)	165.6 (±42.1)	0.366
HDL cholesterol [mg/dL], mean (IQR)	40.0 (34.0–46.9)	42.0 (36.0–50.0)	0.620^u
LDL cholesterol [mg/dL], mean (SD)	102.0 (±42.3)	86.6 (±33.9)	0.131
Triglycerides [mg/dL], mean (SD)	189.6 (±143.3)	198.9 (±131.5)	0.800
Urea before HD [mg/dL], mean (SD)	114.8 (±28.2)	123.6 (±29.4)	0.256
Urea after HD [mg/dL], mean (SD)	34.6 (±13.1)	40.7 (±17.3)	0.149
Creatinine before HD [mg/dL], mean (SD)	7.0 (±2.4)	8.0 (±2.3)	0.073
Creatinine after HD [mg/dL], mean (SD)	3.0 (±1.3)	3.3 (±1.3)	0.238
Na$^+$ before HD [mmol/L], mean (SD)	136.8 (±3.3)	137.7 (±2.1)	0.246
Na$^+$ after HD [mmol/L], mean (SD)	136.5 (±1.3)	137.2 (±1.6)	0.057
K$^+$ before HD [mmol/L], mean (SD)	4.9 (±0.7)	5.3 (±0.7)	0.040
K$^+$ after HD [mmol/L], mean (SD)	4.0 (±0.4)	4.0 (±0.3)	0.756

^{u} – variables compared using Mann–Whitney U test; other variables were compared using Student's t-test; HD – hemodialysis; CRP – C-reactive protein; HDL – high-density lipoprotein; LDL – low-density lipoprotein; SD – standard deviation; IQR – interquartile range.

Table 5. The comparison of the investigated parameters between deceased patients with kidney failure treated with HD depending on the causes (non-CV compared to CV mortality) – basic characteristics

Variables	Deceased non-CV mortality n = 14	Deceased CV-mortality n = 11	p-value
Age [years], mean (SD)	65.0 (±13.5)	68.4 (±10.9)	0.508^t
Male gender, n (%)	7 (50.0)	6 (54.6)	0.859
Duration of HD therapy [months], median (IQR)	51.9 (20.1–68.3)	40.8 (21.3–114.2)	0.978^u
Adequacy of HD [Kt/V], mean (SD)	1.4 (±0.3)	1.5 (±0.4)	0.620^t
Ultrafiltration during HD session [mL], mean (SD)	1742.9 (±989.7)	1854.5 (±872.2)	0.771^t
Hypertension, n (%)	11 (78.6)	9 (81.8)	0.763
Diabetes mellitus, n (%)	8 (57.1)	4 (36.4)	0.529
BMI [kg/m^2], mean (SD)	24.3 (±5.7)	26.3 (±6.5)	0.429^t
The cause of kidney failure			
Chronic glomerular disease, n (%)	3 (21.4)	3 (27.3)	0.895
Diabetic nephropathy, n (%)	2 (14.3)	1 (9.1)	0.823
Polycystic kidney disease, n (%)	0 (0)	0 (0)	1.000
Interstitial nephropathy, n (%)	2 (14.3)	2 (18.2)	0.775
Hypertensive nephropathy, n (%)	6 (42.9)	4 (36.4)	0.742
Other, n (%)	1 (7.1)	1 (9.1)	0.573
Cardiovascular morbidity			
Coronary artery disease, n (%)	9 (64.3)	5 (45.6)	0.592
Myocardial infarction, n (%)	4 (28.6)	2 (18.2)	0.895
PCI, n (%)	7 (50)	2 (18.2)	0.220
CABG, n (%)	2 (14.3)	1 (9.1)	0.823
Stroke, n (%)	2 (14.3)	2 (18.1)	0.775

^{t} – variables compared using Student's t-test; ^{u} – variables compared using Mann–Whitney U test; other variables were compared using χ^2 test; HD – hemodialysis; CV – cardiovascular; PCI – percutaneous coronary intervention; CABG – coronary artery bypass graft; SD – standard deviation; IQR – interquartile range; BMI – body mass index.

stiffness parameters. We hypothesize that in the group of patients with kidney failure, the pathophysiological process and degeneration of the arterial wall are so advanced that in most severe cases, the arteries lose ability to reduce inner diameter after dehydration during HD. This particular phenomenon may predict worse outcome.

There is some evidence stating that among patients with kidney failure treated with HD, a U-curve relationship between change in arterial stiffness and survival may occur. In one study, Lertdumrongluk et al. found that modest decline in pulse pressure, rather than either large reduction or rise in pulse pressure, is associated with the greatest survival.[24] This result may correspond with our findings, leading to a concept in which a potential significant decrease in arterial stiffness would correlate with a worse outcome.

In our study, we used high-resolution echo-tracking as a source of stiffness data. This method has already been used in studies on arterial stiffness in patients undergoing maintenance HD; however, only several of them focused on the role of carotid stiffness as a predictor of mortality in this group. Sato et al. found a correlation between high β and a higher risk of all-cause mortality in a 4-year follow up.[21] Another study on β has shown a predictive value of carotid stiffness on cardiovascular mortality independent of arterial thickness.[22] Blacher et al. investigated a potential role of the common carotid artery incremental

Table 6. The comparison of the investigated parameters between deceased patients with kidney failure treated with HD depending on the causes (non-CV compared to CV mortality) – cardiological and vascular assessment

Variables	Deceased non-CV mortality n = 14	Deceased CV-mortality n = 11	p-value
Echocardiographic features			
LVESd [mm], mean (SD)	35.2 (±7.3)	34.6 (±7.7)	0.848
LVEDd [mm], mean (SD)	52.8 (±6.5)	54.5 (±8.3)	0.580
LA diameter [mm], mean (SD)	43.9 (±7.9)	41.1 (±5.5)	0.328
Aortic diameter [mm], mean (SD)	35.1 (±4.9)	31.8 (±4.4)	0.102
IVSd [mm], mean (SD)	13.7 (±2.6)	13.8 (±1.8)	0.892
PWd [mm], mean (SD)	12.2 (±2.3)	12.0 (±1.3)	0.771
LVEF [%], mean (SD)	50.9 (±11.0)	51.4 (±12.9)	0.930
Echo-tracking parameters			
β before HD, mean (SD)	7.4 (±3.2)	9.1 (±3.8)	0.244
β after HD, mean (SD)	8.0 (±3.5)	6.6 (±1.9)	0.283
Δβ, mean (SD)	0.3 (±3.3)	−2.7 (±3.4)	0.053
Ep [kPa] before HD, mean (SD)	104.8 (±47.8)	131.2 (±67.8)	0.289
Ep [kPa] after HD, mean (SD)	104.4 (±44.9)	92.0 (±30.6)	0.457
ΔEp [kPa], mean (SD)	−2.6 (±44.2)	−43.0 (±59.7)	0.083
AC [mm²/kPa] before HD, mean (SD)	0.87 (±0.32)	0.87 (±0.38)	0.986
AC [mm²/kPa] after HD, mean (SD)	1.04 (±0.47)	1.03 (±0.37)	0.962
ΔAC [mm²/kPa], mean (SD)	0.27 (±0.27)	0.16 (±0.31)	0.388
PWVβ [m/s] before HD, mean (SD)	5.8 (±1.5)	6.4 (±1.6)	0.401
PWVβ [m/s] after HD, mean (SD)	5.7 (±1.2)	5.7 (±0.9)	0.968
ΔPWVβ [m/s], mean (SD)	−0.1 (±1.2)	−0.8 (±1.4)	0.222
Blood pressure and heart rate			
SBP before HD [mm Hg], mean (SD)	144.2 (±24.8)	145.5 (±21.1)	0.895
SBP after HD [mm Hg], mean (SD)	133.5 (±20.5)	133.0 (±28.9)	0.960
DBP before HD [mm Hg], mean (SD)	75.5 (±13.3)	71.8 (±9.3)	0.466
DBP after HD [mm Hg], mean (SD)	71.2 (±13.9)	79.5 (±12.6)	0.155
Heart rate before HD, mean (SD)	83.6 (±13.0)	71.2 (±14.1)	0.031
Heart rate after HD, mean (SD)	83.1 (±13.7)	78.3 (±14.3)	0.425

variables were compared using Student's t-test; CV – cardiovascular; LVESd – left ventricular end-systolic diameter; LVEDd – left ventricular end-diastolic diameter; LA – left atrium; IVSd – intraventricular septum thickness in diastole; PWd – posterior wall thickness in diastole; LVEF – left ventricular ejection fraction; HD – hemodialysis; β – beta stiffness index; Ep – epsilon; AC – arterial compliance; PWVβ – one-point pulse wave velocity; SBP – systolic blood pressure; DBP – diastolic blood pressure; SD – standard deviation.

Table 7. The comparison of the investigated parameters between deceased patients with kidney failure treated with HD depending on the causes (non-CV compared to CV mortality) – laboratory parameters

Variables	Deceased non-CV mortality n = 14	Deceased CV-mortality n = 11	p-value
Hemoglobin [g/dL], mean (SD)	9.6 (±1.6)	10.7 (±2.1)	0.156
Serum total protein [g/dL], mean (SD)	6.6 (±0.7)	6.8 (±0.7)	0.515
Serum albumin [g/dL], mean (SD)	3.5 (±0.5)	3.6 (±0.3)	0.773
Fasting glucose [mg/dL], mean (SD)	145.1 (±61.9)	141.6 (±99.1)	0.915
CRP [mg/L], mean (SD)	16.0 (±18.2)	31.8 (±48.0)	0.267
Uric acid [mg/dL], mean (SD)	5.9 (±1.3)	6.1 (±1.2)	0.699
Total cholesterol [mg/dL], mean (SD)	175.7 (±66.6)	179.2 (±39.1)	0.880
HDL cholesterol [mg/dL], mean (SD)	42.9 (±13.4)	40.5 (±12.7)	0.657
LDL cholesterol [mg/dL], mean (SD)	97.9 (±51.0)	107.2 (±29.4)	0.595
Triglycerides [mg/dL], mean (SD)	169.4 (±113.7)	215.5 (±176.6)	0.595
Urea before HD [mg/dL], mean (SD)	118.0 (±22.9)	110.6 (±34.4)	0.528
Urea after HD [mg/dL], mean (SD)	36.2 (±12.6)	32.5 (±14.0)	0.497
Creatinine before HD [mg/dL], mean (SD)	6.9 (±2.3)	7.0 (±2.1)	0.871
Creatinine after HD [mg/dL], mean (SD)	3.0 (±1.3)	2.9 (±1.3)	0.934
Na⁺ before HD [mmol/L], mean (SD)	136.6 (±2.9)	137.1 (±3.8)	0.740
Na⁺ after HD [mmol/L], mean (SD)	136.5 (±1.3)	136.5 (±1.3)	0.933
K⁺ before HD [mmol/L], mean (SD)	4.8 (±0.7)	5.0 (±0.50)	0.505
K⁺ after HD [mmol/L], mean (SD)	4.0 (±0.5)	4.0 (±0.4)	0.980

variables were compared using Student's t-test; CV – cardiovascular; HD – hemodialysis; CRP – C-reactive protein; HDL – high-density lipoprotein; LDL – low-density lipoprotein; SD – standard deviation.

modulus of elasticity (E_{inc}), showing that E_{inc} is an independent predictor of both cardiovascular and all-cause mortality in patients with kidney failure treated with HD.[25] In contrary to these studies, we explored a wider spectrum of carotid stiffness parameters directly before and after HD. To the best of our knowledge, there are no studies exploring the potential predictive value of change in these particular arterial stiffness parameters during a single HD session.

Apart from the findings considering arterial stiffness, our study has shown the association between the cardiological burden and survival of patients with kidney failure. Deceased patients had lower LVEF and more often

Table 8. Predictors of overall mortality among patients with kidney failure treated with HD using Cox proportional hazards model

Variables	Full model		Multivariate adjusted HR	
	HR (95% CI)	p-value	HR (95% CI)	p-value
Age [years]	1.184 [1.054; 1.331]	0.004	1.129 [1.054; 1.209]	0.001
PCI	77.697 [5.900; 1023.153]	0.001	11.123 [2.245; 55.114]	0.003
LVEF [%]	1.110 [0.995; 1.238]	0.061	1.079 [1.007; 1.157]	0.031
ΔAC [mm^2/kPa]	4687.865 [20.887; 1,052,157.000]	0.002	221.957 [11.250; 4379.027]	<0.001
Fasting glucose [mg/dL]	0.990 [0.980; 1.000]	0.027	0.989 [0.981; 0.998]	0.013
Serum total protein [g/dL]	5.513 [1.581; 19.228]	0.007	5.521 [2.218; 13.744]	<0.001
Na$^+$ after HD [mmol/L]	0.365 [0.163; 0.816]	0.014	0.430 [0.243; 0.762]	0.004
K$^+$ before HD [mmol/L]	0.166 [0.023; 1.213]	0.077	0.142 [0.041; 0.487]	0.002
Hypertension	0.387 [0.059; 2.549]	0.324	N/A	N/A
Heart rate after HD	1.012 [0.965; 1.062]	0.623	N/A	N/A
Hemoglobin [g/dL]	0.646 [0.438; 0.953]	0.027	N/A	N/A
CRP [mg/L]	1.026 [0.998; 1.054]	0.065	N/A	N/A
LDL cholesterol [mg/dL]	1.029 [1.006; 1.053]	0.013	N/A	N/A
Urea after HD [mg/dL]	0.968 [0.916; 1.062]	0.250	N/A	N/A
Creatinine before HD [mg/dL]	0.997 [0.683; 1.454]	0.986	N/A	N/A

R^2 = 0.84; HR – hazard ratio; 95% CI – 95% confidence interval; PCI – percutaneous coronary intervention; LVEF – left ventricular ejection fraction; AC – arterial compliance; HD – hemodialysis; CRP – C-reactive protein; LDL – low-density lipoprotein; N/A – not applicable.
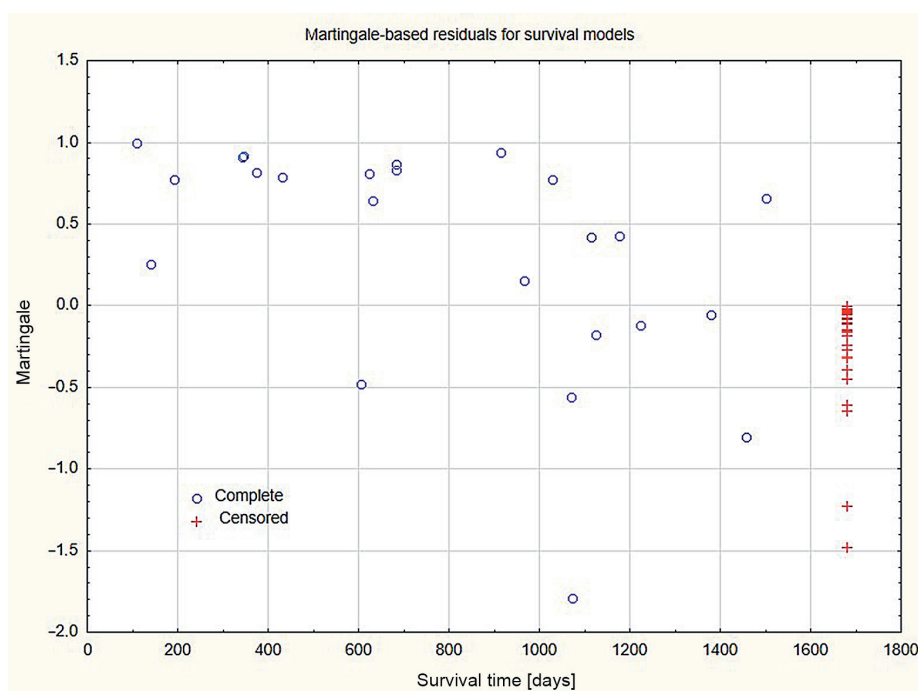
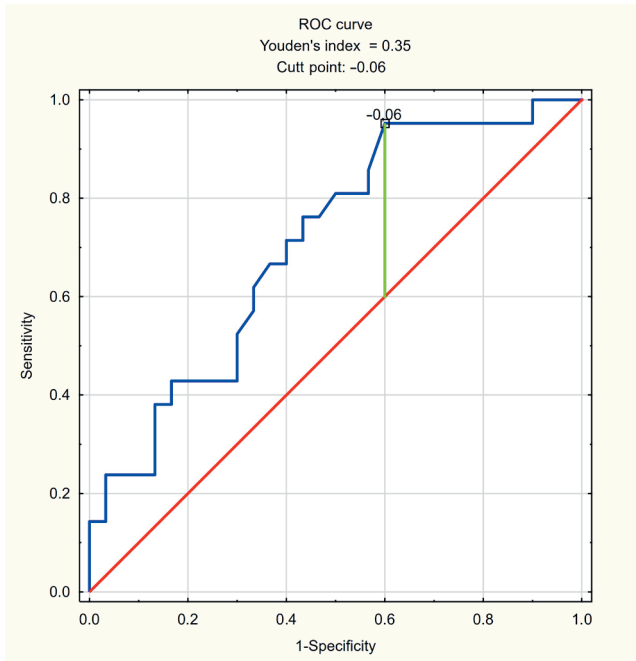**Fig. 1.** Martingale-based residuals for survival models

Fig. 2. Receiver operating characteristic (ROC) curve. The change in arterial compliance (ΔAC) in survivors and non-survivors

Table 9. Spearman's correlations between Schoenfeld residuals and survival

Schoenfeld residual	R Spearman	p-value
Schoenfeld residual for LVEF	0.12	0.599
Schoenfeld residual for Na$^+$ after HD	0.16	0.497
Schoenfeld residual for K$^+$ before HD	0.13	0.583
Schoenfeld residual for serum total protein	−0.40	0.069
Schoenfeld residual for PCI	−0.14	0.531
Schoenfeld residual for age	0.04	0.857
Schoenfeld residual for fasting glucose	−0.23	0.319
Schoenfeld residual for ΔAC	0.26	0.251

LVEF – left ventricular ejection fraction; HD – hemodialysis; PCI – percutaneous coronary intervention; AC – arterial compliance.

had a history of PCI, which are the results of heart failure and coronary artery disease (CAD), respectively. Also, the deceased patients were characterized by a lower serum potassium level, which may be related to a higher risk of tachyarrhythmias.

The assessment of hemodynamic changes in patients with kidney failure is not a simple task. It should be taken
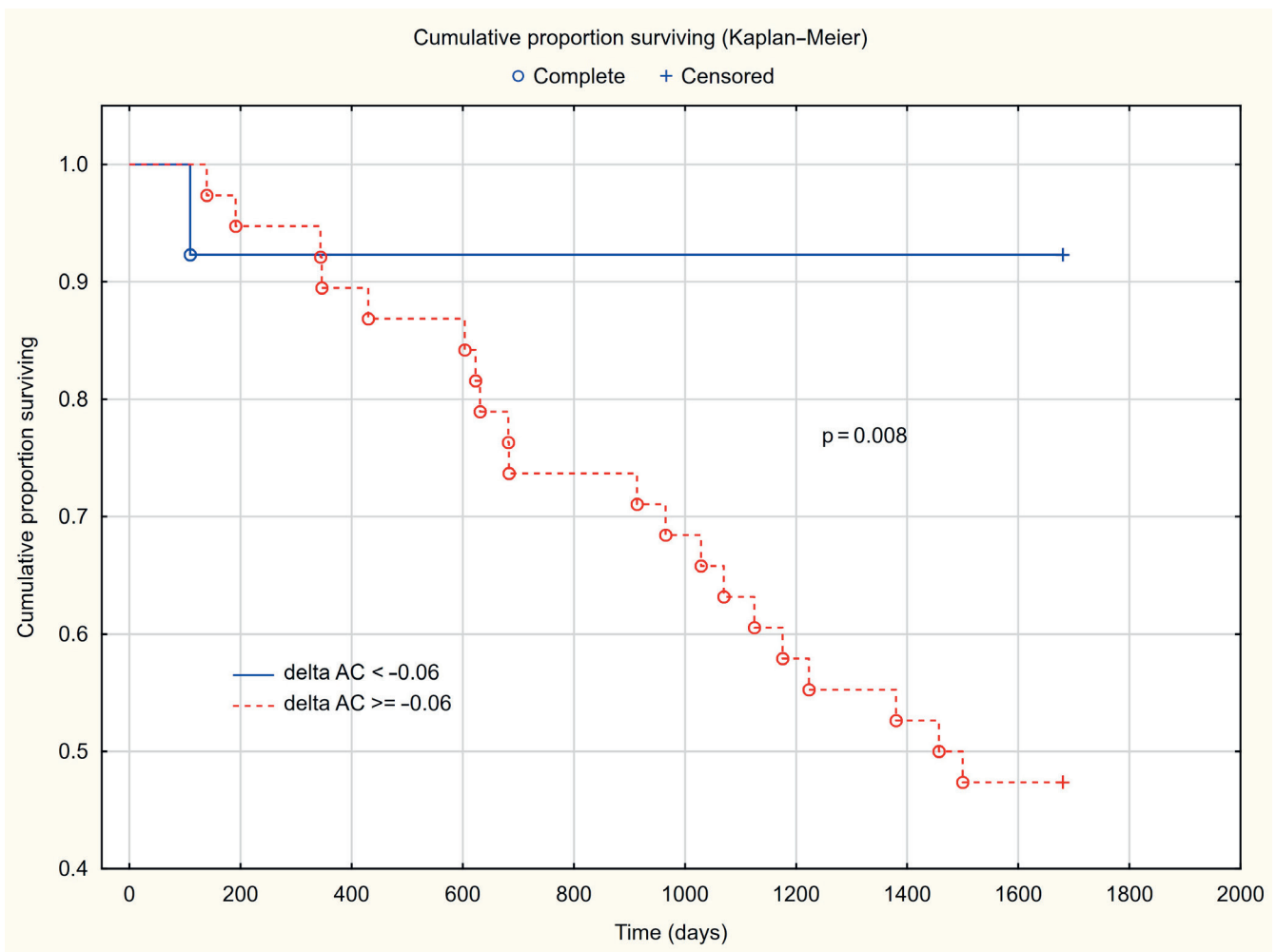

Fig. 3. Kaplan–Meier survival curves. Survival of patients regarding the change in arterial compliance (ΔAC) for patients with ΔAC ≥ −0.06 mm^2/kPa and ΔAC < −0.06 mm^2/kPa

Table 10. Stepwise multiple regression analysis for the association between a dependent variable β and age, gender, diabetes, and the presence of CV complications (at least one of the following: previous MI, stroke, CABG, PCI) in patients with kidney failure treated with HD

Variable	BETA	SE BETA	b	SE b	p-value
Age	0.36	0.13	0.07	0.03	<0.007

$R^2 = 0.13$; adjusted $R^2 = 0.11$; $p < 0.007$. Age was not associated with the remaining echo-tracking parameters. Gender, diabetes and the presence of CV complications were not associated with echo-tracking parameters. Variance inflation factor was less than 2 for all analyses, and the Durbin–Watson test was between 2.4 and 2.5. SE – standard error; BETA – standardized regression coefficients; b – raw regression coefficients; R^2 – coefficient of determination; adjusted R^2 – adjusted coefficient of determination; β – beta stiffness index; HD – hemodialysis; CV – cardiovascular; PCI – percutaneous coronary intervention; CABG – coronary artery bypass graft; MI – myocardial infarction.

Table 11. Stepwise multiple regression analysis for the association between a dependent variable Ep and age, gender, diabetes, and the presence of CV complications (at least one of the following: previous MI, stroke, CABG, PCI) in patients with kidney failure treated with HD

Variable	BETA	SE BETA	b	SE b	p-value
Age	0.42	0.12	1.32	0.39	<0.002

$R^2 = 0.17$; adjusted $R^2 = 0.16$; $p < 0.002$. Age was not associated with the remaining echo-tracking parameters. Gender, diabetes and the presence of CV complications were not associated with echo-tracking parameters. Variance inflation factor was less than 2 for all analyses, and the Durbin–Watson test was between 2.4 and 2.5. SE – standard error; BETA – standardized regression coefficients; b – raw regression coefficients; R^2 – coefficient of determination; adjusted R^2 – adjusted coefficient of determination; Ep – epsilon; HD – hemodialysis; CV – cardiovascular; PCI – percutaneous coronary intervention; CABG – coronary artery bypass graft; MI – myocardial infarction.

Table 12. Stepwise multiple regression analysis for the association between a dependent variable PWVβ and age, gender, diabetes, and the presence of CV complications (at least one of the following: previous MI, stroke, CABG, PCI) in patients with kidney failure treated with HD

Variable	BETA	SE BETA	b	SE b	p-value
Age	0.36	0.13	0.03	0.01	<0.006

$R^2 = 0.13$; adjusted $R^2 = 0.12$; $p < 0.006$. Age was not associated with the remaining echo-tracking parameters. Gender, diabetes and the presence of CV complications were not associated with echo-tracking parameters. Variance inflation factor was less than 2 for all analyses, and the Durbin–Watson test was between 2.4 and 2.5. SE – standard error; BETA – standardized regression coefficients; b – raw regression coefficients; R^2 – coefficient of determination; adjusted R^2 – adjusted coefficient of determination; PWVβ – one-point pulse wave velocity; HD – hemodialysis; CV – cardiovascular; PCI – percutaneous coronary intervention; CABG – coronary artery bypass graft; MI – myocardial infarction.

into account, that changes in stiffness parameters during HD may indicate both pathological changes in the vessels themselves and unfavorable processes in the autonomic system. Some blood pressure changes are provoked by higher fluid or sodium removal. On the other hand, cardiovascular changes can be disturbed in the state of raised sympathetic tone present in CKD patients.[26] Sympathetic hyperactivity is taken into account as one of the reasons of intradialytic blood pressure changes.[27] The hydration status may also be considered a factor impacting arterial stiffness. In a study on a group of HD patients, hypervolemia (assessed as left ventricle end-diastolic volume) was significantly associated with pulse pressure.[28] Moreover, it cannot be ruled out that the increase in AC after HD is a result of decrease in systolic blood pressure following dehydration. Hemodialysis may impact local arterial stiffness in a complex mechanism, in which the decrease of blood pressure, dehydration and individual properties of the cardiovascular system overlap and lead to the change in AC. This reaction of cardiovascular system is correlated with the survival.

The correlation with mortality of other echo-tracking parameters such as β, Ep and PWVβ remained statistically insignificant both before and after the HD, which stays in opposition to the previous findings.[21,22] Because of the existing shortage in the studies on the abovementioned parameters in kidney failure patients, with regard to all-cause mortality, and in particular cardiovascular mortality, the discussion of those relationships would be complex or probabilistic one.

Clinical implications

Our study shows that high-resolution echo-tracking may provide a unique insight into pathophysiology of cardiovascular disease in patients with kidney failure, and particularly, in patients treated with maintenance HD. It also gives hope for a better risk stratification among those patients. Further pathophysiological studies will be needed in order to recognize the underlying cause of paradoxical change in AC and a potential utility of this phenomenon. Moreover, further studies are required to establish how to control arterial stiffness in order to improve the outcomes.

Limitations

Our study has several limitations. It was observational in nature and thus, the causality could not be directly derived from the results. It had also a relatively small number of participants. The mid-term follow-up of 48 months seems to be also a limitation. Nevertheless, the subject did not undergo extensive investigations, so our study adds an important piece of data regarding the studied issue.

Conclusions

Echo-tracking-based arterial stiffness assessment in patients with CKD yields the clinical information regarding mid-term mortality risk. The independent risk factors for mid-term mortality in patients with kidney failure treated with HD are age, PCI, LVEF, ΔAC, fasting glucose, serum total protein, sodium level after HD, and potassium level before HD. The proper estimation of the correlations among vascular, hemodynamic and sympathetic-dependent changes in a given patient with kidney failure is complex.

ORCID iDs

Konrad Rekucki ⬤ https://orcid.org/0000-0002-2570-347X
Agnieszka Sławuta ⬤ https://orcid.org/0000-0001-5671-9864
Dorota Zyśko ⬤ https://orcid.org/0000-0001-9190-0052
Katarzyna Madziarska ⬤ https://orcid.org/0000-0002-3624-3691

References

1. Tonelli M, Wiebe N, Culleton B, et al. Chronic kidney disease and mortality risk: A systematic review. *J Am Soc Nephrol*. 2006;17(7):2034–2047. doi:10.1681/ASN.2005101085
2. Karras A, Haymann JP, Bozec E, et al. Large artery stiffening and remodeling are independently associated with all-cause mortality and cardiovascular events in chronic kidney disease. *Hypertension*. 2012;60(6):1451–1457. doi:10.1161/HYPERTENSIONAHA.112.197210
3. Herzog CA, Asinger RW, Berger AK, et al. Cardiovascular disease in chronic kidney disease: A clinical update from Kidney Disease: Improving Global Outcomes (KDIGO). *Kidney Int*. 2011;80(6):572–586. doi:10.1038/ki.2011.223
4. Kidney Disease: Improving Global Outcomes (KDIGO) CKD Work Group. KDIGO 2012 Clinical Practice Guideline for the Evaluation and Management of Chronic Kidney Disease. *Kidney Inter*. Suppl 2013;3:1–150. https://kdigo.org/wp-content/uploads/2017/02/KDIGO_2012_CKD_GL.pdf. Accessed May 2, 2021.
5. Karthikeyan V, Ananthasubramaniam K. Coronary risk assessment and management options in chronic kidney disease patients prior to kidney transplantation. *Curr Cardiol Rev*. 2009;5(3):177–186. doi:10.2174/157340309788970342
6. Francis GS, Tang WH. Cardiac troponins in renal insufficiency and other non-ischemic cardiac conditions. *Prog Cardiovasc Dis*. 2004;47(3):196–206. doi:10.1016/j.pcad.2004.07.005
7. Iwanaga Y, Miyazaki S. Heart failure, chronic kidney disease, and biomarkers: An integrated viewpoint. *Circ J*. 2010;74(7):1274–1282. doi:10.1253/circj.cj-10-0444
8. Hallan SI, Coresh J, Astor BC, et al. International comparison of the relationship of chronic kidney disease prevalence and ESRD risk. *J Am Soc Nephrol*. 2006;17(8):2275–2284. doi:10.1681/ASN.2005121273
9. Coresh J, Selvin E, Stevens LA, et al. Prevalence of chronic kidney disease in the United States. *JAMA*. 2007;298(17):2038–2047. doi:10.1001/jama.298.17.2038
10. Matsushita K, van der Velde M, Astor BC, et al.; Chronic Kidney Disease Prognosis Consortium. Association of estimated glomerular filtration rate and albuminuria with all-cause and cardiovascular mortality in general population cohorts: A collaborative meta-analysis. *Lancet*. 2010;375(9731):2073–2081. doi:10.1016/S0140-6736(10)60674-5
11. Rao MV, Qiu Y, Wang C, Bakris G. Hypertension and CKD: Kidney Early Evaluation Program (KEEP) and National Health and Nutrition Examination Survey (NHANES), 1999–2004. *Am J Kidney Dis*. 2008;51(4 Suppl 2):S30–S37. doi:10.1053/j.ajkd.2007.12.012
12. Yerkey MW, Kernis SJ, Franklin BA, Sandberg KR, McCullough PA. Renal dysfunction and acceleration of coronary disease. *Heart*. 2004;90(8):961–966. doi:10.1136/hrt.2003.015503
13. Laurent S, Cockcroft J, Van Bortel L, et al. Expert consensus document on arterial stiffness: Methodological issues and clinical applications. *Eur Heart J*. 2006;27(21):2588–2605. doi:10.1093/eurheartj/ehl254
14. Zieman SJ, Melenovsky V, Kass DA. Mechanisms, pathophysiology, and therapy of arterial stiffness. *Arterioscler Thromb Vasc Biol*. 2005;25(5):932–943. doi:10.1161/01.ATV.0000160548.78317.29
15. Jaroch J, Łoboz-Grudzień K, Magda S, et al. The relationship of carotid arterial stiffness and left ventricular concentric hypertrophy in hypertension. *Adv Clin Exp Med*. 2016;25(2):263–272. doi:10.17219/acem/34654
16. Bruno RM, Cartoni G, Stea F, et al. Carotid and aortic stiffness in essential hypertension and their relation with target organ damage: The CATOD study. *J Hypertens*. 2017;35(2):310–318. doi:10.1097/HJH.0000000000001167
17. Uejima T, Dunstan FD, Arbustini E, et al. Age-specific reference values for carotid arterial stiffness estimated by ultrasonic wall tracking. *J Hum Hypertens*. 2020;34(3):214–222. doi:10.1038/s41371-019-0228-5
18. Safar ME, Asmar R, Benetos A, et al. Interaction between hypertension and arterial stiffness. *Hypertension*. 2018;72(4):796–805. doi:10.1161/HYPERTENSIONAHA.118.11212
19. DeLoach SS, Townsend RR. Vascular stiffness: Its measurement and significance for epidemiologic and outcome studies. *Clin J Am Soc Nephrol*. 2008;3(1):184–192. doi:10.2215/CJN.03340807
20. Yu ZX, Wang XZ, Guo RJ, Zhong ZX, Zhou YL. Comparison of ultrasound echo-tracking technology and pulse wave velocity for measuring carotid elasticity among hemodialysis patients. *Hemodial Int*. 2013;17(1):19–23. doi:10.1111/j.1542-4758.2012.00707.x
21. Sato M, Ogawa T, Otsuka K, Ando Y, Nitta K. Stiffness parameter β as a predictor of the 4-year all-cause mortality of chronic hemodialysis patients. *Clin Exp Nephrol*. 2013;17(2):268–274. doi:10.1007/s10157-012-0674-7
22. Shoji T, Maekawa K, Emoto M, et al. Arterial stiffness predicts cardiovascular death independent of arterial thickness in a cohort of hemodialysis patients. *Atherosclerosis*. 2010;210(1):145–149. doi:10.1016/j.atherosclerosis.2009.11.013
23. Inrig JK, Patel UD, Toto RD, et al. Decreased pulse pressure during hemodialysis is associated with improved 6-month outcomes. *Kidney Int*. 2009;76(10):1098–1107. doi:10.1038/ki.2009.340
24. Lertdumrongluk P, Streja E, Rhee CM, et al. Changes in pulse pressure during hemodialysis treatment and survival in maintenance dialysis patients. *Clin J Am Soc Nephrol*. 2015;10(7):1179–1191. doi:10.2215/CJN.09000914
25. Blacher J, Pannier B, Guerin AP, Marchais SJ, Safar ME, London GM. Carotid arterial stiffness as a predictor of cardiovascular and all-cause mortality in end-stage renal disease. *Hypertension*. 1998;32(3):570–574. doi:10.1161/01.hyp.32.3.570
26. Zoccali C, Mallamaci F, Parlongo S, et al. Plasma norepinephrine predicts survival and incident cardiovascular events in patients with end-stage renal disease. *Circulation*. 2002;105(11):1354–1359. doi:10.1161/hc1102.105261
27. Zanoli L, Lentini P, Briet M, et al. Arterial stiffness in the heart disease of CKD. *J Am Soc Nephrol*. 2019;30(6):918–928. doi:10.1681/ASN.2019020117
28. Yazici H, Oflaz H, Pusuroglu H, et al. Hypervolemia rather than arterial calcification and extracoronary atherosclerosis is the main determinant of pulse pressure in hemodialysis patients. *Int Urol Nephrol*. 2012;44(4):1203–1210. doi:10.1007/s11255-011-0024-9

The role and mechanism of TLR4-siRNA in the impairment of learning and memory in young mice induced by isoflurane

Lin Lin[1,A–D,F], Dongping Chen[2,A–C,F], Xiaoli Yu[3,A–C,F], Wensheng Zhong[3,B,C,F], Yanlong Liu[3,B,F], Yu Feng[3,B,F], Heguo Luo[3,A,C,E,F]

[1] Department of Stomatology, Jiangxi Provincial People's Hospital, Nanchang, China
[2] Department of General Surgery, Jiangxi Provincial People's Hospital, Nanchang, China
[3] Department of Anesthesiology, Jiangxi Provincial People's Hospital, Nanchang, China

A – research concept and design; B – collection and/or assembly of data; C – data analysis and interpretation;
D – writing the article; E – critical revision of the article; F – final approval of the article

Address for correspondence
Heguo Luo
E-mail: luoheguo123@126.com

Abstract

Background. Isoflurane can significantly induce inflammation in children without surgical stress. The toll-like receptor 4 (TLR4) is closely related to noninfectious inflammation in the brain.

Objectives. To investigate the role of TLR4-small interfering RNA (siRNA) in learning and memory impairment in young mice induced by isoflurane.

Materials and methods. The C57 newborn mice were randomly allocated into normal control (control), isoflurane anesthesia (isoflurane), TLR4 interference empty vector+isoflurane anesthesia (siRNA-NC), and TLR4 interference+isoflurane anesthesia (TLR-siRNA) groups. Their behavior and pathological condition were detected using Morris water maze and hematoxylin and eosin (H&E) staining, respectively. The TLR4, brain-derived neurotrophic factor (BDNF) and cyclic adenosine monophosphate response element-binding protein 1 (CREB1) mRNA expressions were detected using quantitative real-time polymerase chain reaction (qRT-PCR). Serum tumor necrosis factor alpha (TNF-α) and interleukin (IL)-6 were detected by means of the enzyme-linked immunosorbent assay (ELISA). Apoptosis rate was detected with terminal deoxynucleotidyl transferase dUTP nick end labeling (TUNEL). The TLR4, TNF-α, IL-6, BDNF, CREB1, extracellular signal-regulated kinase 1/2 (ERK1/2), and c-Jun N-terminal kinase (JNK) protein expressions were detected using western blot (WB).

Results. Compared with the control group, the number of times the mice crossed the platform, and the time spent at the circumjacent area I and II of the platform were significantly decreased in the isoflurane group; the TLR4, TNF-α and IL-6 expressions were significantly increased in the isoflurane group, as compared to control; the results were reversed after the TLR4 interference. The hippocampal neurons in the isoflurane and siRNA-NC groups showed arrangement disorder and a high number of inflammatory infiltrates, while in the TLR-siRNA group they were closely and orderly arranged. Compared with the control group, the apoptosis rate and JNK protein expression in the isoflurane group were significantly increased, CREB1 protein expression was significantly decreased, and BDNF and ERK1/2 protein expressions showed no significant changes. Compared with the isoflurane group, the apoptosis rate of the TLR-siRNA group was significantly decreased, BDNF and CREB1 protein expressions were significantly increased, and ERK1/2 and JNK did not change significantly.

Conclusions. Isoflurane stimulates the overexpression of inflammatory response factors, playing an important role in the cognitive impairment process. As a mediator of the innate immune inflammatory response, TLR4 plays an important role in the process of cell injury, which may be delayed by blocking the TLR4 signal.

Key words: TLR4, isoflurane, memory function

Background

Early anesthetic exposure has been strongly linked to learning/behavior impairments in later life.[1–3] Multiple exposures before the age of 3 are related to a higher rate of learning difficulties and attention deficit hyperactivity disorder (ADHD).[1] Animal models confirmed long-lasting learning and memory impairments upon early postnatal exposure to anesthetics.[4–6] Evidence showed that general anesthesia can promote apoptosis and cognitive impairment in the developing brain by exacerbating neuroinflammation.[7]

Isoflurane is a commonly used general anesthesia. Aseptic trauma of surgery can trigger an inflammatory cascade via the innate immune system, affecting synaptic plasticity in brain areas responsible for learning and memory.[8] Besides, a previous study revealed that brief exposure to isoflurane can significantly induce inflammation in children without surgical stress.[9]

The hippocampus and ventromedial prefrontal cortex (vmPFC) play an important role in learning and memory processes, including fear conditioning and processing of safety–threat information.[10–12] The hippocampus and prefrontal areas have a key function in inhibitory control.[13,14] Isoflurane inhalation can induce hippocampal neuroinflammation and cognitive dysfunction in rats.[15,16] Isoflurane inhalation in children may produce neurodegenerative toxic effect[17] and induce hippocampal apoptosis,[15,18] and its prolonged use in early life is considered to be closely related to cognitive impairment in later life.[19] Isoflurane induced persistent and progressive decrease in hippocampal neural stem cell pool and neurogenesis in the developing brain of young rodents, with significant object recognition and reversal learning impairment which became more obvious as they grew older, whereas similar findings were not observed in adult rodents.[20]

Isoflurane anesthesia can alter the hippocampal dendritic spine morphology and development in neonatal mice.[21] The exposure of immature neurons to isoflurane can also induce a long-term loss of synaptic connections.[22] Isoflurane may have neurosynaptic toxic effects, thereby affecting synaptic plasticity and impairing learning and memory functions.

Toll-like receptors (TLRs) are a class of pattern recognition receptors expressed on the membrane of the microglia. The TLRs can recognize pathogens and a variety of harmful substances produced in the body.[23] The activation of microglia produces a corresponding response. In the TLR family, toll-like receptor 4 (TLR4) is considered to be most closely related to the noninfectious inflammation in the brain.[24] Experimental results show that TLR4 has a significant impact on the outcome of noninfectious central nervous system diseases, such as cerebral ischemia and Alzheimer's disease (AD).[25,26] The alterations of the relevant neural structures may affect learning and memory processes.[27] The inflammatory mediators released by the primary innate immune cells of the brain can compromise the neuronal structure and function, thus playing important roles in the pathogenesis of neurodegenerative diseases.[28–30]

Objectives

This study analyzed the function of TLR pathway in the learning and memory impairment in young mice caused by isoflurane. The TLR4-small interfering RNA (siRNA) was injected into the lateral ventricle of the brain[31] to observe whether TLR4-siRNA intervention can alleviate the effects of isoflurane on impaired learning and memory function in young mice, which were assessed using Morris water maze test and hematoxylin and eosin (H&E) staining, in order to provide a feasible method for protecting the cognitive development of children undergoing surgery with isoflurane anesthesia.

Materials and methods

Ethics approval

All experiments in this study has been approved by the Animal Care and Use Committee of the Jiangxi Provincial People's Hospital, Nanchang, China, and conducted in strict accordance with the guidelines of the Committee.

Experimental animals

Specific pathogen-free (SPF) grade, C57 mice (license No. SCXK (Xiang) 2016-002) were purchased from Hunan SJA Lab Animal Co., Ltd. (Hunan, China). The mice were raised in polypropylene cages, maintained at 12-hour light/12-hour dark cycle, at a temperature of 25 ±2°C, and allowed food and water ad libitum.

Laboratory reagents and instruments

Main reagents

The reagents used in the study included: isoflurane (national drug approval No. H20070172; Shanghai Hengrui Pharmaceutical Co., Ltd., Shanghai, China); TLR4-siRNA oligos set (cat. No. i548002; Applied Biological Materials Inc., Richmond, Canada); TRIzon reagent (CW0580S), ultrapure RNA extraction kit (CW0581M), HiFiScript first strand complementary DNA (cDNA) synthesis kit (CW2569M), UltraSYBR Mixture (CW0957M), bicinchoninic acid (BCA) protein assay kit (CW0014S) (Beijing ComWin Biotech Co., Ltd., Beijing, China); polyvinylidene difluoride (PVDF) membrane (IPVH00010; EMD Millipore Corporation, Billerica, USA); marker (PageRuler™ Prestained Protein Ladder; #26617), super enhanced

chemiluminescence (ECL) plus (RJ239676; Thermo Fisher Scientific, Waltham, USA); mouse monoclonal anti-glyceraldehyde-3-phosphate dehydrogenase (GAPDH, 1/2000, TA-08), goat anti-rabbit immunoglobulin G (IgG) (H+L) horseradish peroxidase (HRP) conjugate secondary antibody (1/5000, ZB-2301; ZSGB-BIO, Beijing, China); rabbit anti-TLR4 polyclonal antibody (1/1000, bs-20594R), rabbit anti-interleukin (IL)-6 polyclonal antibody (1/500, bs-6309R; Bioss Antibodies Inc., Woburn, USA); rabbit anti-tumor necrosis factor alpha (TNF-α) polyclonal antibody (1/500, AF7014; Affinity Biosciences, Cincinnati, USA); rabbit anti-brain-derived neurotrophic factor (BDNF) (1/1000, ab108319; Abcam, Cambridge, USA); rabbit anti-cyclic adenosine monophosphate response element-binding protein 1 (CREB1, 1/1000, 12208-1-ap), rabbit anti-extracellular signal-regulated kinase 1/2 (ERK1/2, 1/1000, 16443-1-ap; Proteintech Group, Inc., Rosemont, USA); rabbit anti-c-Jun N-terminal kinase (JNK, 1/1000, df6089; Affinity Biosciences); terminal deoxynucleotidyl transferase dUTP nick end labeling (TUNEL) assay kit (C1088; Beyotime Biotechnology, Shanghai, China); mouse TNF-α enzyme-linked immunosorbent assay (ELISA) kit (MM-0132M1), mouse IL-6 kit (MM-0163M1; Jiangsu Meimian Industrial Co., Ltd., Jiangsu, China); radioimmunoprecipitation assay (RIPA) lysis buffer (C1053), skimmed milk powder (P1622; Applygen Technologies Inc., Beijing, China); and bovine serum albumin (BSA, A8020; Solarbio Life Sciences, Beijing, China).

Main instruments

The instruments used in the study included: small animal ventilator (DW-3000C; Beijing Zhongshidichuang Science and Technology Development Co., Ltd., Beijing, China); isoflurane anesthesia ventilator (ABM-100), stereotaxic apparatus (SA-102), Morris water maze (JLBehv-MWMG; Shanghai Yuyan Instruments Co., Ltd., Shanghai, China); fluorescence microscope (CX41; Olympus Corp., Tokyo, Japan); microtome (BQ-318D; Bona Medical Technology Co., Ltd., Hubei, China); fluorescence quantitative real-time polymerase chain reaction (qRT-PCR) machine (CFX Connect™ Real-Time), ultra-high sensitivity chemiluminescence imaging system (Chemi Doc™ XRS+; Bio-Rad Laboratories Co., Ltd., Shanghai, China); vertical protein electrophoresis system (DYY-6C), automatic microplate reader (WD-2102B; Beijing Liuyi Biotechnology Co., Ltd., Beijing, China); low-temperature high-speed centrifuge (5424R; Eppendorf AG, Hamburg, Germany); and constant temperature shaker (TC-100B; Shanghai Tocan Biotechnology Co., Ltd., Shanghai, China).

Allocation sequence and blinding

Allocation sequence was performed using random numbers generated by a computer. The researchers conducting the experiments, the outcome assessment and the data analysis were blinded to the group allocation.

Sample allocation

First, the adult mice were caged together with female/male ratio of 2:1. Then, the newborn mice were randomly allocated into 4 groups. There was no requirement for gender of the young mice and it was ensured that there were 12 in each group, 6 of which were randomly allocated for qRT-PCR and western blot (WB) analysis. The hippocampal tissue was taken and evenly divided into 2 parts from the midline, one part was used for qPCR and the other for WB analysis. Another 3 mice from each group were used for H&E staining and serum collection for ELISA test. The brain tissue was obtained, placed in 10% formalin and stored at 4°C for H&E staining. The remaining 3 mice from each group were taken for the water maze experiments.

Experimental grouping

The newborn mice were randomly assigned into 4 groups as follows:

(1) Normal control group (control): no isoflurane anesthesia was given;

(2) Isoflurane anesthesia group (isoflurane): the mice were given isoflurane anesthesia;

(3) TLR4 interference empty vector+isoflurane anesthesia group (siRNA-NC): the mice were given intracerebroventricular injection of TLR4 interference negative control plasmid (2 μL, 50 μM/L), followed by isoflurane anesthesia;

(4) TLR4 interference+isoflurane anesthesia group (TLR-siRNA): the mice were given intracerebroventricular injection of TLR4 interference plasmid (2 μL, 50 μM/L), followed by isoflurane anesthesia.

Isoflurane anesthesia was given by inhalation with 3% isoflurane + 60% O_2 induction for the first 3 min, at a flow rate of 2 L/min, followed by maintenance at a flow rate of 1 L/min for 3 h, for 3 consecutive days.

For groups (3) and (4), after 5 days of intracerebroventricular injection (injection into the lateral ventricle of the brain) (6-day-old mice), isoflurane inhalation was given for 3 h for 3 consecutive days (6-day, 7-day and 8-day-old mice).

Mice behavior detected using Morris water maze test

When the mice reached 31 days of age, 3 mice from each group were taken for water maze experiment to observe the changes in animal behavior. The procedures were as follows:

1) Place navigation: The mice memory and learning abilities in the water maze were assessed. One day before the experiment, the mice were placed in the water maze for 60 s to adapt to the environment. The mice were trained for 4 consecutive days, 4 times per day in the afternoon,

with an interval of 15 min between each time. In each experiment, one mouse was placed in the pool with the head facing the side wall in 4 different directions (1 of the 4 directions each time). The order was different each day. The mice were allowed to swim until they found a platform and stayed on it for 20 s to achieve the effect of memory enhancement. The route to the platform that the mice were searching for under the water and the escape latency (the time it took to get from the water to the platform) were noted and recorded by a camera. If the mice did not reach the platform within 60 s, the escape latency was recorded as 60 s, and they were guided by the investigator to the platform and stayed on it for 30 s. The markers around the water maze were fixed, with no sound, no light and no human interference.

2) Spatial probe: It was used to detect the mice ability to remember the spatial position of the platform after learning to find it. The spatial probe test was carried out on the 5th day, following 4 days of training. The platform was removed. The mice were placed in the water on the opposite side of the original platform quadrant. The time the mice spent in the target quadrant and other quadrants was recorded.

Pathological condition in the hippocampal tissue detected with H&E staining

The mice were sacrificed by cervical dislocation. Under aseptic condition, the brain tissue was removed and washed with running water for several hours. The tissues were dehydrated with 70%, 80% and 90% ethanol solutions, and immersed in an equal amount of pure alcohol and xylene for 15 min, followed by xylene I and II (15 min each, until clear). Subsequently, the tissues were placed in an equal amount of xylene and paraffin for 15 min, followed by paraffin I for 50–60 min and paraffin II for another 50–60 min. The tissues were embedded in paraffin, and then sectioned, baked, dewaxed, and hydrated. The sections were placed in distilled water, and then subjected to hematoxylin staining for 3 min. Then, the sections were differentiated with hydrochloric acid ethanol for 15 s, and slightly washed with water. Blueing was performed for 15 s, and the sections were washed with running water, subjected to eosin staining for 3 min, and then again washed with running water. Then, they were dehydrated, cleared, mounted, and viewed under the microscope.

TLR4, BDNF and CREB1 mRNA expressions in the hippocampal tissue detected with fluorescence qPCR

Following RNA extraction, cDNA was synthesized using the reverse transcription kit. With cDNA as the template, the detection was performed with the fluorescent qPCR

Table 1. The operating system, reaction procedure and melting curve analysis of the fluorescence quantitative real-time polymerase chain reaction (qRT-PCR)

A. Operating system	
Reagent	Volume
RNase-Free dH$_2$0	9.5 µL
cDNA/DNA	1 µL
Upstream primer	1 µL
Downstream primer	1 µL
2×UltraSYBR Mixture	12.5 µL

B. Reaction procedure, 3-step method		
Step	Temperature [°C]	Duration
Predenaturation	95	10 min
Denaturation	95	10 s
Annealing	54.3	30 s
Extension	72	30 s
Cycle	40	

C. Melting curve analysis	
Temperature [°C]	Duration
95	15 s
54.3	1 min
95	15 s
54.3	15 s
54.3	15 s

cDNA – complementary DNA.

machine. The expression of TLR4 in each group was estimated using GAPDH as the internal reference.

The operating system, reaction procedure and melting curve analyses were presented in Table 1A–C. The primer information was displayed in Table 2.

TLR4, TNF-α, IL-6, BDNF, CREB1, ERK1/2, and JNK protein expressions in the hippocampal tissues detected with western blot

The samples in each group were added with lysis buffer, put on ice for 30 min and centrifuged for 10 min at 10,000 rpm at 4°C. The supernatant was carefully aspirated for total protein determination. The protein content was measured using the BCA kit. The protein was denatured, and sample loading was performed. Sodium dodecyl sulfate (SDS) gel electrophoresis was conducted for 1–2 h, followed by wet transfer for 30–50 min. Primary antibodies were incubated overnight at 4°C, followed by the secondary antibody for 1–2 h at room temperature. The ECL solution was applied onto the membrane and the image was captured under the gel imaging system. The gray value of each antibody band was determined using the Quantity One software (Bio-Rad Laboratories Co., Ltd.).

Table 2. Primer information

Primer	Primer sequence	Primer length [bp]	Product length [bp]	Annealing temperature [°C]
TLR4 F	AGCTTCTCCAATTTTTCAGAACTTC	25	99	60.4
TLR4 R	TGAGAGGTGGTGTAAGCCATGC	22		
GAPDH F	TCAACGGCACAGTCAAGG	18	357	57.8
GAPDH R	TGAGCCCTTCCACGATG	17		
BDNF F	ATGTCTATGAGGGTTCGGCG	20	256	59.52
BDNF R	GCGAGTTCCAGTGCCTTTG	19		
CREB1 F	GAGCAGACAACCAGCAGAGT	20	100	59.73
CREB1 R	ACCTGGGCTAATGTGGCAAT	20		
β-actin F	AGGGAAATCGTGCGTGAC	18	192	57.3
β-actin R	CATACCCAAGAAGGAAGGCT	20		

TLR4 – toll-like receptor 4; GAPDH – glyceraldehyde-3-phosphate dehydrogenase; BDNF – brain-derived neurotrophic factor; CREB1 – cyclic adenosine monophosphate response element-binding protein 1.

Serum TNF-α and IL-6 levels detected using ELISA

First, all reagents and components were brought back to room temperature. The standards, quality control products and samples were prepared in replicates. The working solution of various components of the kit were prepared according to the kit manual. The aluminum foil bags containing the ELISA-coated plates were removed. The standard and sample wells were established. Each of the standard wells received 50 µL of standards at various concentrations. The blank control wells were not added with samples or enzyme-labeled reagents; the remainder of the procedures were the same as the sample wells. Each sample well received 40 µL of sample diluent, followed by 10 µL of sample (the final dilution of sample was ×5). The samples were placed at the bottom of the wells, avoiding touching the side walls. They were gently shaken and mixed. Except for the blank control wells, each well received 100 µL of enzyme-labeled reagent. The plate was sealed with a film, which was then incubated at 37°C for 60 min. Before use, the wash buffer concentrate (×20) was diluted 20 times with distilled water. The sealing film was removed with care, and the liquid was patted dry. Each well was filled with wash buffer, left for 30 s and then discarded. This was performed 5 times, and each well was patted dry. Then, color reagents A and B (each 50 µL) were added into each well, gently shaken and mixed. Color was developed for 15 min at 37°C in the dark. The reaction was then terminated by adding 50 µL of stop solution to each well. The color was changed from blue to yellow. The blank well was adjusted to zero, and the absorbance (optical density (OD) value) of each well was measured at 450 nm.

Apoptosis rate in the hippocampal tissue detected with TUNEL staining

The tissue sections were placed in oven at 65°C and baked for 2 h. The sections were immersed in xylene for 10 min.

Then, the xylene was replaced with fresh xylene and the sections were left for another 10 min. The sections were put in 100% (twice), 95% and 80% ethanol, and then purified water, for 5 min each. The sections were placed in a wet box and 50 µg/mL proteinase K working solution was applied dropwise to each sample and incubated for 30 min at 37°C. Then, the sections were washed thoroughly with phosphate-buffered saline (PBS) for 5 min 3 times. The PBS around the tissue was absorbed with absorbent paper, an appropriate amount of TUNEL detection solution was added to each slide, and the sections were incubated in the dark for 2 h at 45°C. The slides were then washed with PBS for 5 min 3 times. The liquid on the glass slide was absorbed with absorbent paper. The glass slides were mounted with antifade mounting medium and examined with a fluorescence microscope.

Statistical analyses

The IBM SPSS v. 19 software (IBM Corp., Armonk, USA) was used for data analysis. The measurement data were presented as mean ± standard deviation ($\overline{x}$ ±SD). One-way analysis of variance (ANOVA) was used for the comparisons between the groups. Post hoc test was performed using Tukey's honestly significant difference (HSD) test. The value of $p < 0.05$ was considered statistically significant.

Outcome measures

Primary outcome: The behavior of mice treated with TLR4-siRNA compared with the control, isoflurane and siRNA-NC groups.

Secondary outcomes: The pathological condition, TLR4, BDNF and CREB1 mRNA expressions, serum IL-6 and TNF-α levels, apoptosis rate, and TLR4, IL-6, TNF-α, BDNF, CREB1, ERK1/2, and JNK protein expressions in mice treated with TLR4-siRNA, compared with the control, isoflurane and siRNA-NC groups.

Results

Mice behavior detected using Morris water maze test

As demonstrated in Fig. 1 (and Supplementary Table 1), the number of times the mice in the isoflurane group crossed the platform was significantly smaller, and the time spent at the platform circumjacent area I and II for the spatial probe test was significantly shorter than in the control group (Tukey's HSD; $p < 0.001$, $p < 0.001$, $p = 0.001$, respectively), while these values were significantly higher in the TLR-siRNA group than in the isoflurane group (Tukey's HSD; $p = 0.001$, $p = 0.009$, $p = 0.007$, respectively).

Pathological condition in the hippocampal tissue detected with H&E staining

The results of the pathological staining in each group were shown in Fig. 2. The neurons in each area of the hippocampus in the control group were closely arranged, the cell body size was normal, no obvious edema and degeneration were noted, and the inflammatory cell infiltration was relatively low. Both the isoflurane group and the siRNA-NC group had varying degrees of neuron arrangement disorder as well as a large number of inflammatory infiltrates. The neurons in the TLR-siRNA group were arranged in a relatively close and orderly manner.

TLR4, TNF-α and IL-6 expressions in the hippocampal tissue detected with qPCR and WB

As shown in Fig. 3 (and Supplementary Table 2), the TLR4, TNF-α and IL-6 expressions in the isoflurane group were significantly increased compared with the control group (Tukey's HSD; $p < 0.001$ for TLR4 mRNA expression, all $p < 0.001$ for protein expressions), while in the TLR-siRNA group they were significantly decreased when compared with the isoflurane group (Tukey's HSD; $p = 0.004$ for TLR4 mRNA expression, all $p < 0.001$ for protein expressions).

Serum TNF-α and IL-6 levels detected with ELISA

As presented in Fig. 4 (and Supplementary Table 3), the TNF-α and IL-6 levels in the isoflurane group were significantly increased compared with the control group (Tukey's HSD; $p < 0.001$ both), while in the TLR-siRNA group they were significantly decreased when compared with the isoflurane group (Tukey's HSD; $p < 0.001$ both).

Apoptosis rate in the hippocampal tissue detected with TUNEL staining

As shown in Fig. 5 (and Supplementary Table 4), the apoptosis rate in the isoflurane group was significantly increased compared with the control group (Tukey's HSD; $p = 0.005$), while in the TLR-siRNA group it was significantly decreased when compared with the isoflurane group (Tukey's HSD; $p = 0.004$).

BDNF and CREB1 mRNA expressions in the hippocampal tissue detected with qPCR

As revealed in Fig. 6 (and Supplementary Table 5), the BDNF mRNA expression in the isoflurane group was increased (Tukey's HSD; $p = 0.898$), and the CREB1 mRNA expression was decreased when compared with the control group (Tukey's HSD; $p = 0.654$). The BDNF mRNA expression in the TLR-siRNA group was decreased (Tukey's HSD; $p = 0.660$) and the CREB1 mRNA expression was significantly decreased (Tukey's HSD; $p = 0.013$) compared with the isoflurane group.
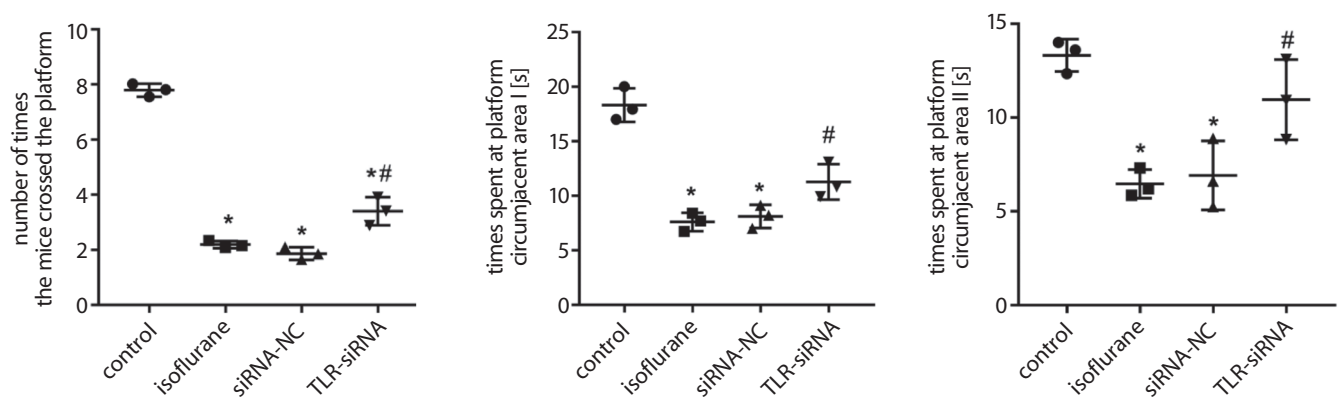

Fig. 1. Morris water maze test results of each group. Tukey's honestly significant difference (HSD); compared with the control group, *$p < 0.05$; compared with the isoflurane group, #$p < 0.05$ ($n = 3$/group). The interval represents the mean value. The ends of the interval represent standard deviation (SD)

siRNA-NC – TLR4 interference empty vector+isoflurane anesthesia group; TLR-siRNA – TLR4 interference+isoflurane anesthesia group.
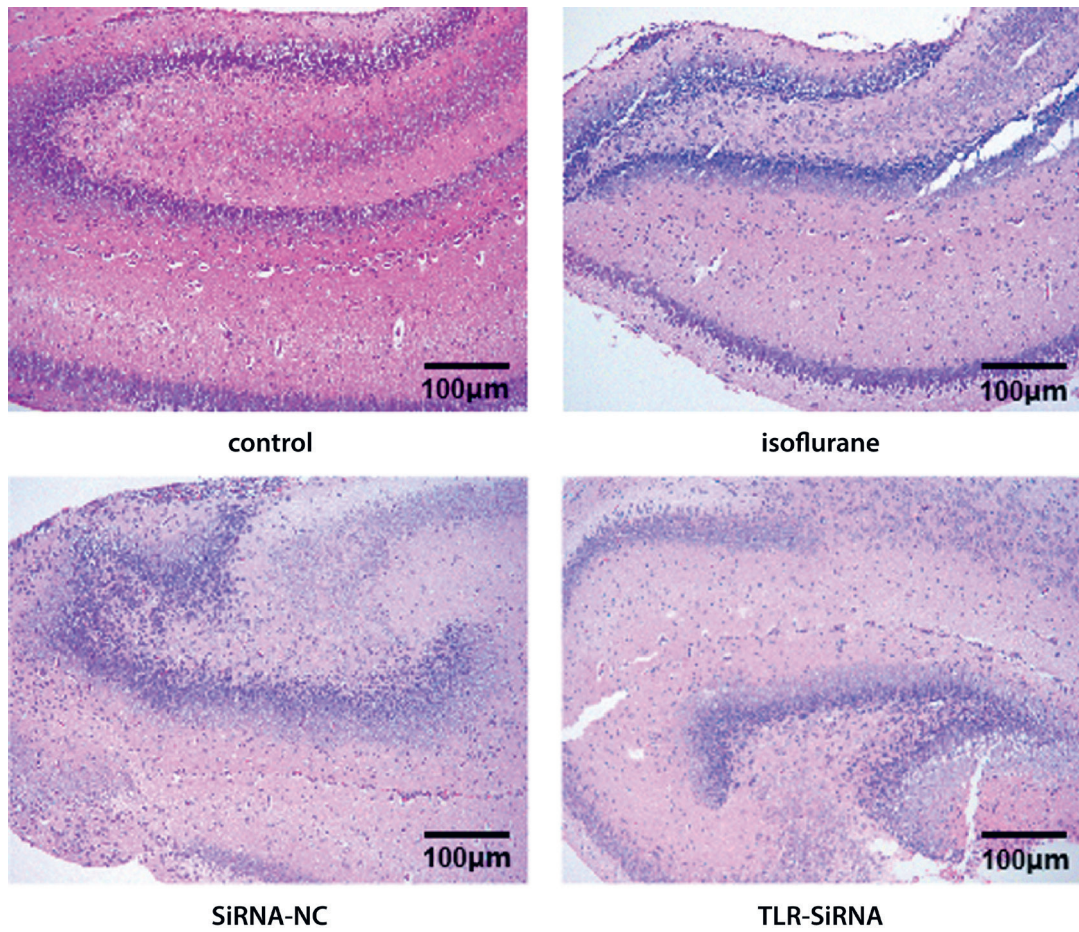
Fig. 2. Hematoxylin and eosin (H&E) staining of the hippocampal tissue in each group

siRNA-NC – TLR4 interference empty vector+isoflurane anesthesia group; TLR-siRNA – TLR4 interference+isoflurane anesthesia group.
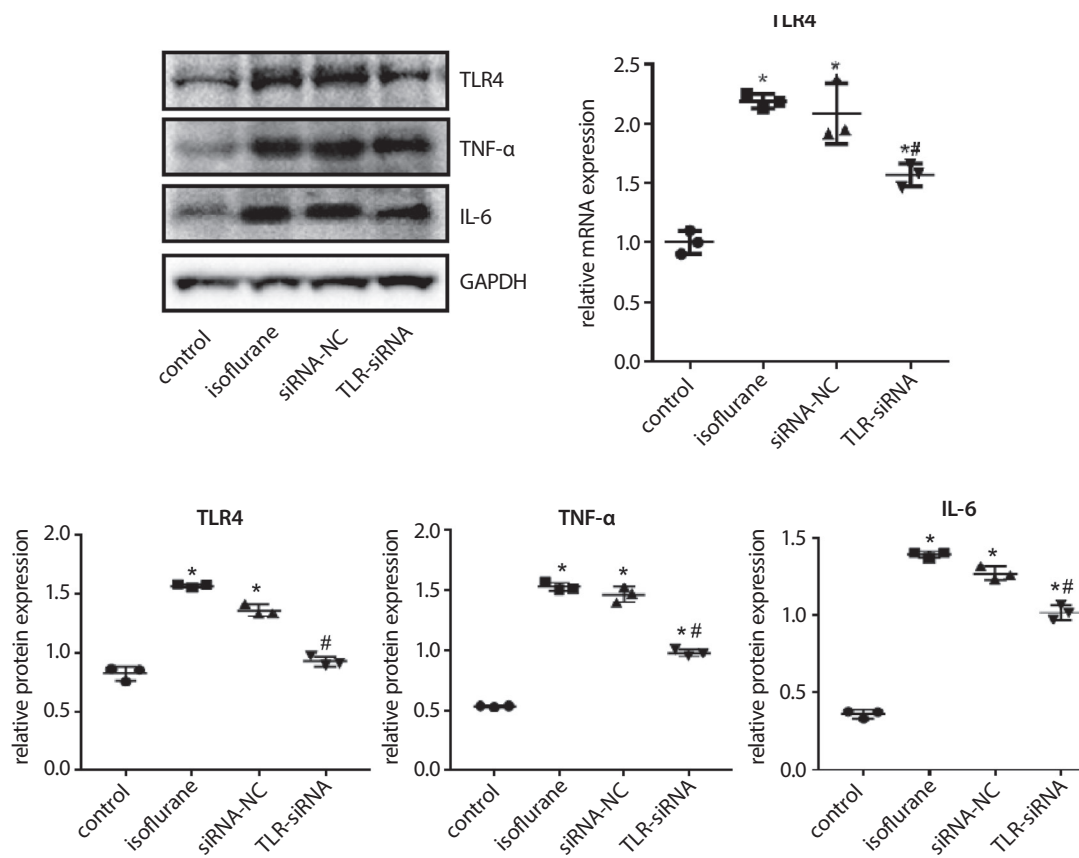

Fig. 3. The toll-like receptor 4 (TLR4), tumor necrosis factor alpha (TNF-α) and interleukin (IL)-6 expressions in the hippocampal tissue of each group detected with quantitative real-time polymerase chain reaction (qRT-PCR) and western blot (WB). Tukey's honestly significant difference (HSD); compared with the control group, *p < 0.05; compared with the isoflurane group, #p < 0.05 (n = 3/group). The interval represents the mean value. The ends of the interval represent standard deviation (SD)

siRNA-NC – TLR4 interference empty vector+isoflurane anesthesia group; TLR-siRNA – TLR4 interference+isoflurane anesthesia group; GAPDH – glyceraldehyde-3-phosphate dehydrogenase.
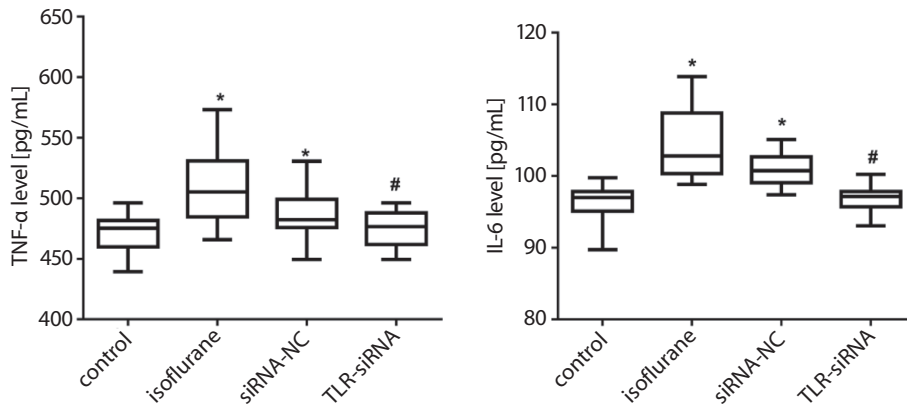
Fig. 4. Serum tumor necrosis factor alpha (TNF-α) and interleukin (IL)-6 levels of mice in each group detected using the enzyme-linked immunosorbent assay (ELISA). Tukey's honestly significant difference (HSD); compared with the control group, *p < 0.05; compared with the isoflurane group, #p < 0.05 (n = 3/group). The box-and-whiskers are built of the ranges without outliers (whiskers), interquartile ranges (IQRs; boxes) and medians

siRNA-NC – TLR4 interference empty vector+isoflurane anesthesia group; TLR-siRNA – TLR4 interference+isoflurane anesthesia group.
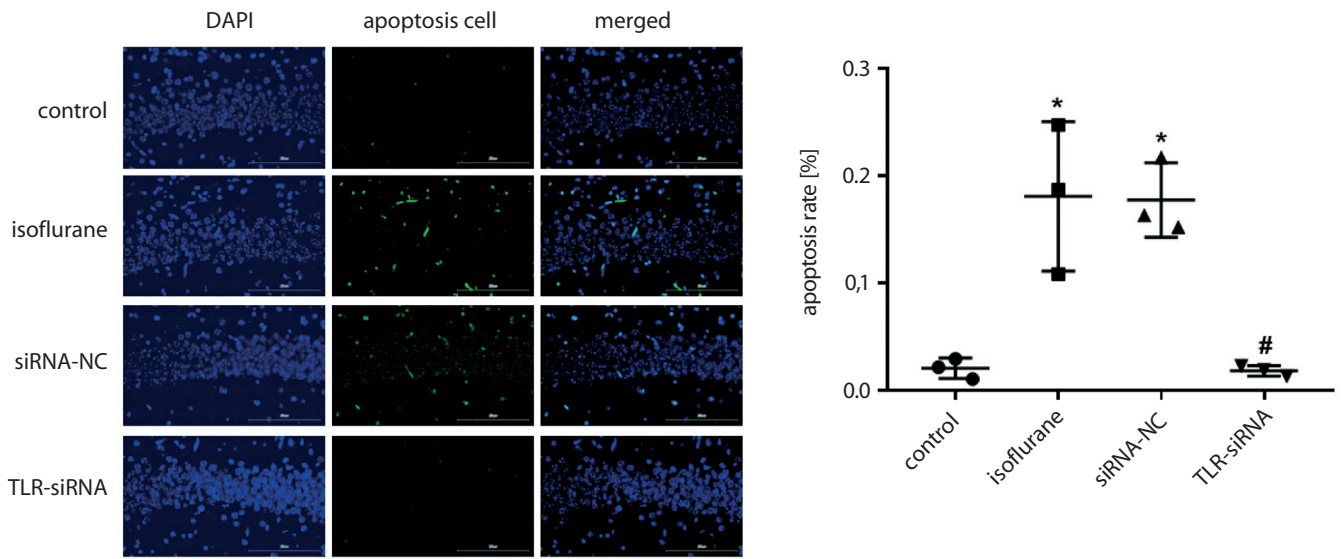

Fig. 5. Apoptosis rate in the hippocampal tissue of each group detected with terminal deoxynucleotidyl transferase dUTP nick end labeling (TUNEL) staining. Tukey's honestly significant difference (HSD); compared with the control group, *p < 0.05; compared with the isoflurane group, #p < 0.05 (n = 3/group). The interval represents the mean value. The ends of the interval represent standard deviation (SD)

siRNA-NC – TLR4 interference empty vector+isoflurane anesthesia group; TLR-siRNA – TLR4 interference+isoflurane anesthesia group.
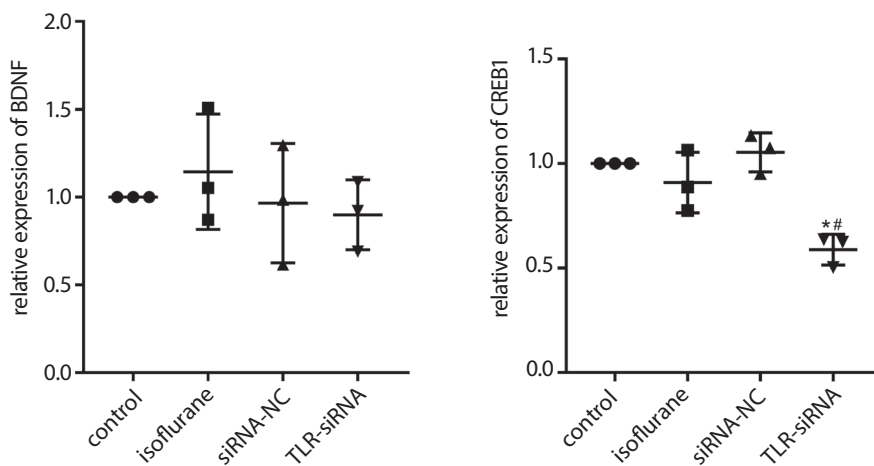
Fig. 6. Brain-derived neurotrophic factor (BDNF) and cyclic adenosine monophosphate response element-binding protein 1 (CREB1) mRNA expressions in the hippocampal tissue of each group detected with quantitative real-time polymerase chain reaction (qRT-PCR). Tukey's honestly significant difference (HSD); compared with the control group, *p < 0.05; compared with the isoflurane group, #p < 0.05 (n = 3/group). The interval represents the mean value. The ends of the interval represent standard deviation (SD)

siRNA-NC – TLR4 interference empty vector+isoflurane anesthesia group; TLR-siRNA – TLR4 interference+isoflurane anesthesia group.

BDNF, CREB1, ERK1/2, and JNK protein expressions in the hippocampal tissue detected with WB

As shown in Fig. 7 (and Supplementary Table 6), the CREB1 protein expression in the isoflurane group was significantly decreased (Tukey's HSD; p = 0.018) and the JNK protein expression was significantly increased (Tukey's HSD; p = 0.004), while the BDNF and ERK1/2 protein expressions did not show significant changes (Tukey's HSD; p = 0.317, p = 0.789, respectively) compared with the control group. The BDNF and CREB1 protein expressions in the TLR-siRNA group were significantly increased (Tukey's HSD; p < 0.001, both), while the ERK1/2 and JNK protein expressions did not show significant changes (Tukey's HSD; p = 0.994, p = 0.547, respectively) when compared with the isoflurane group.
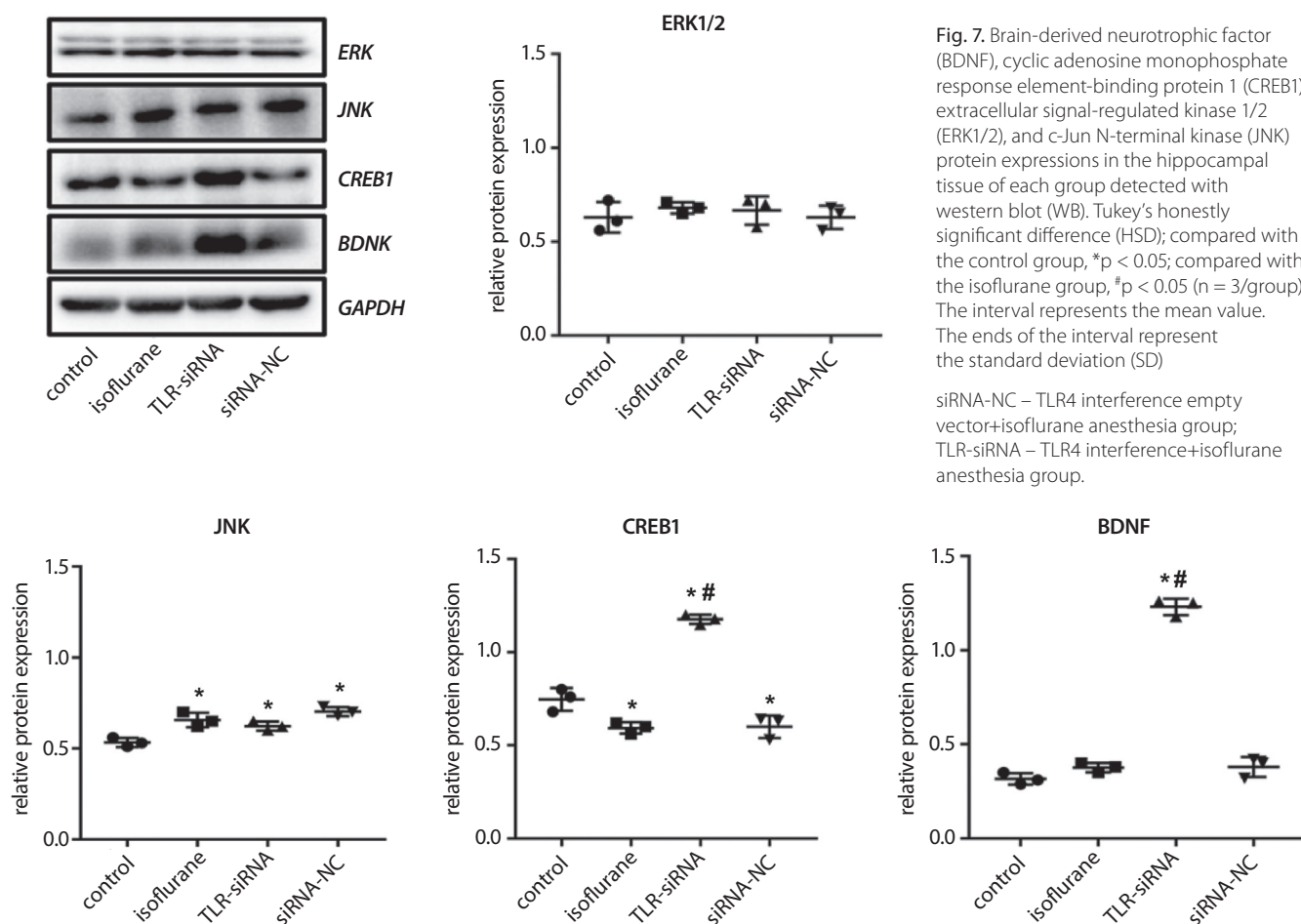
Discussion

A number of studies have found that the inhalation of anesthetics may cause or increase the risk of cognitive impairment in humans and rodents.[32,33] A large number of animal experiments have shown that the current clinical use of inhaled and intravenous general anesthetics can cause obvious and extensive apoptosis of the developing neurons, and cognitive impairment and abnormal function of neural circuit, as well as decline or loss of cognitive behavior ability in adulthood.[4,34,35]

The TLR4 is an important part of the activation of the innate immune system, and is expressed in neurons and glial cells.[36] It does not only mediate the innate immune response, but also participates in the inflammatory reactions and neurodegeneration.[37,38] In this study, the number of times the mice crossed the platform, and the time they spent at the platform circumjacent area I and II for the spatial probe test were significantly decreased in the isoflurane group, indicating that isoflurane can impair the cognitive and behavioral abilities of the mice. The cognitive ability recovered after the TLR4 interference. These findings indicate that the TLR4 expression plays an important role in the cognitive ability of mice.

The TLR4 activation can lead to a substantial number of neuronal deaths.[39] Studies have found that an increased expression of TLR4 aggravates the increase of the inflammatory cytokines in the hippocampus, which may further stimulate the neuroinflammatory response by activating microglia and astrocytes, and eventually lead to neuronal damage and cognitive decline.[40] In this study, basing

Fig. 7. Brain-derived neurotrophic factor (BDNF), cyclic adenosine monophosphate response element-binding protein 1 (CREB1), extracellular signal-regulated kinase 1/2 (ERK1/2), and c-Jun N-terminal kinase (JNK) protein expressions in the hippocampal tissue of each group detected with western blot (WB). Tukey's honestly significant difference (HSD); compared with the control group, *p < 0.05; compared with the isoflurane group, #p < 0.05 (n = 3/group). The interval represents the mean value. The ends of the interval represent the standard deviation (SD)

siRNA-NC – TLR4 interference empty vector+isoflurane anesthesia group; TLR-siRNA – TLR4 interference+isoflurane anesthesia group.

on the H&E staining results, it could be observed that the hippocampal neurons in the control group were closely arranged, and inflammatory cell infiltration was relatively low, whereas the isoflurane and siRNA-NC groups showed varying degrees of neuron arrangement disorder and a high number of inflammatory infiltrates. The neurons in the TLR-siRNA group were arranged in a relatively close and orderly manner.

The increase of peripheral inflammatory cytokines can cause cognitive impairment. At present, more than 30 kinds of cytokines are known, including interleukins (IL-1 to IL-4), TNF and transforming growth factor (TGFβ1-3), among which IL-1, IL-6 and TNF-α are considered to be the typical pro-inflammatory cytokines.[41] The IL-1, produced by the activation of microglia, is the initiating link of the inflammatory response. The IL-1 promotes the proliferation and activation of microglia through the autocrine pathway, initiates the release of cytokines such as IL-6 and TNF-α, and induces the increase in the production of complement and chemokines. In turn, the immune inflammatory cytokines activate microglia, resulting in a continuous increase in cytokines that eventually lead to neuronal degeneration and necrosis, which further stimulates microglia to synthesize and secrete cytokines, and forms a positive feedback loop in the body, resulting in a cascade amplification effect of inflammatory response.[42,43] The TLR4 can promote expressions of the inflammatory factors such as IL-1, IL-6 and TNF-α. At the same time, these inflammatory factors interact with each other, causing an excessive release of inflammatory mediators, which further aggravate tissue and organ damage.[44] The results of this study revealed that the expressions of the inflammatory factors TNF-α and IL-6 increased significantly after the mice were anesthetized with isoflurane, and decreased significantly following the TLR4 expression interference. These results indicated that TLR4, as an innate immune inflammatory response mediator, may mediate the excessive release of the inflammatory response factors, causing nerve cell damage, and long-term excessive damage may lead to a decline in the cognitive function.

In addition, we found that isoflurane anesthesia significantly increased the apoptosis rate of the hippocampal tissue. The apoptosis rate in the TLR-siRNA group was significantly decreased compared with the isoflurane group. Further mechanism study demonstrated that the CREB1 protein expression in the isoflurane group was significantly decreased, and the JNK protein expression was significantly increased compared with the control group; however, the protein expressions of BDNF and ERK1/2 did not show any significant changes. The BDNF and CREB1 protein expressions in the TLR-siRNA group were significantly increased, while the ERK1/2 and JNK protein expressions did not show any significant changes compared with the isoflurane group.

Generalizability of the study

The findings of this study can be generalized to human and validated by further clinical trials.

Limitations

First, this study only shows the protective effect of TLR4-siRNA intervention on learning and memory function of young mice induced by anesthetics, but the mechanism of TLR4 is not clear. Second, surgical anesthesia involves a broad array of drugs. This study only explores the effect of isoflurane anesthesia, which is not comprehensive enough. A variety of anesthetic agents can be explored to illustrate the universality of the role of TLR4 in cognitive impairment.

Future research can be extended in 2 directions. First, to explore the mechanism of TLR4 in microglia at the cellular level. Second, to establish a model of postoperative cognitive impairment induced by a variety of anesthetics to prove the universality of the role of TLR4.

Another limitation is the small sample size of the study; the homogeneity of variance and normality were assumed without checking the assumptions. Future research should involve a larger size sample.

Conclusions

The exposure to isoflurane anesthesia plays a crucial role in the cognitive impairment process in young mice. Isoflurane anesthesia stimulates the inflammatory response factors to overexpress, causing neuronal cell damage and eventually cognitive impairment. An early exposure to isoflurane anesthesia can lead to a persistent impairment in memory and learning function of the developing brain. As a mediator of the innate immune inflammatory response, TLR4 plays a key role in the cell injury process. Blocking TLR4 signal may delay the process of cell inflammatory injury and cognitive impairment.

Supplementary data

Additional data showing the exact statistical analysis data have been deposited at
https://doi.org/10.5281/zenodo.6319656.
The package contains 6 files:
Supplementary Table 1. Morris water maze test results of each group;
Supplementary Table 2. TLR4, TNF-α and IL-6 expressions in the hippocampus of each group detected with qPCR and WB;
Supplementary Table 3. Serum TNF-α and IL-6 levels of mice in each group detected with ELISA;

Supplementary Table 4. Apoptosis rate detected with TUNEL staining;

Supplementary Table 5. BDNF and CREB1 mRNA expressions detected with qPCR;

Supplementary Table 6. BDNF, CREB1, ERK1/2, and JNK protein expressions detected with WB.

ORCID iDs

Lin Lin https://orcid.org/0000-0003-4655-8379
Dongping Chen https://orcid.org/0000-0002-3791-6755
Xiaoli Yu https://orcid.org/0000-0002-4642-2888
Wensheng Zhong https://orcid.org/0000-0001-5046-0935
Yanlong Liu https://orcid.org/0000-0001-7427-2533
Yu Feng https://orcid.org/0000-0003-4800-5612
Heguo Luo https://orcid.org/0000-0002-6602-6591

References

1. Hu D, Flick RP, Zaccariello MJ, et al. Association between exposure of young children to procedures requiring general anesthesia and learning and behavioral outcomes in a population-based birth cohort. *Anesthesiology*. 2017;127(2):227–240. doi:10.1097/ALN.0000000000 001735

2. Block RI, Thomas JJ, Bayman EO, Choi JY, Kimble KK, Todd MM. Are anesthesia and surgery during infancy associated with altered academic performance during childhood? *Anesthesiology*. 2012;117(3): 494–503. doi:10.1097/ALN.0b013e3182644684

3. Ing CH, DiMaggio CJ, Whitehouse AJ, et al. Neurodevelopmental outcomes after initial childhood anesthetic exposure between ages 3 and 10 years. *J Neurosurg Anesthesiol*. 2014;26(4):377–386. doi:10.1097/ANA.0000000000000121

4. Jevtovic-Todorovic V, Hartman RE, Izumi Y, et al. Early exposure to common anesthetic agents causes widespread neurodegeneration in the developing rat brain and persistent learning deficits. *J Neurosci*. 2003;23(3):876–882. doi:10.1523/JNEUROSCI.23-03-00876.2003

5. Yon JH, Daniel-Johnson J, Carter LB, Jevtovic-Todorovic V. Anesthesia induces neuronal cell death in the developing rat brain via the intrinsic and extrinsic apoptotic pathways. *Neuroscience*. 2005;135(3):815–827. doi:10.1016/j.neuroscience.2005.03.064

6. Ma D, Williamson P, Januszewski A, et al. Xenon mitigates isoflurane-induced neuronal apoptosis in the developing rodent brain. *Anesthesiology*. 2007;106(4):746–753. doi:10.1097/01.anes.0000264762. 48920.80

7. Shen X, Dong Y, Xu Z, et al. Selective anesthesia-induced neuroinflammation in developing mouse brain and cognitive impairment. *Anesthesiology*. 2013;118(3):502–515. doi:10.1097/ALN.0b013e3182834d77

8. Saxena S, Maze M. Impact on the brain of the inflammatory response to surgery. *Presse Med*. 2018;47(4 Pt 2):e73–e81. doi:10.1016/j.lpm. 2018.03.011

9. Whitaker EE, Christofi FL, Quinn KM, et al. Selective induction of IL-1β after a brief isoflurane anesthetic in children undergoing MRI examination. *J Anesth*. 2017;31(2):219–224. doi:10.1007/s00540-016-2294-y

10. de Voogd LD, Murray YPJ, Barte RM, et al. The role of hippocampal spatial representations in contextualization and generalization of fear. *Neuroimage*. 2020;206:116308. doi:10.1016/j.neuroimage. 2019.116308

11. Battaglia S, Garofalo S, di Pellegrino G, Starita F. Revaluing the role of vmPFC in the acquisition of Pavlovian threat conditioning in humans. *J Neurosci*. 2020;40(44):8491–8500. doi:10.1523/JNEUROSCI.0304-20.2020

12. Battaglia S, Harrison BJ, Fullana MA. Does the human ventromedial prefrontal cortex support fear learning, fear extinction or both? A commentary on subregional contributions. *Mol Psychiatry*. 2021. doi:10.1038/s41380-021-01326-4

13. Borgomaneri S, Serio G, Battaglia S. Please, don't do it! Fifteen years of progress of non-invasive brain stimulation in action inhibition. *Cortex*. 2020;132:404–422. doi:10.1016/j.cortex.2020.09.002

14. Anderson MC, Bunce JG, Barbas H. Prefrontal-hippocampal pathways underlying inhibitory control over memory. *Neurobiol Learn Mem*. 2016;134(Pt A):145–161. doi:10.1016/j.nlm.2015.11.008

15. Wang W, Chen X, Zhang J, et al. Glycyrrhizin attenuates isoflurane-induced cognitive deficits in neonatal rats via its anti-inflammatory activity. *Neuroscience*. 2016;316:328–336. doi:10.1016/j.neuroscience. 2015.11.001

16. Si J, Jin Y, Cui M, Yao Q, Li R, Li X. Neuroprotective effect of miR-212-5p on isoflurane-induced cognitive dysfunction by inhibiting neuroinflammation. *Toxicol Mech Methods*. 2021;31(7):501–506. doi:10.1080/ 15376516.2021.1919948

17. Eifinger F, Hünseler C, Roth B, et al. Observations on the effects of inhaled isoflurane in long-term sedation of critically ill children using a modified AnaConDa©-system. *Klin Padiatr*. 2013;225(4):206–211. doi:10.1055/s-0033-1345173

18. Yi X, Cai Y, Li W. Isoflurane damages the developing brain of mice and induces subsequent learning and memory deficits through FASL-FAS signaling. *Biomed Res Int*. 2015;2015:315872. doi:10.1155/2015/315872

19. Talpos JC, Chelonis JJ, Li M, Hanig JP, Paule MG. Early life exposure to extended general anesthesia with isoflurane and nitrous oxide reduces responsivity on a cognitive test battery in the non-human primate. *Neurotoxicology*. 2019;70:80–90. doi:10.1016/j.neuro. 2018.11.005

20. Zhu C, Gao J, Karlsson N, et al. Isoflurane anesthesia induced persistent, progressive memory impairment, caused a loss of neural stem cells, and reduced neurogenesis in young, but not adult, rodents. *J Cereb Blood Flow Metab*. 2010;30(5):1017–1030. doi:10.1038/jcbfm. 2009.274

21. Schaefer ML, Wang M, Perez PJ, Coca Peralta W, Xu J, Johns RA. Nitric oxide donor prevents neonatal isoflurane-induced impairments in synaptic plasticity and memory. *Anesthesiology*. 2019;130(2):247–262. doi:10.1097/ALN.0000000000002529

22. Kang E, Jiang D, Ryu YK, et al. Early postnatal exposure to isoflurane causes cognitive deficits and disrupts development of newborn hippocampal neurons via activation of the mTOR pathway. *PLoS Biol*. 2017;15(7):e2001246. doi:10.1371/journal.pbio.2001246. Erratum in: *PLoS Biol*. 2018;16(3):e1002625. doi:10.1371/journal.pbio.1002625

23. Bachour Y, Ritt MJPF, Heijmans R, Niessen FB, Verweij SP. Toll-like receptors (TLRs) expression in contracted capsules compared to uncontracted capsules. *Aesthetic Plast Surg*. 2019;43(4):910–917. doi:10.1007/s00266-019-01368-8

24. Caso JR, Pradillo JM, Hurtado O, Lorenzo P, Moro MA, Lizasoain I. Toll-like receptor 4 is involved in brain damage and inflammation after experimental stroke. *Circulation*. 2007;115(12):1599–1608. doi:10.1161/ CIRCULATIONAHA.106.603431

25. Hua F, Ma J, Ha T, et al. Differential roles of TLR2 and TLR4 in acute focal cerebral ischemia/reperfusion injury in mice. *Brain Res*. 2009; 1262:100–108. doi:10.1016/j.brainres.2009.01.018

26. Walter S, Letiembre M, Liu Y, et al. Role of the toll-like receptor 4 in neuroinflammation in Alzheimer's disease. *Cell Physiol Biochem*. 2007;20(6):947–956. doi:10.1159/000110455

27. Battaglia S, Garofalo S, di Pellegrino G. Context-dependent extinction of threat memories: Influences of healthy aging. *Sci Rep*. 2018;8(1): 12592. doi:10.1038/s41598-018-31000-9

28. Török N, Tanaka M, Vécsei L. Searching for peripheral biomarkers in neurodegenerative diseases: The tryptophan-kynurenine metabolic pathway. *Int J Mol Sci*. 2020;21(24):9338. doi:10.3390/ijms 21249338

29. Tanaka M, Toldi J, Vécsei L. Exploring the etiological links behind neurodegenerative diseases: Inflammatory cytokines and bioactive kynurenines. *Int J Mol Sci*. 2020;21(7):2431. doi:10.3390/ijms21072431

30. Ising C, Heneka MT. Functional and structural damage of neurons by innate immune mechanisms during neurodegeneration. *Cell Death Dis*. 2018;9(2):120. doi:10.1038/s41419-017-0153-x

31. Zhou X, Wu Q, Lu Y, et al. Crosstalk between soluble PDGF-BB and PDGFRβ promotes astrocytic activation and synaptic recovery in the hippocampus after subarachnoid hemorrhage. *FASEB J*. 2019;33(8):9588–9601. doi:10.1096/fj.201900195R

32. Sen T, Sen N. Isoflurane-induced inactivation of CREB through histone deacetylase 4 is responsible for cognitive impairment in developing brain. *Neurobiol Dis*. 2016;96:12–21. doi:10.1016/j.nbd.2016.08.005

33. Cheng B, Zhang Y, Wang A, Dong Y, Xie Z. Vitamin C attenuates isoflurane-induced caspase-3 activation and cognitive impairment. *Mol Neurobiol*. 2015;52(3):1580–1589. doi:10.1007/s12035-014-8959-3

34. Jevtovic-Todorovic V. Anesthesia and the developing brain: Are we getting closer to understanding the truth? *Curr Opin Anaesthesiol*. 2011;24(4):395–399. doi:10.1097/ACO.0b013e3283487247

35. Sanchez V, Feinstein SD, Lunardi N, et al. General anesthesia causes long-term impairment of mitochondrial morphogenesis and synaptic transmission in developing rat brain. *Anesthesiology*. 2011;115(5): 992–1002. doi:10.1097/ALN.0b013e3182303a63

36. Buchanan MM, Hutchinson M, Watkins LR, Yin H. Toll-like receptor 4 in CNS pathologies. *J Neurochem*. 2010;114(1):13–27. doi:10.1111/j. 1471-4159.2010.06736.x

37. Gong CY, Zhou AL, Mao JH, Hu YE, Geng JS. The role of Toll-like receptor 4 on inflammation and Aβ formation in cortex astrocytes. *Sheng Li Xue Bao*. 2014;66(6):631–638. PMID:25516511.

38. Trotta T, Porro C, Calvello R, Panaro MA. Biological role of Toll-like receptor-4 in the brain. *J Neuroimmunol*. 2014;268(1–2):1–12. doi:10. 1016/j.jneuroim.2014.01.014

39. Hua F, Ma J, Ha T, et al. Activation of Toll-like receptor 4 signaling contributes to hippocampal neuronal death following global cerebral ischemia/reperfusion. *J Neuroimmunol*. 2007;190(1–2):101–111. doi: 10.1016/j.jneuroim.2007.08.014.

40. Jou I, Lee JH, Park SY, Yoon HJ, Joe EH, Park EJ. Gangliosides trigger inflammatory responses via TLR4 in brain glia. *Am J Pathol*. 2006; 168(5):1619–1630. doi:10.2353/ajpath.2006.050924

41. Lissoni P, Messina G, Pelizzoni F, et al. The fascination of cytokine immunological science. *J Infectiology*. 2020;3(1):14–28. doi:10.29245 /2689-9981/2020/1.1155

42. Harry GJ, Kraft AD. Neuroinflammation and microglia: Considerations and approaches for neurotoxicity assessment. *Expert Opin Drug Metab Toxicol*. 2008;4(10):1265–1277. doi:10.1517/17425255.4.10.1265

43. Rodríguez-Gómez JA, Kavanagh E, Engskog-Vlachos P, et al. Microglia: Agents of the CNS pro-inflammatory response. *Cells*. 2020;9(7):1717. doi:10.3390/cells9071717

44. Lin XW, Xu WC, Luo JG, et al. WW domain containing E3 ubiquitin protein ligase 1 (WWP1) negatively regulates TLR4-mediated TNF-α and IL-6 production by proteasomal degradation of TNF receptor associated factor 6 (TRAF6). *PLoS One*. 2013;8(6):e67633. doi:10.1371/ journal.pone.0067633

Knockdown of circular RNA *hsa_circ_0003307* inhibits synovial inflammation in ankylosing spondylitis by regulating the PI3K/AKT pathway

Yanyan Fang[A,C], Jian Liu[A,E,F], Yan Long[A,D], Jianting Wen[B], Dan Huang[B], Ling Xin[E]

The First Affiliated Hospital of Anhui University of Chinese Medicine, Hefei, China

A – research concept and design; B – collection and/or assembly of data; C – data analysis and interpretation;
D – writing the article; E – critical revision of the article; F – final approval of the article

Address for correspondence
Jian Liu
E-mail: liujianahzy@126.com

Conflict of interest
None declared

Abstract

Background. Ankylosing spondylitis (AS) has a high disability rate, and an early diagnosis is difficult.

Objectives. To explore the possible functions and underlying mechanism of circular RNAs *Homo sapiens (hsa)_circ_0003307* in ankylosing spondylitis.

Materials and methods. The *hsa_circ_0003307* expression levels were investigated in the peripheral blood mononuclear cells (PBMCs) of 30 AS patients and 30 healthy controls (HC) using quantitative reverse transcription polymerase chain reaction (qRT-PCR) analysis. Primary fibroblast-like synoviocytes (FLS) were separated from synovial tissues, established as cell lines and cultured for subsequent cell experiments involving transfection with different vectors. The qRT-PCR analysis was used for evaluating the levels of *hsa_circ_0003307* in AS-FLS. Phosphoinositide 3-kinase (PI3K)/protein kinase B (AKT) pathway-related protein levels were measured using western blotting and immunofluorescence. Enzyme-linked immunosorbent assay (ELISA) was used to detect the levels of inflammatory cytokines. Spearman's correlation analysis was used to assess the correlation between *hsa_circ_0003307* and clinical characteristics.

Results. The expression level of *hsa_circ_0003307* was significantly high in AS patients and was positively associated with erythrocyte sedimentation rate (ESR), C-reactive protein (CRP), Bath Ankylosing Spondylitis Disease Activity Index (BASDAI), and Bath Ankylosing Spondylitis Functional Index (BASFI). We found that *hsa_circ_0003307* overexpression could promote the activation of the PI3K/AKT pathway and expression of inflammatory cytokines – tumor necrosis factor alpha (TNF-α) and TNF-α-induced protein 2 (TNFAIP2). However, *hsa_circ_0003307* knockdown reduced the expression of TNF-α and TNFAIP2.

Conclusions. The expression level of *hsa_circ_0003307* was associated with inflammatory response, and it was revealed that *hsa_circ_0003307* knockdown could reduce the inflammatory response of AS by regulating the PI3K/AKT pathway.

Key words: ankylosing spondylitis, PI3K/AKT, *hsa_circ_0003307*

Background

Ankylosing spondylitis (AS) is a chronic refractory inflammatory arthritis, characterized by chronic nonspecific inflammation.[1] The sacroiliac joints and spine are the body parts most commonly affected by AS.[2] If not treated in time, it affects the movement of the spine joints, and even spinal joint stiffness and deformity will appear.[3] This seriously worsen the quality of life of patients. This disease is mainly painful in the early stage, when the symptoms of unfavorable spinal joint movement are not obvious, and it is not easy to be diagnosed. Often, when AS is clearly diagnosed, irreversible joint damage has already occurred, and other system diseases may also be observed. The treatment of AS brings a huge economic burden to the families of the patients and the whole community. Therefore, an early diagnosis is very important for AS patients and their families. There is an urgent need to identify new biomarkers that could be used as indicators for the diagnosis or prognosis of AS. The discovery of such biomarkers may have inestimable value for the early diagnosis and treatment of AS.

Circular RNA (circRNA) is a unique RNA composed of exons, introns, or the products of reverse splicing of both.[4] Because circRNA has no 5′ or 3′ ends, it can withstand RNase digestion and is more stable than most linear RNAs.[5] In addition to its characteristics of a relatively high stability, circRNA often exhibits tissue/developmental stage-specific expression,[6,7] and is therefore more suitable as a biomarker than linear RNA.[8] Previous studies have confirmed that circRNA may control gene transcription by isolating target microRNAs (miRNAs) and regulating RNA-binding proteins, thereby acting as an "miRNA sponge".[9] There is increasing evidence that certain circRNAs may be related to the risk of neurological, atherosclerotic vascular, prion, cancer, and autoimmune diseases.[10–13] This supports the hypothesis that circRNAs may become new diagnostic and prognostic biomarkers, and new disease treatment targets.[14,15] However, the current understanding of circRNA in AS patients is limited.

Phosphatidylinositol-3 kinase (PI3K)/protein kinase B (AKT) is an important inflammatory pathway that participates in a variety of physiological and pathological processes in the body. After activation, it participates in cell signal transduction, growth, angiogenesis, and carcinogenic transformation.[16] The PI3K is affected by cytokines to change the protein structure of AKT and activate it, thereby regulating the release of pro-inflammatory mediators.[17] Studies have shown that the PI3K/AKT//mammalian target of rapamycin (mTOR) signaling pathway plays a role in cartilage degeneration, subchondral bone dysfunction and synovial inflammation.[18,19] Therefore, this study verified the diagnostic effect of *circ_0003307* by observing the influence of *circ_0003307* on the PI3K/AKT pathway.

Objectives

The objective of this study was to explore the possible role of a certain circRNA, *Homo sapiens (hsa)_circ_0003307*, in AS. To achieve this, we detected the expression level of *circRNA_0003307* in peripheral blood mononuclear cells (PBMCs) of AS patients. Thereafter, we verified the possible role of the edited *circRNA_0003307* in the inflammatory response of AS-fibroblast-like synoviocytes (AS-FLS).

Materials and methods

Patients and healthy controls

Thirty AS patients were recruited from the Department of Rheumatology, Anhui Provincial Hospital of Traditional Chinese Medicine, Hefei, China. These patients were diagnosed by interviewers in accordance with the New York criteria revised by the American College of Rheumatology.[20,21] At the same time, we also recruited 30 healthy subjects whose age and gender matched those of AS patients as healthy controls (HC). Both the patient and the HC group ruled out the history of other diseases. The research protocol was in line with the Declaration of Helsinki. This study was approved by the Medical Ethics Committee of Anhui Provincial Hospital of Traditional Chinese Medicine (approval No. 2020AH-08).

Isolation of PBMCs and extraction of total RNA

Peripheral blood (5 mL) of the subjects was collected using an ethylenediaminetetraacetic acid (EDTA) anticoagulation tube. A discontinuous density gradient (Histopaque-1077; Sigma-Aldrich, St. Louis, USA) was used to separate PBMCs. Total RNA was extracted using TRI-Reagent (Invitrogen, Carlsbad, USA) and stored at –80°C. The RNA concentration was determined with a NanoDrop spectrophotometer (Thermo Fisher Scientific, Waltham, USA), and RNA integrity was assessed with agarose gel electrophoresis.

Cell culture

Synovial tissue specimens were obtained from AS patients undergoing hip replacement surgery. The specimens were cut into small pieces and mixed with 4 mg/mL collagenase (type I) (Sigma-Aldrich) for 1 h. Then, the cells were digested with 0.25% trypsin. Thereafter, AS-FLS cells were collected and added to Dulbecco's modified Eagle's culture medium (DMEM; HyClone Laboratories, Inc., Logan, USA) containing 10% fetal bovine serum (FBS; Sigma-Aldrich) and 1% streptomycin and penicillin (Beyotime, Shanghai, China). Cells were maintained at 37°C and 5% CO_2. The isolated AS-FLS were cultivated from the 3rd to the 6th generation for further study.

Cell transfection

The pcDNA3.1-*hsa_circ_0003307* was generated by amplifying the coding sequence of *circRNA_0003307* and inserting it into pcDNA3.1(+). Small interfering RNAs (siRNAs) were targeted to *circRNA_0003307* (siRNA1: 5′-AGGCUGGAAACCAUCGACGTT-3′, siRNA2: 5′-C'UGGAAACCAUC GACGAGUTT-3′, siRNA3: 5′-GAAACCAUCGACGAGUACATT-3′). Nonsense control siRNA (si-NC) was purchased from GenePharma (Shanghai, China). Lipofectamine 2000 (Invitrogen) was used for the transient transfection of vectors at room temperature. After that, the cells were incubated for 24 h before their use in subsequent experiments.

qRT-PCR

Extracted total RNA was reverse transcribed to cDNA using the Prime Script™ RT Reagent Kit (TaKaRa, Dalian, China) with gDNA Eraser. After that, according to the manufacturer's instructions, TB Green™ Premix Ex Taq™ (Tli RNase H Plus; TaKaRa, Kusatsu, Japan) was used for the quantitative reverse transcription polymerase chain reaction (qRT-PCR). The internal control β-actin primer sequence is shown in Table 1. Primers were synthesized by Sangon Biotech (Shanghai, China). The $2^{-\Delta\Delta ct}$ method was used to calculate the relative expression level of *circRNA_0003307*.

Western blotting

Table 1. Primer sequences for *hsa_circ_0003307*

Name	Size (bp)	Sequence (5′→3′)
β-actin	96	F: CCCTGGAGAAGAGCTACGAG R: GGAAGGAAGGCTGGAAGAGT
circRNA0003307	77	F: CTGTCATCAACCTGGGAAGG R: ACGGGTTGGTGGTAGCAT

Commercial kits (Pierce, Rockford, USA) were used to extract cytoplasmic and nuclear proteins from AS-FLS. A sample was prepared for electrophoresis on a Novex 10% sodium lauryl sulphate/polyacrylamide gel (Thermo Fisher Scientific). Then, the membrane was blocked with 5% skimmed milk powder in Tris-buffered saline and combined with rabbit anti-human anti-phosphorylated (p)-PI3K (dilution 1:1000; cat. No. ab182651; Abcam, Cambridge, USA) or rabbit anti-human anti-p-AKT (dilution 1:2000; cat. No. 4060s; Abcam) and incubated overnight. After washing 3 times, the membrane was incubated with anti-rabbit immunoglobulin G secondary antibody (dilution 1:20,000; cat. No. ab6721; Abcam) at room temperature for 1.5 h. Proteins were detected using enhanced chemiluminescence (ECL; Merck Millipore, Burlington, USA) and quantified using ImageQuant™ LAS 4000 (GE Healthcare Life Science, Pittsburgh, USA).

Immunofluorescence assay

After 48 h of transfection, AS-FLS were permeabilized with 0.5% Triton X100 in phosphate-buffered saline (PBS), and blocked with 2% bovine serum albumin for 15 min at room temperature. The cells were then incubated with primary antibodies and diluted in blocking buffer at 4°C overnight. This was followed by the incubation with the fluorophore-conjugated secondary antibody (1:1000; Invitrogen) in blocking buffer for 1 h at room temperature. The nuclei were stained with 4,6-diamidino-2-phenylindole (DAPI; Invitrogen). Images were obtained using a Zeiss LSM710 confocal microscope (Carl Zeiss AG, Jena, Germany).

ELISA

Enzyme-linked immunosorbent assay (ELISA) was performed according to the instructions of the tumor necrosis factor alpha (TNF-α; product No. JYM0110Hu) and TNF-α-induced protein 2 (TNFAIP2; product No. JYM2468Hu) kits (Wuhan Genemei Technology, Wuhan, China) to determine the expression levels of TNF-α and TNFAIP2 in the AS-FLS supernatant. Absorbance was determined at the optical density (OD) of 450 nm. The contents were calculated according to standard curves.

Statistical analyses

Statistical analyses were performed and graphs were created using GraphPad Prism v. 8 software (GraphPad Software, San Diego, USA). Age was analyzed using Student's t-test (Supplementary Table 1A,B). The expression of *circRNA_0003307* in PBMCs was analyzed using Welch's t-test (Supplementary Table 2A,B). Categorical variables were compared using the χ^2 test. Correlations were assessed using the Spearman's analysis because clinical characteristics were not normally distributed (Supplementary Table 3). The *circRNA_0003307* expression in AS-FLS was analyzed using a one-way analysis of variance (ANOVA) followed by the Games–Howell test (Supplementary Table 4A–C). The p-PI3K protein expression in AS-FLS was analyzed using a one-way ANOVA followed by the Games–Howell test (Supplementary Table 5A–C). The p-AKT protein expression in AS-FLS was analyzed using a one-way ANOVA followed by the Games–Howell test (Supplementary Table 6A–C). The TNF-α levels in AS-FLS were analyzed using a one-way ANOVA followed by the Games–Howell test (Supplementary Table 7A–C). The TNFAIP2 levels in AS-FLS were analyzed using a one-way ANOVA followed by Games–Howell test (Supplementary Table 8A–C). A receiver operating characteristic (ROC) curve analysis was performed to judge whether *circRNA_0003307* can be used as a diagnostic indicator for AS. A value of p < 0.05 indicates that the difference was statistically significant. All Supplementary Tables with the description of statistical methods and the results of statistical tests are available at https://doi.org/10.5281/zenodo.6244943.

Results

General situation of the research subjects

Thirty AS patients and 30 HC were examined in this study. The general situation of the 2 groups of subjects is exhibited in Table 2. There was no significant difference between AS patients and HC in terms of age (t = 0.1370, p = 0.8915, degrees of freedom (df) = 58) or gender (χ^2 = 0.000, p > 0.999, df = 1) (Table 2).

Expression of *circ_0003307* in PBMCs

To detect the level of *circRNA_0003307* in PBMCs of AS patients, qRT-PCR was performed. The results showed that the level of *circRNA_0003307* in PBMCs of AS patients was significantly higher than that of the HC group (t = 15.32, p < 0.0001, df = 47.30; Fig. 1A). To evaluate the diagnostic value of *circRNA_0003307*, a ROC curve analysis was performed. The area under the curve (AUC) of *circRNA_0003307* was 0.8533 (95% confidence interval (95% CI): [0.7564; 0.9503]). The results indicate that *circRNA_0003307* has potential value in diagnosing AS (Fig. 1B).

Correlation analysis of *circRNA_0003307* and clinical characteristics of AS patients

The results of the Spearman's analysis (the distribution of the correlated variables was non-normal – cf. Supplementary Table 3) showed that the expression

level of *circRNA_0003307* in PBMCs of AS patients was positively correlated with clinical characteristics, including erythrocyte sedimentation rate (ESR; r = 0.7188, p < 0.0001; Fig. 2A), C-reactive protein (CRP) level (r = 0.6309, p = 0.0002; Fig. 2B), Bath Ankylosing Spondylitis Functional Index (BASFI) (r = 0.4126, p = 0.0235; Fig. 2C), and Bath Ankylosing Spondylitis Disease Activity Index (BASDAI) (r = 0.6295, p = 0.0002; Fig. 2D). The overall evidence indicate that the abnormal expression of *circRNA_0003307* may be related to the pathogenesis of AS.

CircRNA_0003307 expression in AS-FLS

The expression of *circRNA_0003307* in AS-FLS was detected using the qRT-PCR. In addition, qRT-PCR was used to detect the expression following overexpression and knockdown. These results showed that, through transfection of the *circRNA_0003307* overexpression vector, *circRNA_0003307* was significantly increased (t = 13.68, p < 0.0001, df = 7.171), while *circRNA_0003307* knockdown with siRNA resulted in a significant decrease (t = 18.15, p < 0.0001, df = 8.776, Fig. 3).

Effect of abnormal expression of *circRNA_0003307* on the PI3K/AKT pathway

To determine the effect of abnormal expression of *circRNA_0003307* on AS-related pathways, we tested the expression of PI3K/AKT pathway-related proteins through

Table 2. General situation of the research subjects

Variables	AS (n = 30)	HC (n = 30)	$\chi^{2/t}$	p-value	df
Sex (M/F)	24/6	24/6	χ^2 = 0.0000	>0.9999	1
Age [years], mean ±SD	36.4300 ±10.3300	36.1000 ±8.4170	t = 0.1370	0.8915	58
ESR [mm/h], median (Q1, Q3)	30.00 (17.00, 45.25)	N/A	N/A	N/A	N/A
CRP [mg/L], median (Q1, Q3)	37.13 (23.03, 71.11)	N/A	N/A	N/A	N/A
BASDAI score, median (Q1, Q3)	5.60 (5.40, 6.60)	N/A	N/A	N/A	N/A
BASFI score, median (Q1, Q3)	6.45 (6.20, 6.80)	N/A	N/A	N/A	N/A

ESR – erythrocyte sedimentation rate; CRP – C-reactive protein; BASDAI – Bath Ankylosing Spondylitis Disease Activity Index; BASFI – Bath Ankylosing Spondylitis Functional Index; N/A – not applicable; SD – standard deviation; Q1 – 1st quartile; Q3 – 3rd quartile; AS – ankylosing spondylitis; HC – healthy controls; df – degrees of freedom.
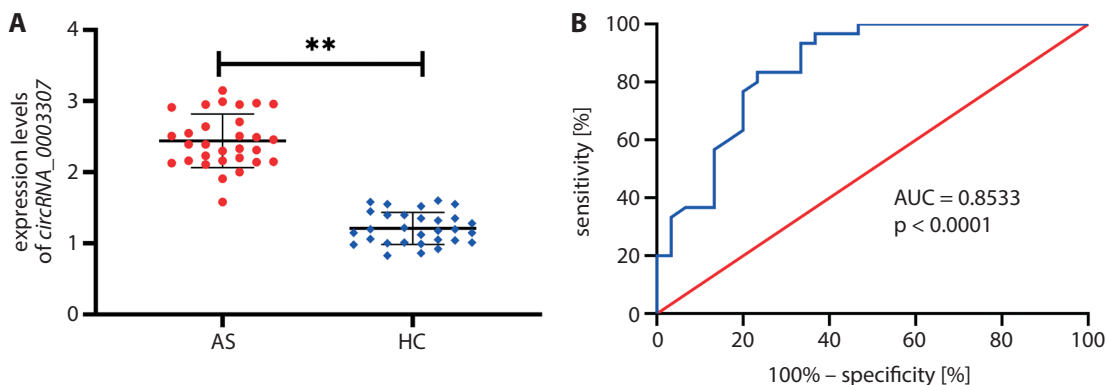

Fig. 1. Validation of abnormal expression of *circRNA_0003307* and receiver operating characteristic (ROC) curve analysis

AUC – area under the curve; AS – ankylosing spondylitis; HC – healthy controls.
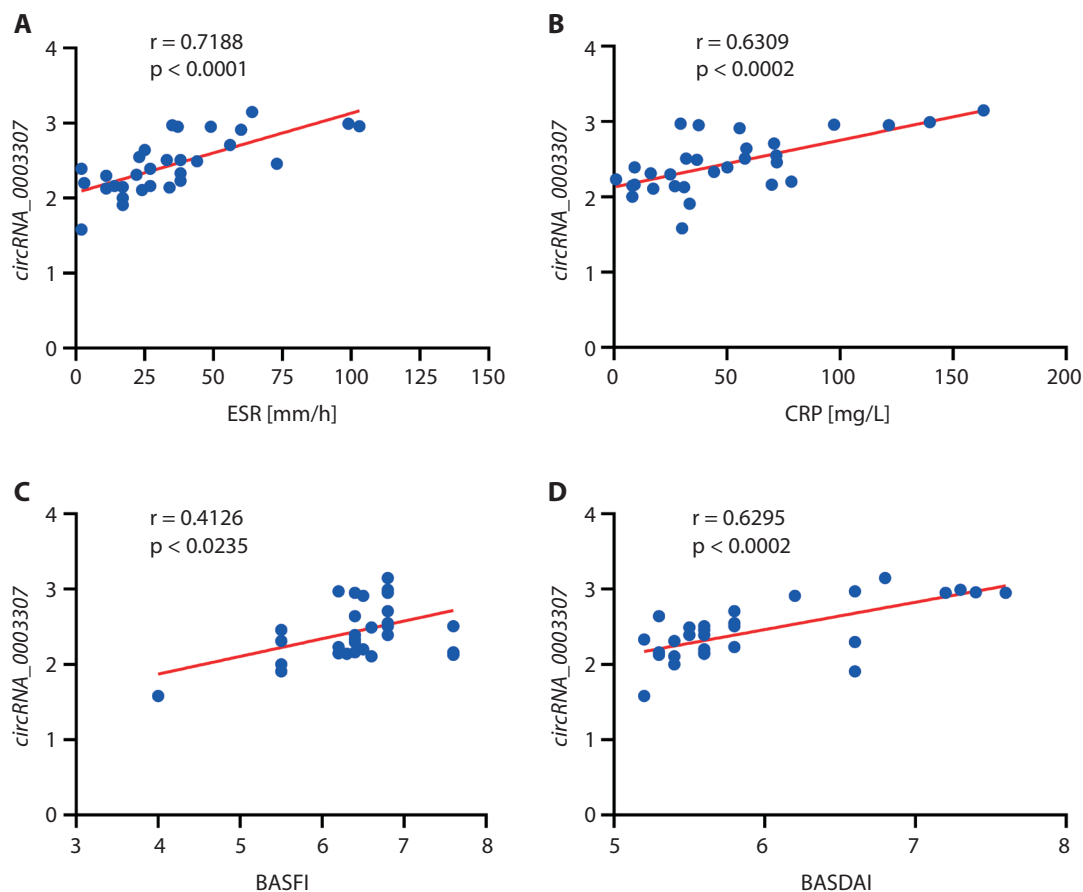
Fig. 2. Spearman's correlation analysis of *circRNA_0003307* and clinical characteristics of ankylosing spondylitis (AS) patients

ESR – erythrocyte sedimentation rate; CRP – C-reactive protein; BASFI – Bath Ankylosing Spondylitis Functional Index; BASDAI – Bath Ankylosing Spondylitis Disease Activity Index.

western blotting and immunofluorescence (IF) assay. Compared with the AS-FLS group, AS-FLS transfected with pcDNA3.1-*hsa_circ_0003307* showed a significant increase in the protein expression of p-PI3K (t = 21.81, p = 0.0015, df = 2.806) and p-AKT (t = 4.744, p = 0.0451, df = 3.768, Fig. 4A–C), whereas these protein levels were significantly decreased in AS-FLS transfected with si-*hsa_circ_0003307* compared with those in the AS-FLS group ($t_{p\text{-PI3K}}$ = 11.13, $p_{p\text{-PI3K}}$ = 0.0050, $df_{p\text{-PI3K}}$ = 3.167; $t_{p\text{-AKT}}$ = 4.851, $p_{p\text{-AKT}}$ = 0.0396, $df_{p\text{-AKT}}$ = 3.884, Fig. 4A–C). The IF assay used to analyze protein expression in these AS-FLS yielded similar results (Fig. 4D,E). These results indicate that the PI3K/AKT signaling pathway can be activated by *circRNA_0003307*, which is highly expressed in AS.

Effects of aberrant *circRNA_0003307* expression on inflammatory cytokines

To study the effect of *circRNA_0003307* on the inflammatory response of AS following the activation of the PI3K/AKT pathway, ELISA was used to detect the expression of the inflammatory factors – TNF-α and TNFAIP2. The results showed that TNF-α and TNFAIP2 levels in AS-FLS significantly decreased when AS-FLS was transfected with si-*hsa_circ_0003307* ($t_{\text{TNF-}\alpha}$ = 4.686, $p_{\text{TNF-}\alpha}$ = 0.0110, $df_{\text{TNF-}\alpha}$ = 7.662; t_{TNFAIP2} = 5.066, p_{TNFAIP2} = 0.0157, df_{TNFAIP2} = 5.536, Fig. 5A,B) compared with si-NC. In addition, AS-FLS induced with pcDNA3.1-*hsa_circ_0003307*

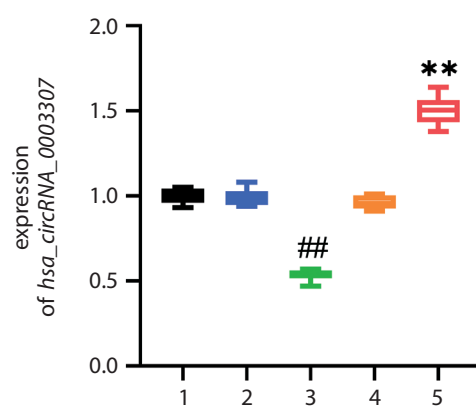Fig. 3. Differential expression of *circRNA_0003307* in ankylosing spondylitis fibroblast-like synovial cells

si-NC – nonsense control siRNA.

showed higher levels of TNF-α and TNFAIP2 than pcDNA3.1-NC ($t_{\text{TNF-}\alpha}$ = 11.51, $p_{\text{TNF-}\alpha}$ < 0.0001, $df_{\text{TNF-}\alpha}$ = 6.077; t_{TNFAIP2} = 28.84, p_{TNFAIP2} < 0.0001, df_{TNFAIP2} = 8.741, Fig. 5A,B).

A

β-actin   42 KDa

p-PI3K   85 KDa

p-AKT   60 KDa

            1   2   3   4   5

B

relative protein expression of p-PI3K

control
si-NC
si-*hsa_circ_0003307*
pcDNA3.1-NC
pcDNA3.1-*hsa_circ_0003307*

C

relative protein expression of p-AKT

control
si-NC
si-*hsa_circ_0003307*
pcDNA3.1-NC
pcDNA3.1-*hsa_circ_0003307*

D

p-PI3K   DAPI   merged

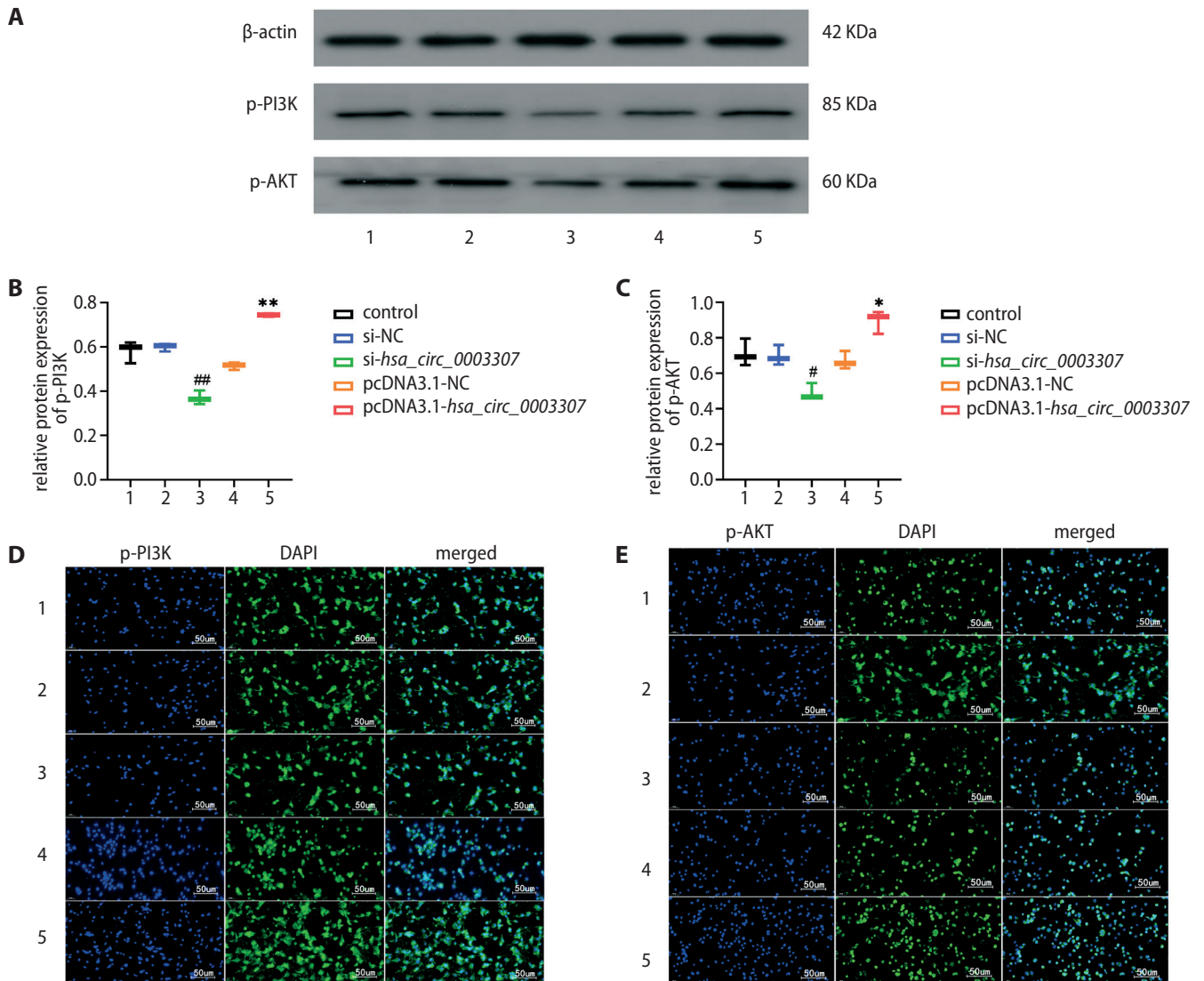**E**

p-AKT   DAPI   merged

Fig. 4. Boxplots of the effect of *circRNA_0003307* on the phosphoinositide 3-kinase (PI3K)/protein kinase B (AKT) pathway
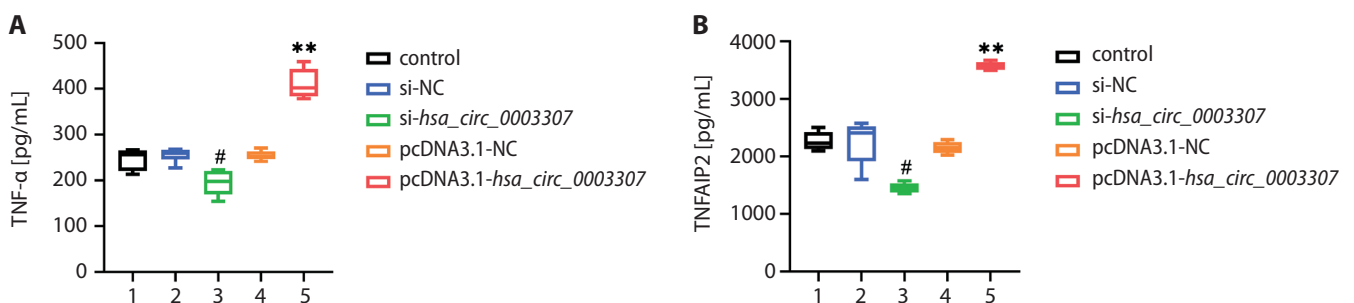
si-NC – nonsense control siRNA.

A

TNF-α [pg/mL]

control
si-NC
si-*hsa_circ_0003307*
pcDNA3.1-NC
pcDNA3.1-*hsa_circ_0003307*

B

TNFAIP2 [pg/mL]

control
si-NC
si-*hsa_circ_0003307*
pcDNA3.1-NC
pcDNA3.1-*hsa_circ_0003307*

Fig. 5. Boxplots of the effect of *circRNA_0003307* on inflammatory cytokines

si-NC – nonsense control siRNA; TNF-α – tumor necrosis factor alpha; TNFAIP2 – TNF- α-induced protein 2.

Discussion

The discovery of circRNAs has provided novel insights into AS treatment, and it is of vital significance for identifying new diagnostic and therapeutic targets for AS.

A growing number of studies in recent years have greatly broadened our horizons regarding circRNA functions and increased its value in disease diagnosis. Many circRNAs are dysregulated in rheumatic disorders, and the clinical significance of dysregulated circRNAs in such disorders

has been investigated previously. For example, Ouyang et al. confirmed that *circRNA_002453* may serve as a diagnostic marker for AS.[22] They have proven that the upregulated circRNA in the plasma of AS patients can aggravate the degree of renal involvement. Wang et al. indicated that circIBTK may also act as a therapeutic target for systemic lupus erythematosus (SLE), and its therapeutic mechanism might regulate DNA demethylation and downstream signaling pathways by targeting miR-29b in SLE.[23]

These findings confirm the existence of useful information about mRNA profiles in the PBMCs of AS patients.[15] In addition, researchers have used bioinformatics methods to predict the genes that were differentially expressed in AS, and research the role of these differential genes in the pathogenesis of AS. This information allows us to better understand the pathogenesis of AS, and it is possible to discover new diagnosis and treatment methods from it. For this study, we selected *circRNA_0003307*. To determine the pathway of *circRNA_0003307* in AS-FLS involved in the pathogenesis, we chose PI3K/AKT as the research pathway. The reason is that PI3K/AKT plays a key role in the pathogenesis of AS and provide a breakthrough in AS treatment. Terlemez et al., Yan et al. and Liu et al. proved that miRNAs affects the phenotype of FLS in rheumatism by regulating the expression of PI3K/AKT, thereby affecting the pathogenesis of rheumatism.[24–26] Therefore, we speculate that there may be a regulatory relationship between *circRNA_0003307* and the PI3K/AKT pathway.

The results of this study showed that high expression level of *circRNA_0003307* was positively correlated with the severity of AS. Li et al. reported that the *circ_0056558* level was highly expressed in AS tissue, and was achieved through the PI3K/AKT pathway.[27] In our study, *circRNA_0003307* was overexpressed in PBMCs of AS patients compared with healthy participants. There was a positive correlation between *circRNA_0003307* levels and ESR, CRP level, BASDAI, and BASFI. Luo et al. demonstrated that low expression of *hsa_circ_0079787* in peripheral blood of AS patients was negatively correlated with BASDAI, which was in concert with our data.[28] Collectively, the expression level of *circRNA_0003307* was associated with disease activity.[29]

CircRNA_0003307 activated the PI3K/AKT signaling pathway and affected the expression of the downstream inflammatory factors – TNF-α and TNFAIP2. The results of the study confirmed our hypothesis stating that the protein expression of p-PI3K and p-AKT was altered by both overexpression and knockdown of *circRNA_0003307*. Li et al. demonstrated that *hsa_circ_0056558* inhibited the PI3K/AKT pathway by targeting miR-1290 in AS, and reduced the protein expression of p-AKT.[27] A further analysis showed that the overexpression of *circRNA_0003307* markedly increased the protein expression level of p-PI3K and p-AKT. However, for *circRNA_0003307* knockdown, the protein expression level was significantly reduced. Thus, PI3K/AKT is involved in immune-mediated inflammatory responses. Simultaneously, the findings showed that the overexpression of *circRNA_0003307* increased the expression of the downstream inflammatory factors – TNF-α and TNFAIP2, while the knockdown of *circRNA_0003307* showed the opposite results, reducing the expression of TNF-α and TNFAIP2.

Kou et al. demonstrated that circRNAs may be involved in the PI3K/AKT signaling pathways associated with inflammation-induced apoptosis in chondrocytes.[30] The activation of p-PI3K could induce downstream p-AKT. Inflammatory cytokines, such as TNF-α and interleukin 17 (IL-17), are involved in the pathogenesis of AS.[31] Taken together, the expression level of *circRNA_0003307* is closely related to the AS inflammatory response.

Limitations

This study has certain limitations. In our subjects, we found that the overexpression of *circRNA_0003307* increased the levels of p-PI3K, p-AKT, TNF-α, and TNFAIP2 in AS-FLS. The knockdown of *circRNA_0003307* showed the opposite results, reducing the expression of p-PI3K, p-AKT, TNF-α, and TNFAIP2. However, the detailed mechanism of *circRNA_0003307*-targeted activation of the PI3K/AKT pathway remains unclear. We also lacked patients with other autoimmune diseases as a control group to clarify that *circRNA_0003307* is specific to AS.

Conclusions

The present study revealed that the knockdown of *circRNA_0003307* inhibits synovial inflammation in AS by regulating the PI3K/AKT pathway. In addition, the expression level of *circRNA_0003307* was associated with disease activity. The *circRNA_0003307* was highly expressed in AS-PBMCs and AS-FLS, and *circRNA_0003307* knockdown reduced the inflammatory response of AS-FLS by regulating the PI3K/AKT pathway. These findings suggest that targeting *circRNA_0003307* offers a promising therapeutic strategy for AS patients and may serve as a potential target for AS treatment. Based on these findings, our research team will explore the possible competing endogenous RNA molecular mechanism of *circRNA_0003307* in future studies of AS.

ORCID iDs

Yanyan Fang https://orcid.org/0000-0001-8754-7786
Jian Liu https://orcid.org/0000-0003-3101-7553
Yan Long https://orcid.org/0000-0002-3247-2446
Jianting Wen https://orcid.org/0000-0003-2757-8462
Dan Huang https://orcid.org/0000-0002-9327-8583
Ling Xin https://orcid.org/0000-0001-9986-4551

References

1. Garcia-Montoya L, Gul H, Emery P. Recent advances in ankylosing spondylitis: Understanding the disease and management. *F1000Res*. 2018;7:F1000–1512. doi:10.12688/f1000research.14956.1

2. Bergman M, Lundholm A. Managing morbidity and treatment-related toxicity in patients with ankylosing spondylitis. *Rheumatology (Oxford)*. 2018;57(3):419–428. doi:10.1093/rheumatology/kex292

3. Maksymowych WP. Disease modification in ankylosing spondylitis. *Nat Rev Rheumatol*. 2010;6(2):75–81. doi:10.1038/nrrheum.2009.258

4. Chen LL, Yang L. Regulation of circRNA biogenesis. *RNA Biol*. 2015; 12(4):381–388. doi:10.1080/15476286.2015.1020271

5. Hentze MW, Preiss T. Circular RNAs: Splicing's enigma variations. *EMBO J*. 2013;32(7):923–925. doi:10.1038/emboj.2013.53

6. Salzman J, Chen RE, Olsen MN, Wang PL, Brown PO. Cell-type specific features of circular RNA expression. *PLoS Genet*. 2013;9(9):e1003777. doi:10.1371/journal.pgen.1003777. Erratum in: *PLoS Genet*. 2013;9(12). doi:10.1371/annotation/f782282b-eefa-4c8d-985c-b1484e845855

7. Szabo L, Morey R, Palpant NJ, et al. Statistically based splicing detection reveals neural enrichment and tissue-specific induction of circular RNA during human fetal development. *Genome Biol*. 2015; 16(1):126. doi:10.1186/s13059-015-0690-5. Erratum in: *Genome Biol*. 2016;17(1):263. doi:10.1186/s13059-016-1123-9

8. Suzuki H, Tsukahara T. A view of pre-mRNA splicing from RNase R resistant RNAs. *Int J Mol Sci*. 2014;15(6):9331–9342. doi:10.3390/ijms 15069331

9. Hansen TB, Jensen TI, Clausen BH, et al. Natural RNA circles function as efficient microRNA sponges. *Nature*. 2013;495(7441):384–388. doi:10.1038/nature11993

10. Kumar L, Shamsuzzama, Haque R, Baghel T, Nazir A. Circular RNAs: The emerging class of non-coding RNAs and their potential role in human neurodegenerative diseases. *Mol Neurobiol*. 2017;54(9): 7224–7234. doi:10.1007/s12035-016-0213-8

11. Wang L, Shen C, Wang Y, et al. Identification of circular RNA *Hsa_circ_0001879* and *Hsa_circ_0004104* as novel biomarkers for coronary artery disease. *Atherosclerosis*. 2019;286:88–96. doi:10.1016/j.atherosclerosis.2019.05.006

12. Qu S, Liu Z, Yang X, et al. The emerging functions and roles of circular RNAs in cancer. *Cancer Lett*. 2018;414:301–309. doi:10.1016/j.canlet.2017.11.022

13. Ouyang Q, Wu J, Jiang Z, et al. Microarray expression profile of circular RNAs in peripheral blood mononuclear cells from rheumatoid arthritis patients. *Cell Physiol Biochem*. 2017;42(2):651–659. doi:10.1159/000477883

14. Wang F, Nazarali AJ, Ji S. Circular RNAs as potential biomarkers for cancer diagnosis and therapy. *Am J Cancer Res*. 2016;6(6):1167–1176. PMID:27429839. PMCID:PMC4937728.

15. Huang D, Liu J, Cao Y, et al. RNA sequencing for gene expression profiles in peripheral blood mononuclear cells with ankylosing spondylitis RNA. *Biomed Res Int*. 2020;2020:5304578. doi:10.1155/2020/5304578

16. Utermark T, Rao T, Cheng H, et al. The p110α and p110β isoforms of PI3K play divergent roles in mammary gland development and tumorigenesis. *Genes Dev*. 2012;26(14):1573–1586. doi:10.1101/gad.191973.112

17. Patel AB, Tsilioni I, Weng Z, Theoharides TC. TNF stimulates IL-6, CXCL8 and VEGF secretion from human keratinocytes via activation of mTOR, inhibited by tetramethoxyluteolin. *Exp Dermatol*. 2018; 27(2):135–143. doi:10.1111/exd.13461

18. Sun K, Luo J, Guo J, Yao X, Jing X, Guo F. The PI3K/AKT/mTOR signaling pathway in osteoarthritis: A narrative review. *Osteoarthritis Cartilage*. 2020;28(4):400–409. doi:10.1016/j.joca.2020.02.027

19. Zhang Y, Cai W, Han G, et al. Panax notoginseng saponins prevent senescence and inhibit apoptosis by regulating the PI3K-AKT-mTOR pathway in osteoarthritic chondrocytes. *Int J Mol Med*. 2020;45(4): 1225–1236. doi:10.3892/ijmm.2020.4491. Erratum in: *Int J Mol Med*. 2021;47(1):408–409. doi:10.3892/ijmm.2020.4786. Erratum in: *Int J Mol Med*. 2022;49(3):30. doi:10.3892/ijmm.2022.5085

20. Van der Linden S, Valkenburg HA, Cats A. Evaluation of diagnostic criteria for ankylosing spondylitis: A proposal for modification of the New York criteria. *Arthritis Rheum*. 1984;27(4):361–368. doi:10.1002/art.1780270401

21. Goie The HS, Steven MM, van der Linden SM, Cats A. Evaluation of diagnostic criteria for ankylosing spondylitis: A comparison of the Rome, New York and modified New York criteria in patients with a positive clinical history screening test for ankylosing spondylitis. *Br J Rheumatol*. 1985;24(3):242–249. doi:10.1093/rheumatology/24.3.242

22. Ouyang Q, Huang Q, Jiang Z, Zhao J, Shi GP, Yang M. Using plasma *circRNA_002453* as a novel biomarker in the diagnosis of lupus nephritis. *Mol Immunol*. 2018;101:531–538. doi:10.1016/j.molimm.2018.07.029

23. Wang X, Zhang C, Wu Z, Chen Y, Shi W. CirclBTK inhibits DNA demethylation and activation of AKT signaling pathway via miR-29b in peripheral blood mononuclear cells in systemic lupus erythematosus. *Arthritis Res Ther*. 2018;20(1):118. doi:10.1186/s13075-018-1618-8

24. Terlemez R, Akgün K, Palamar D, Boz S, Sarı H. The clinical importance of the thyroid nodules during anti-tumor necrosis factor therapy in patients with axial spondyloarthritis. *Clin Rheumatol*. 2017;36(5): 1071–1076. doi:10.1007/s10067-017-3607-8

25. Yan X, Liu Y, Kong X, et al. MicroRNA-21-5p are involved in apoptosis and invasion of fibroblast-like synoviocytes through PTEN/PI3K/AKT signal. *Cytotechnology*. 2019;71(1):317–328. doi:10.1007/s10616-018-0288-3

26. Liu S, Cao C, Zhang Y, et al. PI3K/Akt inhibitor partly decreases TNF-α -induced activation of fibroblast-like synoviocytes in osteoarthritis. *J Orthop Surg Res*. 2019;14(1):425. doi:10.1186/s13018-019-1394-4

27. Li X, Zhou W, Li Z, Guan F. *Hsa_circ_0056558* regulates cyclin-dependent kinase 6 by sponging microRNA-1290 to suppress the proliferation and differentiation in ankylosing spondylitis. *Autoimmunity*. 2021;54(2):114–128. doi:10.1080/08916934.2021.1894417

28. Luo Q, Fu B, Zhang L, Guo Y, Huang Z, Li J. Expression and clinical significance of circular RNA *hsa_circ_0079787* in the peripheral blood of patients with axial spondyloarthritis. *Mol Med Rep*. 2020;22(5): 4197–4206. doi:10.3892/mmr.2020.11520

29. Kook H, Jin S, Park P, Lee S, Shin H, Kim T. Serum miR-214 as a novel biomarker for ankylosing spondylitis. *Int J Rheum Dis*. 2019;22(7): 1196–1201. doi:10.1111/1756-185X.13475

30. Kou J, Liu G, Liu X, et al. Profiling and bioinformatics analysis of differentially expressed circRNAs in spinal ligament tissues of patients with ankylosing spondylitis. *Biomed Res Int*. 2020;2020:7165893. doi:10.1155/2020/7165893

31. Braga M, Lara-Armi FF, Neves JSF, et al. Influence of IL10 (rs1800896) polymorphism and TNF-α, IL-10, IL-17A, and IL-17F serum levels in ankylosing spondylitis. *Front Immunol*. 2021;12:653611. doi:10.3389/fimmu.2021.653611

(—)-Epigallocatechin-3-gallate plays an antagonistic role in the antitumor effect of bortezomib in myeloma cells via activating Wnt/β-catenin signaling pathway

Xi Qiu[1,A–F], Xiao Wu[2,B,C], Weilan He[3,B]

[1] Department of Hematology, Second Affiliated Hospital of Zhejiang University School of Medicine, Hangzhou, China

[2] Department of Hematology, Affiliated Hospital of Medical School of Ningbo University, China

[3] Department of Hematology and Oncology, Longquan People's Hospital, China

A – research concept and design; B – collection and/or assembly of data; C – data analysis and interpretation;
D – writing the article; E – critical revision of the article; F – final approval of the article

Address for correspondence
Xi Qiu
E-mail: 2312060@zju.edu.cn

Abstract

Background. (—)-Epigallocatechin-3-gallate (EGCG) is an active constituent of green tea, whose efficacy on chemoprevention and chemotherapy has been extensively researched. Its anticancer potency with low toxicity and easy administration allows for its widespread use. Bortezomib, a proteasome inhibitor, has a significant influence on multiple myeloma (MM) in chemotherapy. Previous studies about the role of EGCG in the antitumor effect induced by bortezomib remain controversial.

Objectives. In our study, the effect of EGCG on the antitumor activity of bortezomib was investigated in myeloma cell lines U266 and RPMI8226, and the underlying mechanism was explored.

Materials and methods. The effect of EGCG on the antiproliferative and pro-apoptotic activities of bortezomib were investigated in myeloma cells using MTT assay and cell cycle analysis, respectively. The Wnt/β-catenin signaling pathway and related proteins were involved in this antagonistic effect and measured with western blot assay.

Results. Our results showed the inhibitory activity of EGCG on myeloma cells in a time- and dose-dependent manner. The EGCG neutralized the antiproliferative and pro-apoptotic effect induced by bortezomib by activating Wnt/β-catenin signaling pathway with the accumulation of β-catenin. An increase of the downstream target proteins as c-Myc and cyclin D1 was also observed. was also observed. These findings demonstrated the antagonistic role of EGCG in the antitumor effect of bortezomib likely through the activated Wnt/β-catenin signaling pathway and the upregulated target proteins.

Conclusions. When bortezomib is involved in the MM chemotherapy, the consumption of green tea should be avoided in order to maintain the biological efficacy of bortezomib.

Key words: multiple myeloma, bortezomib, Wnt/β-catenin, apoptosis, (—)-epigallocatechin-3-gallate

Background

Multiple myeloma (MM) is one of the most common hematological malignancies, characterized by abnormal and out-of-control proliferation of plasma cells in bone marrow and monoclonal immunoglobulins, or immunoglobulin chain secretion in blood and/or urine in large amounts.[1] Although highly efficient therapeutic agents are constantly emerging to improve the prognosis and the quality of life in a much better way than before, MM remains incurable.[2,3] At the same time, notable adverse effects of drugs and disease recurrence due to drug resistance became the key problems in treatment failure.[4] Therefore, it is paramount to develop novel therapeutic strategies with high efficiency and low toxicity.

Green tea is recognized as one of the favorite beverages for people of all ages worldwide, bringing health benefits and reducing the risk of diseases. (–)-Epigallocatechin-3-gallate (EGCG), the main active ingredient of catechins in green tea, exhibits antioxidative, anti-inflammation, as well as antimicrobial and antitumor activity.[5–7] Recently, many studies have identified the antiproliferative role of EGCG on carcinomas such as osteosarcoma, lung cancer, gastric cancer, melanoma, and so on; it may be involved in cell cycle modulation, induction of apoptosis and inhibition of angiogenesis.[8–11] However, the antitumor activity of EGCG on MM cells, especially when combined with proteasome inhibitors, as well as the related mechanism, is still unknown. Researchers considered that EGCG could counteract the antitumor effects of boronic acid-based proteasome inhibitors. Conversely, the synergistic effect of EGCG and proteasome inhibitors on growth inhibition on myeloma cells was also identified by other researchers.

The Wingless-Int (Wnt)/β-catenin signaling pathway plays an important role in regulating the cell proliferation and differentiation in various human cancers.[12,13] In MM, recent studies indicated that Wnt/β-catenin signaling pathway is activated by Wnt regulatory components, including deletion of tumor suppressor and overexpression of the co-transcriptional activator.[14] Evidence provided by Sukhdeo et al. demonstrated that a small molecular compound, PKF 115-584, downregulates the Wnt/β-catenin signaling pathway, resulting in suppressing tumor growth in vitro and in vivo.[15] Zhao et al. found that miR-30-5p, one of the tumor suppressor microRNAs, is downregulated in MM and further enhances the expression of *BCL9*.[16] The *BCL9*, which is a coactivator for transcription in the Wnt signaling pathway, promotes myeloma cells proliferation, migration and invasion. The reproducibility of miR-30-5p as a therapeutic approach can reduce tumor loading and metastasis in vivo. These findings imply that Wnt/β-catenin signaling pathway is on the way to become a candidate for targeted therapy in MM.

Objectives

The objective of this research was to investigate the effect and underlying mechanism of EGCG on the antitumor activity of bortezomib in myeloma cells.

Materials and methods

Materials

The EGCG (Mw 458.4, purity ≥95%; Sigma-Aldrich, St. Louis, USA) was dissolved in water for storage at 2–8°C. Bortezomib (Velcade; Millennium Predictive Medicine, Inc., Cambridge, USA) was dissolved in saline at 10 mM for storage at –20°C. Rabbit antibody against β-catenin, mouse antibody against cyclin D1, mouse antibody against c-Myc, mouse antibody against β-actin, and fluorescein isothiocyanate (FITC)-conjugated secondary antibody were all purchased from Santa Cruz Biotechnology (Santa Cruz, USA).

Cell lines and cultures

Human MM cell lines RPMI8226 and U266 were provided by Hematology Institute of Zhejiang University, Zhejiang, China, and normal hematopoietic cells were obtained from peripheral blood of healthy volunteers who signed informed consent. Mononuclear cells were harvested using density gradient centrifugation at 3500 rpm for 20 min with Ficoll-Hypaque Solution (Sigma-Aldrich). All cells were cultivated in RPMI-1640 (Gibco, Waltham, USA) supplemented with 10% fetal bovine serum (FBS; Invitrogen, Waltham, USA) and penicillin-streptomycin solution (100 U/mL penicillin and 0.1 mg/mL streptomycin; Siji Qing Biotech, Hangzhou, China), and grown at 37°C in a humidified incubator with 5% carbon dioxide atmosphere.

Cell viability assay

The RPMI8226 and U266 cells were grown with 1×10^4 cells per well in 96-well plates and incubated with increasing concentrations of EGCG as 10 μM, 20 μM and 40 μM for 24 h, 48 h and 72 h, respectively. Then, 20 μL of 5 mg/mL 3-(4, 5-dimethylthiazol-2-yl)-2, 5-diphenyl-tetrazolium bromide (MTT; Sangon Biotech, Shanghai, China) was added for another 4 h. The MTT formazan crystals were then dissolved with Dulbecco's modified Eagle's medium (DMEM) and their optical density (OD) was examined at 570 nm. All the experiments were performed in triplicate independently.

To detect the effect of EGCG combined with bortezomib on cell growth, U266 and RPMI8226 cells were incubated with EGCG (10 μM, 20 μM and 40 μM) alone and in combination with bortezomib (10 nM, 20 nM, 50 nM, 100 nM, and 200 nM) for 24 h. The MTT assay was used to determine the cell viability as described above.

Cell cycle analysis and apoptosis detection

The RPMI8226 cells were incubated with 5×10^5 cells per well in 6-well plates with EGCG (20 μM) for 24 h at a concentration of 0 μM, 10 μM, 20 μM, and 40 μM. The RPMI8226 cells were incubated with the combination of EGCG (20 μM) and bortezomib (20 nM) for 24 h. Then, the cells were collected and fixed using 70% cold ethanol overnight, and stained with 50 μg/mL propidium iodide (PI; Sigma-Aldrich) for 30 min at 4°C. The FACScan flow cytometry (Becton Dickinson Biosciences, San Jose, USA) was used to analyze the cell cycle distribution. Double staining with Anexin-V fluorescein (AV; Sigma-Aldrich) and PI were used to identify the cell apoptosis. After incubation in the dark at room temperature for 15 min, flow cytometry method (FCM) could quantitatively detect the apoptotic cells.

Western blotting assay

The RPMI8226 cells were treated with EGCG (0 μM, 10 μM, 20 μM, and 40 μM) alone and with the combination of EGCG (20 μM) and bortezomib (20 nM) for 24 h. These cells were then collected and dissolved in protein extraction reagent (Pierce Chemical, Rockford, USA). The total cellular protein was extracted, separated using sodium dodecyl sulfate-polyacrylamide gel electrophoresis (SDS-PAGE) and transferred to polyvinylidene difluoride (PVDF) membranes (Bio-Rad, Hercules, USA). Tris-buffered-saline (TBS) with 5% skim milk and 0.1% Tween-20 was supplied to block the nonspecific antibodies binding on the membranes for 2–3 h. After that, primary antibodies were added and allowed to culture overnight with the cells at 4°C. The membranes were washed 3 times with TBS mentioned above and secondary antibodies were used at room temperature for 1 h. The electrochemiluminescence (ECL) kit (Pierce Chemical) was applied to detect the specific immunoreactive bands, according to the manufacturer's protocols.

Statistical analyses

All analyses were conducted using IBM SPSS v. 20.0 (IBM Corp., Armonk, USA) and all data were demonstrated as mean ± standard deviation (SD). The difference of cell viability was analyzed with two-way repeated-measure analysis of variance (ANOVA) with 2 factors – time and drug concentration. The effects of 2 different drugs on cell viability was analyzed with two-way ANOVA. The discrepancies of the percentage of apoptotic cells and the protein levels between groups were analyzed with one-way ANOVA. The pairwise comparisons between each 2 groups were based on the post hoc analysis of least significant difference (LSD). Values of $p < 0.05$ were considered statistically significant.

Results

EGCG inhibits MM cells proliferation

The MTT assay was applied to explore the effects of EGCG on the viability of myeloma cell lines as RPMI8226 and U266. As demonstrated in Fig. 1A,B, EGCG played a significantly inhibitory role on proliferation of both RPMI8226 and U266 cells in a time- and dose-dependent manner, when compared with the control ones. Our results indicated that EGCG had the antiproliferative effect on MM cells without cytotoxic effects on normal hematopoietic cells.

EGCG neutralizes the growth inhibiting effect of bortezomib on MM cells

As was shown in our data, the inhibitory influence of bortezomib on the myeloma cells proliferation was dose-dependent – it increased with concentration. To further investigate the effect of EGCG combined with
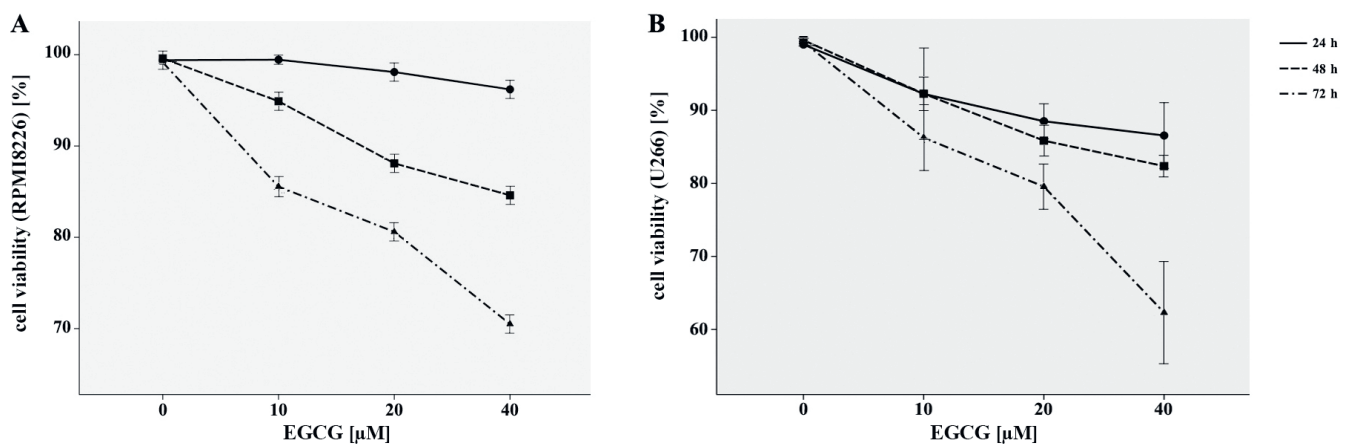

Fig. 1. (−)-Epigallocatechin-3-gallate (EGCG) showed the cell viability inhibition in myeloma cells: (A) RPMI8226 and (B) U266. The myeloma cells were incubated with EGCG at a concentration of 10 μM, 20 μM and 40 μM for 24 h, 10 μM, 20 μM and 40 μM for 48 h and 10 μM, 20 μM and 40 μM for 72 h. The cell viability inhibition in a time- and dose-dependent relationship was detected with MTT assay
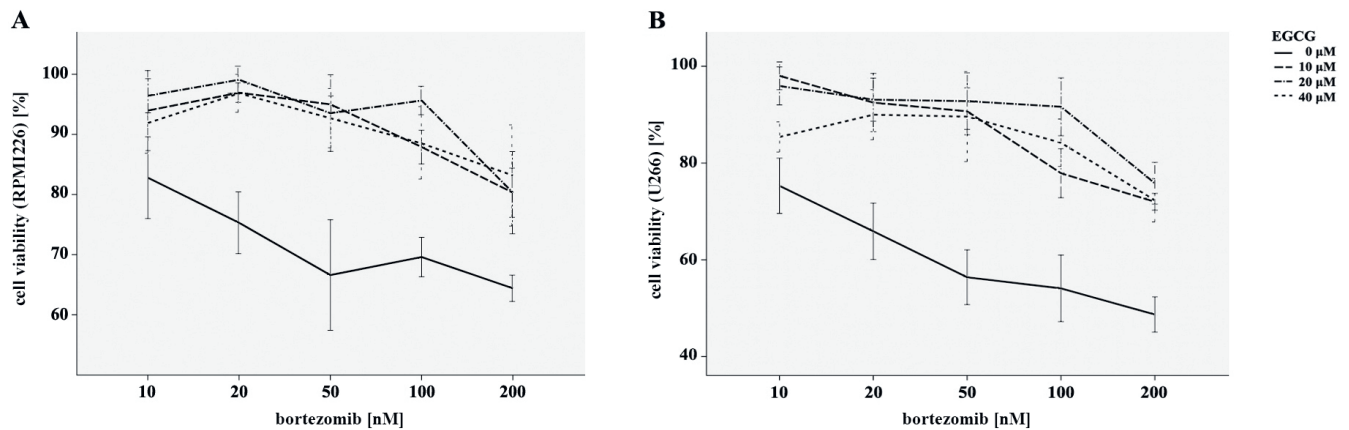
A

B

Fig. 2. The antagonistic effect of (–)-epigallocatechin-3-gallate (EGCG) on the viability inhibition by bortezomib in myeloma cells: (A) RPMI8226 and (B) U266. The myeloma cells were incubated with EGCG at a concentration of 10 µM, 20 µM and 40 µM and bortezomib (10–200 nM) for 24 h. The antagonistic effect of EGCG on the antiproliferative role of bortezomib was detected using MTT assay

bortezomib, RPMI8226 and U266 cells were incubated with EGCG at a concentration of 10 µM, 20 µM and 40 µM and bortezomib (10–200 nM) for 24 h in vitro. Figure 2 shows that the myeloma cell viability was significantly increased under the combination of 2 drugs when measured with MTT assay, as compared with the group treated with bortezomib alone. These results demonstrated that EGCG could minimize the antitumor efficacy of bortezomib on myeloma cells.

EGCG neutralizes the apoptosis of MM cells induced by bortezomib

The percentages of apoptotic cells were analyzed after RPMI8226 cells were treated with EGCG, at a concentration of 10 µM, 20 µM and 40 µM alone and with the combination of 2 drugs (20 µM of EGCG and 20 µM of bortezomib) for 24 h. As shown in Fig. 3A, cell apoptosis increased significantly along with the rise in concentration of EGCG, as compared with the controls. Additionally, the combination of EGCG and bortezomib obviously

reduced cell apoptosis when compared with bortezomib alone, which demonstrated that EGCG reversed the cell apoptosis induced by bortezomib.

Wnt/β-catenin signaling pathway is activated when EGCG combined with bortezomib

To further explore the mechanism of blocking the antiproliferative and pro-apoptotic effect of bortezomib on MM cells by ECCG, the proteins related to Wnt/β-catenin signaling pathway were investigated using western blot assay. As mentioned in Fig. 4, β-catenin was largely unchanged when RPMI8226 cells were exposed to EGCG (10 µM, 20 µM and 40 µM) alone. Furthermore, β-catenin was downregulated when exposed to bortezomib alone, which could be highly expressed when EGCG and bortezomib were added together. Similar results were also observed in the protein levels of downstream target genes like *c-Myc* and *cyclin D1*, which are responsible for promoting cell proliferation and inhibiting cell apoptosis. The upregulated
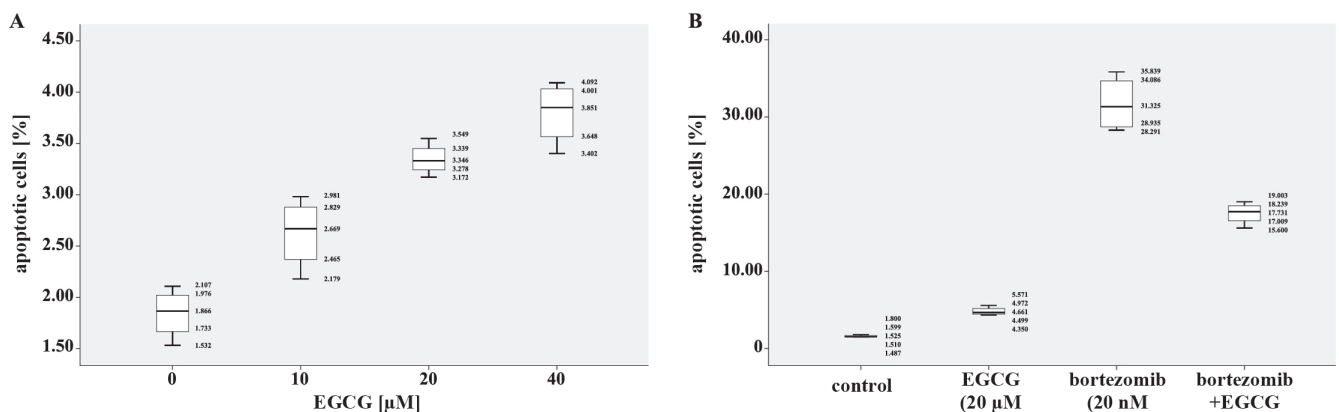
A

B

Fig. 3. A. (–)-Epigallocatechin-3-gallate (EGCG) induced the apoptosis of myeloma cells. The myeloma cells RPMI8226 were incubated with EGCG at a concentration of 10 µM, 20 µM and 40 µM for 24 h. The percentage of apoptotic cells was detected with cell cycle analysis. The result showed that cell apoptosis was induced by EGCG in a dose-dependent manner; B. The neutralizing effect of EGCG on the apoptosis of myeloma cells RPMI8226 induced by bortezomib. The myeloma cells RPMI8226 were incubated with EGCG at a concentration of 20 µM in combination with bortezomib at a concentration 20 nM for 24 h. The neutralizing effect of EGCG on the pro-apoptotic role of bortezomib was observed.
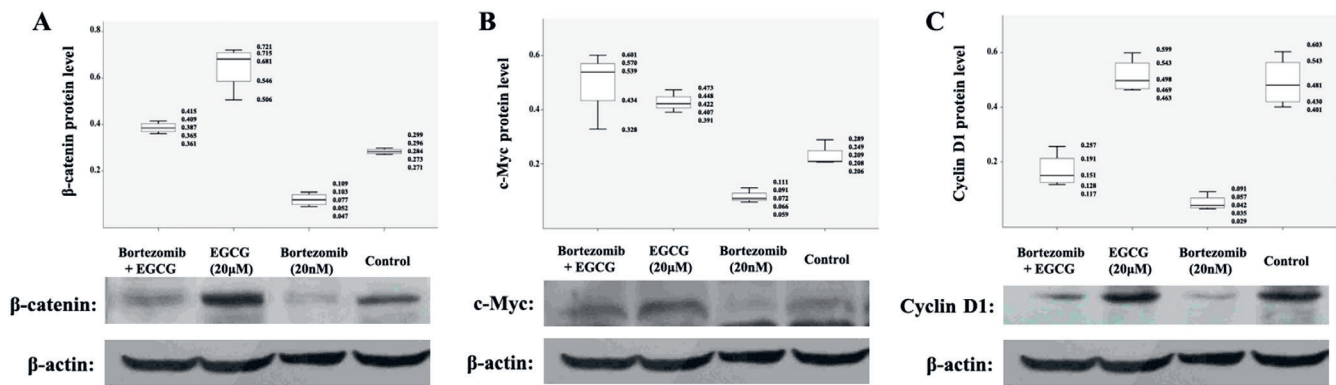
Fig. 4. Wnt/β-catenin signaling pathway and the downstream targets (*c-Myc* and *cyclin-D1*) were involved in the neutralizing effect of the combination of (−)-epigallocatechin-3-gallate (EGCG) and bortezomib in myeloma cells. The myeloma cells RPMI8226 were incubated with EGCG at a concentration of 20 μM in combination with bortezomib at a concentration of 20 nM for 24 h. Compared with the cells treated with bortezomib alone, upregulated expressions of β-catenin, *c-Myc* and *cyclin-D1* were observed.

expressions of *c-Myc* and *cyclin D1* were significant when RPMI8226 cells were exposed to the combination of 2 (EGCG and bortezomib), compared with the exposure to bortezomib alone. Our results indicate that EGCG has an antagonistic effect on the antitumor effect of bortezomib through the cumulation of β-catenin and activation of downstream proteins.

Discussion

The promising effects produced by EGCG against the development of various cancers have received a great deal of attention for decades. In hematological malignancy like MM, EGCG also exhibits remarkable antitumor effect properties and the underlying mechanism has been investigated. Masood et al. identified the efficacy of EGCG on growth arrest and apoptosis promotion in MM cells in vitro and in vivo, and they found that the 67-kDa laminin receptor1 (*LR1*) played a crucial part in mediating the biological activity of EGCG.[17] Furthermore, Zhou et al. confirmed the enhancer of zeste homolog2 (EZH2), which was a member of Pc-G family, to be inactivated in the antitumor effect of EGCG on MM cells.[18] The mitochondrial apoptosis pathway was also involved. *MST-312* is an another modified derivative of EGCG which was named as telomerase inhibitor and induces apoptosis of myeloma cells via modulating apoptotic-related genes.

As EGCG can be administered orally, researchers had high hopes for augmenting the antitumor outcome of chemotherapy in clinical use when EGCG was added. Unexpectedly, Encouse et al. discovered that EGCG effectively blocked myeloma cells death induced with bortezomib in vitro and in vivo.[20] This antagonistic function was performed via a direct reaction with the boronic acid group of bortezomib, which resulted in the discontinuation of endoplasmic reticulum stress induction and inactivation

of caspase-7. Qing et al. demonstrated that when the concentration of EGCG increased, the combination of EGCG and bortezomib played a synergistic role in inhibiting cell proliferation and inducing apoptosis, and that the NF-κB pathway was involved.[21] These results implied that various concentrations of EGCG had completely opposite effects on the anticancer role of bortezomib, and the underlying mechanism was still not clear and required further investigation.

In our study, the proliferation inhibition and apoptosis-inducing effect of EGCG on MM cells was demonstrated. The EGCG played an antagonistic role in growth inhibition induced by bortezomib. Moreover, we found that the number of apoptotic cells was decreased significantly in combination with bortezomib when compared with the effect of bortezomib alone. Especially with the concentrations of bortezomib of 20 nM and EGCG also of 20 μM, the combination of these 2 drugs maximized the impact of antagonism. Based on this result, we chose these concentrations to study the underlying mechanism further. As it is commonly known, the canonical Wnt signaling pathway, which is one of the most essential regulators for embryogenesis and homeostasis, is conserved evolutionarily in mammals.[22,23] Abnormal inactivation of Wnt/β-catenin signaling pathway is closely correlated with tumorigenesis.[24] When β-catenin is accumulated in the cell nucleus, its binding to the *TCF/LEFs* makes the downstream target genes upregulate.[25] Our study demonstrated that significant accumulation of β-catenin was found when EGCG and bortezomib were combined as compared to the effect of bortezomib alone; such accumulation subsequently activated the downstream target genes as *c-Myc* and *cyclin-D1*, and finally induced the growth, proliferation and differentiation of tumor cells. These results indicate that EGCG exerts an antagonistic effect on the antitumor effect of bortezomib in MM cells, probably by activating Wnt/β-catenin signaling pathway.

Limitations

Our study has some limitations. Although the inhibitory role of EGCG on the antiproliferative and pro-apoptotic effect of bortezomib in myeloma cells was verified, we also found that the combination of bortezomib (20 nM) and EGCG (20 μM) maximized the antagonism, which was not in a dose-dependent relationship, and the mechanism was still unclear. Moreover, whether other crucial signaling pathways also took part in this antagonistic function requires further investigations.

Conclusions

Our results illustrate that EGCG had the anti-proliferative and pro-apoptotic effects on myeloma cells. Furthermore, it neutralized the antiproliferative and pro-apoptotic effects of bortezomib on myeloma cells. The underlying mechanism was probably involved in the activation of Wnt/β-catenin signaling pathway. In summary, we further identified the antagonistic effect of EGCG in combination with bortezomib, and provided another insight into the underlying mechanism. As a widely consumed drink throughout the world, green tea, in which EGCG is the most abundant and active ingredient, should be avoided by MM patients regularly receiving the chemotherapy including bortezomib.

ORCID iDs

Xi Qiu   https://orcid.org/0000-0002-8653-9968

References

1. Gerecke C, Fuhrmann S, Strifler S, Schmidt-Hieber M, Einsele H, Knop S. The diagnosis and treatment of multiple myeloma. *Dtsch Arztebl Int*. 2016;113(27–28):470–476. doi:10.3760/cma.j.issn.0253-2727.2021.10.008

2. Pulte D, Jansen L, Castro FA, et al. Trends in survival of multiple myeloma patients in Germany and the United States in the first decade of the 21ˢᵗ century. *Br J Haematol*. 2015;171(2):189–196. doi:10.1111/bjh.13537

3. Blade J, Rosinol L, Cibeira MT, Rovira M, Carreras E. Hematopoietic stem cell transplantation for multiple myeloma beyond 2010. *Blood*. 2010;115(18):3655–3663. doi:10.1182/blood-2009-08-238196

4. Kumar SK, Lee JH, Lahuerta JJ, et al. Risk of progression and survival in multiple myeloma relapsing after therapy with IMIDs and bortezoimib: A multicenter international myeloma working group study. *Leukemia*. 2012;26(1):149–157. doi:10.1038/leu.2011.196

5. Chen ZP, Schell JB, Ho CT, Chen KY. Green tea epigallocatechin gallate shows a pronounced growth inhibitory effect on cancerous cells but not on their normal counterparts. *Cancer Lett*. 1998;129(2):173–179. doi:10.1016/s0304-3835(98)00108-6

6. Reygaert WC. The antimicrobial possibilities of green tea. *Front Microbiol*. 2014;5:434. doi:10.3389/fmicb.2014.00434

7. Singh BN, Shankar S, Srivastava RK. Green tea catechin, epigallocatechin-3-gallate (EGCG): Mechanisms, perspectives and clinical applications. *Biochem Pharmacol*. 2011;82(12):1807–1821. doi:10.1016/j.bcp.2011.07.093

8. Wang WC, Chen D, Zhu K. SOX2OT variant 7 contributes to the synergistic interaction between EGCG and doxorubicin to kill osteosarcoma via autophagy and stemness inhibition. *J Exp Clin Cancer Res*. 2018;37(1):37. doi:10.1186/s13046-018-0689-3

9. Li M, Li JJ, Gu QH, et al. EGCG induces lung cancer A549 cell apoptosis by regulating Ku70 acetylation. *Oncol Rep*. 2016;35(4):2339–2347. doi:10.3892/or.2016.4587

10. Ma J, Shi M, Li GM, et al. Regulation of Id1 expression by epigallocatechin-3-gallate and its effect on the proliferation and apoptosis of poorly differentiated AGS gastric cancer cells. *Int J Oncol*. 2013;43(4):1052–1058. doi:10.3892/ijo.2013.2043

11. Siddiqui IA, Bharali DJ, Nihal M, et al. Excellent anti-proliferative and pro-apoptotic effects of (−)-epigallocatechin-3-gallate encapsulated in chitosan nanoparticles on human melanoma cell growth both in vitro and in vivo. *Nanomedicine*. 2014;10(8):1619–1626. doi:10.1016/j.nano.2014.05.007

12. Yao H, Ashihara E, Maekawa T. Targeting the Wnt/beta-catenin signaling pathway in human cancers. *Expert Opin Ther Targets*. 2011;15(7):873–887. doi:10.1517/14728222.2011.577418

13. Reya T, Clevers H. Wnt signalling in stem cells and cancer. *Nature*. 2005;434(7035):843–850. doi:10.1038/nature03319

14. Andel HV, Kocemba KA, Spaargaren M, Pals ST. Aberrant Wnt signaling in multiple myeloma: Molecular mechanism and targeting options. *Leukemia*. 2019;33(5):1063–1075. doi:10.1038/s41375-019-0404-1

15. Sukhdeo K, Mani M, Zhang YY, et al. Targeting the beta-catenin/TCF transcriptional complex in the treatment of multiple myeloma. *Proc Natl Acad Sci U S A*. 2007;104(18):7516–7521. doi:10.1073/pnas.0610299104

16. Zhao JJ, Lin JH, Zhu D, et al. miR-30-5p functions as a tumor suppressor and novel therapeutic tool by targeting the oncogenic Wnt/beta-catenin/BCL9 pathway. *Cancer Res*. 2014;74(6):1801–1813. doi:10.1158/0008-5472.CAN-13-3311-T

17. Masood AS, Paola N, Hemanta K, et al. Specific killing of multiple myeloma cells by (−)-epigallocatechin-3-gallate extracted from green tea: Biologic activity and therapeutic implications. *Blood*. 2006;108(8):2804–2810. doi:10.1182/blood-2006-05-022814

18. Zhou CG, Hui LM, Luo JM. Epigallocatechin gallate inhibits the proliferation and induces apoptosis of multiple myeloma cells via inactivating EZH2. *Eur Rev Med Pharmacol Sci*. 2018;22(7):2093–2098. doi:10.26355/eurrev_201804_14742

19. Ameri Z, Ghiasi S, Farsinejad A, Hassanshahi G, Ehsan M, Fatemi A. Telomerase inhibitor MST-312 induces apoptosis of multiple myeloma cells and down-regulation of anti-apoptotic, proliferative and inflammatory genes. *Life Sci*. 2019;228:66–71. doi:10.1016/j.lfs.2019.04.060

20. Encouse BG, Philip YL, Adel K, et al. Green tea polyphenols block the anticancer effects of bortezomib and other boronic acid-based proteasome inhibitors. *Blood*. 2009;113(23):5927–5937. doi:10.1182/blood-2008-07-171389

21. Qing W, Juan L, Jing LG, et al. Potentiation of (−)-epigallocatechin-3-gallate-induced apoptosis by bortezomib in multiple myeloma cells. *Acta Biochim Biophys Sin*. 2009;41(12):1018–1026. doi:10.1093/abbs/gmp094

22. Clevers H, Nusse R. Wnt/beta-catenin signaling and disease. *Cell*. 2012;149(6):1192–1205. doi:10.1016/j.cell.2012.05.012

23. Verkaar F, Cadigan KM, Amerongen RV. Celebrating 30 years of Wnt signaling. *Sci Signal*. 2012;5(254):mr2. doi:10.1126/scisignal.2003714

24. Kretzchmar K, Clevers H. Wnt/beta-catenin signaling in adult mammalian epithelial stem cells. *Dev Biol*. 2017;428(2):273–282. doi:10.1016/j.ydbio.2017.05.015

25. Clevers H. Wnt/beta-catenin signaling in development and disease. *Cell*. 2006;127(3):469–480. doi:10.1016/j.cell.2006.10.018

Hypoxia-inducible factor-2α promotes EMT in esophageal squamous cell carcinoma through the Notch pathway

Zhiqi Ji[1,A,B], Shihao Bao[1,B], Liang Li[1,C], Dong Wang[2,E], Mo Shi[2,D], Xiangyan Liu[1,2,A,F]

[1] Department of Thoracic Surgery, Shandong Provincial Hospital, Cheeloo College of Medicine, Shandong University, Jinan, China

[2] Department of Thoracic Surgery, Shandong Provincial Hospital Affiliated to Shandong First Medical University, Jinan, China

A – research concept and design; B – collection and/or assembly of data; C – data analysis and interpretation;
D – writing the article; E – critical revision of the article; F – final approval of the article

Address for correspondence
Xiangyan Liu
E-mail: liuxiangyan1@163.com

Conflict of interest
None declared

Abstract

Background. Esophageal cancer is one of the most lethal tumors worldwide. The most common histological type in China is esophageal squamous cell carcinoma (ESCC), accounting for 90% of cases. Esophageal cancer occurs at a high incidence in certain areas, among which China has the highest incidence. Although various therapeutic strategies have been used in clinical treatment, the 5-year survival rate is still not satisfactory, as it is only 15–20%. The reason for the poor prognosis of ESCC is that the distant metastasis easily occurs in these tumors. However, the mechanism of metastasis has not been studied clearly.

Objectives. To investigate the function of hypoxia-inducible factor-2α (hif-2α) in ESCC.

Materials and methods. Immunohistochemistry and immunofluorescence were used to detect the expression of hif-2α in tissues and cells. Clinicopathological data from 100 ESCC patients were used to investigate the relationship between hif-2α and prognosis. Cell experiments (Cell Counting Kit-8 (CCK-8) assay and transwell migration assays) were utilized to verify the roles of hif-2α on the ESCC cells. Western blotting was used to explore the mechanism of hif-2α in ESCC. Mouse model was used to clarify the effect of hif-2α on ESCC cells in vivo.

Results. The hif-2α was overexpressed both in ESCC tissues and cells, and was related with poor prognosis in ESCC patients. The CCK-8 assay evidenced that silencing hif-2α suppressed the proliferation of ESCC cells, while transwell assay – that overexpression of hif-2α promoted the migration of ESCC cells. Western blot assay indicated that hif-2α regulated epithelial–mesenchymal transition (EMT) through Notch pathway in ESCC cells. Mouse model showed that silencing hif-2α significantly suppressed the proliferation of ESCC cells in vivo.

Conclusions. The hif-2α promotes EMT in ESCC through the Notch pathway.

Key words: esophageal squamous cell carcinoma, Notch signaling pathway, epithelial–mesenchymal transition, hypoxia-inducible factor-2α

Background

Esophageal cancer is one of the most lethal tumors worldwide. The most common histological type in China is esophageal squamous cell carcinoma (ESCC), accounting for 90% of cases.[1] Esophageal cancer occurs at a high incidence in certain areas, among which China has the highest incidence.[1] Although various therapeutic strategies have been used in clinical treatment, the 5-year survival rate is still not satisfactory, as it is only 15–20%.[2] The reason for the poor prognosis of ESCC is that the distant metastasis easily occurs in these tumors,[3] especially lymphatic metastasis.[4] However, the mechanism of metastasis has not been studied clearly.

It has been reported that hypoxia can induce ESCC to undergo EMT through several mechanisms, in which hypoxia-inducible factor-1α (hif-1α) plays an important role.[5] The overexpression of hif-1α correlates with lymph node metastasis and poor prognosis in patients with ESCC.[6] The hif-2α is a member of the hypoxia-inducible factor family and is homologous to hif-1α. It has been reported to play important roles in several cancers.[7] The hif-2α is persistently upregulated under mild hypoxia conditions and can regulate the epithelial–mesenchymal transition (EMT) process through crosstalk with Wnt/β-catenin signaling in pancreatic cancer.[8] However, there have been no studies on the role of hif-2α in ESCC yet. Therefore, the role of hif-2α in ESCC is still unknown and requires further investigation.

The Notch signaling pathway is an evolutionarily conserved local cell signaling pathway that participates in a variety of cellular processes. These processes include cell differentiation, proliferation, apoptosis, adhesion, EMT, migration, and angiogenesis, and Notch signaling pathway affects embryonic development, tissue balance and whole-body immunity.[9] The Notch signaling pathway has been reported to act as an oncogene in various cancers, including lung cancer, breast cancer, colorectal cancer, prostate cancer, T-cell acute lymphoblastic leukemia (T-ALL), and other malignancies.[10] The Notch signaling has been proven to have crosstalk with hif-1α in some types of cancers, and this crosstalk consequently results in changes in EMT markers, such as breast cancer.[11] Moreover, some studies have shown that aberrant activation of Notch signaling plays important roles in the progression of ESCC and predicts poor prognosis in ESCC patients.[12] However, the specific mechanism of Notch signaling in ESCC remains unknown, especially the mechanism by which it regulates the EMT process.

Objectives

In this study, we investigated the role of hif-2α by regulating EMT in ESCC through the Notch signaling pathway and identified hif-2α as a factor that predicts poor prognosis in ESCC patients.

Materials and methods

Patients

One hundred patients who were diagnosed with ESCC and underwent esophageal cancer surgery in the Department of Thoracic Surgery at Shandong Provincial Hospital, Jinan, China, from January 2014 to December 2015, were included in this project. The inclusion and exclusion criteria were as follows:

1. ESCC confirmed by pathology after surgery;
2. chemotherapy and radiotherapy not administered to patients before surgery;
3. contraindications of surgery excluded during preoperative examination;
4. patients who died due to complications or accidents after surgery were excluded.

The tumor was completely excised in all patients, and no tumors were visible to the naked eye in the surgical field. The upper and lower resection margins were determined to be cancer cell-negative by pathology. The TNM stage was determined using the 8th edition of TNM staging criteria for esophageal cancer in 2017 according to the International Union Against Cancer.

The experimental protocol and informed consent procedure were in compliance with the Declaration of Helsinki. The study was approved by the ethics committee of the institutional ethics committee of Shandong Provincial Hospital Affiliated to Shandong First Medical University (approval No. SWYX:NO.2022-109) according to the Guide for Chinese Ethics Review Committees, and informed consent was obtained from all individual participants included in the study. Written informed consent was obtained from the patients for publication of their individual details and accompanying images in this manuscript.

Cell culture and reagents

Esophageal squamous cell carcinoma cell lines (Eca-109 and KYSE-150) were obtained from the Shanghai Institutes for Biological Sciences (Shanghai, China). The KYSE-150 cells were cultured in Roswell Park Memorial Institute (RPMI)-1640 medium (GE Healthcare Life Science, Logan, USA). The Eca-109 cells were cultured in high-glucose Dulbecco's modified Eagle's medium (DMEM; Gibco, Logan, USA). Both media were supplemented with 10% fetal bovine serum (FBS, Biological Industries, Kibbutz Beit Haemek, Israel). All cells were cultured at 37.0 ±0.2°C in a humidified incubator with 5.0% CO_2. Before exposure to the hypoxic environment (3.0% O_2), cells were cultured under normoxic conditions and grown to approx. 60% confluence. Then, the cells were cultured in a low-oxygen environment in a hypoxic incubator (Thermal Tech, Orlando, USA) for the indicated duration. Cobalt chloride ($CoCl_2$) was purchased from Sigma-Aldrich (St. Louis, USA) and used at 50 mM concentration for 48 h. The Notch

antagonist CB-103 was purchased from MCE (HY-135145; MedChem Express, Monmouth Junction, USA) and was used at 20 mM for 48 h.

Transfection

Transfections were performed using Lipofectamine 3000 (Invitrogen, Carlsbad, USA) according to the manufacturer's instructions. All experiments were performed after the transfection medium was replaced by complete medium after 24 h of treatment. The hif-2α overexpression plasmid and silencing siRNAs were designed by and purchased from GeneChem Company (Shanghai, China).

CCK-8 assay

Prior to using Cell Counting Kit-8 (CCK-8), the cells were seeded in 96-well plates at 2000 cells per well for specific treatments. Cell viability was evaluated using CCK-8 (Dojindo, Kumamoto, Japan). After incubating the cells with CCK-8 working solution for 30 min, the absorbance was measured at 450 nm using an ELx808 microplate reader (BioTek, Santa Clara, USA). Relative cell viability was expressed as a percentage of a particular control.

Transwell assay

The tumor cell infiltration activity was evaluated by its ability to penetrate the gel matrix (Matrigel; Becton Dickinson, Franklin Lakes, USA). In short, the Matrigel solution was diluted 1:8 in FBS-free medium and filtered with 6.5 mm diameter (8-μm holes) polycarbonate in a 24-well transwell box (Corning, USA) for film coverage. All filters were filled with 40 mL of working solution, and the plates were cured at 37°C for at least 5 h. Tumor cells were seeded at a density of 2×10^5 in each chamber. They were cultured in the upper compartment of the chamber in FBS-free medium for 48 h, and the lower chamber was filled with complete medium. The filter was wiped with a cotton swab, and the cells attached to the bottom were fixed with 4% formaldehyde polyphosphate (Beyotime, Shanghai, China). After staining with crystal violet (Beyotime), the cells with greater infiltration capacity were counted. The experiment was independently repeated 3 times.

Immunohistochemistry and immunofluorescence

The immunohistochemistry study was carried out using the streptavidin-peroxidase method. Formalin-fixed and paraffin-embedded ESCC tissue was cut into 5-μm thick sections, deparaffinized and then incubated with hydrogen peroxide. Goat serum was used at room temperature for 1 h for blocking before the primary antibody was applied. The primary antibodies used to perform immunohistochemistry were as follows: anti-hif-2a (NB100-122;

Novus, St Charles, USA), anti-E-cadherin (20874-1-AP), anti-N-cadherin (22018-1-AP), and anti-vimentin (10366-1-AP). These antibodies were purchased from Proteintech (Beijing, China). The primary antibody was added to tissue slides and incubated overnight at 4°C. The next step followed the instructions of the secondary biotinylated antibody kit (Zhongshan Biotech, Guangzhou, China). The stained slides were independently evaluated by 2 observers.

Before immunofluorescence staining was performed, 4% polyphosphate formaldehyde was used to fix the cells for 15 min. After incubation with 1% Triton for 30 min, the cells were blocked with goat serum for 1 h at room temperature. Then, the cells were incubated overnight at 4°C with rabbit anti-hif-2α antibody (NB100-122; Novus) and incubated with secondary antibodies conjugated to fluorescent dyes for 1 h at room temperature in the dark. After counterstaining with 4′,6-diamidino-2-phenylindole (DAPI) (C0065; Solarbio, Beijing, China) for 5 min, the cells were observed under an inversion fluorescence microscope.

Protein extraction and western blotting

Mouse model

The Eca-109 cells transfected with siRNA and negative-control lentivirus were used to investigate the effect of hif-2α on tumor progression in vitro. Sixteen 5-week-old female BALB/c nude mice were randomly divided into 2 groups, with 8 mice in each group. The negative control (NC)-siRNA and siRNA cells (1×10^6) were independently injected subcutaneously into the flanks of mice. Then, the tumor sizes were measured every 5 days and weighed after 20 days. The following formula was used to calculate the volume of the tumor: $V = L \times W2/2$, in which L is the largest and W is the smallest diameter. The protocol was approved by the ethics committee of the Provincial Hospital affiliated with Shandong First Medical University, Jinan, China (approval No. LCYJ:NO.2019-164).

Statistical analyses

The statistical data are presented as the mean ± standard deviation (SD). Tests of normality and homogeneity of variance were performed before the analysis of differences (Supplementary Table 1). The analysis of differences between the 2 groups was performed using Student's t test and multiple groups were compared using one-way analysis of variance (ANOVA) if the data were normally distributed and had uniform variance. Otherwise, Mann–Whitney test was used to analyze differences between the 2 groups and multiple groups were compared using Welch's test. Regarding the post hoc analysis among multiple groups, Bonferroni's test was used if the data had uniform variance. Otherwise, Tamhane's T2 test was used. The relationships between hif-2α

and clinicopathological information displayed in Table 1 were calculated using Fisher's test. The information of Kaplan–Meier curve is presented in Supplementary Table 2. The multivariate Cox regression and verification of assumption of proportional hazard (Supplementary Table 3) were performed using IBM SPSS software v. 24.0 (IBM Corp., Armonk, USA). In the multivariate Cox regression, age, gender, hif-2α, maximal dimension of tumor, lymph node metastasis, and TNM stage were explanatory variables, while response variables were survival time and outcome status. Differences were considered to be significant if the p-value <0.05. The IBM SPSS v. 24.0 and GraphPad Prism v. 7 (GrahPad Software, San Diego, USA) statistical software were used to perform all statistical calculations and to construct graphs.

Results

Hif-2α is overexpressed in ESCC and relates with poor prognosis

To investigate whether hif-2α is overexpressed in ESCC tissues and cell lines, immunohistochemistry and immunofluorescence were performed. Immunohistochemistry showed that ESCC tissues expressed high levels of hif-2α, but hif-2α was hardly detected in normal esophageal epithelial cells (Fig. 1A,B). In addition, the results show that hif-2α is mainly aggregated in the nucleus, which is consistent with the transcription factor role of hif-2α. Immunofluorescence results suggested that hif-2α could be detected in the ESCC cell lines Eca-109 and KYSE-150 under normoxia conditions and was located mainly in the nucleus (Fig. 1C,D), which is consistent with the immunohistochemistry results.

The relationship between hif-2α expression levels and clinical factors in ESCC patients was also studied. The expression level of hif-2α was divided into high and low groups according to the H-score. The overexpression of hif-2α was significantly related with lymph node metastasis (p = 0.009) and tumor stage (p = 0.018) (Table 1). In addition, the hif-2α expression level was a predicting factor for prognosis (hazard ratio (HR): 4.538; 95% confidence interval (95% CI): [1.426; 14.44], p = 0.01) (Table 2). Moreover, lymph node metastasis was also indicated to be a prognostic factor (HR: 2.411; 95% CI: [1.284; 4.527], p = 0.006) (Table 2). To investigate the relationship between the hif-2α expression level and overall survival (OS) of patients with ESCC, a Kaplan–Meier curve was constructed, and the results showed that patients with a low expression level of hif-2α had a greatly improved OS rate (p = 0.015) (Fig. 1E).

Hypoxia induces EMT and hif-2α overexpression in ESCC

Two esophageal cancer cell lines were used to mimic hypoxia-induced EMT. As expected, morphological changes

Table 1. Relationships between hypoxia-inducible factor-2α (hif-2α) expression and the clinicopathological information in 100 esophageal squamous cell carcinoma (ESCC) patients

Variable	hif-2α low	hif-2α high	p-value (Fisher's test)
Gender			
Male	38	50	0.062
Female	9	3	
Age			
<60	28	24	0.167
≥60	19	29	
Maximal dimension of tumor			
<5	26	30	1.000
≥5	21	23	
Lymph node metastasis			
Yes	17	34	0.009
No	30	19	
Stage			
I–II	30	21	0.018
III–IV	17	32	

Table 2. Multivariate Cox regression analysis of the indicated factors for patient survival

Variable	HR (95% CI)	p-value
Age (≥60/<60)	1.008 [0.573; 1.775]	0.978
Gender (male/female)	1.204 [0.542; 2.676]	0.648
Hif-2α (high/low)	4.538 [1.426; 14.44]	0.01
Maximal dimension of tumor (≥5/<5)	1.174 [0.265; 5.204]	0.833
Lymph node metastasis (yes/no)	2.411 [1.284; 4.527]	0.006
Stage (I–II/III–IV)	0.207 [0.37; 1.155]	0.073

95% CI – 95% confidence interval; HR – hazard ratio; hif-2α – hypoxia-inducible factor-2α.

of the cells were observed after treatment with hypoxic conditions for 48 h (Fig. 2A). These findings were accompanied by a decreased expression of E-cadherin and increased expression of hif-2α, N-cadherin, vimentin, and Snail (Fig. 2B–D). We also used $CoCl_2$ to mimic hypoxia.[13] The expression of E-cadherin was decreased, and the expression of N-cadherin, vimentin and Snail was increased (Fig. 2E–G).

Hif-2α promotes the proliferation and invasion of esophageal cells

The hif-2α has been reported to promote cell proliferation and invasion in different tumors, but the role of hif-2α in esophageal cancer cells has not yet been studied. To investigate whether hif-2α could promote proliferation and invasion in esophageal cells, CCK-8 and transwell assays were performed. The CCK-8 assay showed that the optical density (OD) value (450 nm) of the hif-2α-silenced group was significantly decreased at 24 h, 48 h, 72 h, and 96 h in both Eca-109 and KYSE-150 ESCC cells (Fig. 3A).
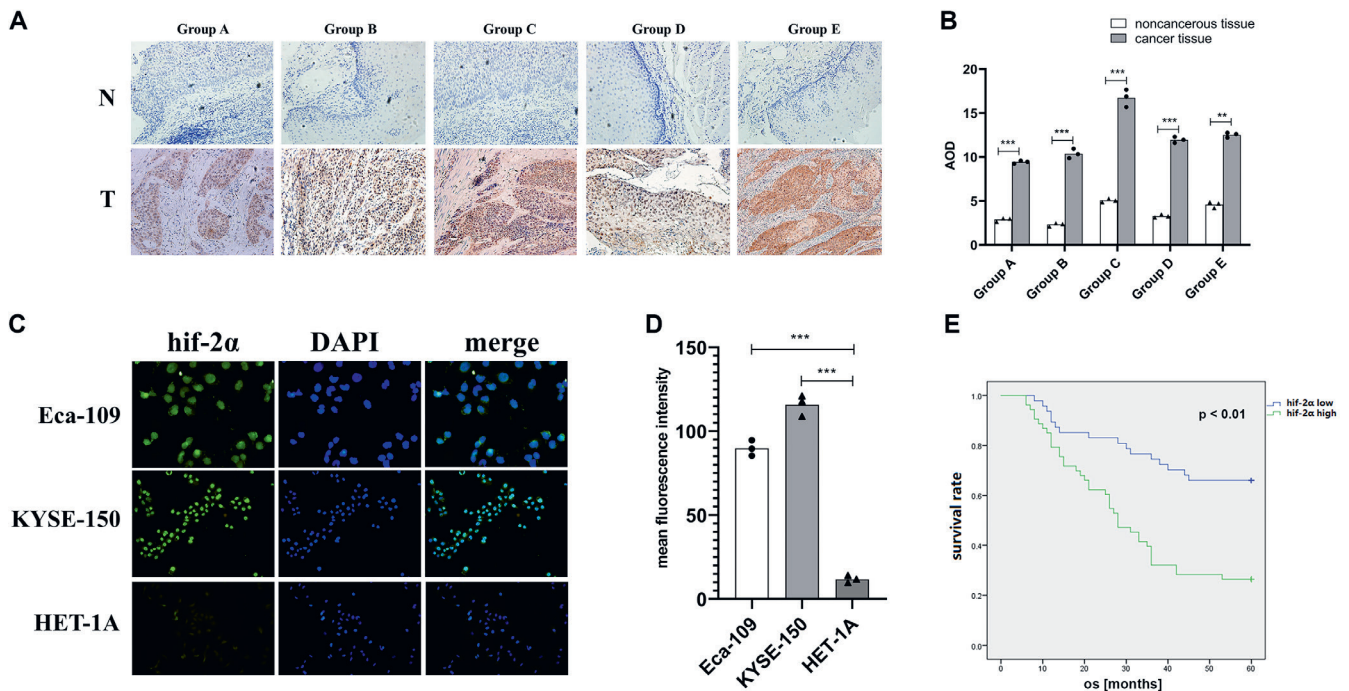
Fig. 1. Hypoxia-inducible factor-2α (hif-2α) is overexpressed in esophageal squamous cell carcinoma (ESCC) and correlates with poor prognosis.
A,B. Immunohistochemistry showing that the hif-2α level in ESCC tissue was significantly higher than in normal tissue (N – noncancerous tissue; T – tumor tissue; Student's t-test was used to calculate the significant difference); C,D. Immunofluorescence showing that hif-2α was overexpressed in ESCC cells compared with normal esophageal epithelial cells (one-way analysis of variance (ANOVA) test was used to calculate the significant difference); E. Kaplan–Meier curve showing that patients with lower expression levels of hif-2α had significantly longer survival times than those with higher expression levels of hif-2α

OS – overall survival; DAPI – 4',6-diamidino-2-phenylindole; AOD – average optical density; *p < 0.05; **p < 0.01; ***p < 0.001.

Moreover, silencing hif-2α resulted in a strong inhibitory effect on proliferation in Eca-109 cells. For the transwell assay, compared to the control and NC-siRNA groups, the number of hif-2α-silenced ESCC cells entering the transwell membrane was significantly reduced (Fig. 3B,C). This finding suggests that the invasion capability of ESCC cells was suppressed when hif-2α was silenced. In contrast, the hif-2α-overexpressing group showed significantly increased cell numbers penetrating the membrane compared to the control and negative control to overexpression (NC-OE) groups (Fig. 3D,E). This finding indicates that the overexpression of hif-2α enhances the invasion ability of ESCC cells. These results suggest that hif-2α plays an important role in the proliferation and invasion of ESCC cells.

Hif-2α regulates EMT through the Notch pathway

To determine whether hif-2α could regulate EMT in ESCC cells, western blot assay was performed to detect the protein levels of EMT markers. Compared to the control and NC-siRNA groups, the hif-2α-silenced group showed increased levels of E-cadherin and decreased expression levels of N-cadherin, vimentin and Snail in both Eca-109 and KYSE-150 ESCC cells (Fig. 4A–C). Furthermore, the hif-2α overexpression group demonstrated the opposite results (Fig. 4D–F). In addition, the expression

level of NICD, which is the active form of Notch and functions as a transcriptional regulator, showed the same trend as hif-2α (Fig. 4A,D). These results show that both EMT and Notch could be regulated by hif-2α. Next, the inhibitor CB-103 was used to study whether the Notch pathway could regulate EMT. The CB-103 is a specific and highly effective inhibitor of the Notch pathway. The results showed that CB-103 could significantly reverse the EMT process in ESCC cells (Fig. 4G–I). Furthermore, a retrial experiment was carried out to investigate whether hif-2α regulated EMT in ESCC cells through the Notch pathway. The EMT process was reversed in hif-2α-overexpressing ESCC cells after the Notch pathway inhibitor was used (Fig. 4J–L). These results suggest that hif-2α could regulate EMT through the Notch pathway in ESCC cells.

Silencing hif-2α suppressed tumor growth in a mouse model

A xenograft mouse model was used to confirm the effect of hif-2α in vivo. Compared to the NC group, the tumor volume and weight of the siRNA group were markedly decreased (Fig. 5A–C), and no significant difference in the body weight of nude mice was observed (Fig. 5D). Besides the comparison of tumor volume between groups, comparisons within groups were also performed (Supplementary Fig. 1). This result suggests that inhibiting hif-2α significantly suppresses the growth of tumors
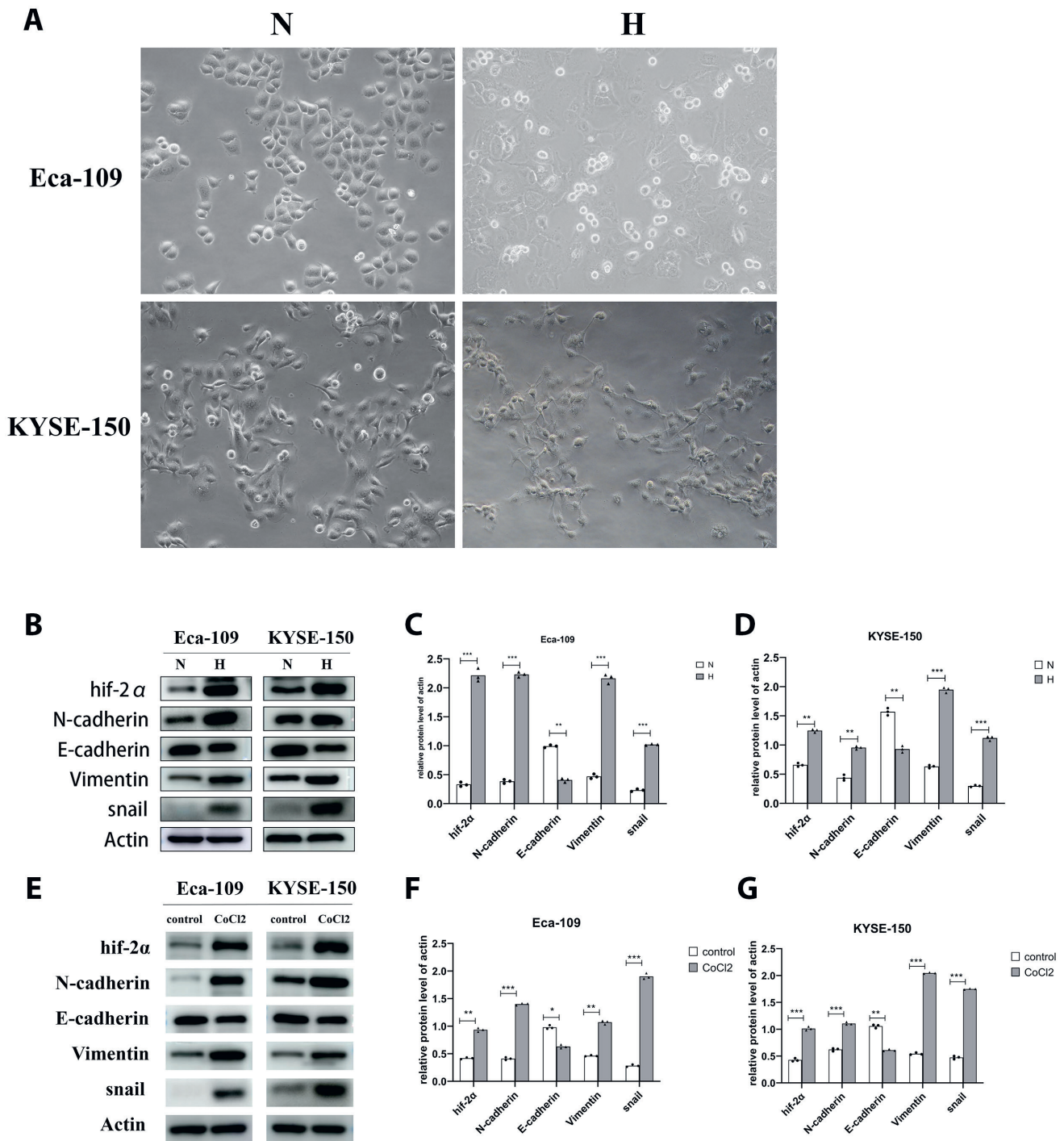
Fig. 2. Hypoxia induces epithelial–mesenchymal transition (EMT) and hypoxia-inducible factor-2α (hif-2α) overexpression in esophageal squamous cell carcinoma (ESCC). A. Morphological changes in ESCC cells after hypoxia treatment for 48 h; B–D. Changes in the expression of hif-2α and EMT markers in ESCC cells after hypoxia treatment; E–G. CoCl$_2$ was used to mimic hypoxia and induce EMT. Student's t-test was used to calculate the significant difference

N – normoxia; H – hypoxia; *$p < 0.05$; **$p < 0.01$; ***$p < 0.001$.

without any apparent impacts on mouse growth. Immunohistochemistry and western blot analyses were performed using xenograft tumors to confirm that hif-2α could regulate EMT through the Notch pathway (Fig. 5E–G). The results showed that hif-2α deficiency could significantly suppress Notch signaling and reverse EMT in vivo.

Discussion

Surgical resection is still considered the first line of treatment for early and local ESCC.[14] However, ESCC is generally resistant to conventional therapeutic agents. In addition, the newest ESCC inhibitors are clinically ineffective. Therefore, finding new biological targets that may
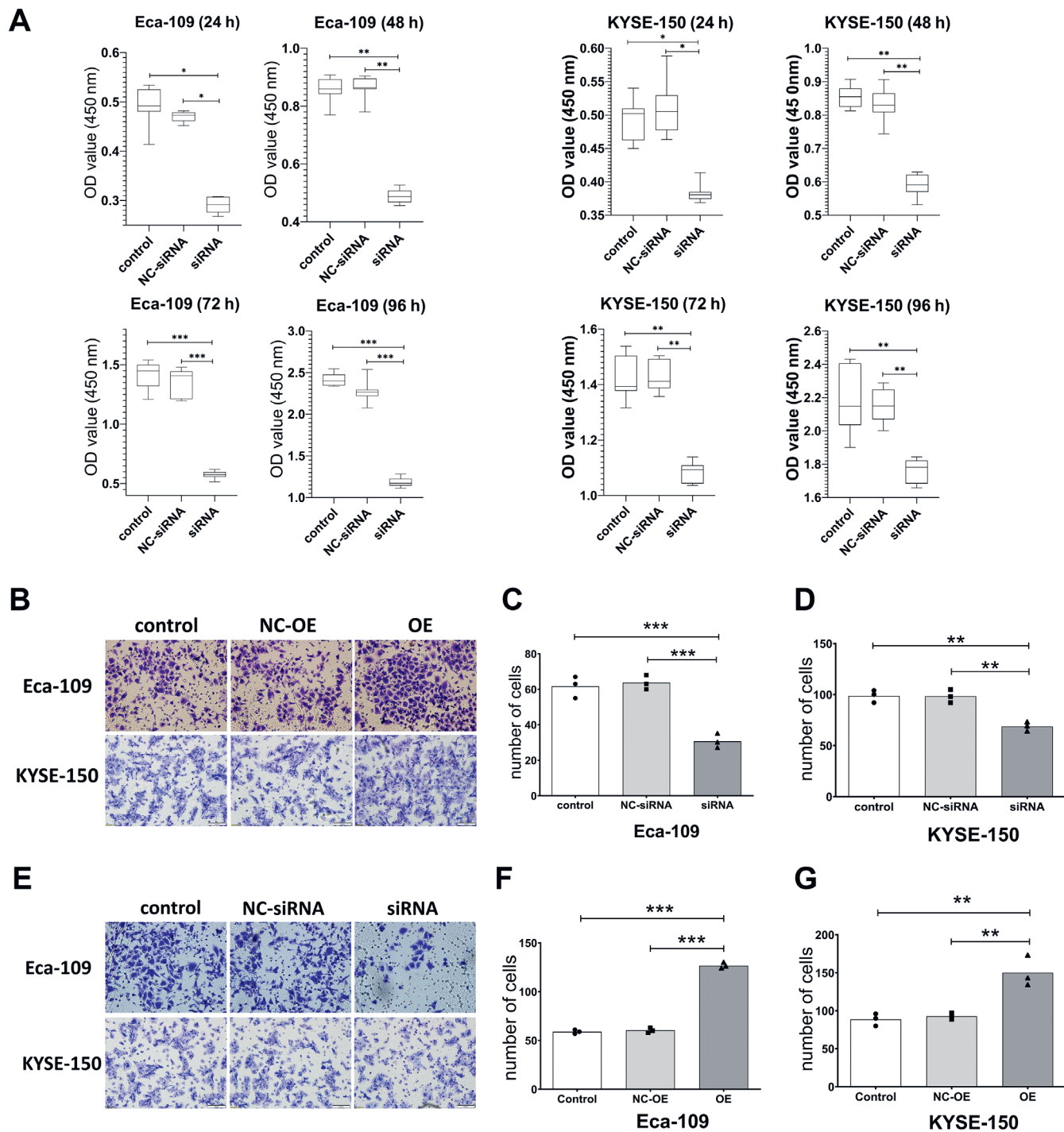
Fig. 3. Hypoxia-inducible factor-2α (hif-2α) promotes the proliferation and invasion of esophageal cells. A. Cell Counting Kit-8 (CCK-8) assay showing that silencing hif-2α inhibited the proliferation of esophageal squamous cell carcinoma (ESCC) cells (top of box – upper quartile; bottom of box – lower quartile; upper whisker – maximum value; lower whisker – minimum value; middle whisker – median). B. Transwell assays showing that silencing hif-2α reduced the invasion ability of ESCC cells; C,D. The cell numbers on the lower surface of the membrane were counted in 3 randomly selected fields; E. Transwell assays showing that overexpressing hif-2α enhanced the invasion ability of ESCC cells; F,G. The cell numbers on the lower surface of the membrane were counted in 3 randomly selected fields

siRNA – silencing RNA of hif-2α; NC-siRNA – negative control to siRNA; OE – overexpression of hif-2α; NC-OE – negative control to OE; OD – optical density. One-way analysis of variance (ANOVA) test and Welch's test were used to calculate the significant difference. *$p < 0.05$, **$p < 0.01$, ***$p < 0.001$.

be useful in improving the prognosis of patients with ESCC has been a central issue in recent years.

In recent decades, hypoxia-inducible factor (HIF) has been widely and comprehensively researched. It is a key regulator in cells responsible for preventing damage from hypoxia, which is mainly regulated by the oxygen level in cells.[15] Under normoxic conditions, HIF is modified by HIF-specific prolyl hydroxylases (PHDs), which lead
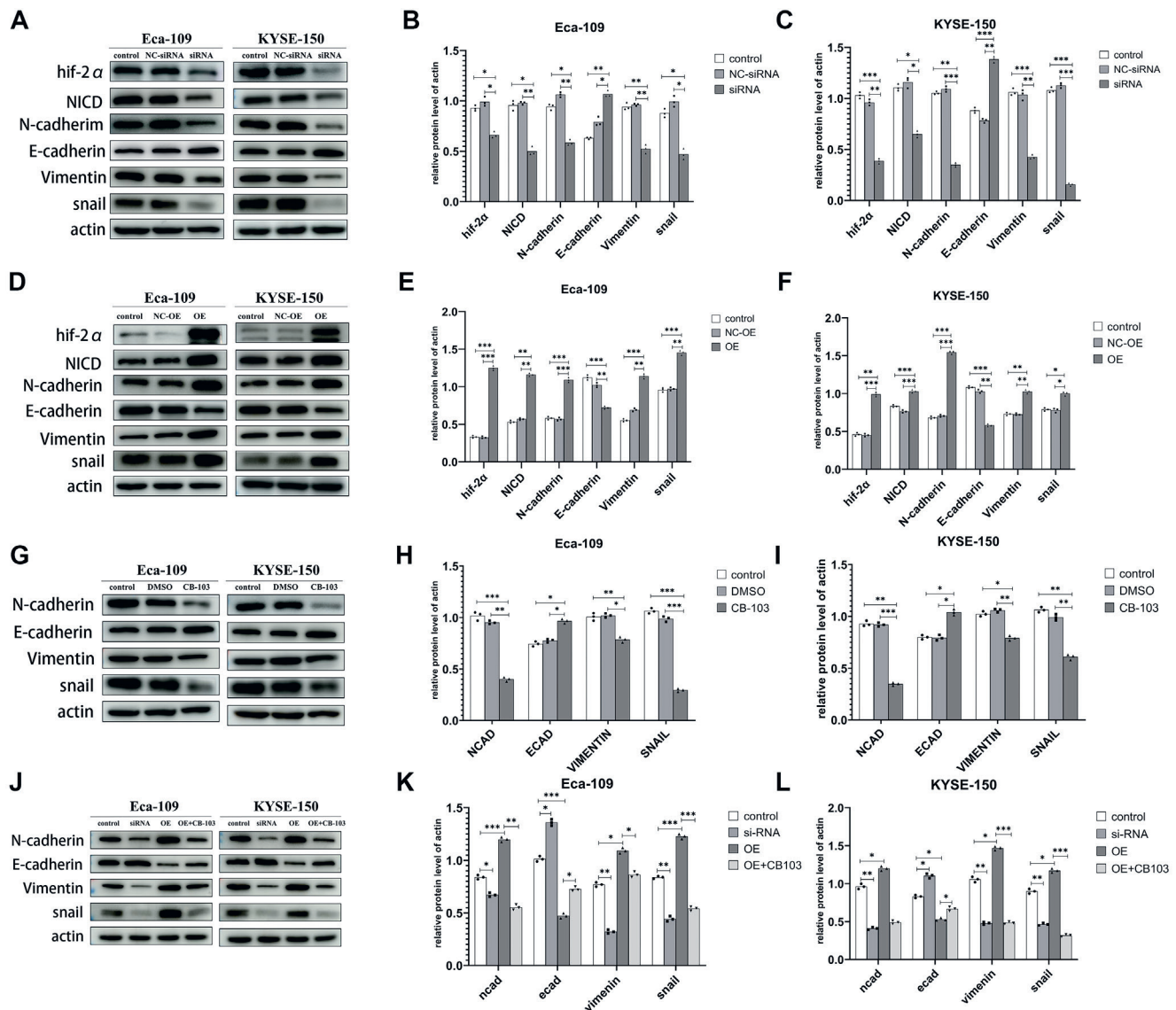
Fig. 4. Hypoxia-inducible factor-2α (hif-2α) regulates epithelial–mesenchymal transition (EMT) through the Notch pathway. A–C. Silencing hif-2α reduced Notch signaling and EMT in esophageal squamous cell carcinoma (ESCC) cells; D–F. Overexpressing hif-2α enhanced Notch signaling and EMT in ESCC cells; G–I. A notch inhibitor reduced EMT in ESCC cells; J–L. Using a Notch inhibitor in hif-2α-overexpressing cells reversed the EMT process. One-way analysis of variance (ANOVA) test was used to calculate the significant difference

siRNA – silencing RNA of hif-2α; NC-siRNA – negative control to siRNA; OE – overexpression of hif-2α; NC-OE – negative control to OE; DMSO – dimethyl sulfoxide; *p < 0.05; **p < 0.01; ***p < 0.001.

to its degradation by von Hippel–Lindau tumor suppressors (pVHLs).[16] When the cell is under hypoxic conditions, PHDs are inactivated and the VHL-dependent degradation pathway is blocked. This results in the accumulation of HIF and the activation of downstream genes. As a member of HIF, hif-2α has been reported to be associated with a poor prognosis in various cancers, such as non-small-cell lung carcinoma (NSCLC), breast cancer, colorectal cancer, hepatocellular cancer, and glioblastoma.[7] However, the role of hif-2α in ESCC has not yet been studied. In this study, we identified hif-2α as a key molecule that regulates EMT, and we revealed that it can be a prognostic factor in ESCC patients. We found that hif-2α was overexpressed in both ESCC tissues and cell lines. The overexpression of hif-2α in tumor tissue might be due to the hypoxic

tumor microenvironment, but the mechanism by which hif-2α is overexpressed under normoxia in ESCC cell lines remains unclear. A possible hypothesis could be that the transcription is increased or that the degradation pathway of hif-2α is impacted. However, these hypotheses require further investigation. In addition, we discovered the function of hif-2α in promoting proliferation and metastasis in ESCC. Both the in vitro and in vivo experiments verified the role of hif-2α in promoting the growth of ESCC cells. The function of hif-2α in promoting metastasis and regulating the expression of EMT markers was also confirmed in our investigation. In addition, we confirmed that hif-2α was associated with poor prognosis in patients with ESCC, characterized by a lower 5-year survival rate and a higher incidence of lymph node metastasis.
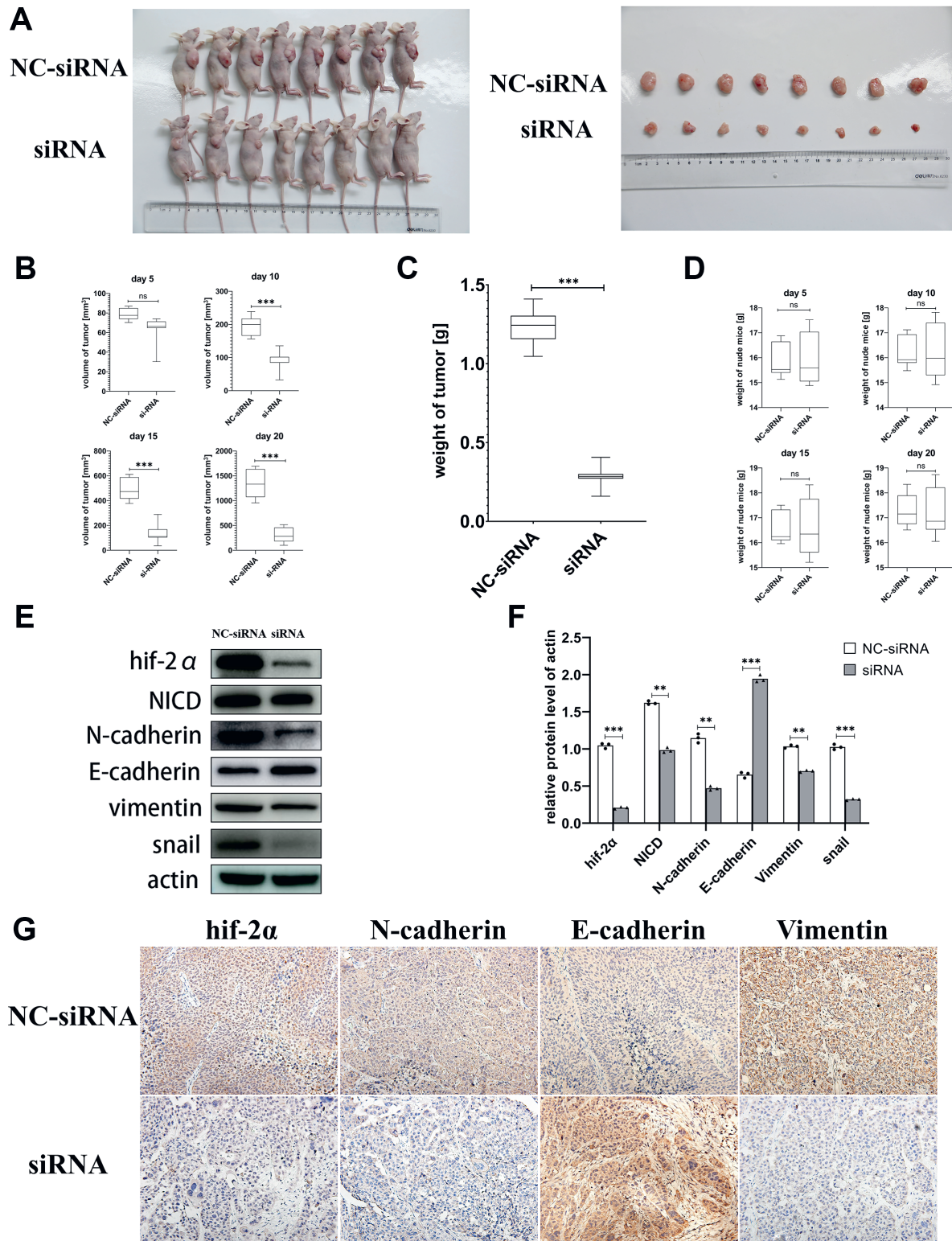
Fig. 5. Silencing hypoxia-inducible factor-2α (hif-2α) suppressed tumor growth in a mouse model. A. NC-siRNA or siRNA Eca-109 cells (1 × 10⁶) were injected subcutaneously into the flanks of mice. Xenografts from siRNA were much smaller than those from NC-siRNA; B. Tumor volume comparison between the NC-siRNA and siRNA groups. Tamhane's T2 test was used to calculate the significant differences (top of box – upper quartile; bottom of box – lower quartile; upper whisker – maximum value; lower whisker – minimum value; middle whisker – median); C. Tumor weight of the NC-siRNA and siRNA groups. Student's t-test was used to calculate the significant differences (top of box – upper quartile; bottom of box – lower quartile; upper whisker – maximum value; lower whisker – minimum value; middle whisker – median); D. The body weight of mice injected with NC-siRNA- or siRNA-transfected cells (top of box – upper quartile; bottom of box – lower quartile; upper whisker – maximum value; lower whisker – minimum value; middle whisker – median); E. Western blot analysis showed changes in the expression of hif-2α, NICD and epithelial–mesenchymal transition (EMT) markers in the NC-siRNA and siRNA groups; F. Western blot analysis showed changes in the expression of hif-2α, NICD and EMT markers in the NC-siRNA and siRNA groups. Student's t-test was used to calculate the significant differences; G. Immunohistochemistry showed changes in the expression of hif-2α and EMT markers in the NC-siRNA and siRNA groups

siRNA – silencing RNA of hif-2α; NC-siRNA – negative control to siRNA;*p < 0.05; **p < 0.01; ***p < 0.001.

The Notch signaling pathway has been studied for over 100 years; it was first described by Thomas Hunt Morgan in 1917.[9] Previous studies have proven that Notch functions as an oncogene in many types of cancers, and the mechanism of how the Notch signaling pathway works has been clearly interpreted.[17] The transduction process of the Notch signaling pathway mainly includes the classical pathway that relies on CSL and CSL-independent transduction pathways.[18] The classical pathway of Notch signaling is triggered by the interaction between the Notch ligand and the receptor. Then, the Notch receptor releases the active form of the Notch protein, that is, the intracellular segment of the ICN (NICD).[19] The NICD enters the nucleus, where it acts as a transcription regulator. In recent decades, it has been confirmed that Notch signaling plays important roles in regulating the EMT process in different cancers, including esophageal cancer.[20] The crosstalk between signaling pathways in cells is an extremely complicated network, which is not an exception for Notch signaling. It has been reported that both hif-1α and hif-2α can regulate Notch signaling in different cancers.[21,22] However, the relationship between HIF signaling and Notch signaling in ESCC remains unclear. In this study, Notch signaling was found to be downstream of hif-2α. We observed that the expression of NICD, the active form of Notch, could be regulated by hif-2α. As a modulator of EMT, NICD can enter the nucleus and regulate the transcription of downstream genes. Both EMT markers and NICD can be regulated by hif-2α, but whether EMT is regulated by hif-2α through the Notch signaling pathway remains unknown. Therefore, we carried out a retrieval experiment, and the results verified our speculation that Notch is the intermediary of hif-2α in regulating EMT in ESCC. As an oncogene, hif-2α is a potential target in cancer therapy, and a specific inhibitor of hif-2α has been proven to be efficient in clear cell renal cell carcinoma.[23] According to this study, hif-2α plays an important role in the progression of ESCC. Thus, hif-2α inhibitors may be a new treatment target in ESCC therapy strategies and may improve the prognosis of ESCC patients in the future.

Limitations

This study still has some limitations in spite of clarifying the function of hif-2α in ESCC. For instance, we confirmed that Notch signaling pathway was downstream of hif-2α, but the in-depth mechanism of how hif-2α regulate Notch signaling pathway, by pre-translational or post-translational modification, was not clear. Furthermore, we confirmed that hif-2α could enhance the invasion ability of ESCC in vitro, but the experiment investigating whether hif-2α could promote metastasis of ESCC in vivo was not conducted because of the limitations of experimental conditions. Therefore, more in-depth and extensive research is still needed.

Conclusions

In general, this project illuminated a protumor role of hif-2α in esophageal cancer. The hif-2α enhanced the proliferation and invasion ability of ESCC cells and promoted EMT through the Notch signaling pathway. In addition, we identified hif-2α as an indicator of poor prognosis in ESCC patients and found that it was associated with shorter OS and lymph node metastasis. Hence, hif-2α may become a potential target for treating esophageal cancer and might serve as a new strategy to prolong the survival time of ESCC patients.

Supplementary data availability

The Supplementary material is available at doi:10.5281/zenodo.6316427. The Supplementary data consist of:

Supplementary Table 1. Verification of assumption for Student's t test and ANOVA analysis.

Supplementary Table 2. Information of Kaplan–Meier analysis.

Supplementary Table 3. Verification of proportional-hazard assumption for COX model.

Supplementary Fig. 1. Comparison of tumor volume within NC-siRNA and siRNA groups.

References

1. Abnet CC, Arnold M, Wei WQ. Epidemiology of esophageal squamous cell carcinoma. *Gastroenterology*. 2018;154(2):360–373. doi:10.1053/j.gastro.2017.08.023
2. Mitin T, Hunter JG, Thomas CR Jr. Esophageal carcinoma. *N Engl J Med*. 2015;372(15):1471–1472. doi:10.1056/NEJMc1500692
3. Li J, Qi Z, Hu YP, Wang YX. Possible biomarkers for predicting lymph node metastasis of esophageal squamous cell carcinoma: A review. *J Int Med Res*. 2019;47(2):544–556. doi:10.1177/0300060518819606
4. Isik A, Soran A, Grasi A, Barry N, Sezgin E. Lymphedema after sentinel lymph node biopsy: Who is at risk? [published online as ahead of print on June 30, 2021]. *Lymphat Res Biol*. 2021. doi:10.1089/lrb.2020.0093
5. Zhu Y, Zang Y, Zhao F, et al. Inhibition of HIF-1α by PX-478 suppresses tumor growth of esophageal squamous cell cancer in vitro and in vivo. *Am J Cancer Res*. 2017;7(5):1198–1212. PMID:28560067. PMCID:PMC5446484.
6. Shao JB, Li Z, Zhang N, Yang F, Gao W, Sun ZG. Hypoxia-inducible factor 1α in combination with vascular endothelial growth factor could predict the prognosis of postoperative patients with oesophageal squamous cell cancer. *Pol J Pathol*. 2019;70(2):84–90. doi:10.5114/pjp.2019.87100
7. Albadari N, Deng S, Li W. The transcriptional factors HIF-1 and HIF-2 and their novel inhibitors in cancer therapy. *Expert Opin Drug Discov*. 2019;14(7):667–682. doi:10.1080/17460441.2019.1613370
8. Zhang Q, Lou Y, Zhang J, et al. Hypoxia-inducible factor-2α promotes tumor progression and has crosstalk with Wnt/β-catenin signaling in pancreatic cancer. *Mol Cancer*. 2017;16(1):119. doi:10.1186/s12943-017-0689-5
9. Siebel C, Lendahl U. Notch signaling in development, tissue homeostasis, and disease. *Physiol Rev*. 2017;97(4):1235–1294. doi:10.1152/physrev.00005.2017
10. Majumder S, Crabtree JS, Golde TE, Minter LM, Osborne BA, Miele L. Targeting Notch in oncology: The path forward. *Nat Rev Drug Discov*. 2021;20(2):125–144. doi:10.1038/s41573-020-00091-3
11. Kar R, Jha NK, Jha SK, et al. A "NOTCH" deeper into the epithelial-to-mesenchymal transition (EMT) program in breast cancer. *Genes*. 2019;10(12):961. doi:10.3390/genes10120961

12. Natsuizaka M, Whelan KA, Kagawa S, et al. Interplay between Notch1 and Notch3 promotes EMT and tumor initiation in squamous cell carcinoma. *Nat Commun*. 2017;8(1):1758. doi:10.1038/s41467-017-01500-9

13. Tripathi VK, Subramaniyan SA, Hwang I. Molecular and cellular response of co-cultured cells toward cobalt chloride (CoCl(2))-induced hypoxia. *ACS Omega*. 2019;4(25):20882–20893. doi:10.1021/acsomega.9b01474

14. Yang YM, Hong P, Xu WW, He QY, Li B. Advances in targeted therapy for esophageal cancer. *Signal Transduct Target Ther*. 2020;5(1):229. doi:10.1038/s41392-020-00323-3

15. Balamurugan K. HIF-1 at the crossroads of hypoxia, inflammation, and cancer. *Int J Cancer*. 2016;138(5):1058–1066. doi:10.1002/ijc.29519

16. Dang CV, Kim JW, Gao P, Yustein J. The interplay between MYC and HIF in cancer. *Nat Rev Cancer*. 2008;8(1):51–56. doi:10.1038/nrc2274

17. Meurette O, Mehlen P. Notch signaling in the tumor microenvironment. *Cancer Cell*. 2018;34(4):536–548. doi:10.1016/j.ccell.2018.07.009

18. Kopan R, Ilagan MX. The canonical Notch signaling pathway: Unfolding the activation mechanism. *Cell*. 2009;137(2):216–233. doi:10.1016/j.cell.2009.03.045

19. Gordon WR, Vardar-Ulu D, Histen G, Sanchez-Irizarry C, Aster JC, Blacklow SC. Structural basis for autoinhibition of Notch. *Nat Struct Mol Biol*. 2007;14(4):295–300. doi:10.1038/nsmb1227

20. Li Y, Ma J, Qian X, et al. Regulation of EMT by Notch signaling pathway in tumor progression. *Curr Cancer Drug Targets*. 2013;13(9):957–962. doi:10.2174/15680096113136660101

21. Jiang N, Zou C, Zhu Y, et al. HIF-1α-regulated miR-1275 maintains stem cell-like phenotypes and promotes the progression of LUAD by simultaneously activating Wnt/β-catenin and Notch signaling. *Theranostics*. 2020;10(6):2553–2570. doi:10.7150/thno.41120

22. Yan Y, Liu F, Han L, et al. HIF-2α promotes conversion to a stem cell phenotype and induces chemoresistance in breast cancer cells by activating Wnt and Notch pathways. *J Exp Clin Cancer Res*. 2018;37(1):256. doi:10.1186/s13046-018-0925-x

23. Chen W, Hill H, Christie A, et al. Targeting renal cell carcinoma with a HIF-2 antagonist. *Nature*. 2016;539(7627):112–117. doi:10.1038/nature19796

Bibliometric analysis of acute respiratory distress syndrome (ARDS) studies published between 1980 and 2020

Fatma Yildirim[1,A–F], Pinar Yildiz Gulhan[2,A–F], Irem Karaman[3,C–F], Mehmet Nurullah Kurutkan[4,B–D,F]

[1] Pulmonary Intensive Care Unit, Clinic of Chest Diseases, Dışkapı Yıldırım Beyazıt Training and Research Hospital, University of Health Sciences, Ankara, Turkey

[2] Department of Chest Diseases, Faculty of Medicine, Düzce University, Turkey

[3] School of Medicine, Bahçeşehir University, Istanbul, Turkey

[4] Department of Health Management, Faculty of Management, Düzce University, Turkey

A – research concept and design; B – collection and/or assembly of data; C – data analysis and interpretation;
D – writing the article; E – critical revision of the article; F – final approval of the article

Abstract

Background. Acute respiratory distress syndrome (ARDS), an acute respiratory failure caused by noncardiogenic pulmonary edema, was first defined by Ashbaugh et al. in 1967. The number of publications increased enormously after the Berlin definition of ARDS was first described in 2012.

Objectives. This article intends to provide the physicians and the scientists with a reference guide to assess the most influential publications written about ARDS.

Materials and methods. We performed an exhaustive bibliometric analysis to identify publication trends by year, and the most influential research articles, authors, co-authors, journals, and countries. Articles on ARDS published in Science Citation Index (SCI) and Emerging Sources Citation Index (ESCI) journals between 1980 and 2020 were examined. On December 20, 2020, the keywords "ARDS" and "acute respiratory distress syndrome" were searched using the Web of Science Core Collection (WoSCC) database, and data including titles, author information, abstracts, journals, and references were analyzed.

Results. A total of 4564 articles related to ARDS published between 1980 and 2020 were identified. After excluding 192 proceedings papers, 19 early access papers, 1 book chapter, 1 research paper, and 1 retracted article, 4350 articles published in SCI and ESCI journals were analyzed. The largest number of articles (n = 557, 12.8%) appeared in 2020. The average citations per article was 38.21, and 4350 articles were cited 166,885 times altogether. The USA was at the top of the list of the most productive countries with 5025 articles. Harvard University was the most contributing institution with 244 articles. M.A. Matthay ranked as the most productive author in ARDS research with 87 published publications.

Conclusions. The present study provided a comprehensive, illustrative analysis of ARDS articles published in SCI and ESCI journals over the past 40 years.

Key words: intensive care, bibliometric analysis, acute respiratory distress syndrome

Background

Acute respiratory distress syndrome (ARDS) is a progressive form of sudden respiratory failure characterized by severe hypoxemia and dyspnea. This condition, which involves refractory hypoxemia and diffuse bilateral infiltrates in lung radiology, was first described in 1967 by Ashbaugh et al.[1] After this definition was introduced in a case series with acute respiratory failure, it has been revised many times. In 1988, the definition of ARDS was expanded to include a 4-point lung injury score (0−4), the degree of hypoxemia and static lung compliance, the positive end-expiratory pressure level, and the extent of radiological infiltrations.[2] At the American-European Consensus Conference in 1994, a partial oxygen pressure/fraction of inspired oxygen (PaO_2/FiO_2) <300 mm Hg was defined as acute lung injury, and PaO_2/FiO_2 ratio <200 mm Hg was defined as ARDS.[3] The clinical criteria for ARDS have also changed over time, and the current diagnostic criteria and severity (classification) for ARDS are based on the Berlin definition.[4] Currently, the diagnostic criteria include bilateral opacities in chest imaging, an acute onset (within 1 week of a new clinical insult), arterial hypoxemia with a PaO_2/FiO_2 ratio <300 mm Hg, and noncardiogenic origin of pulmonary edema. The severity of ARDS is determined by the degree of hypoxemia, with mild ARDS defined as a PaO_2/FiO_2 ratio of 200−300 mm Hg, moderate as a PaO_2/FiO_2 ratio of 100−200 mm Hg, and severe as a PaO_2/FiO_2 ratio <100 mm Hg.

Since its first description, ARDS has become a major worldwide clinical problem, with a high morbidity, mortality and healthcare cost burden.[5] Studies from Europe have reported an ARDS incidence of between 5 and 7 cases per 100,000 individuals.[6] In a large observational study conducted in 2016 across 459 intensive care units (ICUs) in 50 countries, it was revealed that 23% of mechanically ventilated patients and 10% of critically ill patients met the diagnostic criteria for ARDS, and that ARDS represented 0.42 cases per ICU bed over 4 weeks. The investigators also found that the hospital mortality was 34.9% for patients with mild ARDS, 40.3% for those with moderate ARDS and 46.1% for those with severe ARDS.[7] Although there is a lack of epidemiological studies on ARDS in lower- and middle-income countries, a recent study from Vietnam reported a 57% ICU mortality rate for critically ill ARDS patients.[8]

Several risk factors triggering the onset of ARDS have been identified. The most common risk factors include pneumonia, non-pulmonary sepsis, pancreatitis, aspiration, shock, drug overdose, surgery, and trauma.[7,9] After exposure to these triggers, alveolar macrophages secrete mediators, neutrophils and alveolar epithelial cells activate, and proinflammatory mediators and chemokines are secreted, which cause impaired vascular permeability, gaps in the alveolar epithelial barrier and necrosis of alveolar cells. The intravascular coagulation cascade is also activated, and microthrombus formation occurs. These processes result in pulmonary edema, loss of surfactant, and debris deposition in the alveoli, in consequence decreasing pulmonary compliance and making gas exchange difficult.[10] Although this condition is severe and life-threatening, and several clinical studies have been carried out since its first description, there is no effective pharmacotherapy for ARDS apart from supportive therapies, such as lung-protective ventilation and conservative volume strategies.[11]

To quantify the impact of scientific articles, citation data have been used as indicators. Academic effectiveness is understood as authorship of highly cited articles. Bibliometric analysis can identify influential articles, journals and authors, and can guide future research.[12,13] In medicine, bibliometric methods estimate how much impact a selected article has on future research or how much impact an author's published article will have on the number of citations of a given issue of a journal. This method usually quantifies the number of times an article or author is cited after publication, and it has been used more and more often to determine the influence of articles, books or journals.[14] In some medical fields, such as oncology,[15] cardiology[16] and gynecology,[13] bibliometric analyses are widely used. Although they have been performed in some areas of intensive care medicine like sepsis, acute kidney injury and neurocritical care,[17−20] very few studies on ARDS were undertaken.[21,22]

Thus, in the present study, an exhaustive bibliometric analysis was carried out to identify publication trends by year, and the most influential research articles, authors, co-authors, journals, and countries associated with ARDS research between 1980 and 2020.

Objectives

Materials and methods

Web of Science (WoS) is one of the most commonly used databases among academics. It provides current and detailed information on many leading journals, including publications with worldwide impact.[23] On December 30, 2020, the keywords "ARDS" and "acute respiratory distress syndrome" were searched using the WoS Core Collection (WoSCC) database. As stated above, the definition of ARDS used within the year of publication of each article was accepted. The publication period was between 1980 and 2020. Original research articles published in Science Citation Index (SCI) and Emerging Sources Citation Index (ESCI) journals were included, and WoSCC data, including titles, author information, abstracts, journals, and references, were downloaded in plain TXT format.

A bibliometric analysis of the raw data was performed, and the specific analyses carried out are presented in Table 1. An online bibliometric analysis platform and Microsoft Excel 2016 (Microsoft Corp., Redmond, USA) were used to generate the figures. Authors from different

Table 1. Software and analysis

Software	Analysis
Bibliometrix Biblioshiny	annual production of articles in the years 1980–2020 top 15 institutions productive authors most-cited articles in ARDS research top 25 countries contributing to ARDS papers top 10 journals
VOSviewer	citation visualization map of the countries

ARDS – acute respiratory distress syndrome.

countries and the countries of publication were analyzed separately for each article. For articles with more than 2 authors affiliated with 2 different countries, the article was accounted for both countries.

Results

A total of 4564 articles related to ARDS published between 1980 and 2020 were identified. After excluding 192 proceedings papers, 19 early access papers, 1 book chapter, 1 research paper, and 1 retracted article, 4350 articles published in SCI and ESCI journals were analyzed. The largest number of articles (n = 557, 12.8%) appeared in 2020. The trend for the number of the articles published by year is shown in Fig. 1. The average citations per article was 38.21, and 4350 articles were cited 166,885 times altogether.
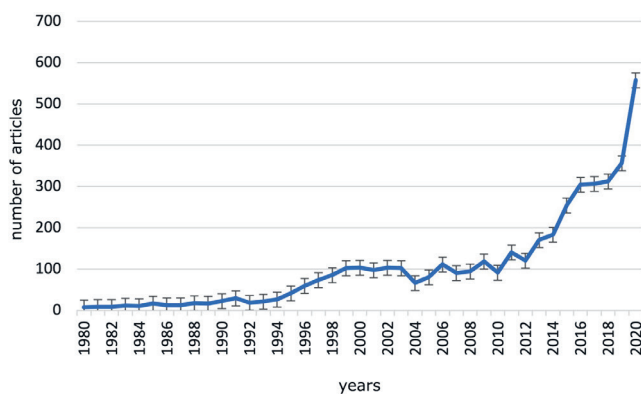

Fig. 1. Articles published in the years 1980–2020

Analysis of countries

According to the WoSCC database, 4350 articles originated from 129 countries. The top 25 countries contributing to ARDS articles between 1980 and 2020 are depicted in Fig. 2. The USA was at the top of the list with 5025 articles. China (n = 2146), France (n = 1676), Germany (n = 974), Italy (n = 941), Canada (n = 883), Japan (n = 781), Spain (n = 756), the UK (n = 516), Brazil (n = 503), and the Netherlands (n = 425) followed the USA.
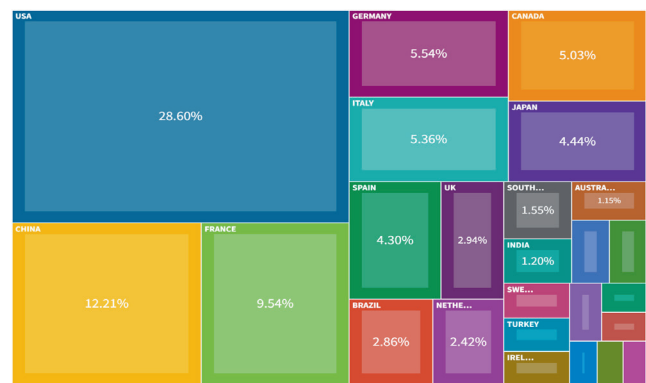

Fig. 2. The top 25 countries contributing to acute respiratory distress syndrome (ARDS) publications between 1980 and 2020

Analysis of institutions

We also analyzed the most productive institutions in ARDS research. Harvard University (USA) was the most contributing institution with 244 articles, followed by the Assistance-Publique Hôpitaux de Paris (France; n = 213), the University of California System (USA; n = 198), the University of Toronto (Canada; n = 178), Massachusetts General Hospital (USA; n = 176), and the Institut national de la santé et de la recherche médicale (INSERM; France; n = 173). The top 15 most productive institutions are listed in Table 2.

Table 2. Top 15 institutions in acute respiratory distress syndrome (ARDS) research

Institution	Number of articles
Harvard University, USA	244
Assistance-Publique Hôpitaux de Paris, France	213
University of California System, USA	198
University of Toronto, Canada	178
Massachusetts General Hospital, USA	176
Institut national de la santé et de la recherche médicale (INSERM), France	173
University of California San Francisco, USA	146
University of Washington, USA	119
University of Pennsylvania, USA	100
St. Michael's Hospital, Toronto, Canada	93
Pennsylvania State System of Higher Education, USA	92
University of Milan, Italy	92
University of Michigan, USA	88
Vanderbilt University, USA	86
Sorbonne University, France	85

Analysis of authors and citations

In the present study, we analyzed the total number of ARDS publications by author. M.A. Matthay (University of California San Francisco, USA) ranked first

Table 3. Top 15 most productive authors in acute respiratory distress syndrome (ARDS) research

Author	Country	Number of publications
Matthay MA	USA	87
Thompson BT	USA	79
Brochard L	Canada	57
Slutsky AS	Canada	57
Calfee CS	USA	56
Gattinoni G	Germany	52
Pesenti A	Italy	52
Pelosi P	Italy	50
Papazian P	France	49
Schultz MJ	the Netherlands	48
Christiani DC	USA	43
Ware LB	USA	41
Hudson LD	USA	39
Chiumello D	Italy	36
Gong MN	USA	35

with 87 publications, followed by B.T. Thompson (Massachusetts General Hospital, USA) with 79 publications, L. Brochard (St. Michael's Hospital, Toronto, Canada) with 57 publications, A.S. Slutsky (St. Michael's Hospital, Toronto, Canada) with 57 publications, and C.S. Calfee (University of California San Francisco, USA) with 56 publications. The top 15 most productive authors in ARDS research are shown in Table 3.

All publications on ARDS were cited 166,815 times altogether (139,359 times without self-citation). The average number of citations per article was 38.24, with an h-index of 172. The citation visualization map by country is shown in Fig. 3.

Analysis of publications and journals

The 10 most cited ARDS articles are shown in Table 4. With 6412 citations, the article entitled "Ventilation with lower tidal volumes as compared with traditional tidal volumes for acute lung injury and the acute respiratory distress syndrome" by R.G. Brower, published in *New England*
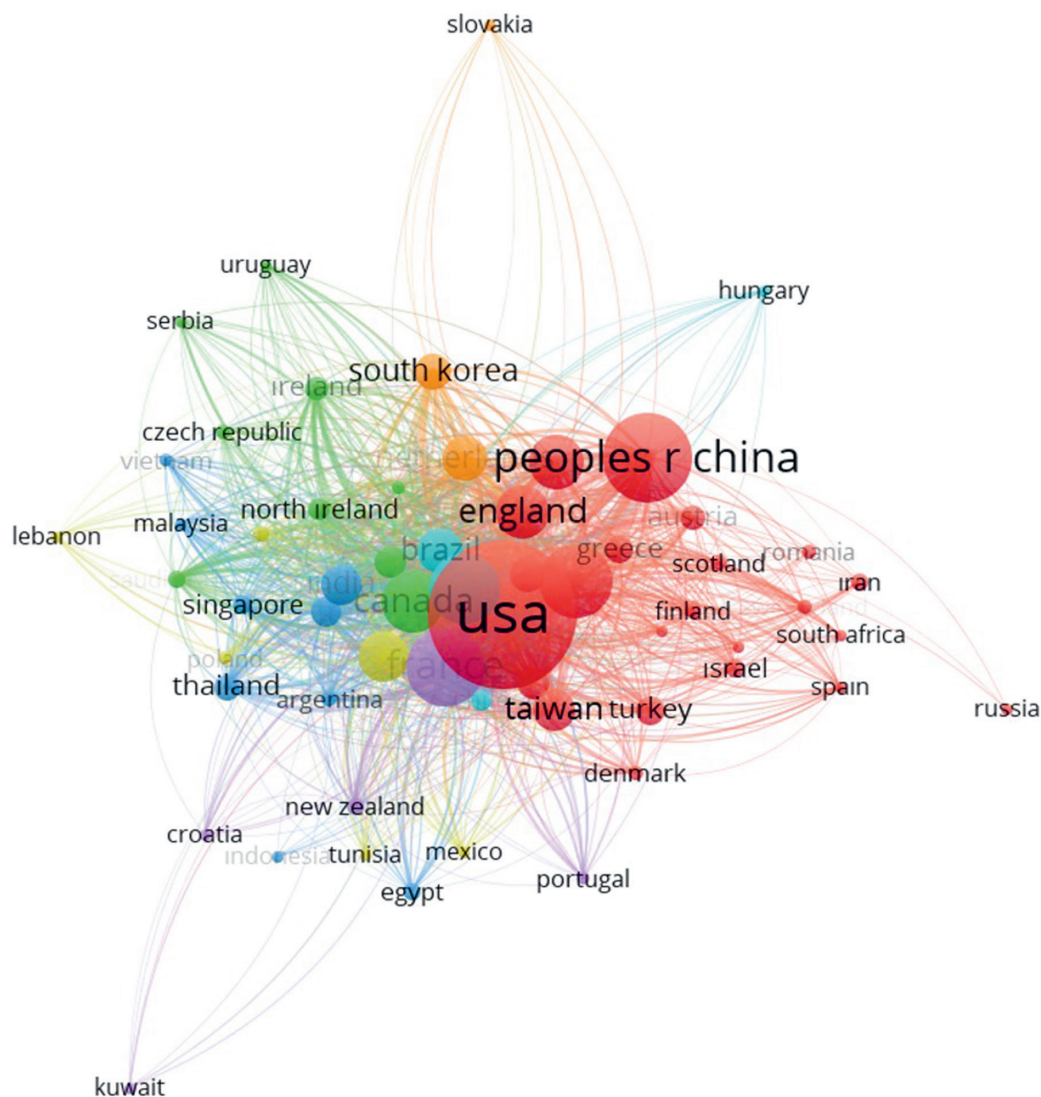

Fig. 3. Citation visualization map of the countries

Table 4. The most cited 10 articles in acute respiratory distress syndrome (ARDS) research

| Title	Publication year	First author	Journal	Number of citations
Ventilation with lower tidal volumes as compared with traditional tidal volumes for acute lung injury and the acute respiratory distress syndrome	2000	Brower RG[24]	*New England Journal of Medicine*	6412
Acute respiratory distress syndrome: The Berlin definition	2012	Ranieri VM[4]	*Journal of the American Medical Association (JAMA)*	3987
Pathological findings of COVID-19 associated with acute respiratory distress syndrome	2020	Xu Z[25]	*Lancet Respiratory Medicine*	2597
Effect of a protective-ventilation strategy on mortality in the acute respiratory distress syndrome	1998	Amato MB[26]	*New England Journal of Medicine*	2183
Risk factors associated with acute respiratory distress syndrome and death in patients with coronavirus disease 2019 pneumonia in Wuhan, China	2020	Wu C[27]	*JAMA Internal Medicine*	1901
Epidemiology, patterns of care, and mortality for patients with acute respiratory distress syndrome in intensive care units in 50 countries	2016	Bellani G[7]	*Journal of the American Medical Association (JAMA)*	1518
Prone positioning in severe acute respiratory distress syndrome	2013	Guérin C[28]	*New England Journal of Medicine*	1381
Higher versus lower positive end-expiratory pressures in patients with the acute respiratory distress syndrome	2004	Brower RG[29]	*New England Journal of Medicine*	1359
One-year outcomes in survivors of the acute respiratory distress syndrome	2003	Herridge MS[30]	*New England Journal of Medicine*	1266
Neuromuscular blockers in early acute respiratory distress syndrome	2010	Papazian L[31]	*New England Journal of Medicine*	1238
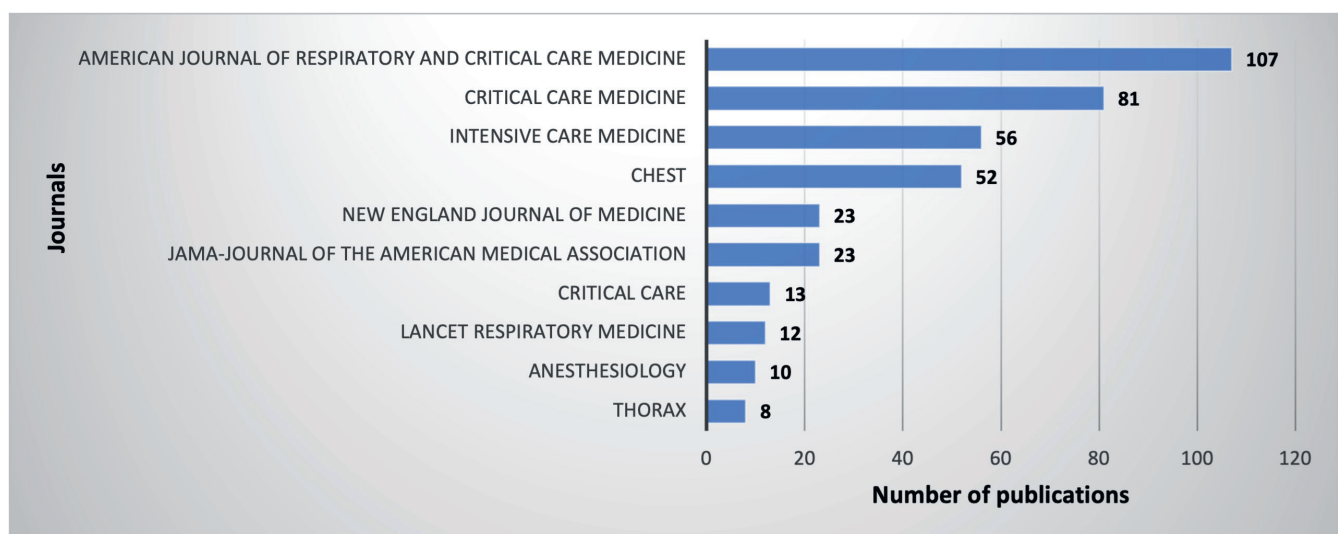
Fig. 4. Top 10 journals that published the 500 most cited acute respiratory distress syndrome (ARDS) articles

Journal of Medicine (impact factor (IF): 91.25) ranked first. It was followed by the article titled "Acute respiratory distress syndrome: The Berlin definition" by V.M. Ranieri, published in *Journal of American Medical Association* (*JAMA*; IF: 56.3; 3987 citations) and "Pathological findings of COVID-19 associated with acute respiratory distress syndrome" by Z. Xu, published in *Lancet Respiratory Medicine* (IF: 30.7; 2597 citations). Six of the top 10 most cited articles were published in *New England Journal of Medicine*, while 2 articles were published in *JAMA*. After the analysis of the top 500 most cited ARDS articles, we found that *American Journal of Respiratory and Critical Care Medicine* (IF: 21.41) ranked first with 107 articles

published. *Critical Care Medicine* (IF: 7.60), *Intensive Care Medicine* (IF: 17.44) and *Chest* (IF: 9.41) were in the 2nd, 3rd and 4th place with 81, 56 and 53 articles, respectively, followed by *New England Journal of Medicine* (n = 23) and *JAMA* (n = 23). The top 10 journals that published the 500 most highly cited articles are listed in Fig. 4.

Discussion

Although bibliometric analyses have been recently used in almost all medical fields, there were almost no investigations on ARDS papers. We believe that our study will

contribute to summarizing and better understanding the literature on the subject. To the best of our knowledge, our study is the 3rd to investigate ARDS articles.[19,20] Nevertheless, the present study analyzed articles published in the last 40 years, the most extended period used for a bibliometric analysis of ARDS articles.

In the 1980s, the period immediately after ARDS was first described, we did not observe a significant increase in the number of ARDS studies. After the mid-1990s, the number of ARDS articles increased each year. In 1994, the American-European Consensus Conference on ARDS published a consensus report to bring clarity and uniformity to the ARDS definition and attract attention to mechanisms of the disease.[3] In this report, the need for studies on ARDS was strongly emphasized, and a large part of the report was devoted to recommendations for future studies. Therefore, the effect of this consensus report on increasing the number of ARDS studies cannot be ignored. A 2nd increase in the number of ARDS studies came after 2012 when the Berlin definition of ARDS was released.[2] Finally, in 2019 and 2020, the number of publications related to ARDS in coronavirus disease 2019 (COVID-19) increased, likely due to the fact that COVID-19 leads to ARDS in 16–31% of hospitalized patients.[32]

The main result of our study is that the USA is the most productive country in ARDS research, and 8 out of the 15 most cited authors were from the USA. Similarly, a previous study by Wang et al.,[21] which evaluated the publication trends of 7890 studies on ARDS between 2009 and 2019, revealed that the USA was the most contributing country with 2612 articles published (15.0%). In the current study, China was the 2nd largest contributor with 2146 ARDS articles. Wang et al.[21] also reported China as the 2nd most productive country between 2009 and 2019; however, since 2016, China has exhibited a rapid increase in the number of ARDS articles and has surpassed the USA in the number of articles per year. On the other hand, China could not reach the citation frequency or the h-index of the USA. This suggests that China conducts relatively fewer randomized clinical trials and more observational studies. Two previous bibliometric analyses of ARDS articles reported Germany as the 3rd most productive country, whereas in our research France ranked 3rd.[21,22] This may be due to more extended period of analysis in our study.

Two of the 10 most cited articles focus on COVID-19-associated ARDS. These articles were published in 2020 and have received a large number of citations in just 2 years. Pathophysiologically, ARDS is characterized by acute and diffuse inflammatory damage to the alveolar–capillary barrier, leading to an increased vascular permeability, decreased compliance, and hypoxemia due to impaired gas exchange.[23,24] Since COVID-19 has emerged, the central question of intensivists was whether COVID-19-related ARDS is a typical ARDS.[33,34] Numerous studies have examined the different pathophysiological features, characteristics and outcomes of patients with COVID-19-related

ARDS and non-COVID-19-related ARDS. Gattinoni et al. described 2 different COVID-19-related ARDS patterns at the beginning of the disease course.[35,36] The 1st, termed Type L, is characterized by low elastance, low lung recruitability, low ventilation-to-perfusion ratio, and low lung weight. The 2nd, known as Type H, has a high elastance, high lung recruitability, high right-to-left shunt, and high lung weight. Gattinoni et al. suggested different ventilatory management strategies for these 2 types of cases.[36] Although there is not enough evidence to support the existence of these 2 types of COVID-19-related ARDS and the effectiveness of the different ventilatory management strategies, this hypothesis may direct researchers to perform more epidemiological and physiological investigations on COVID-19-related ARDS.

Eight of the 10 most cited ARDS articles were published in *New England Journal of Medicine* (n = 6) and *JAMA* (n = 2). In contrast, 107, 81, 56, and 52 of the top 500 most cited articles were published in *American Journal of Respiratory and Critical Care Medicine*, *Critical Care Medicine*, *Intensive Care Medicine*, and *Chest*, respectively. These findings suggest that journals with the highest IFs and those categorized as "general medicine" have published fewer but more influential articles than others classified as "critical care medicine" or "intensive care medicine." Since ARDS is still a syndrome with a high mortality in critically ill patients in ICUs, it is not surprising that ARDS articles are published in these journals.

Limitations

The present study produced a comprehensive, illustrative analysis of ARDS articles published in SCI and ESCI journals over the past 40 years. However, due to the nature of the bibliometric research, it has some limitations. First, the WoSCC database is constantly updated, meaning that our results will need to be validated over time. Second, as we excluded non-English articles, we may have ignored some influential and important non-English-language studies.

Conclusions

This study provides insight into the publications on ARDS. The number of publications has increased over the last 40 years, especially after the Berlin definition of ARDS was first formulated in 2012. The USA is the leading country contributing to the literature in terms of publication numbers, and most of the top-cited researchers are from the USA. M.A. Matthay, B.T. Thompson, R.L. Brochard, A.S. Slutsky, and C.S. Calfee are the most contributing authors in the ARDS field. This study can be helpful to future studies on ARDS. Although this study reported the numbers, countries, authors, and citations of ARDS-related studies (epidemiology, pathogenesis, pre-clinical,

clinical and treatment), it did not cover the content of these studies. More detailed bibliometric studies are needed to determine which areas (genetic, phenotype, microbiota, etc.) of ARDS research require more thorough exploration.

ORCID IDs

Fatma Yildirim https://orcid.org/0000-0003-3715-3097
Pinar Yildiz Gulhan https://orcid.org/0000-0002-5347-2365
Irem Karaman https://orcid.org/0000-0001-7559-9095
Mehmet Nurullah Kurutkan https://orcid.org/0000-0002-3740-4231

References

1. Ashbaugh DG, Bigelow DB, Petty TL, Levine BE. Acute respiratory distress in adults. *Lancet*. 1967;2(7511):319–323. doi:10.1016/s0140-6736(67)90168-7

2. Murray JF, Matthay MA, Luce JM, Flick MR. An expanded definition of the adult respiratory distress syndrome. *Am Rev Respir Dis*. 1988; 138(3):720–723. doi:10.1164/ajrccm/138.3.720

3. Bernard GR, Artigas A, Brigham KL, et al. The American-European consensus conference on ARDS: Definitions, mechanisms, relevant outcomes, and clinical trial coordination. *Am J Respir Crit Care Med*. 1994;149(3 Pt 1):818–824. doi:10.1164/ajrccm.149.3.7509706

4. Ferguson ND, Fan E, Camporota L, et al. The Berlin definition of ARDS: An expanded rationale, justification, and supplementary material. *Intensive Care Med*. 2012;38(10):1573–1582. doi:10.1007/s00134-012-2682-1

5. Villar J, Blanco J, Añón JM, et al. The ALIEN study: Incidence and outcome of acute respiratory distress syndrome in the era of lung protective ventilation. *Intensive Care Med*. 2011;37(12):1932–1941. doi:10.1007/s00134-011-2380-4

6. Villar J, Blanco J, Kacmarek RM. Current incidence and outcome of the acute respiratory distress syndrome. *Curr Opin Crit Care*. 2016; 22(1):1–6. doi:10.1097/MCC.0000000000000266

7. Bellani G, Laffey JG, Pham T, et al. Epidemiology, patterns of care, and mortality for patients with acute respiratory distress syndrome in intensive care units in 50 countries. *JAMA*. 2016;315(8):788–800. doi:10.1001/jama.2016.0291

8. Chinh LQ, Manabe T, Son DN, et al. Clinical epidemiology and mortality of patients with acute respiratory distress syndrome (ARDS) in Vietnam. *PLoS One*. 2019;14(8):e0221114. doi:10.1371/journal.pone. 0221114

9. Parhar KKS, Zjadewicz K, Soo A, et al. Epidemiology, mechanical power, and 3-year outcomes in acute respiratory distress syndrome patients using standardized screening: An observational cohort study. *Ann Am Thorac Soc*. 2019;16(10):1263–1272. doi:10.1513/AnnalsATS. 201812-910OC

10. Saguil A, Fargo MV. Acute respiratory distress syndrome: Diagnosis and management. *Am Fam Physician*. 2020;101(12):730–738. PMID:32538594.

11. Confalonieri M, Salton F, Fabiano F. Acute respiratory distress syndrome. *Eur Respir Rev*. 2017;26(144):160116. doi:10.1183/16000617. 0116-2016

12. van Eck NJ, Waltman L. Software survey: VOSviewer, a computer program for bibliometric mapping. *Scientometrics*. 2010;84(2):523–538. doi:10.1007/s11192-009-0146-3

13. Brandt JS, Hadaya O, Schuster M, Rosen T, Sauer MV, Ananth CV. A bibliometric analysis of top-cited journal articles in obstetrics and gynecology. *JAMA Netw Open*. 2019;2(12):e1918007. doi:10.1001/jamanetworkopen.2019.18007

14. Cooper ID. Bibliometrics basics. *J Med Libr Assoc*. 2015;103(4):217–218. doi:10.3163/1536-5050.103.4.013

15. Akmal M, Hasnain N, Rehan A, et al. Glioblastome multiforme: A bibliometric analysis. *World Neurosurg*. 2020;136:270–282. doi:10.1016/j.wneu.2020.01.027

16. Devos P, Menard J. Bibliometric analysis of research relating to hypertension reported over the period 1997–2016. *J Hypertens*. 2019;37(11): 2116–2122. doi:10.1097/HJH.0000000000002143

17. Yao RQ, Ren C, Wang JN, et al. Publication trends of research on sepsis and host immune response during 1999–2019: A 20-year bibliometric analysis. *Int J Biol Sci*. 2020;16(1):27–37. doi:10.7150/ijbs.37496

18. Ramos MB, Koterba E, Rosi Júnior J, Teixeira MJ, Figueiredo EG. A bibliometric analysis of the most cited articles in neurocritical care research. *Neurocrit Care*. 2019;31(2):365–372. doi:10.1007/s12028-019-00731-6

19. Tao T, Zhao X, Lou J, et al. The top cited clinical research articles on sepsis: A bibliometric analysis. *Crit Care*. 2012;16(3):R110. doi:10. 1186/cc11401

20. Liu YH, Wang SQ, Xue JH, et al. Hundred top-cited articles focusing on acute kidney injury: A bibliometric analysis. *BMJ Open*. 2016; 6(7):e011630. doi:10.1136/bmjopen-2016-011630

21. Wang C, Wang X, Long X, Xia D, Ben D, Wang Y. Publication trends of research on acute lung injury and acute respiration distress syndrome during 2009–2019: A 10-year bibliometric analysis. *Am J Transl Res*. 2020;12(10):6366–6380. PMID:33194036.

22. Zhang X, Wang C, Zhao H. A bibliometric analysis of acute respiratory distress syndrome (ARDS) research from 2010 to 2019. *Ann Palliat Med*. 2021;10(4):3750–3762. doi:10.21037/apm-20-2050

23. Falagas ME, Pitsouni EI, Malietzis GA, Pappas G. Comparison of PubMed, Scopus, Web of Science, and Google Scholar: Strengths and weaknesses. *FASEB J*. 2008;22(2):338–342. doi:10.1096/fj.07-9492LSF

24. Brower RG, Matthay MA, Morris A, et al; Acute Respiratory Distress Syndrome Network. Ventilation with lower tidal volumes as compared with traditional tidal volumes for acute lung injury and the acute respiratory distress syndrome. *N Engl J Med*. 2000;342(18):1301–1308. doi:10.1056/NEJM200005043421801

25. Xu Z, Shi L, Wang Y, Zhang J, et al. Pathological findings of COVID-19 associated with acute respiratory distress syndrome. *Lancet Respir Med*. 2020;8(4):420–422. doi:10.1016/S2213-2600(20)30076-X

26. Amato MB, Barbas CS, Medeiros DM, et al. Effect of a protective-ventilation strategy on mortality in the acute respiratory distress syndrome. *N Engl J Med*. 1998;338(6):347–354. doi:10.1056/NEJM1998 02053380602

27. Wu C, Chen X, Cai Y, et al. Risk factors associated with acute respiratory distress syndrome and death in patients with coronavirus disease 2019 pneumonia in Wuhan, China. *JAMA Intern Med*. 2020;180(7):934–943. doi:10.1001/jamainternmed.2020.0994

28. Guérin C, Reignier J, Richard JC, et al; PROSEVA Study Group. Prone positioning in severe acute respiratory distress syndrome. *N Engl J Med*. 2013;368(23):2159–2168. doi:10.1056/NEJMoa1214103

29. Brower RG, Lanken PN, MacIntyre N, et al; National Heart, Lung, and Blood Institute ARDS Clinical Trials Network. Higher versus lower positive end-expiratory pressures in patients with the acute respiratory distress syndrome. *N Engl J Med*. 2004;351(4):327–336. doi:10.1056/NEJMoa032193

30. Herridge MS, Cheung AM, Tansey CM, et al; Canadian Critical Care Trials Group. One-year outcomes in survivors of the acute respiratory distress syndrome. *N Engl J Med*. 2003;348(8):683–693. doi:10.1056/NEJMoa022450

31. Papazian L, Forel JM, Gacouin A, et al; ACURASYS Study Investigators. Neuromuscular blockers in early acute respiratory distress syndrome. *N Engl J Med*. 2010;363(12):1107–1116. doi:10.1056/NEJMoa1005372

32. Li X, Ma X. Acute respiratory failure in COVID-19: Is it "typical" ARDS? *Crit Care*. 2020;24(1):198. doi:10.1186/s13054-020-02911-9

33. Yıldırım F, Yıldız Gülhan P, Şimşek M. COVID-19 related acute respiratory distress syndrome: Pathological, radiological and clinical concordance. *Tuberk Toraks*. 2021;69(3):360–368. doi:10.5578/tt.20219708

34. Katzenstein AL, Bloor CM, Leibow AA. Diffuse alveolar damage: The role of oxygen, shock, and related factors: A review. *Am J Pathol*. 1976; 85(1):209–228. PMID:788524.

35. Gattinoni L, Chiumello D, Rossi S. COVID-19 pneumonia: ARDS or not? *Crit Care*. 2020;24(1):154. doi:10.1186/s13054-020-02880-z

36. Gattinoni L, Chiumello D, Caironi P, et al. COVID-19 pneumonia: Different respiratory treatments for different phenotypes? *Intensive Care Med*. 2020;46(6):1099–1102. doi:10.1007/s00134-020-06033-2